Universidade de Aveiro Departamento de Química
2010

JOSÉ ALEXANDRE RIBEIRO DE CASTRO FERREIRA

STRUCTURAL CHARACTERIZATION OF *HELICOBACTER PYLORI* CELL-SURFACE LIPOPOLYSACCHARIDES AND EXOPOLYSACCHARIDES

Universidade de Aveiro Departamento de Química
2010

JOSÉ ALEXANDRE RIBEIRO DE CASTRO FERREIRA

STRUCTURAL CHARACTERIZATION OF *HELICOBACTER PYLORI* CELL-SURFACE LIPOPOLYSACCHARIDES AND EXOPOLYSACCHARIDES

Dissertation submitted to the University of Aveiro to fulfil the requirements for the degree of Doctor of Philosophy in the field of Biochemistry, done under the scientific supervision of Doctor Manuel António Coimbra Rodrigues da Silva, Associated Professor with Aggregation of the Department of Chemistry of the University of Aveiro and Doctor Mário Artur Monteiro from the Department of Chemistry of the University of Guelph (Guelph, Ontario, Canada).

Financial support from POCI 2004 under the III Community Support Framework

Financial support from FCT and ESF under the III Community Support Framework

To my dearest family and friends

«Entre o sono e sonho,
Entre mim e o que em mim
É o quem eu me suponho
Corre um rio sem fim.
Passou por outras margens,
Diversas mais além,
Naquelas várias viagens
Que todo o rio tem.

Chegou onde hoje habito
A casa que hoje sou.
Passa, se eu me medito;
Se desperto, passou.
8
E quem me sinto e morre
No que me liga a mim
Dorme onde o rio corre -
Esse rio sem fim.»

Fernando Pessoa

Examining Committee

President

Professor José Carlos Esteves Duarte Pedro
Cathedratic professor of the University of de Aveiro

Professor Ivonne Delgadillo Giraldo
Associated professor with Aggregation of the University of de Aveiro

Professor Manuel António Coimbra Rodrigues da Silva
Associated professor with Aggregation of the University of de Aveiro

Professor Mário Artur Monteiro
Associated professor of the University of Guelph, Canada

Professor Maria do Céu Fontes Herdeiro Figueiredo
Auxiliary professor of the Faculty of Medicine of the University of Porto

Professor Maria do Rosário Gonçalves Reis Marques Domingues
Auxiliary professor of the Faculty of Medicine of the University of Porto

Professor Celso Albuquerque Reis
Researcher from the Institute of Molecular Pathology and Immunology of the University of Porto

Acknowledgements

"No man stands alone"…

Therefore, I feel it was an honour and a privileged to have worked under the supervision of Professor Manuel António Coimbra and Professor Mário Monteiro. I am most grateful for their strong scientific guidance, patience, inspiration and friendship. A word in particular for Professor Manuel António that casted me in this journey, taught me about Carbohydrate Chemistry, Glycobiology and so many other things. I also wanted to thank Professor Mario for receiving me in his research group at the University of Guelph. I am most grateful for his hospitality and all the leisure moments we spent together.

A special thanks the Organic Chemistry, Natural and Agro-Food Products research unit from the Department of Chemistry of the University of Aveiro for accepting me as a PhD student and providing me with all the necessary conditions to carry my research and financial support from Fundação para a Ciência e a Tecnologia (FCT) through project Pylori E&LPS (POCI/QUI/59337/2004), PhD grant (SFRH/BD/19929/2004) and the Natural Sciences and Engineering Research Council of Canada (NSERC).

My gratitude also goes to all those involved in project Pylori E&LPS. A special thanks to Professor Céu Figueiro for providing the clinical isolates used in this study, and for PCR analysis. In addition I would like to thank Lurdes Monteiro from Instituto Nacional de Saúde Ricardo Jorge for kindly providing *H. pylori* strain 968.

It all started in Braga… Therefore I would like to express my gratitude to all the people from the Centre of Biological Engineering of the University of Minho, in particular those from the Applied Microbiology Laboratory. I am most thankful to Professor Maria João Vieria and Nuno Azevedo for all the scientific guidance throughout the world of "bugs" and for introducing me to *H. pylori*. A word to my good friend Nuno Guimarães who put the PNA probes "up and running" and Carina and Laura for keeping me busy by providing me with biomass when I returned to Aveiro.

Because it's never easy to spend time away from home, especially when you love it so much, I am most grateful to all those I met during my stay in Guelph. In particular I would like to thank my landlady Krystina, the Longfield's, Diana and all my other neighbours at Shirley's Av. Thank you for your kindness and hospitality, I enjoyed every moment! I was also lucky enough to meet the wonderful people from Mario's group! Thank you Rudy for your friendship, endless patience and all that time spent in the NMR room. To Shariff, a true friend and without a doubt a fan of Portugal and Portuguese people! To Yu-Han for her true kindness! To Xuan Tang, you can beat me at skateboarding but forget about surfing! …and to the sweet Jeya that left us way too soon. You keep on living in our harts.

I also would like to thank to my colleagues from the Department of Chemistry of the University of Aveiro. It would be unfair to be pointing out names since they all have been amazing!

However, I would like to thank Elisabete Coelho for the helpful discussions and friendship through out the years.

Also, I can not forget my good friend Pedro Vasco that got me started, Cristiana Pires and Marina Paulo who shared my interest for *H. pylori*. Thank you for all your help and dedication. My gratitude goes in particular to Cristiana Pires for her belief in me when everything just seemed to be falling apart. She showed me that battles are made to be fought and won! Thanks to Catarina Ferreira for always be watching my back, Susana Cardoso for her friendship and nice cooking's, Gonçalo Graça for his patience and a lot of NMR analysis and João Rodrigues for lots o funny relaxed chats over the years.

Finally I would like to express my appreciation to all the people I have worked with in Mass Spectrometry Group, in particular Professor Rosário Domingues for her scientific supervision, her sympathy and friendships, to Ana Reis for guidance in mass spectrometry essays, interpretation of results the revision of manuscripts and Cristina Barros for all the time spent together in the mass spectrometers. I also would like to thank Rui Vitorino for all the positive discussion we have been having over the past two years and for the proetomic approach you brought to this thesis.

I gratefully acknowledge the access to research infrastructures within the 6th Framework Programme of the EC (Contract # RII3-026145, EU-NMR) and the opportunity to conduct experiments at the RALF-NMR facility, Professor Brian Goodfellow (UA) and Dr. Adrien Favier (RALF-NMR facility) for all the help and conduction of NMR experiences.

Can not forget Filipe Teixeira Gil for is true friendship. Thank you for having the open mind to discuss ideas, to share thoughts and enjoyable conversations throughout the years. Your good advices were sometimes a light in those dark days that come and go.

I also want to show appreciation for all those that believed, like I do, in the beauty of creating something and seeing it grow. To those that, after learning so much and having yet so much to learn, believe that we have the mission of giving back to the community. Therefore a special thanks to the good friends who embraced the project GlyConStruct, namely Pedro Maia, Rafael Costa and Frederico Mendes. We have learned already so much already and I fell good things are yet to come.

Finally I would like to express my gratitude to my close friends André Pinho, Gonçalo Prista, Gonçalo Silva, Hugo Silva Gomes, José Nuno Martins, Miguel Serrano, Manuel Salgueiro, Rogério Queiroz.

I also would like to thank who ever was responsible for all those amazing surfing days over the last four years! It definitely kept me going!

Last but not the least... to my family, for their love.

palavras-chave

Helicobacter pylori, lipopolissacarideos, exopolissacarídeos, glicosídeos das superfície celular, antigénios de Lewis, amilose, manana

resumo

O *Helicobacter pylori* é um patogénico gástrico que coloniza mais de 50% da população mundial e é considerado um agente carcinogénico de classe 1. No *Helicobacter pylori*, tal como acontece com outras bactérias Gram-negativas, a membrana externa é revestida por lipopolissacarídeos (LPS) formados por três domínios distintos: o lípido A, o core e uma cadeia alongada denominada *O*-chain (LPS, *O*-chain-core-lipid A~célula). As *O*-chains dos LPS expressam frequentemente antigénios de Lewis (Le^a, Le^b, Le^x, Le^y) que possuem um papel determinante na interacção com o hospedeiro, colonização e modulação/evasão do sistema imunitário.

Nesta tese, demonstrou-se o potencial analítico da espectrometria de massa de electrospray (ESI-MS^n) em modo positivo usando três tipos de analisadores (LIT, Q-TOF, QqQ) para identificar quantidades vestigiais de antigénios Le. Observou-se, após fomentar a sua fragmentação por colisão com um gás, que os antigénios de Lewis do Tipo 1 (Le^a e Le^b) podiam ser distinguidos dos de Tipo 2 (Le^x e Le^y) com base em fragmentações do resíduo de GlcNAc. Assim, enquanto açúcares ligados na posição *O*-4 do GlcNAc fragmentam apenas como resíduos (unidade-18 Da), resíduos ligado pelo *O*-3 eram perdidos como resíduos e como unidade. Observou-se ainda que os resíduos de GlcNAc apresentavam uma fragmentação característica $^{0,2}A_2$ do seu anel. Como resultado propõe-se que os iões resultantes da fragmentação, a *m/z* 372, e os iões a *m/z* 388 e 305 possam ser usados para distinguir o par de isómeros Le^a/Le^x, respectivamente, e os iões a *m/z* 372 e 534, 305 para distinguir o par Le^b/Le^y. Aplicou-se este conhecimento ainda na identificação dos antigénios de Tipo 2 (Le^x e Le^y) nos LPS da estirpe de *H. pylori* NCTC 11637.

Nesta tese também se descreve que, para além das estruturas glicosiladas acima descritas, a *H. pylori* também produz glicosídeos ricos em manose e expressa/bio-acumula amilose (polissacarídeos constituído por α-(1→4)-D-Glc.

Observou-se que o fenómeno de bioacumulação era potenciado pela manutenção da bactéria em meio de agar, ao mesmo tempo que a quantidade de LPS expressa diminuía. Por outro lado, durante uma fase de crescimento exponencial em meio líquido F12, observou-se o comportamento oposto, isto é, um aumento da expressão de LPS e diminuição na expressão de amilose. Assim, sugere-se que, quando submetida a uma pressão selectiva induzida por condições ambientais específicas, o *H. pylori* seja levado a expressar amilose.

Estudos por RMN permitiram ainda a caracterização estrutural dos glicosídeos ricos em manose produzidos na estirpe virulenta *H. pylori* 968. A manana produzida por esta estirpe é constituída por resíduos de *O*-6 Man apresentando aproximadamente 80% destes resíduos ramificações na posição *O*-2. Nas cadeias laterais foram identificados resíduos de *O*-2 Man tanto em configuração α como β. Esta manana foi observada como parte de um heteropolissacarídeo constituído também por Glc, Gal e GlcNA e um domínio proteico.

Estudos levados a cabo na estirpe virulenta *H. pylori* PTAV79 isolada de um paciente com refluxo gastro-esofágico revelaram LPS com *O*-chains compostas por unidades de LacNAc (antigénio i). Mesmo não apresentando *O*-chains fucosiladas determinantes para a interacção com o hospedeiro, esta estirpe manteve a capacidade de colonizar a mucosa gástrica e promover um quadro patológico. No *H. pylori* PTAV79 foram ainda detectadas elevadas quantidades de ácido esteárico e amilose ligada a resíduos de glicerol (Gro). Os resíduos de Gro foram observados ligados a grupos fosfodiéster, sugerindo a expressão de glicoglicerofosfolípidos. Estes resultados apontam para que a amilose se encontre ligada à membrana externa da bactéria através de glicerofosfolípidos. Com base em estudos estruturais por GC-EI-MS, FTIR, ESI-MS, MALDI-TOF-MS e RMN foi ainda possível identificar um polissacarídeo ainda não descrito para a *H. pylori* composto pela seguinte unidade repetitiva de ácido aldobiourónico: [→3)-α-D-GlcA(1→4)-α-D-Glc(1→]. Uma abordagem proteómica permitiu ainda a primeira descrição para o *H. pylori* de uma proteína glicosilada não pertencente ao flagelo.

keywords

Helicobacter pylori, lipopolysaccarides, exopolysaccharides, cell surface glycans, Lewis antigens, amylose, mannan, cell-surface glycans

abstract

Helicobacter pylori is a widespread gastroduodenal pathogen recognized as a category 1 (definitive) human carcinogen. Like other Gram-negative bacteria, it expresses cell-surface lipopolysaccharides comprising a lipid A moiety, a conserved core oligosaccharide and an elongated *O*-chain (LPS, *O*-chain-core-lipid A~cell). *H. pylori O*-chains have been recognized to contain mammalian Le blood group determinants (Le^a, Le^b, Le^x, Le^y) that exert much influence in the interaction with the host, namely adhesion to gastric cells, colonization, and modulation/evasion of immune responses.

In this work, underivatized Lewis blood groups were studied by electrospray mass spectrometry (ESI-MS^n) in the positive mode with three different mass analysers (Q-TOF, QqQ, and LIT) in order to establish the analytical basis for a reliable determination of trace amounts of Lewis antigens. It was observed that, under collision induced fragmentations, Type 1 Lewis antigens (Le^a and Le^b) could be distinguished from Type 2 (Le^x and Le^y) on the basis of specific fragmentations of the GlcNAc unit. While *O*-4 linked sugars of the GlcNAc are lost as residues, the *O*-3 linked sugars undergo fragmentation both as sugar units as well as sugar residues (unit -18 Da). Type 2 Le antigens also showed a characteristic cross-ring cleavage $^{0,2}A_2$ of the GlcNAc. As a result, the product ions at *m/z* 388 and 305, characteristic of Le^x, and 372, characteristic of Le^a, are proposed to distinguish the trisaccharide isomers Le^x/Le^a. Also, the product ions at *m/z* 534 and 305, characteristic of Le^y, and 372, characteristic of Le^b, are proposed to distinguish the tetrasaccharide isomers Le^b/Le^y. These diagnostic fragment ions were further applied in the identification of Lewis Type 2 antigens (Le^x and Le^y) in the cell-surface of *H. pylori* NCTC 11637.

In this thesis it is also described that, in addition to LPS, *H. pylori* is able to produce cell-surface mannan-rich glycosides and express/accumulate amylose-like glycans (α-(1→4)-Glc polysaccharide).

Bioaccumulation of amylose was found to be enhanced with the subcultivation of the bacterium on agar medium, while LPS *O*-chains expression decreased. During exponential growth of the bacterium in F12 liquid medium, an opposite behaviour is observed, i.e. there is an increase in the overall amount of LPS and decrease in amylose content. As such, it is suggested that under certain selective pressures induced by specific environmental conditions, *H. pylori* might be led to express a phase-variable cell-surface α-(1→4)-D-Glc polysaccharide.

NMR structural studies carried out in mannose-rich glycans isolated from virulent strain *H. pylori* 968 allowed a characterization of this moiety. This strain was found to express a highly branched mannan formed by a backbone of α-(1→6)-linked mannopyranose units showing up to 80% substitution in the *O*-2 position. The side chains were found to contain *O*-2 linked Man residues both in α- and β- configurations.

In addition, studies conducted in virulent strain PTAV79 isolated from a gastric biopsy specimen of a patient with gastroesophageal reflux disease revealed semi-rough LPS having *O*-chains composed of LacNAc (i-antigen) units. Even though lacking fucosylated *O*-chains this strain was still able to colonize the human stomach and promote disease. This strain also found expressed high amounts of stearic acid and amylose-like glycans that were observed linked to glycerol (Gro) residues. Furthermore, Gro was detected carrying phosphodiester moieties suggesting the existence of glycerophospholipids. These structures are thought to act as anchoring points of amylose-like glycans to the outer cell-surface lipidic bilayer. Fine analytical and spectroscopic techniques, namely GC-EI-MS, FTIR, ESI-MS, MALDI-TOF-MS and NMR further permitted the identification of an unusual polysaccharide composed of aldobiouronic acid repeating units, [→3)-α-D-GlcA(1→4)-α-D-Glc(1→].. In addition, a proteomic approach allowed the first report of a non-flagelar *H. pylori* glycoprotein exhibiting *O*-glucuronosyl Ser residues.

Publications

Publications in peer revised international scientific journals

Ferreira, J.A.; Pires, C.; Paulo, M.; Azevedo, N.F.; Domingues, M.R.; Vieira, M.J.; Monteiro, M.A.; Coimbra, M.A. Bioaccumulation of amylose-like glycans by *Helicobacter pylori*. Helicobacter. 2009 14: 559-570.

Ferreira, J.A.; Domingues, M.R.; Reis, A.; Monteiro, M.A.; Coimbra, M.A. Differentiation of isomeric Lewis blood groups by positive ion electrospray tandem mass spectrometry. Anal Biochem. 2010 397: 186-196.

Ferreira, J.A.; Vitorino, R.; Reis, A.; Domingues, M.R.M.; Figueiredo, C.; Monteiro, M.A.; Coimbra, M.A. Helicobacter pylori virulent strain expressing cell-surface lipopolysaccharides lacking fucosylated Lewis *O*-chains. Observation of α-glucans and glucuronic acid-containing serine *O*-glycoproteins (submitted to Glycobiology November 2009)

Ferreira, J.A. Azevedo, N.F.; Vieira, M.J.; Figueiredo, C.;. Goodfellow, B.J; Vitorino, R.; Monteiro, M.A.; Coimbra, M.A. Identification of mannose-rich heteropolymeric glycans in the cell-surface of a virulent *Helicobacter pylori* wild type strain. (submitted to Carbohydr. Res. November 2009).

Oral communications by invitation

Ferreira, J.A. Search for *Helicobacter pylori* exopolysaccharides. Workshop: *Helicobacter pylori* – Bases químicas e bioquímicas para o desenvolvimento de vacinas e para a compreensão dos mecanismos de adesão. 2006. Aveiro, Portugal.

Ferreira, J.A. *Helicobacter pylori*: A wolf in sheep's clothing. Encontro Nacional de Estudantes de Biologia (ENEB). 2007. Aveiro, Portugal.

Ferreira, J.A. Envelope glicosídico da *H. pylori* - da estrutura à função. Jornadas de Bioquímica do Departamento de Química da Universidade de Aveiro. 2009. Aveiro, Portugal.

Other oral communications

Ferreira, J.A. Cell-surface mannan polysaccharide in *Helicobacter pylori*. (A candidate for a glycoconjugated vaccine?). Portuguese-French meeting on *Helicobacter pylori*. 2008. Lisbon, Portugal.

Poster in conferences

Ferreira, J.A.; Pires, C.; Azevedo, N.; Domingues, M.R.; Vieira, M.J.; Monteiro, M.A.; Coimbra, M.A. Bioaccumulation of amylose-like glycans by *Helicobacter pylori*. MICROBIOTEC'09. 2009 Vilamoura, Portugal.

Ferreira, J.A.; Domingues, M.R.; Reis, A.; Monteiro, M.A.; Coimbra, M.A. Differentiation of isomeric Lewis blood groups by positive ion electrospray tandem mass spectrometry. Glupor 09. Braga, Portugal.

Coimbra, M.A.; Dias, E.; **Ferreira, J.A.;** Azevedo, N.; Vieira, M.J.; Rocha, S.M. Process of detection of *Helicobacter pylori* using aliphatic amides. MICROBIOTEC'07. 2007 Lisbon, Portugal.

Ferreira, J.A.; Azevedo, N.; Vieira M.J.; Monteiro, M.A.; Coimbra, M.A. Cell-surface mannan polysaccharide in *Helicobacter pylori*. European Helicobacter Study Group XX International Workshop. 2007. Istanbul, Turkey.

Ferreira, J.A.; Azevedo, N.; Vieira M.J.; Monteiro, M.A.; Coimbra, M.A. Structural screening of *Helicobacter pylori* Lipolysaccharides from clinical isolates of Portuguese based patients Glupor 07. Oeiras, Portugal.

Ferreira, J.A.; Azevedo, N.; Coimbra, M.A.; Vieira, M.J. Exopolysaccharide production by *H. pylori*. Summer Course Glycosciences – 9th European Training Course on Carbohydrates. 2006. Wageningen, the Netherlands.

Ferreira, J.A.; Azevedo, N.; Coimbra, M.A.; Vieira, M.J. Evidences of Exopolysaccharide production by *H. pylori*. MICROBIOTEC'05. 2005. Povoa do Varzim, Portugal.

National Patents

Coimbra, M.A.; Rocha, S.M.; Dias, E.; **Ferreira, J.A.** Processo de detecção de *Helicobacter pylori* através da utilização de amidas alifáticas. Patent application PT/2006/103630.

International Patents

Coimbra, M.A.; Rocha, S.M.; Dias, E.; **Ferreira, J.A.** Process for detecting *Helicobacter pylori* using aliphatic amides. Patent application WO/2008/081398.

Contents

CHAPTER I.

CHAPTER II.

List of abbreviations

AA	Alditol acetates
AEP	2-aminoethylphosphate
Ara	Arabinose
BCA	Biocinchronic acid
cagA	Cytotoxin-associated protein
CBA	Columbia blood agar
COSY	Correlation spectroscopy
CPS	Capsular polysaccharide
Da	Dalton
DD-Hep	D-*glycero*-D-*manno*-heptose
LD-Hep	L-*glycer*o-D-*manno*-heptose
DMSO	Dimethylsulfoxide
DNA	Deoxyribonucleic acid
DOSY	Diffusion ordered spectroscopy
EI	Electronic impact
ELISA	Enzyme-linked immunosorbent assay
ELSD	Evaporative Light Scattering Detector
EPS	Exopolysaccharide
ESI-MS	Electronic Impact-Mass Spectrometry
Fuc	Fucose
FTIR	Fourier Transform Infrared Spectroscopy;
Gal	Galactose
GC	Gas chromatography
Glc	Glucose
GlcA	Glucuronic Acid
GlcNAc	2-acetamido-2-deoxy-glucose
Gro	Glycerol
Hex	Hexose
HexNAc	2-acetamido-2-deoxy-hexose
HMBC	Heteronuclear multiple bond correlation
HMQC	Heteronuclear Multiple Quantum Correlated Spectroscopy

HPLC	High Performance Liquid Chromatography
kdo	3-deoxy-D-*manno*-octulosonic acid
LacNAc	*N*-acetyl-β-lactosamine
Le	Lewis blood group determinant
Le^a	Lewis A
Le^b	Lewis B
Le^x	Lewis X
Le^y	Lewis Y
LIT	Linear Ion Trap
LPS	Lipopolysaccharide
MALDI	Matrix-assisted laser-desorption/ionisation
Man	Mannose
MS	Mass spectrometry
MS^n	Tandem mass spectrometry
*M*w	Molecular weight
m/z	Mass-to-charge ratio
NCTC	National Collection of Type Cultures
NeuAc	5-acetamido-neuraminic acid
NMR	Nuclear Magnetic Ressonance
NOE	Nuclear Overhauser Effect
NOESY	Nuclear Overhauser Enhancement Spectroscopy
OS	Oligosaccharides
P	Phosphate
PAGE	Polyacrylamide gel electrophoresis
PAS	Periodic Acid Schiff
PCR	Polymerase Chain Reaction
PMAA	Partially Methylated Alditol Acetates
PNA	Peptide Nucleic Acid
PS	Polysaccharide
R-LPS	Rough-form Lipopolysaccharide
rt	Retention time
S-LPS	Smooth LPS

QqQ	Triple quadrupole;
Q-TOF	Quadrupole time-of-flight;
Rha	Rhamnose
Rib	Ribose
RNA	Ribonucleic acids
SEC	Size exclusion chromatography
Ser	Serine
SDS	Sodium-dodecylsulfate
TFA	Trifluoroacetic acid;
TOCSY	Total correlation spectroscopy
TOF	Time-of-flight
vacA	Vacuolating cytotoxin

Structure of monosaccharides observed in the *H. pylori* cell-surface glycans mentioned in the present thesis

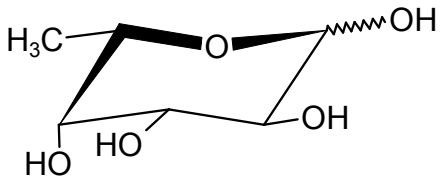

6-deoxy-L-Galactose or L-Fuc (L-Fuc*p*)

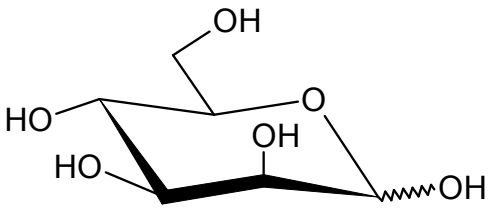

D-Mannose (D-Man*p*)

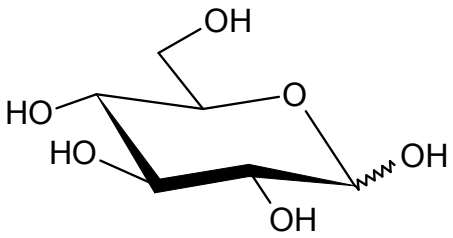

D-Glucose (D-Glc*p*)

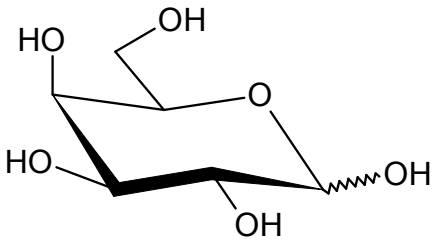

D-Galactose (D-Gal*p*)

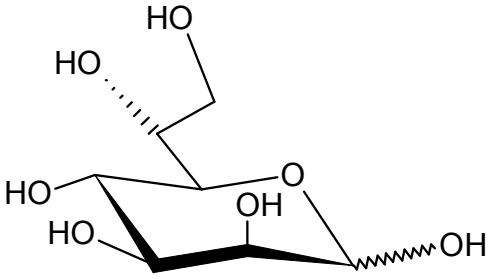

D-glycero-D-*manno*-heptose (DDHep*p*)

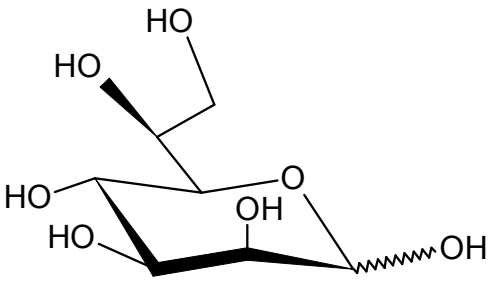

L-glycero-D-*manno*-heptose (LDHep*p*)

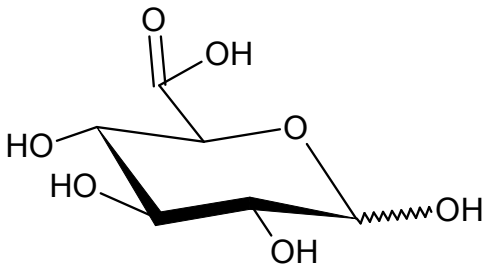

D-Glucuronic acid (D-GlcA*p*)

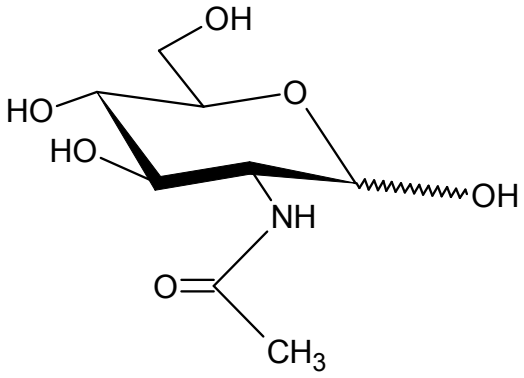

N-acetyl-D-Glucosamine (D-Glc*p* Nac*p*)

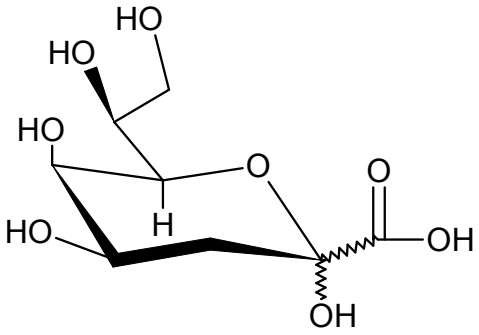

3-deoxy-D-*manno*-octulosonic acid

(D-Kdo*p*)

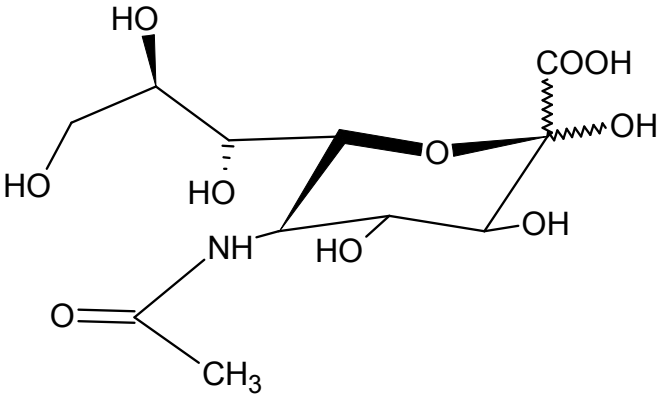

5-acetamido-neuraminic acid

(Neu5Ac*p*)

Lewis blood group related structures mentioned in the present thesis

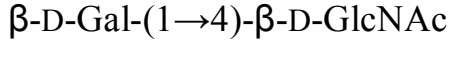

***i*-antigen**

(Type 1 chain: β-D-Gal-(1→3)-β-D-GlcNAc)

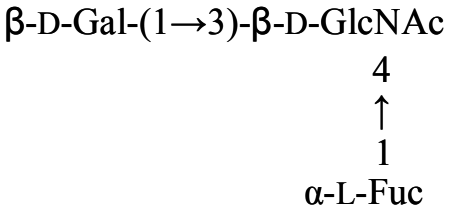

Le^a

(Type 1 chain)

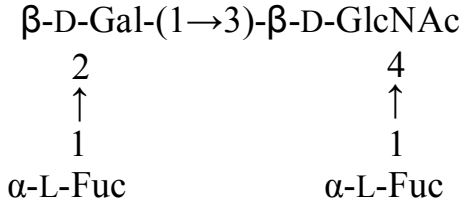

Le^b

(Type 1 chain)

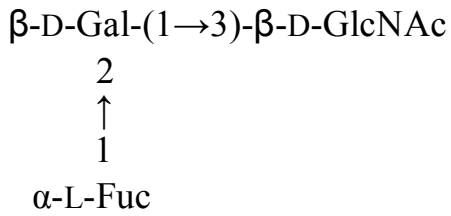

Le^d

(Type 1 chain)"

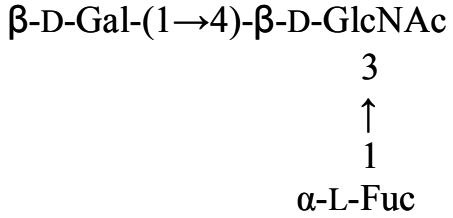

Le^x

(Type 2 chain: β-D-Gal-(1→4)-β-D-GlcNAc)

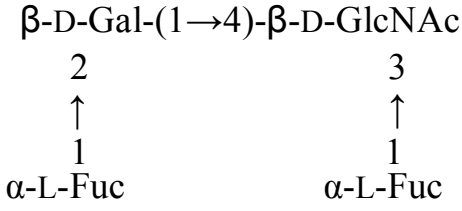

Le^y

(Type 2 chain)

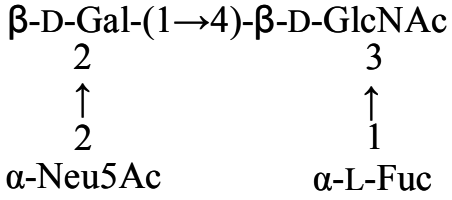

Sialyl-Le^x

(Type 2 chain)

CHAPTER I

GENERAL INTRODUCTION

Helicobacter pylori

Helicobacter pylori is a microaerophilic, Gram-negative bacterium taxonomically related to *Campylobacter spp* that colonizes the human gastric mucosa. *H. pylori* is one of the most widespread bacterial pathogens with a prevalence of up to 90% in developing countries and a worldwide infection rate of around 50%[1]. Its first isolation from the human stomach less than 30 years ago and the correlation of infection with gastric burdens was achieved by Robin Warren and Barry Marshall[2,3] and resulted in dramatic changes in the field of gastroenterology. In addition, the persistence of a pathogen in an environment long thought to be sterile revealed one of the most sophisticated colonizers of humans.

This knowledge had a major clinical impact in the management of gastric diseases such as gastritis and peptic ulcers initially regarded as resulting from unhealthy habits such as drink, smoking or unbalanced diet has well as nervous disorders. Additionally, in 1994, the International Agency for Cancer Research, an arm of the World Health Organization, declared *H. pylori* a class 1 (definite) human carcinogen[4]. These events and the peculiarities behind *H. pylori* further enhanced research and made these bacteria one of the hot-topics for scientists worldwide. In 2005 Warren and Marshall's discovery was recognize with the award of a Nobel Prize of Physiology and Medicine and triggered what has now been considered one of the most studied microorganism in the world

1.1.1. Microbiology

H. pylori (Fig. 1.1) is a helix-shaped Gram-negative bacterium, about 3 μm long ad with a diameter of about 0.5 μm[1]. It is microaerophilic; that is, it requires oxygen, but at lower concentration than is found in the atmosphere. It contains a hydrogenase which can be used to obtain energy by oxidizing molecular hydrogen (H_2) that is produced by intestinal bacteria[5]. It also produces oxidase, catalase, and urease which have been used to access the presence of the bacteria. *H. pylori* has further been described as having the ability to form biofilms both *in vitro*[6] as *in vivo*[7] and can change from the spiral to a possibly viable but nonculturable coccoid form[8]. This transformation is thought to occur when facing unfriendly environments, namely outside the human reservoir thus contributing to the epidemiology of the bacterium[9]. However, the coccoid form has demonstrated to be able to adhere to gastric epithelial cells *in vitro*[10].

H. pylori possesses five major outer membrane protein (OMP) families[1]. The largest family includes known and putative adhesins thought to play a critical role in the interaction with the host. The other four families include porins, iron transporters, flagellum-associated proteins, and proteins with still unknown function.

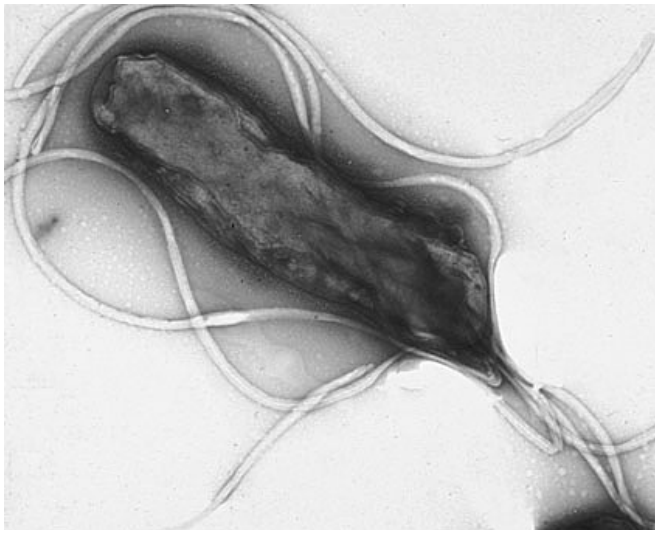

Figure 1.1. Electron micrograph of *H. pylori* (negative staining)[11].

Like other typical Gram-negative bacteria, the outer membrane of *H. pylori* consists of phospholipids and lipopolysaccharide (LPS) whose structures will be discussed in detail in sections 1.3 and 1.4. The outer membrane also contains cholesteryl glucosides, which have been found in few other bacteria[1]. *H. pylori* further exhibit 4–6 flagella responsible for its high mobility and colonization of the gastric mucous[12].

1.1.2. Pathogenicity factors

Although infection with *H. pylori* almost always results in chronic active gastritis, most infected patients develop no complications and are free of any obvious clinical symptoms of this infection[13]. This led to the notion that some strains may be more virulent than others. Some of the most relevant virulence factors that have been responsible for aiding bacterial colonization and/or inducing pathology are further discussed bellow.

- *CagA*

The cytotoxin associated gene A (*CagA*) protein is a highly immunogenic protein with a molecular mass of approximately 149 kDa encoded by the *cagA* gene, which is present in 50 to 70% of *H. pylori* strains[1] and is a marker for the presence of a genomic PAI (pathogenicity island). Eighteen of the *cag* PAI-encoded proteins serve as building blocks of a type IV secretion apparatus, which forms a syringe like structure capable of penetrating the gastric epithelial cells and facilitating the translocation of *CagA*, peptidoglycan, and possibly other bacterial factors into host cells, thus inducing morphological change and proinflammatory response[1]. Patients infected with $CagA^+$ strains usually have a higher inflammatory response and are significantly more at risk for developing a symptomatic outcome (peptic ulcer or gastric cancer) in Western populations, though not in Asian populations[1].

- *VacA*

Approximately 50% of all *H. pylori* strains secrete *VacA* (vacuolating cytotoxyn), a highly immunogenic 95 kDa protein that induces massive vacuolization in epithelial cells *in vitro*. The *VacA* protein plays an important role in the pathogenesis of both peptic ulceration and gastric cancer[1]. Although *VacA* is not essential for *in vitro* growth of *H. pylori*, it was reported to significantly contribute to murine gastric colonization by *H. pylori*[1]. *VacA* forms pores in epithelial cell membranes. It also increases transcellular permeability, leading to the release of nutrients and cations[1].

Helicobacter pylori strains from different geographic areas exhibit clear phylogeographical differentiation; therefore, the *CagA* and *VacA* genotypes of *H. pylori* strains can serve as markers for the migration of human populations[14].

- *Acid resistance*

The pH of the gastric mucosa is thought to vary between 4.0 and 6.5, but occasional acid shocks may occur. *H. pylori* thus requires mechanisms to protect itself from acute acid shocks and mechanisms to grow at pH values around 5.5[1]. One of such features is urease, an enzyme that catalyzes the hydrolysis of urea into carbon dioxide and ammonia thus

creating a buffered environment around the cells[15]. *H. pylori* also produces amidases, enzymes responsible for the degradation of amides into volatile carboxylic acids and ammonia that further assisting in the buffering of the surrounding medium[16].

Another strategy to avoid the acid environment of the human stomach is the spiral shape of *H. pylori* and the seven sheathed flagella present in one of its poles. It allows the bacterium to be highly motile even in very viscous mucus, allowing it to migrate to the mucus layer overlaying the gastric mucosa[17,18].

- *Adhesins*

H. pylori express many adhesins, responsible for the mediation of *H. pylori* to the gastric epithelium[1,18]. However, given the narrow host range, the multitude of adhesins probably reflects their importance for the bacterium. In this context the expression of lectins such as BabA and SabA and carbohydrates play a key role in host-bacteria interplay.

The 78 kDa BabA protein probably represents the best-characterized *H. pylori* adhesion protein; it is encoded by the *babA* gene. BabA mediates binding to fucosylated Lewis b (Le^b) blood group antigens on the human host cells[19].

SabA mediates binding to sialic acid containing glycoconjugates. *H. pylori*-induced gastric inflammation and gastric carcinoma are associated with the replacement of nonsialylated Lewis antigens by sialylated Le^x and sialylated Le^a. Thus, the role of SabA is probably during the chronic inflammatory and atrophic disease stages[20].

1.1.3. Epidemiology

There appears to be no substantial reservoir of *H. pylori* aside from the human stomach. Other animals harbour organisms that resemble *H. pylori*, but with the exception of nonhuman primates[21] and, under particular circumstances, cats[22], no others were found to be able to be colonized by *H. pylori*; thus *H. pylori* is considered to be host-specific.

At least half the world's population is infected by the bacterium, making it the most widespread infection in the world[23]. In developing countries, 70 to 90% of the population carries *H. pylori*; while in developed countries (Western Europe, North America,

Australia) the prevalence of infection is lower with rates estimated around 25% and 50%[24]. World wide distribution of *H. pylori* thus suggests a correlation between socio-economic status and infection, which has shown to be usually acquired in early childhood in all countries[1,25]. The infection rate of children in developing nations is higher than in industrialized nations, probably due to poor sanitary conditions. In developed countries it is currently uncommon to find infected children, but the percentage of infected people increases with age, with about 50% infected for those over the age of 60 compared with around 10% between 18 and 30 years[23]. Thus, in an era of "emerging" microbes, we might think of *H. pylori* as gradually "submerging" from probably near-universality several hundred years ago to the present situation when fewer than 10% of children in developed countries are becoming infected[26,27].

H. pylori is contagious, although the exact route of transmission is not yet known[9,28,29]. At present, the route of transmission is perhaps one of the most controversial areas of *H. pylori* research. Several reservoirs outside the human gastrointestinal tract have been suggested as sources of infection, but evidence is not conclusive. Person-to-person transmission by either the oral-oral or fecal-oral route is most likely[30]. Consistent with these transmission routes, the bacteria have been isolated from feces, saliva and dental plaque of some infected people[30]. Interfamilial spread appears to play a central role in transmission of the infection in both developing and developed countries[25]. *H. pylori* may also be transmitted orally by means of fecal matter through the ingestion of waste-tainted water, so a hygienic environment could help decrease the risk of *H. pylori* infection[30].

1.1.4. Clinical relevance of *H. pylori* infection

Colonization with *H. pylori* is not a disease in itself but a condition that affects the relative risk of developing various clinical disorders of the upper gastrointestinal tract and possibly the hepatobiliary tract. Therefore, although gastric colonization with *H. pylori* induces histological gastritis in all infected individuals, only a minority develop any apparent clinical signs of this colonization[13]. It is estimated that *H. pylori*-positive patients have a 10 to 20% lifetime risk of developing ulcer disease and a 1 to 2% risk of developing distal gastric cancer[1]. The risk of development of these disorders in the presence of *H. pylori* infection depends on a variety of bacterial, host, and environmental factors that mostly relate to the pattern and severity of gastritis (Fig. 1.2).

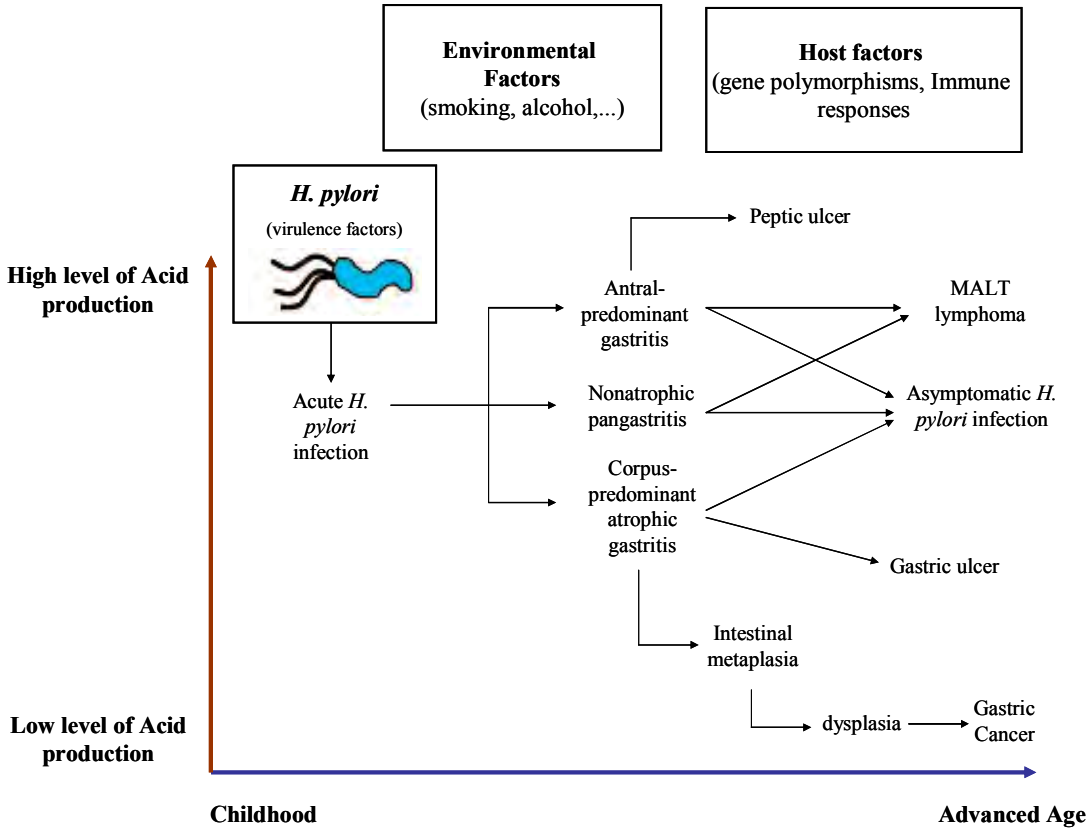

Figure 1.2. Schematic representation of the factors contributing to gastric pathology and disease outcome in *H. pylori* infection (adapted from Kusters *et. al.*[1]).

H. pylori infection also has been further associated with the development of gastric non-Hodgkin's lymphomas[31] and with another lymph proliferative disorder, gastric mucosa-associated lymphoid tissue (MALT) lymphoma (MALToma)[32,33]. Importantly, treatment of gastric MALToma patients with antibiotics that eradicate *H. pylori* often leads to regression of the tumour[34-36].Thus, in total, *H. pylori*, a previously obscure organism, has now been associated with many of the most important diseases involving gastroduodenal tissue[26].

1.2. Gram-negative cell wall architecture

Almost all prokaryotes possess cell walls external to their plasma membrane. Cell-surface architecture is used to divide bacteria into two groups based on staining with Gram stain; Gram positive bacteria remain stained by crystal violet on washing, Gram negative bacteria do not.

In both Gram-negative and Gram-positive bacteria, the cell wall is most exclusively formed by peptidoglycan, also known as murein, a composite of long polymeric strands of glycans crosslinked by stretchable peptides. The sugar moiety consists of alternating residues of β-(1,4) linked *N*-acetylglucosamine (GlcNAc) and *N*-acetylmuramic acid (MurNAc) residues. Attached to the MurNAc is a peptide chain of three to five D-amino acids that can be cross-linked to the peptide chain of another strand resulting in a 3D elastic mesh-like network. However, while Gram-positive bacteria are characterized by a relatively thick cell wall consisting of multiple layers of protective peptidoglycan, Gram-negative bacteria exhibit a single and thinner layer. Still, Gram-negative cell walls (Fig. 1.3) have been found strong enough to withstand ~3 atm of turgor pressure[37], tough enough to endure extreme temperatures[38] and pHs[39] and elastic enough to be capable of expanding several times their normal surface area[40]. Thus the Gram-negative cell wall is regarded as a remarkable strong, tough, and elastic structure and the main responsible for the protection of cellular contents[41,42].

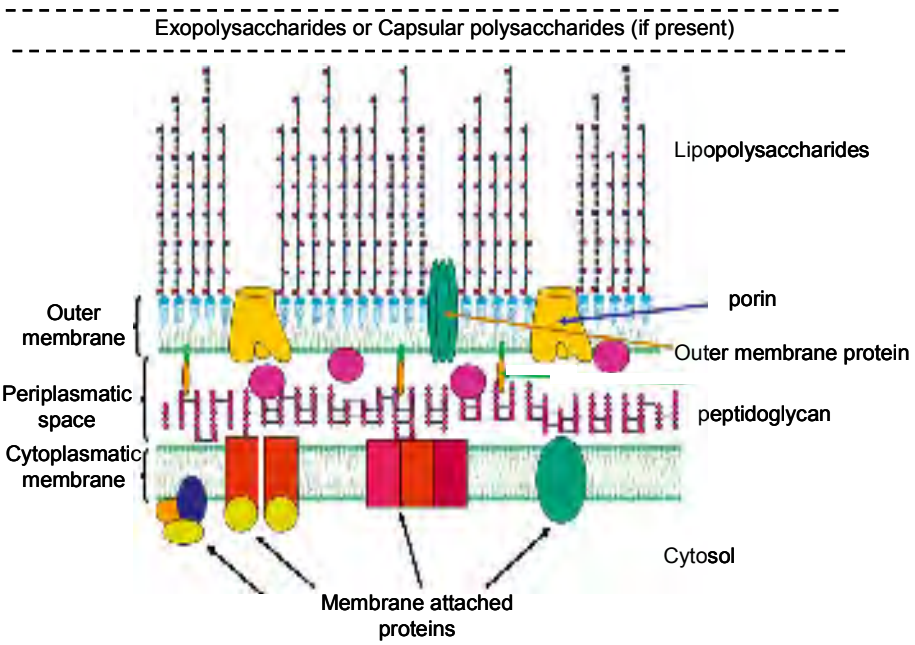

Figure 1.3. Schematic representation of a Gram-negative cell wall (adapted from[43]).

Gram-negative bacteria also present an additional outer surface membrane decorated with lipopolysaccharides (LPS) originating a much more complex cell-surface architecture than the one of Gram-positive bacteria. Some bacteria further produce capsular or extracellular polysaccharides (CPS/EPS) responsible for conferring extra protection to the cell, thus frequently regarded as pathogenicity phenotypes.

1.2.1. Lipopolysaccharides (LPS)

Lipopolysaccharides (LPSs) are vital to both the structural and functional integrity of the Gram-negative bacterial outer membrane. Ubiquitously expressed by all Gram-negative bacteria, and containing several well-conserved domains, LPS also serves as one of the primary targets of the innate arm of the mammalian immune system[44]. The presence of LPS in the outer membrane confers stability to the bacterial membrane, protection against bacteriophages and certain antibiotics, as well as protection against the host defence mechanism during infections[44,45]. LPS are also regarded as powerful immunomodulators in infected hosts, and may cause endotoxic shock[43]. Most of them share a common architecture but vary considerably in structural motifs from one genus to another, species, and even within strains. The LPS are commonly formed by three distinct domains: a lipidic moiety termed lipid A that acts as anchoring point to the cell-surface; an inner oligosaccharide moiety termed core; and often elongated domains yielding repeating units termed *O*-chains.

The lipid A endows the LPS with its range of immunological and endotoxic activities, although the degree of bioactivity of lipid A may be modulated by the saccharide portion of the LPS[46]. The structure of the lipid A moiety is highly conserved within each species, whereas the core oligosaccharide is more variable and the *O*-chain exhibits the higher variability[46].

The inner core is proximal to the lipid A and contains a high proportion of unusual sugars such as 3-deoxy-D-*manno*-octulosonic acid (Kdo) and L-glycero-D-*manno* heptose (Hep)[43.46]. The outer core extends further from the bacterial surface and is more likely to consist of more common sugars such as hexoses and hexosamines[43]. Onto this is attached, in most cases, a polymer of repeating saccharide subunits called the *O*-polysaccharide, or *O*-chain, also typically composed of common hexoses and hexosamines. This *O*-chain is not ubiquitous, however, it appears truncated or lacking in a number of Gram-negative

strains[43]. Bacteria which colonise mucosal surfaces, for example, often express LPS with a truncated non-repeating *O*-chain known as lipo-oligosaccharide (LOS; oligomeric *O*-chain-Core-Lipid A~cell)[43]. In addition, certain strains carry mutations in the well-conserved *rfb* locus (which contains a selection of genes involved in *O*-chain synthesis and attachment) and are termed rough mutants (Core-Lipid A~cell) to differentiate them from the wild-type smooth (S) strains which express *O*-chain bearing LPS (polymeric *O*-chain-Core-Lipid A~cell) (Fig. 1.4). LPS phenotypes yielding a complete core oligosaccharides (OS) and a small number of *O*-chain repeating blocks are sometimes also observable and termed semi-rough (*O*-chain OS-Core-Lipid A~cell, SR). This classification in rough, semi-rough or smooth phenotypes had its origin on the characteristic shape of their colonies on agar plates.

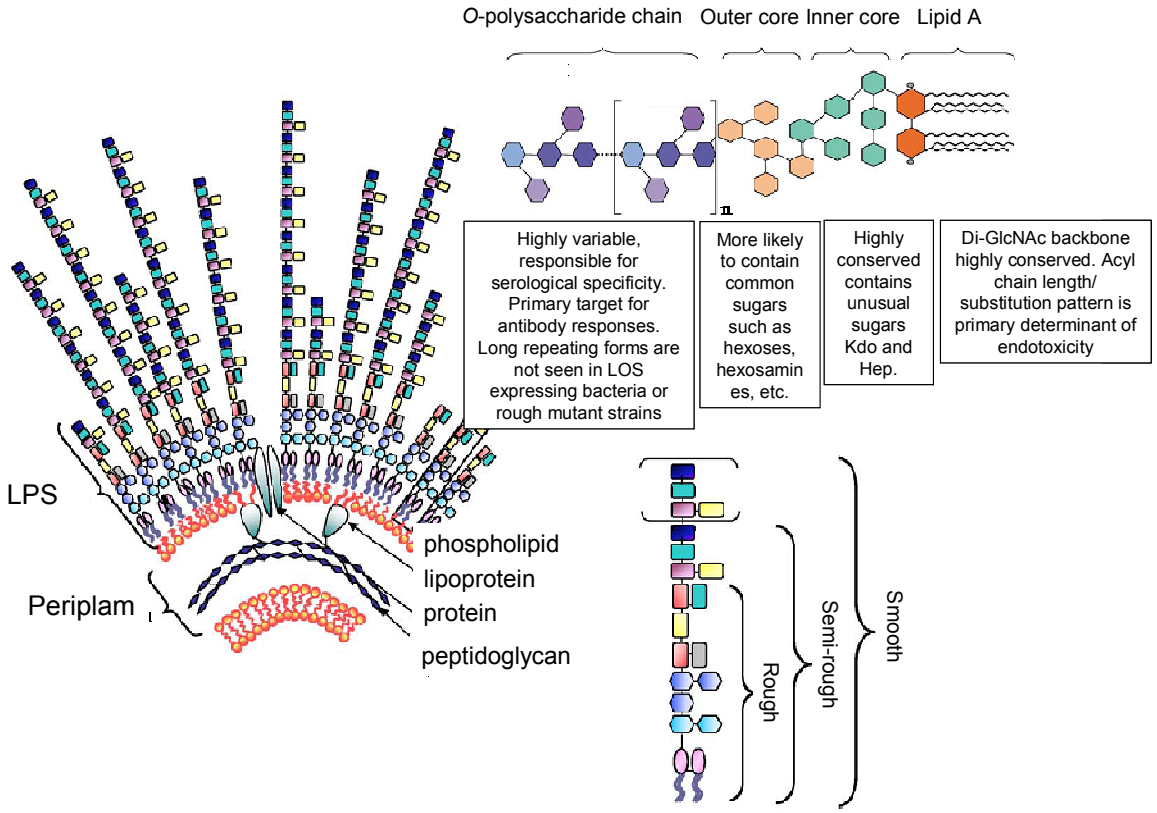

Figure 1.4. Schematic representations of the enterobacterial Gram-negative cell envelope (left), a lipopolysaccharide structure (right), R, SR, and S indicate the structures of rough-type, semi-rough type (with only one O-chain subunit) and smooth-type lipopolysaccharides, respectively (adapted C. Erridge *et al*.[44] and Caroff and Karibian[47])

1.2.2. Extracellular polysaccharides and Capsular polysaccharides (EPS/CPS)

A broad range of bacterial species are known to produce polysaccharide envelopes normally referred as capsules (CPS) or excrete polysaccharides (exopolysaccharides, EPS) to the surrounding media thus creating a strong and sticky framework[43]. Even though some controversy might prevail as far as differentiating CPS form EPS, distinction is generally based on presence of absence of cell bonding. While CPS, like the LPS, are considered to be covalently attached to the cell wall, the EPS molecules appear to be released onto the cell surface with no discernable means of attachment. The EPS and CPS are also, like the *O*-antigen in the LPS, normally built up by oligosaccharide repeating units into homo- or hetero-polymers. Inter-strain and specie variations are frequently observed as well as the introduction of branches and decoration elements such as substitution of both organic and inorganic molecules rendering additional structure complexity.

These structures are considered virulence factors as they are recognized as protection agents for the bacterial cell. They protect the cell against phagocytosis, retain water thus preventing cell from desiccation, and confer shielding against external aggressions, both biological such as virus and chemical (detergents or antibiotics)[43]. Furthermore they are responsible for bacteria adhesion to surfaces and other cells and the main cement in formation and maintenance of an alternative bacterial life style outside the natural reservoir providing harsh environments.

1.3. *Helicobacter pylori* cell-surface LPS

Like other typical Gram-negative bacteria, *H. pylori* cell-envelope is composed of LPS that, when biosynthetically completed, are composed by the three distinct structural domains mentioned in section 1.2: a polysaccharide (PS) known as *O*-chain (OPS), an oligosaccharide (OS) termed Core, and a fatty-acid rich endotoxin moiety named Lipid A (LPS: O-chain →Core→Lipid A~cell)[48], that has demonstrated to yield low biological activity compared when with the Lipid A from other bacteria[49]

Even though *H. pylori* clinical isolates were recognized to produce high-molecular weight (smooth) LPS with extended *O*-antigenic chains, strains yielding semi-rough LPS have also been observed. Long term subcultivation solid medium leads *H. pylori* strains that express smooth LPS phenotypes to express semi-rough and rough forms. However, when recovered to liquid medium this strains regain the capability to express smooth LPS[50,51]. Some strains were also found to express an additional DD-Hep oligomeric domain between the core OS and the Lewis *O*-chain (*O*-chain → Heptoglycan → Core→Lipid A~cell)[48,52,53.]

Studies carried out less than ten years ago by Monteiro and colleagues resulted in the structural definition of the LPS polysaccharide moiety[48]. Furthermore, the classification for *H. pylori* LPS into glycotype families based on their structures has been purposed[48,54].

1.3.1. Lipid A

H. pylori lipid A (Fig. 1.5) is formed by a hydrophilic backbone of β-(1→6)-linked D-GlcNAc disaccharide 1-phosphate or, in lower abundance, ethanolaminephosphate[55]. In smooth-LPS, but not in rough-LPS, the *O*-4 position was partially substituted by another phosphate group. The fatty acid moiety comprises hexadecanoic (16:0), 3-hydroxyhexadecanoic acids [16:0(3-OH)], and 3-hydroxyoctadecanoic [18:0(3-OH)] acids with minor amounts of dodecanoic (12:0) and tetradecanoic (14:0) acids.

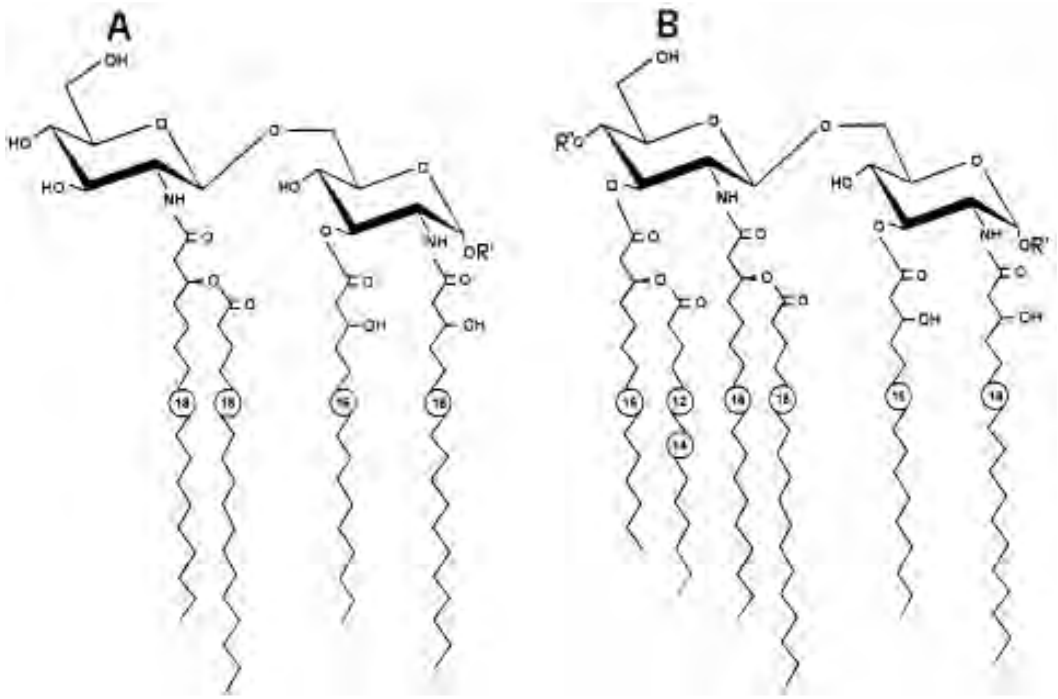

Figure 1.5. Proposed chemical structures of (A) the predominant lipid A molecular structure found in *H. pylori* rough and smooth LPS and (B) a minor lipid A species found only in *H. pylori* smooth LPS. Numbers in circles refer to the number of carbon atoms in acyl chains. Further heterogeneity occurs by nonstoichiometric replacement of 3-(18:0)-*O*-18:0. Polar headgroups are indicated by R' (phosphate or ethanolaminephosphate) and R'' (H or phosphate)[46].

1.3.1. The Core oligosaccharide

The core region is covalently attached through the reducing end of the lipid A by an acid-sensitive ketosidic linkage from 3-deoxy-D-*manno*-octulosonic acid (Kdo), an immutable component of the core, to the *O*-6 of the outer glucosamine unit of lipid A[48]. In *H. pylori* the core region has been found so far to be a conserved region formed by a linear phosphorylated (by a monoester phosphate or by a 2-aminoethylphosphate) backbone, αDGlc*p*-(1→3)-αDGlc*p*-(1→4)-βDGal*p*-(1→7)-DαDHep*p*-(1→2)-LαDHep*p* (1→3)[P/AEP →7]-LαDHepp-(1→5)-Kdo, that is extended by an additional side-branch DαDHep*p* residue appended to the *O*-2 position of the distal of the backbone glycan (Fig.1.6)[48]. A few *H. pylori* core oligossacharides also contain *O*-2 and *O*-6 substituted DDHep units as members of the DDHep side-branch. In some strains also a (1→6)-α-glucan antenna, αDGlc*p*-1-[→6-αDGlc*p*-1]$_n$→, was found to be connected to the *O*-2 site of the side-branch DαDHepp.

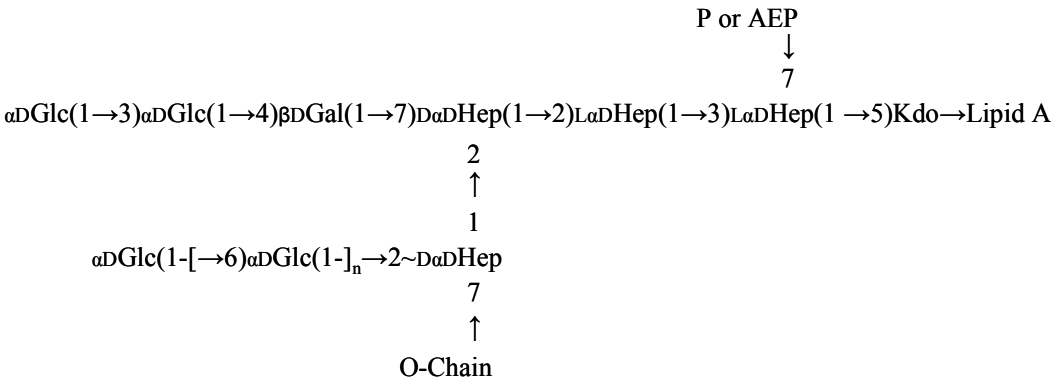

Figure 1.6. *H. pylori* LPS core structure.

1.3.2. The Heptoglycan domain

As mentioned in the beginning of section 1.3, some *H. pylori* strains, namely strain MO19 and those from serogroups O:3 and O:6 have shown to express elongated *3*-substituted D-glycero-α-D-*manno*-Hep*p* oligomers thus forming an heptoglycan domain between the core and the *O*-chain (Fig. 1.7)[52].

O-chain-[→3)DαDHep(1-]$_n$ →6 or 2)DαDHep(1→2 or 6)DαDHep(1→Core

Figure 1.7. Hepoglycan domain in strains MO19 and serogroups O:3 and O:6.

Furthermore, strains isolated from asymptomatic hosts, which were found untypeable using monoclonal antibodies (mAbs) specific for Lewis antigens (Le^x, Le^b, Le^x, or Le^y) commonly expressed in *H. pylori O*-chains, contained instead elongated heptoglycans sometimes capped by an incomplete Lewis antigen[53]. This family of strains also yielded *O-6* substituted DD-Hep as a common component of the inner region of the LPS.

1.3.3. The *O*-chain

Contrarily to the core, whose structure up until now has demonstrated to be conserved, the *O*-antigen chain (*O*-chain) region of *H. pylori* LPS shows considerable variability[48].

In the early stages of *H. pylori* research, Penner et al.[56] developed a serotyping system based on different antigenicity of LPS molecules, which resulted mostly from structural variations in the *O*-antigenic chains and the presence of heptaglycan domains, whereby they defined six distinct *H. pylori* serotypes (O1 to O6). Subsequently, detailed structural[48] and serological[57] studies have shown that the *H. pylori* O-chains are unique in their structure as they express structures homologous to mammalian histo-blood group antigens termed Lewis antigens. Data arising from those studies allowed establishing a correspondence between *O*-chain structures and their serological classification (Fig. 1.8).

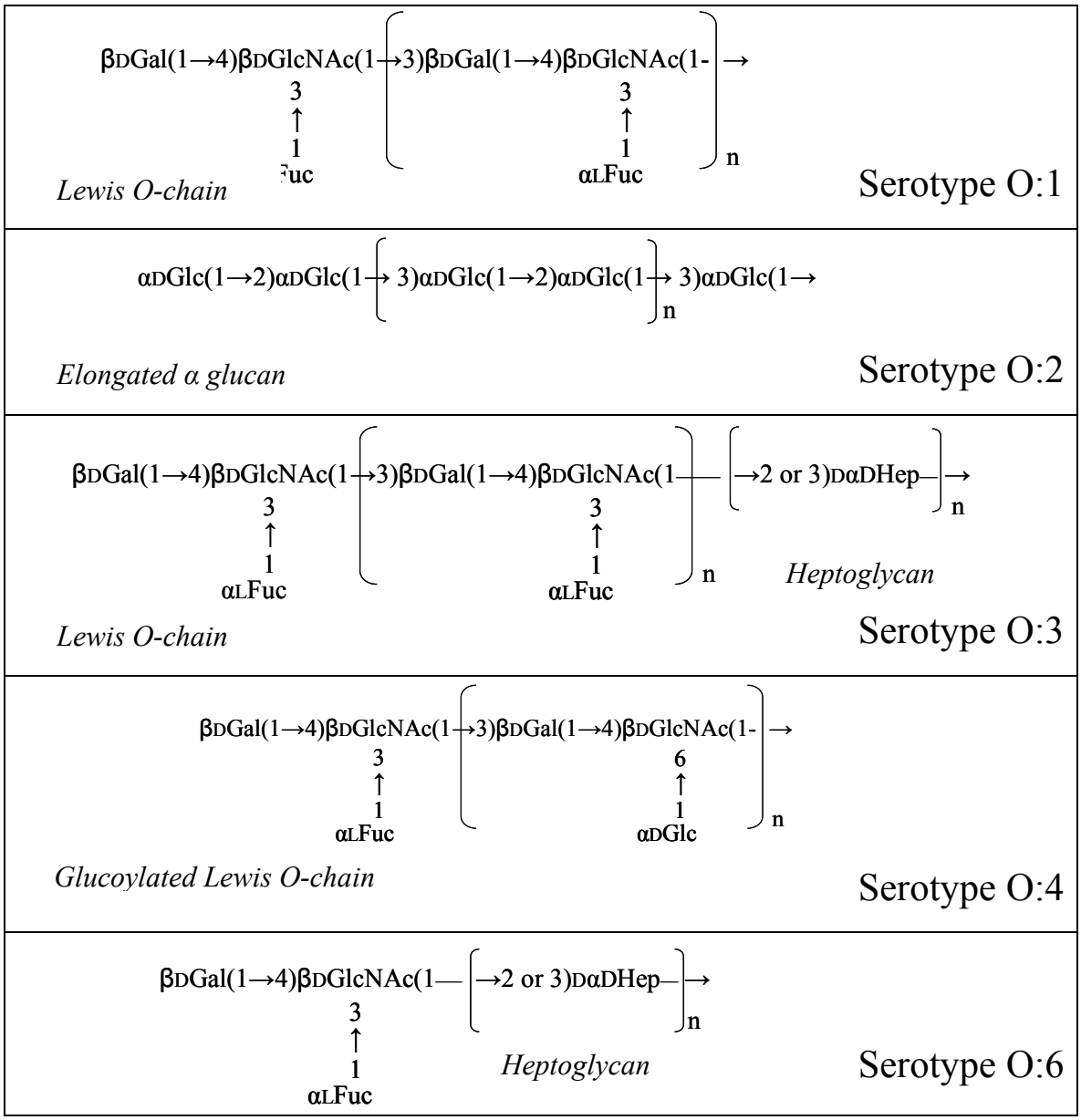

Figure 1.8. Known *O*-chain PS domains for serotypes O:1, O:2, O:3, O:4 and O:6 (adapted from Britton *et al.*[58]).

H. pylori normally expresses *O*-chains exhibiting a poly-LacNAc [→3)-β-D-Gal(1→4)-β-D-GlcNAc(1→] structures decorated with multiple side chains of α-L-Fuc residues forming Type 2 internal Le^x determinants with terminal Type 2 Le^x and Le^y. In some strains additional Type 1 Le^a, Le^b and tumour associated sialyl-Le^x and H-1 determinants, as well as the related blood groups A and B can be also observable in association with Le^x and LacNAc chains[48] (Fig. 1.9).

O-chains comprising typical Type 2 polyLacNAc backbones adorned with branches of α-D-Glc*p* or α-D-Gal*p* linked to the *O*-6 position of the β-D-Gal*p*NAc {→3)-β-D-Gal*p*-(1→4)[α-D-Glc*p* or Gal*p*-(1→6)]-β-D-Glc*p*NAc(1→} were further identified in some strains. Structural studies carried out in *H. pylori* strain UA861 highlighted the presence in the non-reducing end of the galactosylated LPS O-chain of Le^x and Le^y and also of non-fucosylated LacNAc and β-D-Gal*p*NAc [→3)-β-D-Gal*p*-(1→4. A limited number of internal Le^x units were further detected in this galactosyl polyLacNAc chain[48].

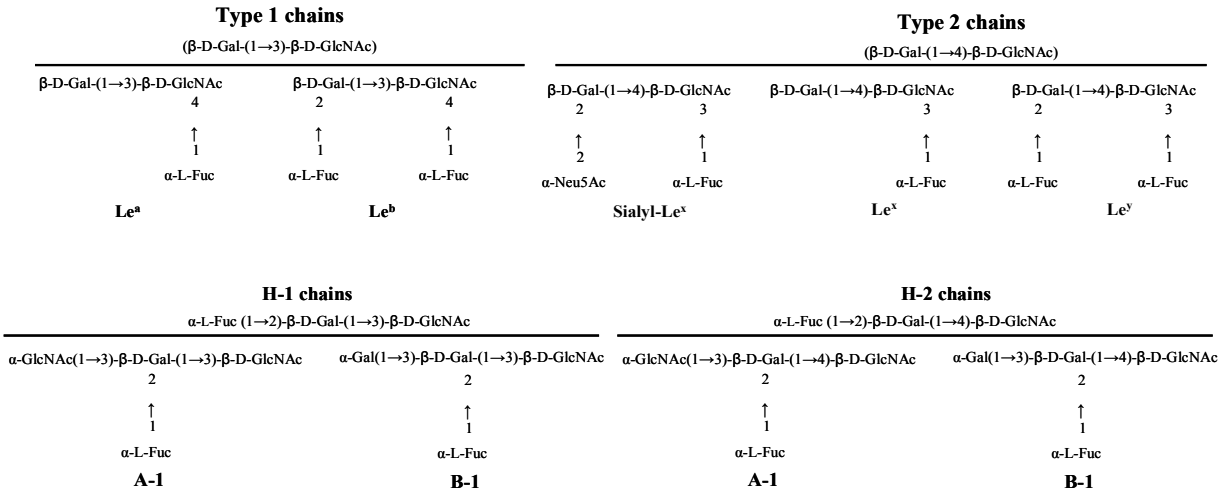

Figure 1.8. Blood group structures found in *H. pylori* LPS *O*-chains.

Frequently incomplete Le antigens are observed implying that the building of Le determinants in *H. pylori* takes place through a sugar-by-sugar addition and not by a block-by-block synthesis, as observed for other enteric bacteria[48].

In addition to the vast diversity of *O*-chain motifs between strains, there is also apparent micro-diversity within a population of cells[59-61]. Such is a consequence of strong phase variation (antigenic variation), a common phenomenon in microorganisms, characterized by a on or off switching in the expression cell surface epitopes such as outer

membrane proteins and LPS. The antigenic variation is most probably beneficial to *H. pylori* during the micro-environmental changes that the bacterium encounters in the course of colonization and persistent infection and as given *H. pylori* a selective advantage in its long history of evolution[62].

1.3.4. Classification of *Helicobacter pylori* LPS into glycotype families

The LPS of *H. pylori* strains share the common characteristic of expressing *O*-chains exhibiting structural homology with human histo-blood group antigens. However, particular fine structural details can be observed to differentiate these LPS molecules. Based on such assumptions, Monteiro[48] proposed a classification to create a systematic grouping of *H. pylori* LPSs that could systematize and aid further investigation (Table 1.1).

Table 1.1. Classification of *H. pylori* LPS into Glycotype families (adapted from Monteiro[49]).

Glycotype (Lewis Type)	Strain	O-Chain[a]	Heptoglycan	Core[b]	(LPS-form)
					Smooth-form LPS
A (Type 2)	NCTC 11 637	Le^x-$[Le^x]_n$		Core	
A	P466	$Le^{x/y}$-$[Le^x]_n$		Core	
		Sialyl-Le^x-$[Le^x]_n$		Core	
A	26695	Le^x-$[Le^x]_n$		Core	
A	J99	$Le^{x/y}$-$[Le^x]_n$		Core	
A	SS1	Le^x-$[Le^x]_n$		Core	
A	AF1,007	$Le^{x/y}$-$[Le^x]_n$		Core	
A	UA1182	$Le^{x/y}$-$[Le^x]_n$		Core	
					Smooth-form LPS
B[c] (Type 2)	O:3	$Le^{x/y}$-$[Le^x]_n$	Heptoglycan		
					Smooth-form LPS
C[d]	MO19	$Le^{y\pm}$	Heptoglycan	Core	
C[d]	1C2, 12C2	$(Fuc, GlcNAc)^{\pm}$	Heptoglycan	Core	
	62C, 7A, 15A		Heptoglycan	Core	
	77C, PJ1		Heptoglycan	Core	
C	O:6	$Le^{y\pm}$	Heptoglycan	Core	
					Smooth-form LPS
D[e] (Type 2)	UA861, O:4	$[LacNAc\text{-}\alpha Glc]_n$		Core	
					Smooth-form LPS
E[e](Type 2)	471	$LacNAc\text{-}\alpha Glc]_n$		Core	

Glycotype (Lewis Type)	Strain	O-Chain[a]	Heptoglycan	Core[b]	(LPS-form)
					Smooth-form LPS
F(Type 1 and 2)	UA948	$Le^{a/x}$-$[Le^{x}]_{n}$		Core	
F	UA955	$Le^{dis/x/y}$-$[Le^{x}]_{n}$		Core	
F	J223	$Le^{c/d}$~$[LacNAc]_{n}$		Core	
F	NCTC 11 637	$Le^{d/x/y}$-Le^{x}		Core	
F	R-7A/H608	Type 1 A blood-group-LacNAc		Core	
F				Core	
					Semi rough-rough LPS
G (Type 1 and 2)	26695	$Le^{dis/x/y}$		Core	
		Fuc-1→3-Fuc-1→4-GlcNAc		Core	
		GlcNAc-1→3-Fuc			
		Linear B blood-group		Core	
G	SS1	Le^{y}		Core	
		Fuc-1→3-Fuc-1→4-GlcNAc		Core	
		Linear B blood-group		Core	
G	F-15A	$Le^{a/y}$		Core	
		Fuc-1→3-Fuc-1→4-GlcNAc		Core	
		Linear B blood-group		Core	
G	CA6	$Le^{a/x}$		Core	
					Semi rough-form LPS
H (Type 1)	UA915	$Le^{b/d}$		Core	
H	UA1111	Le^{b}		Core	
H	F-58C	Le^{a}		Core	
		Linear B blood-group		Core	
H	R-58A	Le^{a}		Core	

Glycotype (Lewis Type)	Strain	O-Chain[a]	Heptoglycan	Core[b]	(LPS-form)
I		H. pylori strains not expressing histo-blood group LPS molecules			Smooth-form LPS
J	O2	[→2)-α-D-Glc*p*-(1→3)-α-D-Glc*p*-(1→]$_n$ Fuc-1→3-Fuc-1→4-GlcNAc Linear B blood group			

[a]The Le^x elongated O-chains also contain randomly placed LacNAc units.
[b]All cores share a similar structure. However, the inner most ld-Hep unit may either carry a monoester phosphate or a 2-aminoethyl phosphate at position O-7.
[c]The solidus (/) indicates that either structure is possible.
dFound in asymptomatic hosts.
[e]The a-D-Glc and a-D-Gal side chains are attached to the O-6 position of the GlcNAc. The UA861 O-antigen chain also expresses one internal Le^x. The 471 LPS also contains O-3 fucosylated GlcNAc unit

1.3.5. Role of Le antigens in *H. pylori* pathogenesis

H. pylori cell-surface glycans and in particular Le antigens are active actors in the microbe-host interplay. They influence bacterial colonization and adhesion and have an active role in the establishment and persistence of infection and evasion of the immune responses[63]. Also, as chronic infection progresses, Le antigens have also been suggested to contribute to gastric autoimmunity that leads to gastric atrophy, a precursor state of gastric cancer[63].

Le phenotypes and gastric adaptation

In the human stomach, Le^a and Le^b are mainly expressed on the surface of foveolar epithelia, whereas Le^x and Le^y are expressed predominantly by the mucus, chief and parietal cell of the gastric glands[64]. Thus, a variety of Le antigens are expressed within the ecological niche of *H. pylori*. Based on the recognition of Le antigen expression both by *H. pylori* and by the gastric mucosa, it has been purposed that bacterial molecular mimicry could be part of a long-term survival strategy[65,66]. This camouflage would allow *H. pylori* an escape from humoral response by preventing the formation of antibacterial antibodies because of cross-reaction with the host[63,65,66]. Therefore, selective pressure from the host is thought to have great influence in the establishment of a given *H. pylori* phenotype[65].

Of note is the fact that *H. pylori* strains expressing Le^x and those expressing Le^y can be isolated from the same host[67] and that extensive diversity in expression of Le^x and Le^y in *H. pylori O*-chains can occur overtime and in different regions of the human stomach[59]. Furthermore, simultaneous expression of Le^x and Le^y by one strain can also occur[48] as well as strains expressing both type 1 and type 2 Le determinants[48]. Moreover, genetic modification have been detected in *H. pylori* FucT genes that could be attributable to recombination events within and between genes resulting in genetic diversity that together with phase variation contributes to divergent LPS expression within an *H. pylori* community[68]. This reflects an ability and potential of the bacterium to adapt to different microniches and environmental conditions within the human stomach[63]. Thus, a combination of several factors might contribute to the observed diversity[63], namely a selective pressure from the host, strong phase variation and genetic exchange by the bacteria[62,69,70], and environmental pressures such as pH[71] and availability of certain micronutrients such as iron[72] within the gastric niche.

Role in adhesion

Le^x in the *O*-chains has been shown to mediate *H. pylori* adhesion to the human antral gastric mucosa[73] by interaction with the gastric receptor galectin-3[74], a galactose-binding lectin. It is also known that strains with high Le^x expression exhibit higher colonization densities[75]. By assisting bacterial adhesion and interaction with the gastric mucosa, the expression of Le^x may enhance the delivery of secreted products into the gastric mucosa, thus promoting the development of gastric malignancies[76,77].

Noteworthy is the influence that pH gradients between the luminal side of the gastric mucus layer (pH ~2) and the surface of gastric cells (pH 7) may exert in *H. pylori* adhesion[63]. Le^x expression by *H. pylori* was found optimal at neutral pH and reduced at lower pH like the one observed in the mucus layer. By modulating expression of Le^x, pH promotes free-swimming *H. pylori* in the mucus layer and adhesion at the epithelial cell-surface[63]. Potentially, these bacteria in the mucus layer can act as a reservoir for continuous infection of the mucosa[63].

Influence in colonization

H. pylori wild type strains and mutants lacking the ability to express *O*-chains and Le^x epitopes exhibit a significant decrease in the capability of colonizing mice[62], thus suggesting its key role in human colonization. Furthermore, knock-out in the expression of GDP-D-mannose pyrophosphorylase required for GDP-fucose synthesis thus resulting in a fucose-lacking *O*-chain (*i*-antigen) retrieved reduced mouse colonization and ablated interaction with the human gastric mucosa *in situ*[78]. However, some controversy still stands as far as upon the dependence of Le blood group expression to guarantee a successful colonization. Reports have been presented of clinical isolates from asymptomatic hosts lacking Lewis *O*-chains and expressing either elongated heptoglycans[48] or α-(1→6) glucans that were able to colonize mice[79]. Such evidences suggest that the presence of Lewis *O*-chain, even though not absolutely required for colonization, might result in the incapability of cells to induce significant pathology. Such phenomena might arise from the inability in adhering to human receptor cells and/or the presence of elongated heptoglycans may prevent exposure of disease-causing bacterial cell-surface molecules[48].

Modulation of immune responses

In order to evade immune recognition, several variants often arise within a bacterial cell population with modifications in cell-surface glycosylations, especially at the *O*-chain level[80].

H. pylori have been recognized to interact with surfactant protein D (SP-D), a lectin involved in antibody-independent pathogen recognition and elimination[81]. SP-D binds with *H. pylori O*-chain moiety resulting in bacterial immobilization and aggregation[80]. Also, there are reports demonstrating that *H. pylori* infection is more common in the absence of SP-D[81,82], emphasizing an important influence of SP-D binding on the establishment of infection.

Strain-to-strain and especially inner strain variability resulting from strong phase variation can also modulate interaction with gastric dentric cells[83-85]. The existence of Le-negative variants within a population allows escaping binding to dentric cells and induces a strong Th1 cell response[84]. On the other hand, strains in the same population expressing Le^x/Le^y bind dentric cells and enhance the production of IL-10 production, thus promoting Th2-cell response and blocks Th1-cell activation[84], resulting in a mixed Th1/Th2-cell response[83]. The modulation of the host response allows a switch from an acute infection response to one that supports development of chronic infection since humoral response and antibody production are not associated with *H. pylori* eradication and protection[63,85].

It has also been advanced that upon prolonged *H. pylori* infection the patients might develop autoimmune responses leading to gastric damage[63]. These observations were backed by several studies describing the existence of anti-Le^x and anti-Le^y antibodies in the sera of host with acute prolonged infections[86-88].

1.3.6. *H. pylori* Lewis expression and human geographical distribution

LPS from *H. pylori* isolated so far from North American and European populations predominantly express Type 2 Le^x and Le^y blood group epitopes[89]; conversely the expression of Type 1 chains among those populations is relatively rare[89]. In Latin America the Type 1 (but only Le^b) was found dominant[90], whereas in Asia, the prevalence rate of Type 1 can be up to 35% and both Le^a and Le^b can exist. It has been purposed that such differences arise from adaptation of *H. pylori* to the host Lewis phenotype. Furthermore, it has been demonstrated that *H. pylori* is submitted to selective pressure to express certain

types of LPS phenotypes[68]. Thus, the milieu in a host will select for bacterial variants with particular characteristics that facilitate adaptation and survival in the gastric mucosa of that individual, and will shape the bacterial community structure. Following these considerations, it has been purposed that, Type 1 or 2 Lewis antigens from *H. pylori* isolates can be used as potential markers for identifying the geographical distribution in the worldwide human population.

Moreover, since Lewis antigens of *H. pylori* are regarded as virulence factors facilitating colonization or inflammation, the selection of vaccine targeting the Lewis antigens will be different for patients from different geographical populations. However, further and broader studies are yet to be conducted until a trustful correlation can be established.

1.3.7. *H. pylori* unusual cell-surface glycosides

In addition to LPS there have been reports of the production of other cell-surface glycans by *H. pylori*. Kocharova *et al.*[91] described the expression of an unusual polysaccharide containing D-rhamnose (D-Rha), L-rhamnose (L-Rha) and 3-C-methyl-D-mannose (D-Man3CMe), a sugar that up until then had never been observed in nature. The mentioned polysaccharide was composed by the following trisaccharide repeating unit: →2)-α-D-Manp3CMe-(1→3)-α-L-Rha*p*-(1→3)-α-D-Rha*p*-(1→ and was isolated from three Danish strains (D1, D3 and D6) found nontypeable using a variety of anti-Lewis and anti-blood-group monoclonal antibodies.

In addition, Monteiro et al.[92] described an immunogenic formulation against *H. pylori* comprising a highly branched polymeric mannan formed by trisaccharide repeating units composed of terminal, *O*-2 and *O*-2,6 α-D-Man residues. This polysaccharide was isolated from *H. pylori* mutant strain NCTC 11637 *pgm* having a knock-out of the phosphomannomutase gene.

1.4. Aims of the thesis

The work that is being carried out by Professor Monteiro over the past ten years has clarified and brought into the spotlight several structural characteristics of *H. pylori* LPS isolated from a broad range of strains and clinical isolates. As discussed in section 1.3 cell-surface glycans, and particularly Le antigens, have shown to be important legislators in the host-*H. pylori* interactions[63]. However, *H. pylori O*-chains often co-express trace amounts of isomeric Le determinants making their analysis challenging from the analytical point of view. Therefore, in this thesis attention is devoted to the establishment of analytical basis for the distinction of isomeric Le determinants relying on the capability of ESI-MS techniques to detect trace amounts of biological samples.

Awareness of the biological implications of cell-surface sugars and their potential as therapeutic agents, namely as carbohydrate vaccines, the objective of this thesis is also to extend the current knowledge on the chemical structure of *H. pylori* glycans. Studies were carried out in *H. pylori* clinical isolates from Portuguese patients previously characterized in relation to their virulence profile. Special attention was devoted to the search and structural characterization of new cell-surface glycans (LPS, CPS/EPS, and glycoproteins) and their possible implication in the interaction with the human reservoir in pathology. The impact of *in vitro* growth in routinely used solid medium Columbia blood agar (CBA)[93] and Ham's F12[94] liquid medium in the definition of *H. pylori* cell-surface glycan phenotypes was also evaluated. This knowledge will allow new insights on the influence of environmental pressures outside the human reservoir in the definition of *H. pylori* surface.

REFERENCES

1. Kusters, J.G.; van Vliet, A.H.M.; Kuipers, E.J.; Pathogenesis of *Helicobacter pylori* infection. Clin. Microbiol. Rev. **2006**. 19: 449-490.
2. Warren, J.R.; Marshall, B.J. Unidentified curved bacilli on gastric epithelium in active chronic gastritis. Lancet. **1983**. 1: 1273-1275.
3. Warren, J.R.; Marshall, B.J. Unidentified curved bacilli in the stomach of patients with gastritis and peptic ulceration. Lancet. **1984**. 323: 1311-1315
4. NIH Consensus Conference *Helicobacter pylori* in peptic ulcer disease, NIH Consensus Development Panel on *Helicobacter pylor*i in peptic ulcer disease. J.A.M.A. **1994**. 272: 65-69.
5. Olson, J.W.; Maier, R.J. Molecular hydrogen as an energy source for *Helicobacter pylori*. Science. **2002** 298: 1788-90.
6. Stark, R.M.; Gerwig, G.J.; Pitman, R.S. Biofilm formation by *Helicobacter pylori*. Lett. Appl. Microbiol. **1999**. 28: 121-126.
7. Carron, M.A.; Tran, V.R.; Sugawa, C.; Coticchia, J.M. Identification of *Helicobacter pylori* biofilms in human gastric mucosa. J. Gastrointest. Surg. **2006**. 10: 712-717
8. Chan, W.Y.; Hui, P.K.; Leung, K.M.; Chow, J.; Kwok, F.; Ng, C.S. Coccoid forms of *Helicobacter pylori* in the human stomach. Am. J. Clin. Pathol. **1994**. 102: 503-507.
9. Azevedo, N.F.; Huntington, J.; Goodman, K.J. The epidemiology of *Helicobacter pylori* and public health implications. Helicobacter. **2009**. 14:1-7.
10. Liu, Z.F.; Chen, C.Y.; Tang, W.; Zhang, J.Y.; Gong, Y.Q.; Jia, J.H. Gene-expression profiles in gastric epithelial cells stimulated with spiral and coccoid *Helicobacter pylori*. J. Med. Microbiol. **2006**. 55 1009-1015.
11. Tsutsumi Y. Department of Pathology Fujita Health University School of Medicine (Toyoake, Japan). web: http://info.fujita-hu.ac.jp/~tsutsumi/photo/photo002-6.htm.
12. Josenhans, C.; Eaton, K.A.; Thevenot, T.; Suerbaum, S. Switching of flagellar motility in *Helicobacter pylori* by reversible length variation of a short homopolymeric sequence repeat in fliP, a gene encoding a basal body protein. Infect. Immun. **2000**. 68: 4598-4603.
13. Blaser, M.J.; Atherton, J.C. *Helicobacter pylori* persistence: biology and disease. J. Clin. Investig. **2004**. 113: 321-333.

14. Yamaoka Y. *Helicobacter pylori* typing as a tool for tracking human migration. Clin Microbiol Infect. **2009**. 15(9): 829-34.

15. Stingl, K.; Altendorf, K.; Bakker, E.P. Acid survival of *Helicobacter pylori*: how does urease activity trigger cytoplasmic pH homeostasis? Trends Microbiol. **2002**. 10: 70-74.

16. Bury-Moné, S.; Skouloubris, S.; Dauga, C.; Thiberge, J.M.; Dailidiene, D.; Berg, D.E.; Labigne. A.; De Reuse, H. Presence of active aliphatic amidases in Helicobacter species able to colonize the stomach. Infect Immun. 2003. 71:5613-5622.

17. Anderson, L.P.; Wadstrom, T.. Basic bacteriology and culture. In: Hazell, S.L. (Eds.) *Helicobacter pylori*: physiology and genetics. ASM press (Washington D.C., U.S.A.) **2001**. 27-38.

18. Andersen, LP. Colonization and infection by *Helicobacter pylori* in humans. Helicobacter. **2007**. 2: 12-15.

1. Yamaoka Y. Roles of *Helicobacter pylori* BabA in gastroduodenal pathogenesis. World J. Gastroenterol. **2008**. 14: 4265-4272.

19. Maeda, S.; Mentis, A.. Pathogenesis of *Helicobacter pylori* infection. Helicobacter. **2007**. 12:10-14.

20. Dubois, A.; Fiala, N.; Heman-Ackah, L.M.; Drazek, E.S.; Tarnawski, A.; Fishbein, W.N.; Perez-Perez, G.I.; Blaser. M.J. Natural gastric infection with *Helicobacter pylori* in monkeys: a model for spiral bacteria infection in humans. Gastroenterology. **1994**. 106 1405-1417.

21. Fox, J.G.; Batchelder, M.; Marini, R.; Yan, L.; Handt, L.; Li, X.; Shames, B.; Hayward, A.; Campbell, J.; Murphy, J.C. *Helicobacter pylori* induced gastritis in the domestic cat. Infect. Immun. **1995**. 63: 2674-2681.

22. Pounder, R.E.; Ng, D.. The prevalence of *Helicobacter pylori* infection in different countries. Aliment. Pharmacol. Ther. **1995**. 9: 33-9.

23. Taylor, D.N.; Parsonnet, J. Epidemiology and natural history of *H. pylori* infections, In: Blaser, M.J.; Smith, P.F.; Ravdin, J.; Greenberg, H.; Guerrant, R.L. (Eds.) Infections of the gastrointestinal tract. Raven Press (New York, U.S.A.). **1995**. 551-564

24. Perez-Perez, G.I.; Rothenbacher, D.; Brenner. H. Epidemiology of *Helicobacter pylori* Infection. Helicobacter. **2004**. 9: 1-6

25. Dunn, B.E.; Cohen, H.; Blaser, M.J.. *Helicobacter pylori*, Clin. Microbiol. Rev. **1997**. 10 720-741.

26. Malaty, H.M. Epidemiology of *Helicobacter pylori* infection. Best Pract. Res. Clin. Gastroenterol. **2007**. 21: 205-214.

27. Mégraud, F. Transmission of *Helicobacter pylori*: faecal-oral versus oral-oral route. Aliment. Pharmacol. Ther. **1995**. 9: 85-91.

28. Cave, D.R. Transmission and epidemiology of *Helicobacter pylori*. Am. J. Med. **1996**. 100: 12S–17S.

29. Brown, L.M., *Helicobacter pylori*: epidemiology and routes of transmission. Epidemiol. Rev. **2000**. 22: 283-297.

30. Parsonnet, J.; Hansen, S.; Rodriguez, L.; Gelb, A.B.; Warnke, R.A.; Jellum, E.; Orentreich, N.; Vogelman, J.H.; Friedman, G.D. *Helicobacter pylori* infection and gastric lymphoma. N. Engl. J. Med. **1994**. 330: 1267-1271.

31. Eidt, S.; Stolte, M.; Fischer, R.. *Helicobacter pylori* gastritis and primary gastric non-Hodgkin's lymphomas. J. Clin. Pathol. **1994**. 47: 436-439.

32. Wotherspoon, A.C.; Ortiz-Hidalgo, C.; Falzon, M.R.; Isaacson, P.G.. *Helicobacter pylori*-associated gastritis and primary B-cell gastric lymphoma. Lancet. **1991**. 338: 1175-1176.

33. Bayerdorffer, E.; Neubauer, A.; Rudolph, B.; Thiede, C.; Lehn, N.; Eidt, S.; Stolte, M.. Regression of primary gastric lymphoma of mucosa-associated lymphoid tissue type after cure of *Helicobacter pylori* infection. Lancet. **1995**. 345: 1591-1594.

34. Walt, R.P.. Regression of MALT lymphoma and treatment for *Helicobacter pylori*. Lancet. **1996**. 348: 1041-1042.

35. Wotherspoon, A.C.; Doglioni, C.; Diss, T.C.; Pan, L.; Moschini, A.; De Boni, M.; Isaacson, P.G.. Regression of primary low-grade B-cell gastric lymphoma of mucosa-associated lymphoid tissue type after eradication of *Helicobacter pylori*. Lancet. **1993**. 342: 575-577.

36. Koch, A.L. The biophysics of the Gram-negative periplasmic space. Crit. Rev. Microbiol. **1998**. 24: 23-59.

37. Silipo, A.; Molinaro, A.; De Castro, C.; Ferrara, R.; Romano, I.; Nicolaus, B.; Lanzetta, R.; Parrilli, M. Structural Analysis of a novel polysaccharide of the

lipopolysaccharide-deficient extremophile Gram-negative bacterium *Thermus thermophilus* HB8. European J .Org. Chem. **2004**. 24: 504 -5054

38. Arredondo, R; García, A; Jerez, CA. Partial removal of lipopolysaccharide from *Thiobacillus ferrooxidans* affects its adhesion to solids. Appl Environ Microbiol. **1994**. 60: 2846-2851.
39. Koch, A.L.; Woeste, S.W. The elasticity of the sacculus of *Escherichia coli*. J. Bacteriol. **1992**. 174: 4811-4819.
40. Beveridge, T.J.. Structures of Gram-negative cell walls and their derived membrane vesicles. J. Bacteriol. **1999**. 181: 4725-4733.
41. Huanga, K.C.; Mukhopadhyay, R.; Wena, B.; Gitaia, Z.; Wingreena, N.S.. Cell shape and cell-wall organization in Gram-negative bacteria. PNAS. **2008**. 105 19282-19287.
42. Holst, O.; Moran, A.P; Brennan, B.J. Overview of the glycosylated components of the bacterial cell envelope. In: Moran, A.P. (Eds.) Microbial Glicobiology. Academic Press (London, U.K.) **2009**. 3-53
43. Erridge, C.; Bennett-Guerrero, E.; Poxton, I.R.. Structure and function of lipopolysaccharides. Microbes Infect. **2002**. 4: 837-851.
44. Rietschel, E.T.; Brade, H. Bacterial endotoxins. Sci. Am. *1992*. 267: 54-61.
45. Moran, A.P. Molecular structure, biosynthesis, and pathogenic roles of Lipopolysaccharides. In: Harry, L.; Mobley, T.; Mendz, G.L.; Stuart, L. Hazell (Eds.) *Helicobacter pylori*: Physiology and Genetics. ASM Press (Washington D.C., U.S.A.) **2001**. 81-96.
46. Caroff, M.; Karibian, D. Structure of bacterial lipopolysaccharides. Carbohydr. Res. **2003**: 338 2431-2447
47. Monteiro, M.A.. *Helicobacter pylori*: a wolf in sheep's clothing: the glycotype families of *Helicobacter pylori* lipopolysaccharides expressing histo-blood groups: structure, biosynthesis, and role in pathogenesis. Adv. Carbohydr. Chem. Biochem. **2001**. 57: 99-158.
48. Muotiala, A.; Helander, I.M.; Pyhala, L.; Kosunen, T.U.; Moran, A.P. Low biological activity of *Helicobacter pylori* lipopolysaccharide. Infect. Immun. **1992**. 60: 1714-1716.

49. Walsh, E.J.; Moran, A.P.. Influence of medium composition on the growth and antigen expression of *Helicobacter pylori*. J. Appl. Microbiol. **1997**. 83: 67-75.

50. Moran, A.P.; Knirel, Y.A.; Senchenkova, S.N.; Widmalm, G.; Hynes, S.O.; Jansson, P.E. Phenotypic variation in molecular mimicry between *Helicobacter pylori* lipopolysaccharides and human gastric epithelial cell surface glycoforms. Acid-induced phase variation in Lewis x and Lewis y expression by *H. pylori* lipopolysaccharides. J. Biol. Chem. **2002**. 277: 5785-5795

51. Aspinall, G.O.; Monteiro, M.A.; Shaver, R.T.; Kurjanczyk, L.A.; Penner, J.L.. Lipopolysaccharides of *Helicobacter pylori* serogroups O:3 and O:6: Structures of a class of lipopolysaccharides with reference to the location of oligomeric units of D-glycero-D-manno-Heptose residues. Eur. J. Biochem. **1997**. 248 592-601.

52. Monteiro, M.A.; Michael, F.St.; Rasko, D.A.; Taylor, D.E.; Conlan, J.W.; Chan, K.H.; Logan, S.M.; Appelmelk, B.J.; Perry, M.B.. *Helicobacter pylori* from asymptomatic hosts expressing heptoglycan but lacking Lewis *O*-chains: Lewis blood-group *O*-chains may play a role in *Helicobacter pylori* induced pathology. Biochem. Cell Biol. **2001.** 79: 449-459.

53. Monteiro, M.A.; Appelmelk, B.J.; Rasko, D.A.; Moran, A.P.; Hynes, S.O.; MacLean, L.L.; Chan, K.H.; St. Michael, F.; Logan, S.M.; O'Rourke, J.; Lee, A.; Taylor, D.E.; Perry, M.B. Lipopolysaccharide structures of *Helicobacter pylori* genomic strains 26695 and J99, mouse model H. pylori Sydney strain, *H. pylori* P466 carrying sialyl Lewis X, and *H. pylori* UA915 expressing Lewis B. Classification of *H. pylori* lipopolysaccharides into glycotype families. Eur. J. Biochem. **2000**. 267: 305-320.

54. Moran, A.P.; Lindner, B.; Walsh, E.J. Structural characterization of the lipid A component of *Helicobacter pylori* rough- and smooth-form lipopolysaccharides. J. Bacteriol. **1997**. Vol. 179: 6453-6463.

55. Mills, S.D., L.A. Kurjanczyk, J.L. Penner, Antigenicity of Helicobacter pylori lipopolysaccharides. J. Clin. Microbiol. **1992**. 30: 3175-3180.

56. Simoons-Smit, I.M.; Appelmelk, B.J; Verboom, T.; Negrini, R.; Penner, J.L.; Aspinall, G.O.; Moran, A.P.; Fei, S.F.; Shi, B.S.; Rudnica, W.; Savio, A.; de Graaff, J.. Typing of *Helicobacter pylori* with monoclonal antibodies against Lewis antigens in lipopolysaccharide. J. Clin. Microbiol. **1996**. 342196-2200.

57. Britton, S.; Papp-Szabo, E.; Simala-Grant, J.; Morrison, L.; Taylor, D.E.; Monteiro, M.A. A novel *Helicobacter pylori* cell-surface polysaccharide. Carbohydr. Res. **2005**. 340: 1605-1611.

58. Nilsson, C.; Skoglund, A.; Moran, A.P.; Annuk, H.; Engstrand, L.; Normark, S. . An enzymatic ruler modulates Lewis antigen glycosylation of *Helicobacter pylori* LPS during persistent infection. Proc. Natl. Acad. Sci. U.S.A. **2006**. 103: 2863-2868.

59. Appelmelk, B.J.; Shiberu, B.; Trinks, C.; Tapsi, N.; Zheng, P.Y. Phase variation in *Helicobacter pylori* lipopolysaccharide. Infect. Immun. **1998**. 66: 70-76

60. Wirth, H.P.; Yang, M.; Peek, R.M.J.; Hoök-Nikanne, J.; Fried, M.; Blaser, M.J. Phenotypic diversity in Lewis expression of *Helicobacter pylori* isolates from the same host. J. Lab. Clin. Med. **1999**. 133: 488-500.

61. Moran, A.P. Relevance of fucosylation and Lewis antigen expression in the bacterial gastroduodenal pathogen *Helicobacter pylori*. Carbohydr. Res. **2008**. 343: 1952-1965.

62. Moran, A.P. Molecular mimicry of host glycosylated structures by bacteria. In: Moran, A.P. (Eds.) Microbial Glicobiology. Academic Press (London, U.K.) 2009. 847-869.

63. Kobayashi, K.; Sakamoto, J.; Kito, T.; Yamamura, Y.; Koshikawa, T.; Fujita, M.; Watanabe, T.; Nakazato, H. Lewis blood group-related antigen expression in normal gastric epithelium, intestinal metaplasia, gastric adenoma, and gastric carcinoma. Am. J. Gastroenterol. **1993**. 88: 919-924.

64. Wirth, H.P.; Yang, M.; Peek, R.M.; Tham, K.T.; Blaser, M.J.. *Helicobacter pylori* Lewis expression is related to the host Lewis phenotype. Gastroenterology. **1997**. 113: 1091-1098.

65. Appelmelk, B.J.; Faller, G.; Claeys, D.; Kirchner, T.; Vandenbroucke-Grauls, C.M.J.E. Bugs on trial: the case of *Helicobacter pylori* and autoimmunity. Immunol. Today. **1998**. 19: 296-299.

66. Wirth, H.P.; Yang, M.; Peek, R.M.; Tham, K.T.; Blaser, M.J. *Helicobacter pylori* Lewis expression is related to the host Lewis phenotype. Gastroenterology. **1997**. 113: 1091-1098.

67. Nilsson, C.; Skoglund, A.; Moran, A.P.; Annuk, H.; Engstrand, L.; Normark, S. Lipopolysaccharide diversity evolving in *Helicobacter pylori* communities through genetic modifications in fucosyltransferases. PLoS ONE. **2008**. 3: 1-14.

68. Appelmelk, B.J.; Martin, S.L.; Monteiro, M.A., Clayton, C.A.; McColm, A.A.; Zheng, P.; Verboom, T.; Maaskant, J.J.; van den Eijnden, D.H.; Hokke, C.H.; Perry, M.B.; Vandenbroucke-Grauls, CM.; Kusters, J.G. Phase variation in *Helicobacter pylori* lipopolysaccharide due to changes in the lengths of poly(C) tracts in α-3-fucosyltransferase genes. Infect. Immun. **1999**. 67: 5361-5366.

69. Ma, B.; Simala-Grant, J.L.; Taylor, D.E. Fucosylation in prokaryotes and eukaryotes. Glycobiology. **2006.** 16: 158R-184R.

70. Moran, A.P.;BKnirel, Y.A.;Senchenkova, S.N.; Widmalm, G.; Hynes, S.O.; Jansson, P.-E. Phenotypic variation in molecular mimicry between *Helicobacter pylori* lipopolysaccharides and human gastric epithelial cell surface glycoforms. Acid-induced phase variation in Lewis x and Lewis y expression by *H. pylori* lipopolysaccharides. J. Biol. Chem. **2002**. 277: 5785-5795.

71. Keenan, J.I.; Davis, K.A.; Beaugie, C.R.; McGovern, J.J.; Moran, A.P. Alterations in *Helicobacter pylori* outer membrane and outer membrane vesicle-associated lipopolysaccharides under iron-limiting growth conditions. Innate Immun. **2008**. 14: 279-290.

72. Edwards, N.J.; Monteiro, M.A.; Faller, G.; Walsh, E.J.; Moran, A.P.; Roberts, I.S.; High, N.J. Lewis x structures in the *O*-ntigen side-chain promote adhesion of *Helicobacter pylori* to the gastric epithelium. Mol. Microbiol. **2000.** 35: 1530-1539.

73. Fowler, M.; Thomas, R.J.; Atherton, J.; Roberts, I.S.; High, N.J.; Galectin-3 binds to *Helicobacter pylori O*-antigen: it is upregulated and rapidly secreted by gastric epithelial cells in response to *H. pylori* adhesion. Cell. Microbiol. **2006**. 8: 44-54.

74. Heneghan, M.A.; McCarthy, C.F.; Janulaityte, D.; Moran, A.P. Relationship of anti-Lewis x and anti-Lewis y antibodies in serum samples from gastric cancer and chronic gastritis patients to *Helicobacter pylori*-mediated autoimmunity. Infect. Immun. **2001**. 69: 4774-4781.

75. Rieder, G.; Hatz, R.A.; Moran, A.P.; Walz, A.; Stolte, M.; Enders, G. Role of adherence in interleukin-8 induction in *Helicobacter pylori*-assisted gastritis. Infect. Immun. **1997**. 65: 3622-3630.

76. Moran, A.P. *Helicobacter pylori* lipopolysaccharides mediate gastric and extragastric pathology. J. Physiol. Pharmacol. **1999**. 50: 787-805.

77. Moran, A.P.; Sturegård, E.; Sjunnesson, H.; Wadström, T.; Hynes, S.O. The relationship between *O*-chain expression and colonisation ability of *Helicobacter pylori* in a mouse model. FEMS Immunol. Med. Microbiol. **2000**. 29: 263-270.

78. Altman, E.; Smirnova, N.; Li, J.; Aubry, A.; Logan, S.M. Occurrence of a nontypable *Helicobacter pylori* strain lacking Lewis blood group *O*-antigens and DD-heptoglycan: evidence for the role of the core a1,6-glucan chain in colonization. Glycobiology. **2003**. 13: 777-783.

79. Khamri, W., Moran, A.P., Worku, M.L., Karim, Q.N.; Walker, M.M.; Annuk, H.; Ferris, J.A.; Appelmelk, B.J.; Eggleton, P.; Reid, K.B.; Thursz, M.R. Variations in *Helicobacter pylori* lipopolysaccharide to evade the innate immune component surfactant protein D. Infect. Immun. **2005**. 73, 7677–7686.

80. Moran, A.P.; Kharmi, W.; Walker, M.M.; Thursz, M.R. Role of surfactant protein D (SP-D) in innate immunity in the gastric mucosa: evidence of interaction with Helicobacter pylori lipopolysaccharide. J. Endotoxin Res. **2005**. 11: 357-362.

81. Khamri, W.; Worku, M.L.; Anderson, A.E., Walker, M.M.; Hawgood, S.; Reid, K.B.; Clark, H.W.; Thursz, M.R. *Helicobacter* infection in the surfactant protein D-deficient mouse. Helicobacter. **2007.** 12, 112–123.

82. Bergman, M.; Del Prete, G.; van Kooyk, Y.; Appelmelk, B. *Helicobacter pylori* phase variation, immune modulation and gastric autoimmunity. Nat. Rev. Microbiol. **2006**. 4: 151-159.

83. Bergman, M.P.; Engering, A.; Smits, H.H., van Vliet, S.J.; van Bodegraven, A.A.; Wirth, H.P.; Kapsenberg, M.L.; Vandenbroucke-Grauls, C.M.; van Kooyk, Y.; Appelmelk, B.J. *Helicobacter pylori* modulates the T helper cell 1/T helper cell 2 balance through phase-variable interaction between lipopolysaccharide and DC-SIGN. J. Exp. Med. **2004**. 200: 979-990.

84. O'Keeffe, J.; Moran, A.P. Conventional, regulatory and unconventional T-cells in the immunological response to *Helicobacter pylori*. Helicobacter **2008**. 13: 1-19.

85. Appelmelk, B.J.; Simoons-Smit, I.; Negrini, R.; Moran, A.P.; Aspinall, G.O.; Forte, J.G.; De Vries, T.; Quan, H.; Verboom, T.; Maaskant, J.J.; Ghiara, P.; Kuipers, E.J.; Bloemena, E.; Tadema, T.M.; Townsend, R.R.; Tyagarajan, K.; Crothers,

J.M.Jr.; Monteiro, M.A.; Savio, A.; De Graaff, J. Potential role of molecular mimicry between *Helicobacter pylori* lipopolysaccharide and host Lewis blood group antigens in autoimmunity. Infect. Immun. **1996**. 64: 2031-2040.

86. Heneghan, M.A.; McCarthy, C.F.; Janulaityte, D.; Moran, A.P. Relationship of anti-Lewis x and anti-Lewis y antibodies in serum samples from gastric cancer and chronic gastritis patients to *Helicobacter pylori*-mediated autoimmunity. Infect. Immun. **2001**. 69: 4774-4781.
87. Hynes, S.O.; Keenan, J.I.; Ferris, J.A.; Annuk, H.; Moran, A.P. Lewis epitopes on outer membrane vesicles of relevance to *Helicobacter pylori* pathogenesis. Helicobacter. **2005**. 10: 146-156.
88. Bor-Shyang, S.; Jiunn-Jong; W. Type 1 and 2 Lewis antigens of *Helicobacter pylori* – a potential marker of the human geographical distribution J. Med. Microbiol. **2008**. 57: 543-544.
89. Altman, E.; Fernández, H.; Chandan, V.; Harrison, B.A.; Schuster, M.W.; Rademacher, L.O.; Toledo. C. Analysis of *Helicobacter pylori* isolates from Chile: occurrence of selective type 1 Lewis b antigen expression in lipopolysaccharide. J. Med. Microbiol. **2008**: 57:585-591.
90. Kocharova, N.A.; Knirel, Y.A., Widmalm, G.; Jansson, P.E.; Moran, A.P. Structure of an atypical *O*-antigen polysaccharide of *Helicobacter pylori* containing a novel monosaccharide 3-C-Methyl-D-mannose. Biochemistry. **2000.** 39: 4755-4760.
91. Monteiro, M.A.; Fulginiti, J.; Dilts, D.A. U.S. Patent US 0118197 A1, **2005**.
92. Stevenson, T.H.; Castillo, A.; Lucia, L.M.; Acuff, G.R. Growth of *Helicobacter pylori* in various liquid and plating media. Lett Appl Microbiol. **2000**, 30, 192–196.
93. Testerman, T.L.; McGee, D.J.; Mobley, H.L.T. J. *Helicobacter pylori* growth and urease detection in the chemically defined medium Ham's F-12 nutrient mixture. Clin. Microbiol. 2001, 39, 3842-3850.

CHAPTER II

SAMPLES PRE-CHARACTERIZATION AND OVERVIEW ON ANALYTICAL STRATEGIES

2.1. Identification of the Samples

The following stains were used in this thesis:

- *H. pylori* reference strain NCTC 11637, obtained from the National Collection of Type Cultures (London, England) and gently provided by Doctor Maria João Vieira from the Centre of Biological Engineering of the University of Minho (Braga, Portugal). *H. pylori* NCTC 11637 is *vacA*$^+$ (s1,m1) and *cagA*$^+$.

- *H. pylori* clinical isolate 968 that was kindly provided by Dr. Maria de Lurdes Monteiro from the National Health Institute Dr. Ricardo Jorge (Lisbon, Portugal). It was isolated from a patient with a gastric ulcer and characterized as *vacA*$^+$ (s1,m1) and *cagA*$^+$.

- *H. pylori* clinical PTAV79 that was kindly provided by Prof. Maria do Céu Figueiredo from the Institute of Molecular Pathology and Immunology at the University of Porto (Porto, Portugal). It was isolated from a patient with reflux esophagitis and characterized as *vacA*$^+$ (s1,m1) and *cagA*$^+$.

- *H. pylori* clinical isolate 14255 that was kindly provided by Prof. Maria do Céu Figueiredo from the Institute of Molecular Pathology and Immunology at the University of Porto (Porto, Portugal). It was isolated from a patient with reflux esophagitis and characterized as *vacA*$^+$ (s1,m1) and *cagA*$^+$.

2.2. Analytical approaches used in the characterization of *H. pylori* cell-surface glycans

The global strategy used in this thesis for the structural characterization of *H. pylori* cell-surface glycans comprised an initial step of isolation from the bacterial cell wall. Subsequent actions involved an interactive combination of purification steps and evaluation of the extracts in relation to their sugars profile (composition, linkage, anomeric configuration). This approach allowed the isolation of fractions that were then analysed by fine analytical methods such as Nuclear Magnetic Ressonance (NMR) and Mass

Spectrometry (MS) and Fourier-Transformed Infrared Spectroscopy (FT-IR) as summarized in Fig. 2.1.

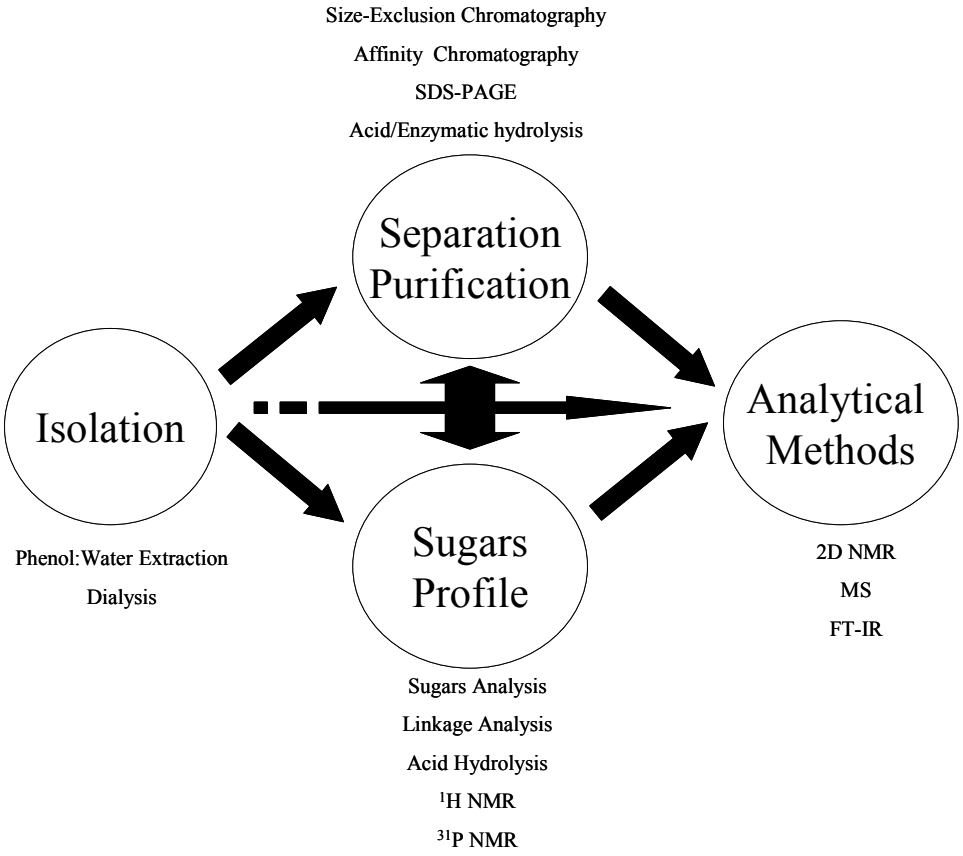

Figure 2.1. Rough scheme of the strategy used in the structural analysis of *H. pylori* cell-surface glycans.

2.2.1. Isolation of cell-surface glycans

The initial step in the isolation of *H. pylori* glycans comprised the isolation from their complex matrix, *H. pylori* cell-surface. The isolation of LPS/CPS or EPS from dry bacterial mass is conventionally initiated with phenol/water extraction[1] (Fig. 2.2). In this step the bulk of the proteins are removed with the phenol-phase while glycan-rich biomolecules remain in the water-phase together with salts and residual phenol. The glycan-rich water extracts were then subjected to a dialysis against distilled water using membranes with a cut-off of 1,000 Da with the purpose of desalting the sample and remove the toxic phenol without losing oligomeric material. The material recovered from dialysis was found to contain LPS/CPS and/or EPS residual but also residual amounts of nucleic acids and frequently peptides and low *M*w proteins.

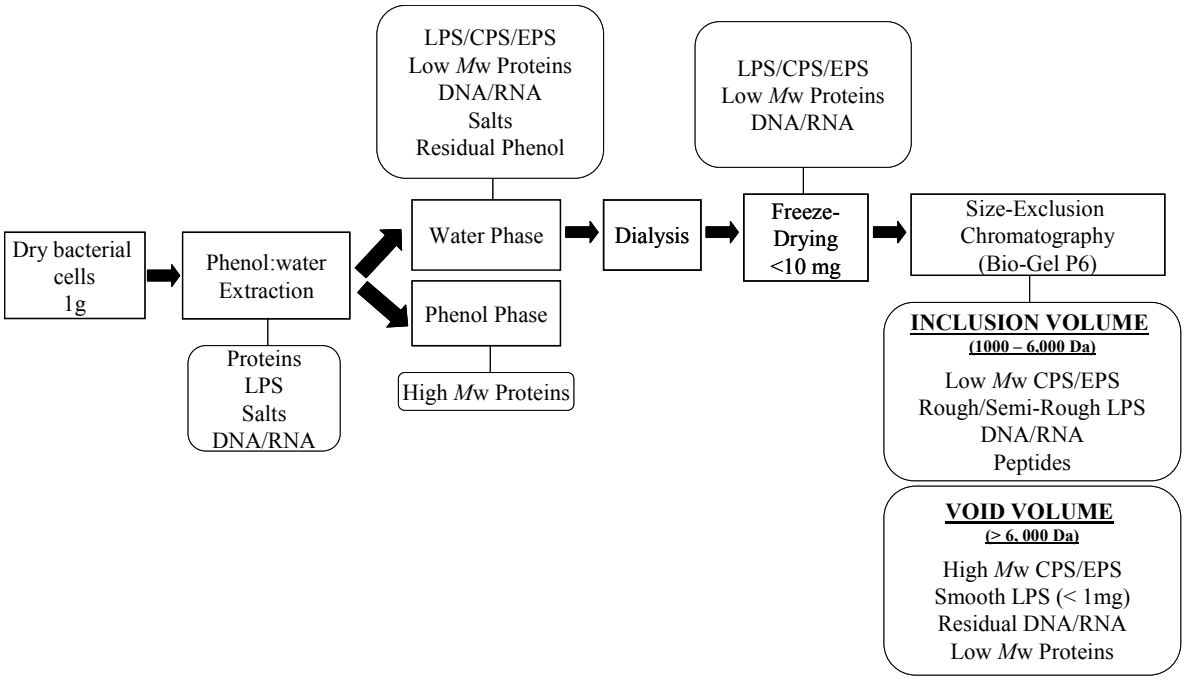

Figure 2.2. The main steps in the purification of *H. pylori* cell-surface glycans. The weight values of 1 g of dry bacterial cells, < 10 mg of freeze-dried material and < 1 mg of smooth LPS result from medium values observed for *H. pylori* NCTC 11637.

The molecular complexity of carbohydrate structures like the ones expressed at the cell-surface of *H. pylori* makes their characterization a challenging task from the analytical point of view. Furthermore, the presence of impurities and high heterogeneity at the glycan level makes the interpretation of analytical data difficult or sometimes impossible. Pure extracts are therefore essential to achieve a successful characterization. In this thesis samples were subjected to a pre-purification step by Size Exclusion Chromatography on a Bio-Gel P6 (separation limit: 1,000 - 6,000 Da). This procedure allowed separating semi-rough and rough LPS (LOS) and other oligomeric glycans from high *M*w smooth LPS and CPS and/or EPS. Furthermore, it revealed effective in the removal of DNA and peptides from the high *M*w fraction. It can also be seen in Fig. 2.2 that, generally, from an initial biomass of approximately 1 g less than 1 mg of LPS was obtained.

2.2.2. Purification of cell-surface glycans

The high heterogeneity and complexity shown by the high *M*w glycan-rich water extracts frequently led to additional purification steps, namely by affinity chromatography and SDS-PAGE.

Affinity chromatography

In this thesis glycans were fractionated based on their affinity to the amphiphilic polypeptide polymyxin-B, an antibiotic recognized for its affinity for LPS[2,3]. They were also fractionated according to their affinity to concanavalin A, a lectin that binds terminal α-D-mannosyl and α-D-glucosyl residues[4].

SDS-PAGE

Sodium dodecyl sulfate polyacrylamide gel electrophoresis (SDS-PAGE) is a technique used to separate biomolecules, in particular proteins according to their electrophoretic mobility (a function of length of polypeptide chain or molecular weight). In SDS gel electrophoresis, samples acquire identical charge per unit mass due to binding of SDS which results in fractionation by size. In this thesis this technique was employed to highlight possible protein-carbohydrate interactions in samples recognized to contain both classes of biomolecules. Different staining agents were used to reveal the bands, namely coomassie[5] for proteins and periodic acid-Shiff for carbohydrates[6]. The bands stained with both agents where considered to exhibit protein-carbohydrate associations[6].

2.2.3. Chemical degradation/derivatization of glycans

De-lipidation

To increase solubility and to simplify the analysis of LPS, the lipid part was sometimes removed. This was accomplished by mild acidic hydrolysis, which selectively cleaves the ketosidic linkage of Kdo[7]. In this thesis mild hydrolysis was performed by treatment with 1% acetic acid at 100 °C for 30-60 min and centrifugation to remove the water insoluble lipid A[7].

Smith degradation

In this thesis the presence of glycans in SDS-PAGE gels has been accessed by the formation of aldehydes in the sugar rings that further react with Schiff reagent creating a purple-magenta colour[6]. The formation of aldehydes is accomplished based on a Smith degradation involving a sequential treatment of sugars with $NaIO_4$ (sodium metaperiodate), sodium borohydride and dilute acid[8]. The oxidation yields a product in which vicinal hydroxyl groups have been oxidised to aldehydes by cleavage of carbon-carbon bonds (Fig. 2.3). Residues without any vicinal hydroxyl groups should thus remain unaffected.

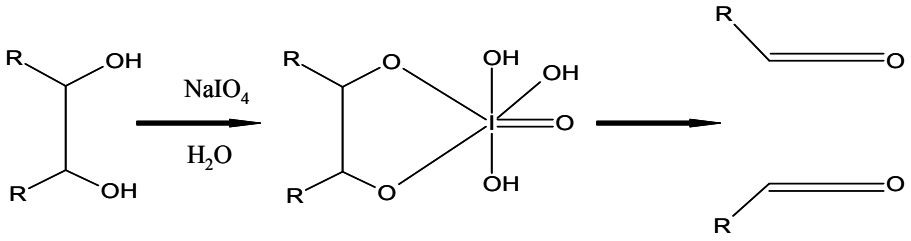

Figure 2.3. Illustration of a periodate oxidation.

Determination of monossaccharide composition

The monosaccharide composition of the isolated extracts was evaluated by the alditol acetate (aa) method as described by Harris *et al.*[9] (Fig. 2.4). The first step comprises the hydrolysis of all glycosidic linkages in the polysaccharide. The rate of hydrolysis of glycosidic bonds can differ significantly. For example, 6-deoxyglycosides hydrolyses 10 times faster than glycosides while uronic acids are partially resistant to normal acid-catalysed hydrolysis because of the inductive effect of the carboxyl group[10]. In this thesis polysaccharides have been degraded to their monomers by acid hydrolysis using 4 M trifluoroacetic acid (TFA) at 100ºC for 3h as reported by Monteiro et al.[11]. TFA is easy to evaporate and therefore preferable. The monosaccharides are then reduced by $NaBH_4$ to alditols to simplify the chromatogram obtained by gas chromatography (GC). The mutarotation is hereby overcome and a single derivative for each monosaccharide is formed. To promote the volatility, the alditols are acetylated originating alditol acetates (AA) (Fig. 2.4).

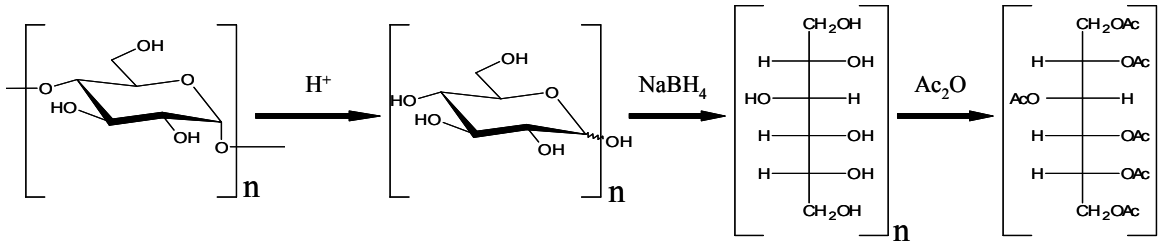

Figure 2.4. General representation of sugars analysis on a polysaccharide composed of *O*-4 linked α-Glc units.

The derivatives are identified from retention times compared to standards and by their mass spectra, if necessary.

Linkage analysis

The linkage pattern of each monosaccharide in a given polysaccharide was given by derivatization to partially methylated alditol acetates (pmaa) according to Ciucanu and Kerek[12] (Fig. 2.5). Although this information can be obtained non-destructively by NMR spectroscopy, methylation analysis can be used alone or complemented with NMR spectroscopy. The polysaccharides are first dissolved in dimethyl sulfoxide (DMSO), a polar aprotic solvent that dissolves both polar and nonpolar compounds, and an excess of NaOH is then added to the medium. Sodium hydroxide acts as an exsiccating agent and at the same time allowing the deprotonation of DMSO forming the dimethylsulphinyl anion ($DMSO^-$). DMSO- is the responsible for the deprotonation of hydroxyl groups of the sugar residues yielding a polyanion. The alkoxy groups are further reacted with methyl iodide and a fully methylated polysaccharide is obtained. The sample is then hydrolysed, reduced, and acetylated to produce volatile partially methylated alditol acetates (PMAA). The PMAA are identified from their retention times on GC as well as from their characteristic electron ionization (EI) mass spectra. Reduction was performed with $NaBD_4$ to label anomeric carbon (C-1).

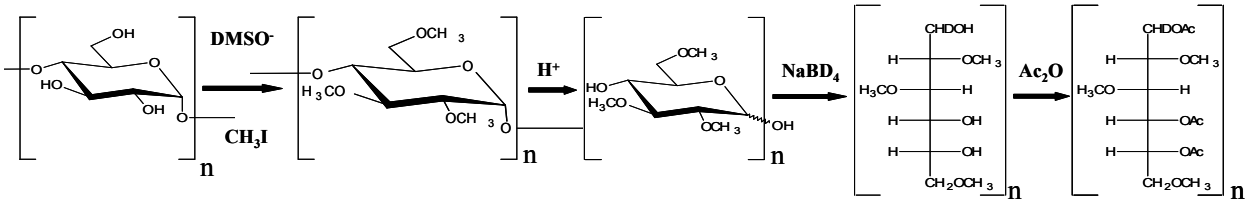

Figure 2.5. General representation of linkage analysis on a polysaccharide composed of *O*-4 linked α-Glc units.

The linkage analysis of sugars with carboxyl function raises some problems due to the conversion of the carboxyl group into a non-volatile sodium carboxylate. This problem was overcome in the present thesis by reducing the carboxylic group with $LiAlD_4$ according to what was described by Lindberg and Lönngren[13] and Redgwell and Selvendran[14] prior to the above described procedure (Fig. 2.6).

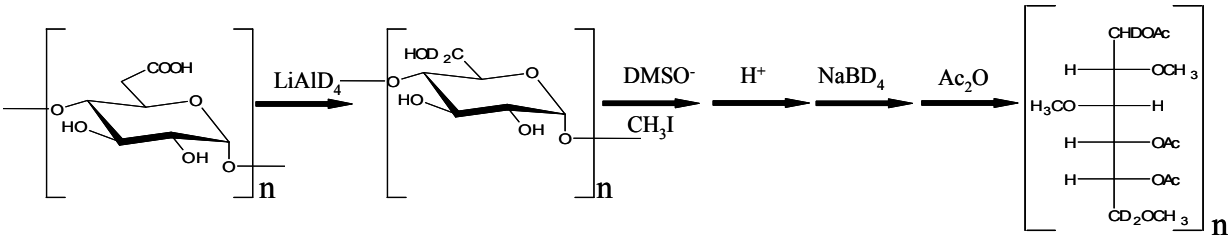

Figure 2.6. General representation of linkage analysis on a polysaccharide composed of *O*-4 linked α-GlcA units.

Partial Acid hydrolysis

In order to obtain fragments suitable for Electrospray ionization (ESI) mass spectrometry analysis, isolated glycans were subjected to partial acid hydrolysis using TFA. TFA was easily evaporated at 40ºC under a steam of N_2 and the resulting oligosaccharides were recovered by Size-Exclusion Chromatography using a Bio-Gel P2 (100 – 1800 Da).

2.2.4 Gas chromatography (GC)

Gas Chromatography (GC) was used in this thesis to separate volatile components of a mixture, namely alditol acetates from sugars analysis (Fig. 2.7) and partially methylated alditol acetates from linkage analysis.

In GC, a small amount of the sample to be analyzed (1 µL) is drawn up into a syringe and injected in a hot injector port of the gas chromatograph where it is volatilized. Separation of the different components of a mixture occurs from the interaction with a mobile phase, in this case He and a stationary phase (Fig. 2.8). The stationary phase used in this thesis was a DB-1 capillary column (30 m length, 0.32 mm internal diameter, and 0.25 µm film thicknesses), a non-polar stationary phase composed of 100% dimethyl-polysiloxane.

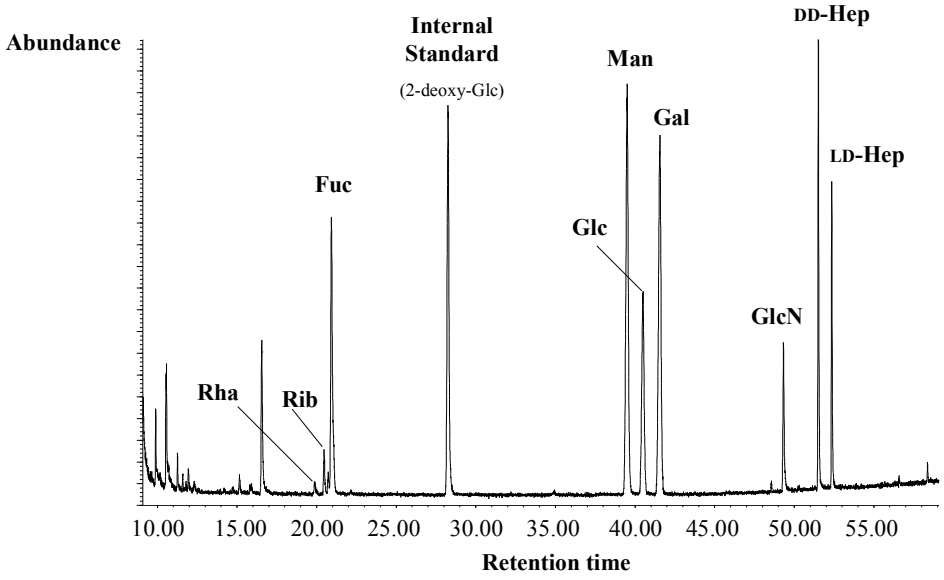

Figure 2.7. Sugar analysis GC chromatogram on a DB-1 column of *H. pylori* 968 glycan-rich water extracts.

Since the partitioning behaviour is dependant on temperature, the separation column is usually contained in a thermostat-controlled oven. Separating components with a wide range of boiling points is accomplished by starting at a low oven temperature and increasing the temperature over time to elute the high-boiling point components.

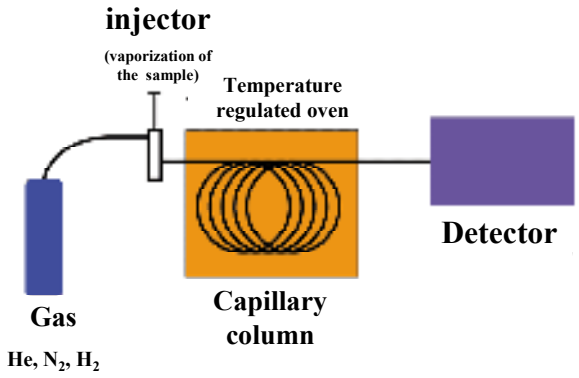

Figure 2.8. Schematic representation of a GC.

Coupling the GC separation with MS detector allowed the identification and quantification of trace amounts of compounds (nano-fentomole range). This was of primary importance when dealing with complex biological matrices and low abundance of starting material. In the present thesis 2-deoxy-Glc was used as internal standard for the quantification of the identified sugars[15].

2.2.5. Nano High performance liquid chromatography (HPLC)

High-performance liquid chromatography (or High pressure liquid chromatography, HPLC), as its designation says, allows fractioning of samples in a liquid phase. It uses a column that holds chromatographic packing material (stationary phase), a pump that moves the mobile phase(s) through the column, and a detector that shows the retention times of the molecules. Retention time varies depending on the interactions between the stationary phase, the molecules being analyzed, and the solvent(s) used. Nano HPLC uses a capillary column and, by decreasing of inner diameter of the stationary phase, it allows injecting a small amount of sample with and increasing sensitivity[16]. Therefore, it was used in this thesis to separate trace amounts of protein digests prior to MALDI-TOF analysis.

2.2.6. Nuclear Magnetic resonance

NMR is widely used for structure analysis of carbohydrates. About 1 mg of sample can be enough for a complete structural assignment. The method is non-destructive and relies on the magnetic properties of some nuclei. In this thesis the NMR active isotopes ^{1}H, ^{13}C, and ^{31}P nuclei are used for structural analysis.

Sample preparation

All NMR experiments in the present thesis were acquired in D_2O to reduce the complexity of the obtained NMR spectra since deuterium and protons are not observed at the same frequency[17]. By doing so, also the protons of hydroxyl, carboxyl, amine and amide groups are exchanged with deuterium further simplifying the sepctra. However, to achieve 100% exchange of deuterium with water protons is difficult and usually an intense, broad signal from HDO was observed in the spectrum. In order to decrease its intensity, the samples were repeatedly dissolved in D_2O and lyophilised. Furthermore, the spectra of unknown samples were acquired with increased temperatures in relation to the defined

temperature. By doing so it was possible to move the HDO signal allowing the visualization of overlapped signals[18].

One dimentional (1D) spectra and the structural reporter region

1D ^{1}H spectra are easy to acquire and do not require high amounts of material. Visual observation can readily provide information on the purity, concentration, and heterogeneity of the sample. Based on the anomeric region (~4.5 and 5.5. ppm) it is possible to estimate the number of different type of sugars in the samples[17]. The existence of acetate or methyl groups (δ_H 1.2-2.3 ppm) can also be easily accessed from the 1D spectrum. Samples containing sialic acids or 3-deoxy-D-manno-oct-2-ulosonic acid (Kdo) will be immediately obvious as well[17]. Therefore, 1D ^{1}H NMR was routinely used to screen samples and easily access their purity and composition. Furthermore, both by observation of the chemical shift ($\delta\alpha > \delta\beta$) and measuring the vicinal coupling constant between H-1 and H-2 ($^{3}J_{1,2}$), it was possible to get information on the anomeric configuration[17,19]. If the sugars have axial-equatorial orientation they present a $^{3}J_{1,2}$ α ~3 Hz (α-anomer) and if they have an axial-axial orientation $^{3}J_{1,2}$ β ~7 Hz (α-anomer)[17,20]. However, if the sugar residue is in a *manno*-configuration (chair configuration D-$^{4}C_1$ or L-$^{1}C_4$) like for Man of the heptoses observed in *H. pylori* core, this distinction is not straightforward. In these cases couplings are less than 3 Hz and the signals are usually not resolved due to line broadening[17,19]. In these cases the $^{3}J_{C1,H1}$ values can be used, being 168-174 Hz for α-pyranosyl residues and 160-167 Hz for β- pyranosyl residues[17,19,20].

2D homonuclear techniques

Nuclear Magnetic Resonance (NMR) of glycans can be challenging, primarily due to spectral overlap; carbohydrate ring protons generally resonate over a relatively narrow spectral region (3.2-4.0 ppm)[20]. Therefore, it was frequently necessary to apply 2D homonuclear techniques such as correlated spectroscopy (COSY) and total correlated spectroscopy (TOCSY) to reduce the overlap by resolving the proton signals over two dimensions[20]. 2D COSY shows correlations between directly coupled protons allowing for example to determine H-2 from its correlation with the anomeric proton and from H-2 determine H-3 and so on[20]. However, problems arise from strong coupled spins such as H-6 and H-6' that resonate close to the spectrum diagonal[17]. In the 2D TOCSY the magnetization can be transferred through the coupled network of spins of a given sugar

from the anomeric position through the ring protons and even beyond in heptoses or octoses[17]. Due to high signal overlapping in complex spectra, the cross-peaks with the anomeric have been used as a reference region[20]. By crossing data from COSY and TOCSY it was possible to assign the majority of the ring protons from the observed sugars. Another NMR technique used was the 2D nuclear Overhauser enhancement spectroscopy (NOESY) which provided through-space information about nucleus less than 5 Å apart[20]. Also, in NOESY spectra, the intensity of the signal is directly correlated with the spatial distance between protons[20].

Backed by proton chemical shifts determined by COSY and TOCSY, it was possible to identify NOE patterns in the NOESY spectra that were used primarily to confirm the anomeric configuration of sugars[17,20]. NEOSY experiments were also used to establish the order of monosaccharide units in a given glycan and permitted the confirmation of previously assigned glycosidic linkages[17,20].

2 D heteronuclear techniques

^{1}H detected ^{1}H-^{13}C correlated NMR methods take advantage of the chemical shift dispersion of the ^{13}C nucleus and are more sensitive than ^{13}C direct detection[17,20]. In this thesis two experiences have been used, the heteronuclear single quantum coherence (HSQS) and heteronuclear multiple bond correlation (HMBC). The HSQC experience correlate directly linked ^{1}H to ^{13}C nuclei and was extensively used in this thesis to assign carbon chemical shifts without the need to acquire much less sensitive ^{13}C spectra[17,20]. An HSQC spectrum highlighting characteristic ^{1}H and ^{13}C chemical shift ranges are presented in Fig. 2.9 and chemical shifts are resumed in Table 2.1.

Additionally, the HMBC allowed the identification of two and three-bond correlations and was most useful in the identification of glycosidic linkages[20]. However this experience is much less sensitive than HSQC, requiring long acquisition times to obtain information[17]. For that reason its utilization was sometimes prohibitive due to the low amounts of glycans available in this work (<200 μg).

^{1}H-^{31}P NMR HMBC correlations were also used to determine phosphorilation sites in sugars.

Table 2.1. Characteristic carbon and proton chemical shifts for cabohydrates[20]

Spectral region	$\delta_{H\ (ppm)}$	$\delta_{C(ppm)}$
Carbonyl Carbons (uronic acids, acetyl or 1-carboxyethyl ethers)		165-185
Anomeric region	4.4-5.5	95 and 110
Ring region	3.2-4.5	50-85
Nitrogen-bearing carbons		50-60
Carbons linking other sugars		75-85
unsubstituted ring carbons		65-75
O-substitution	1.2-0.6	15-30

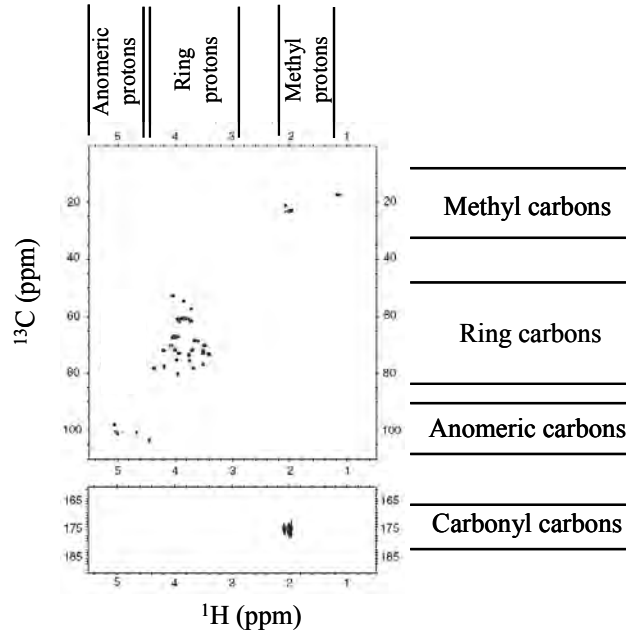

Figure 2.9. The typical chemical shift ranges of signals from the carbon and proton in carbohydrates.

Diffusion ordered spectroscopy (DOSY)

DOSY experiments provide a way to separate the different compounds in a mixture based on the differing translation diffusion coefficients[21]. Therefore, differences in the size and shape of the molecule, as well as physical properties of the surrounding environment such as viscosity and temperature of each chemical species in solution can contribute to the separations. Similar to an analytical chromatographic experiment, the DOSY spectrum presents an individual component ^{1}H spectrum along a diffusion (molecular mass) axis. It was therefore used in this thesis to evaluate the heterogeneity of samples[22].

Databases of chemical shift information

Tabulated chemical shift data for monosaccharides and polysaccharides are a valuable resource for aiding structural assignment of polysaccharides. In this context the existence of databases capable of gathering information is a precious help in NMR interpretation. One of the most important is the database CASPER[23,24] having a web interface at http://www.casper.organ.su.se/casper. This database has been tested extensively and used to simulate ^{13}C spectra of grater than 200 structures with excellent reliability[17]. Therefore, this database has been used in this thesis to evaluate the accuracy of both ^{1}H and ^{13}C chemical shift assignments and the accuracy of the proposed structures.

2.2.7. Mass spectrometry

Mass-spectrometry (MS) is a highly sensitive analytical technique, allowing structural characterization within the nano-fentomole range[25]. An MS experience comprises three general steps: ionization of the sample, separation according to mass/charge ratio, and detection (Fig. 2.10). In this thesis three types of ionization methods were used, Electron impact (EI), eletrospray ionization (ESI), and Matrix Assisted Laser Desorption Ionization Time-of-Flight (MALDI). Different types of analyzers were also used to separate the generated ions, namely

quadrupole, a linear ion-trap (LIT), a quadruple-orthogonal acceleration time-of-flight (Q-TOF) and a triple quadrupole (QqQ).

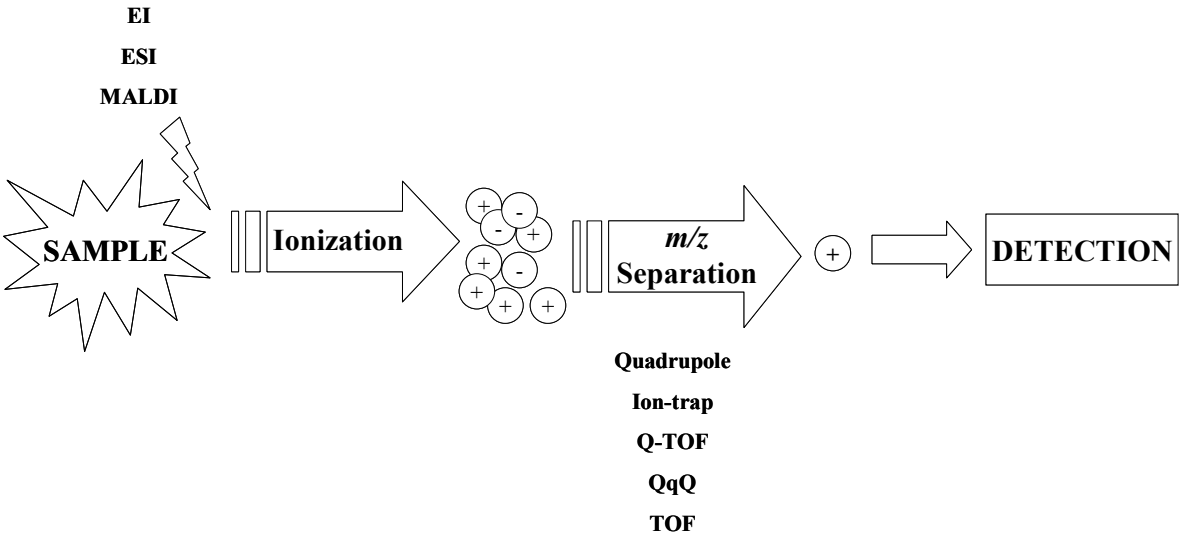

Figure 2.10. Schematic observation of a mass spectrometry experience.

EI-MS

EI was used in the ionization of gas-phase alditol acetates and partially methylated alditol acetates generated during sugar and linkage analysis. These low molecular weight molecules were volatilized and separated by GC and then ionized and fragmented by EI and detected by a quadrupole detector in positive mode[26]. Therefore, only positively charged ions are detected.

EI is a relatively harsh form of ionization producing a wide range of molecular fragments. The electron impact source consists of a heated filament that produces electrons which are accelerated to another electrode called the ion trap. Sample vapour diffuses into the electron beam and become ionized and fragmented. The size of the fragment ion depends on the electron energy, which is controlled by the accelerating potential on the ion trap electrode[26]. Both aa and pmaa were bombarded by electrons with a kinetic energy of 70 electron volts which was enough to break the molecules into smaller fragments[26]. The ions produced are driven by a potential applied to an ion-repeller electrode away from the ion source into the accelerating region of the mass spectrometer, where mass analysis takes place[26]. By coupling GC separative technique to MS analysis it is possible to generate a chromatogric profile associated with an array of MS spectra. This allows the detection of compounds based on retention time and their characteristic fragmentation spectrum under EI conditions.

The mass detector of the GC-MS used was a quadrupole (Fig. 2.11) consisting of 4 circular rods, set perfectly parallel to each other. In quadrupoles, the ions are separated in relation to their mass/charge ratio (*m/z*) based on the stability of their trajectories under a constant voltage and oscillating electric fields that are applied to the rods[26].

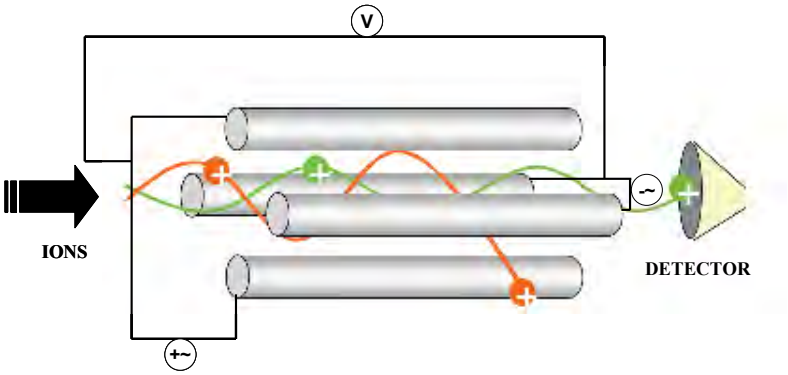

Figure 2.11. Schematic representation of a quadrupole.

ESI-MS

ESI-MS was extensively used in this thesis to analyze oligosaccharides resulting from partial acid hydrolysis and enzymatic treatments previously separated by size-exclusion chromatography in Bio-Gel P2.

During standard electrospray ionisation (Fig. 2.12) the sample is dissolved in a polar, volatile solvent and pumped through a narrow stainless steel capillary[27]. A high voltage is applied to the tip of the capillary, which is situated within the ionisation source of the mass spectrometer and, as a consequence of this strong electric field, the sample emerging from the tip is dispersed into an aerosol of highly charged droplets, a process that is aided by a co-axially introduced nebulising gas flowing around the outside of the capillary (Fig. 2.12). This gas, usually nitrogen, helps to direct the spray emerging from the capillary tip towards the mass spectrometer. The charged droplets diminish in size by solvent evaporation, assisted by a warm flow of nitrogen known as the drying gas which passes across the front of the ionisation source (Fig. 2.12). Eventually charged sample ions, free from solvent, are released from the droplets, some of which pass through a sampling cone or orifice into an intermediate vacuum region, and from there through a small aperture into the analyser of the mass spectrometer, which is held under high vacuum.

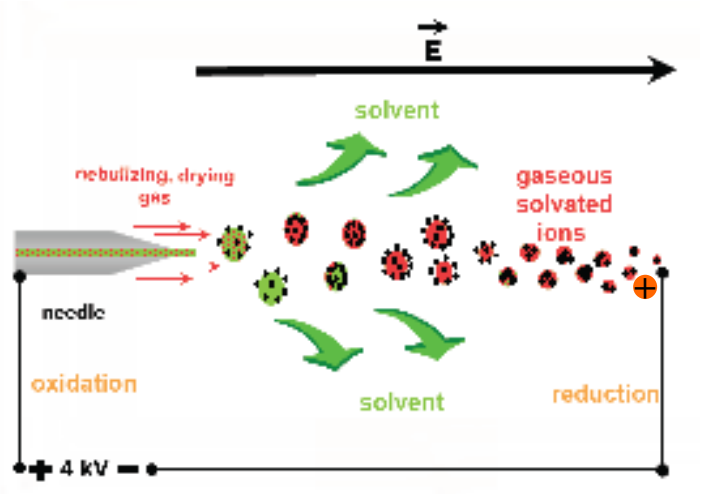

Figure 2.12. Schematic representation of ionization by ESI.

Electrospray ionisation is known as a "mild" ionisation method as the sample is ionised by the addition or removal of a proton, with very little extra energy remaining to cause fragmentation of the sample ions. This technique was used to study oligosaccharides with molecular weight lower than 1200-1600 Da and all experiments relied on positive mode detection. Resulting from the high affinity of carbohydrates for alkali metals, they were mainly detected as sodium adducts ($[M+Na]^+$)[25]. However, in cases where the concentration of H^+ is high or when there is a lower concentration of sodium ions, the protonated specie was found predominant ($[M+H]^+$). Higher molecular weight material generally originates multiple charged molecular-related ions such as $(M+nH)^{n+}$ in positive ionisation mode which are not easy to interpret[25]. In those cases, analysis was carried out by MALDI-TOF-MS.

All available ESI-MS analyzers (LIT, Q-TOF, and QqQ) further allowed tandem mass spectrometry (MS^2) experiments by allowing the fragmentation of the $[M+Na]^+$ ions. Fragmentation of these ions occurs mainly in the glycosidic linkage even though some cross-ring fragmentations can be observed thus generating valuable structural information[25].

The ion-trap mass spectrometer uses three electrodes to trap ions in a small volume[27] (Fig. 2.13). The mass analyzer consists of a ring electrode separating two hemispherical electrodes. A mass spectrum is obtained by changing the electrode voltages to eject the ions from the trap. The advantages of the ion-trap mass spectrometer include compact size, and the ability to trap and accumulate ions to increase the signal-to-noise ratio of a measurement. The pulsing of the ion gate differentiates ion traps from "beam"

instruments such as quadrupoles where ions continually enter the mass analyzer. The time during which ions are allowed into the trap, termed the "ionization period", is set to maximize signal while minimizing space-charge effects. Space-charge results from too many ions in the trap that causes a distortion of the electrical fields leading to an overall reduction in performance. The ion trap is typically filled with helium to a pressure of about 1 mtorr. Collisions with helium dampen the kinetic energy of the ions and serve to quickly contract trajectories toward the centre of the ion trap, enabling trapping of injected ions. Trapped ions are further focused toward the centre of the trap through the use of an oscillating potential, called the fundamental radio-frequency (rf), applied to the ring electrode. An ion will be stably trapped depending upon the values for the mass and charge of the ion, the size of the ion trap, the oscillating frequency of the fundamental rf, and the amplitude of the voltage on the ring electrode.

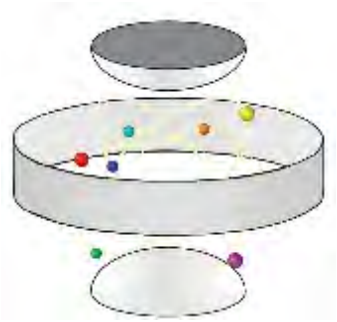

Figure 2.13. Ions are trapped by electric and magnetic potentials. This design has the advantage of allowing the selection of specific ions thus rejecting the rest.

The capability of ion trap analyzers to hold ions for long periods allowed further fragmentations (MS^n experiments) thus resulting in additional structural information.

Oligosaccharides were also analyzed in an ESI-Q-TOF-MS mass spectrometer, that comprised both a quadrupole and TOF analyzers arranged orthogonally with a collision cell separating the two[27] (Fig. 2.14). When operating in MS mode the quadrupole is not used as an analyser, merely as a lens to focus the ion beam into the second (time-of-flight) analyser which separates the ions according to their mass-to-charge ratio. In the TOF analyzer the ions are accelerated by an electric field of known strength[27]. As a result, ions with the same charge have an equal kinetic energy and therefore their velocity becomes dependent on the mass, thus lighter ions reach the detector first. When in MS^2 mode, the molecular ions of each of the species present fragments that can be independently selected and transmitted through the quadrupole, which is now used as an analyzer, to transmit

solely the ions of interest into the collision cell which lies in-between the first and second analyzers. An inert gas such as argon is introduced into the collision cell and the sample ions are bombarded by the collision gas molecules which cause them to fragment prior to entering the TOF analyzer[27].

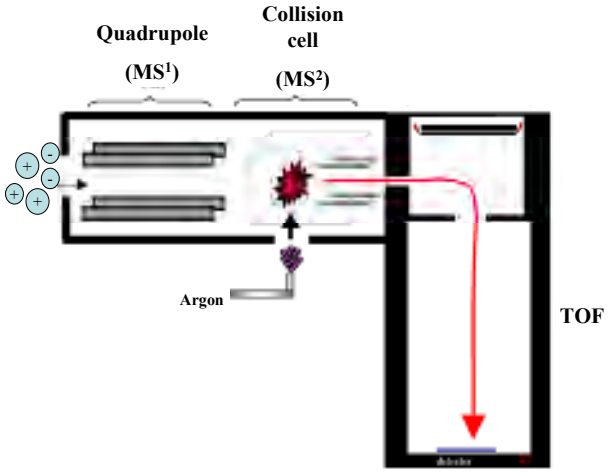

Figure 2.14. Schematic representation o a Q-TOF-MS apparatus.

Analysis of oligosaccharides was also carried out in a triple quadrupole mass spectrometer where there is an arrangement of three quadrupoles[27] (Fig. 2.15). The first (Q1) and third (Q3) quadrupoles serve as mass filters, whereas the middle (q2) quadrupole serves as a collision cell. This collision cell is a radiofrequency only quadrupole (non-mass filtering) using an inert gase such as Ar, He or N gas to provide collision-induced dissociation of a selected precursor ion that is selected in Q1. Subsequent fragments are passed through to Q3 where they may be filtered or scanned[27].

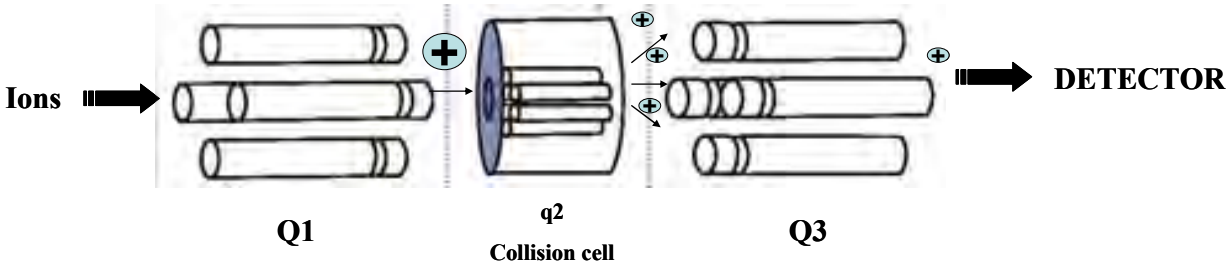

Figure 2.15. Schematic representation of a Q-TOF-MS apparatus.

MALDI-MS

MALDI-MS and MS/MS experiments were used in this thesis both to analyse high molecular weight oligosaccharides and to identify peptides resulting from trypic digestion of high molecular weight glycoproteins. In MALDI, the analyte has to be pre-embedded in

an excess of low molecular weight mass UV-absorbing matrix. For sugars, it was used 2,5-dihydroxybenzoic acid[28] while for peptide analysis it was used α-cyano-4-hydroxycinnamic acid. A pulse is fired at the matrix, which absorbs enough energy to transfer some of this to the sample, which leads to sputtering of analyte and matrix ions from the surface of the mixture[27]. In this way energy transfer is efficient and also the analyte molecules are spared excessive direct energy that may otherwise cause decomposition (Fig. 2.16).

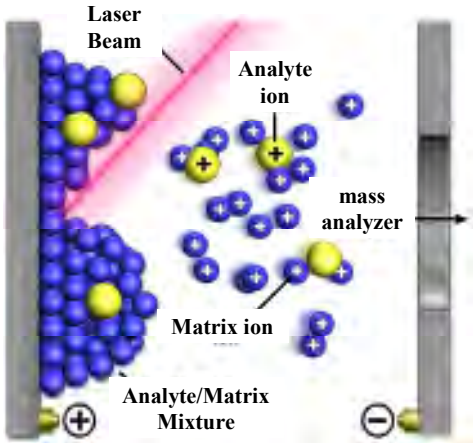

Figure 2.16. Schematic representation of the ionization of the sample in MALDI.

MALDI is also a "mild" ionisation method, resulting predominantly in the generation of singly charged molecular-related ions regardless of the molecular mass, hence the spectra are relatively easy to interpret. Fragmentation of the sample ions does not usually occur. The produced ions are then analysed by TOF. Even though the mass accuracy depends on the type and performance of the analyser of the mass spectrometer, most modern instruments should be capable of measuring masses to within 0.01% of the molecular mass of the analyzed ions[27]. Furthermore, the MALDI-TOF mass spectrometer also allowed tandem mass experiments that provided additional structural information

2.2.8. Fourier transform infrared (FTIR) spectroscopy

Infrared spectroscopy relies on the fact that bonds and groups of bonds vibrate at characteristic frequencies. A molecule that is exposed to infrared radiation absorbs infrared energy at frequencies which are a characteristic of the molecule. Therefore, it was of great usefulness in this

thesis to evaluate the purity of samples as well as, taking advantage of characteristic bands, infer the presence of certain classes of molecules. One of the most informative regions in the study of polysaccharides is fingerprint region from 800-1200 cm^{-1} [29]. The presence of proteins could also be inferred by the characteristic amide bands at 1650 resulting from C=O group (amide I band) and at 1550 from N-H group (amide II band)[30] and lipids by characteristic absorvances in the region between 2959-2852 cm^{-1} resulting from CH, CH_2 and CH_3 asymmetric and symmetric stretching modes of fatty acids[31].

The Fourier Transform Infrared (FTIR) spectrometer obtains infrared spectra by first collecting an interferogram of a sample signal with an interferometer, which measures all of infrared frequencies simultaneously. An FTIR spectrometer acquires and digitalizes the interferogram, performs the FT function, and outputs the spectrum.

REFERENCES

1. Westphal, O.; Jann, K. Bacterial lipopolysaccharides: extraction with phenol–water and further applications of the procedure. Methods Carbohydr. Chem. **1965.** 5: 83–91.
2. Issekutz, A.C. Removal of gram-negative endotoxin from solutions by affinity chromatography. *J.* Immunol. Methods. **1983**. 61: 275-281.
3. Molvig, H.; Baek, L. Removal of endotoxin from culture media by a polymyxin B sepharose column. The activity of contaminating endotoxin in culture media measured by the interleukin 1 inducing effect on human monocyte cultures and by the Limulus test. Scand. J. Immunol. **1987**. 26: 611-619.
4. Goldstein, I.J.; Hollerman, C.E.; Smith, E.E. Protein-carbohydrate interaction. II. Inhibition studies on the interaction of concanvalin A with polysaccharides. Biochemistry. **1965** 4: 876-883.
5. Merril C.R. Gel-staining techniques. Methods Enzymol. **1990**. 182: 477-88.
6. Doerner, K.C.; White, B. Detection of glycoproteins separated by nondenaturing polyacrylamide gel electrophoresis using the periodic acid-Schiff stain. Anal. Biochem. **1990**. 187: 147-150.
7. Aspinall, G.O.; Monteiro, M.A.; Pang, H.; Walsh, E.J.; Moran, A.P. Lipopolysaccharide of the *Helicobacter pylori* type strain NCTC 11637 (ATCC 43504): structure of the O antigen chain and core oligosaccharide regions. Biochemistry. **1996**. 35: 2489-2497.
8. Goldstein, I.J.,; Hay, G.W.; Lewis, B.A.; Smith, F. Controlled degradation of polysaccharides by periodate oxidation, reduction and hydrolysis. Methods Carbohydr. Chem. **1965**. 5: 361-370.
9. Harris, P.J.; Blakeney, A.B.; Henry, R.J.; Stone, B.A. Detection of neutral and aminosugars from glycoproteins and polysaccharides as their alditol acetates. J Chromatogr. **1983**. 256: 419-427.
10. BeMiller, J.N. Acid-catalyzed hydrolysis of glycosides. Adv. Carbohydr. Chem. Biochem. **1967**. 22: 25-108.
11. Monteiro, M.A.; Appelmelk, B.J.; Rasko, D.A.; Moran, A.P.; Hynes, S.O.; MacLean, L.L.; Chan, K.H.; Michael, F.St.; Logan, S.M.; O'Rourke, J.; Lee, A.; Taylor, D.E.;

Perry, M.B. Expression of Type 1 and Type 2 Lewis Blood Group Antigens by *Helicobacter pylori* Lipopolysaccharides. J. Biol. Chem. **1998**. 273:. 11533-11543.

12. Ciucanu, I.; Kerek, F. A simple and rapid method for the permethylation of carbohydrates. Carbohydr. Res. **1984**, 131, 209–217.
13. Lindberg, B.; Lönngren, J. Methylation analysis of complex carbohydrates: general procedure and application for sequence analysis. Methods Enzymol. **1978**. 50: 3-33.
14. Redgwell, R.J.; Selvendran, R.R. Structural features of cell-wall polysaccharides of onion *Allium cepa*. Carbohydr Res. **1986**. 157: 183-199.
15. Cardoso, S.M.; Ferreira, J.A.; Mafra, I.; Silva, A.M.; Coimbra, M.A. Structural ripening-related changes of the arabinan-rich pectic polysaccharides from olive pulp cell walls. J Agric Food Chem. **2007**. 55: 7124-7130.
16. Schmid, D.G.; Behnke, B.; Kempter, C.; Metzger, J.W.; Kuhn, R. Nano-HPLC of oligosaccharides: Method development and optimization. Mikrochim Acta. **2001**. 137: 111-118.
17. Grice, I.D.; Wilson, J.C. Analytical approaches towards the structural characterization of microbial wall glycopolymers. In: Moran, A.P. (Eds.) Microbial Glycobiology. Academic press (London, UK) **2009**. 281-304.
18. Schweda, E.K.H.; Richards, J.C. Structural profiling of short-chain lipopolysaccharides from *Haemophilus influenzae*. Methods Mol. Med. **2002**. 71: 161-183.
19. Rao, V.S.R.; Qasba, P.K.; Balaji, P.V.; Chandrasekaran, R. Conformation of monosaccharides.. In: Conformation of carbohydrates. Haarwood academic publisher (Amsterdam, Netherlands). **1998**. 49-91
20. Duus, J.Ø.; Gotfredsen, C.H.; Bock, K. Carbohydrate structural determination by NMR spectroscopy: modern methods and limitations. Chem. Rev. **2000**. 100: 4589-4614.
21. Kählig, H.; Dietrich, K.; Dorner, S. Analysis of carbohydrate mixtures by diffusion difference NMR spectroscopy. *Monatsh. Chem.* **2002**. 133: 589-598.
22. Suárez, E.R.; Syvitski, R.; Kralovec, J.A.; Noseda, M.D.; Barrow, C.J.; Ewart, H.S.; Lumsden, M.D.; Grindley, T.B. Immunostimulatory polysaccharides from *Chlorella pyrenoidosa*. A new galactofuranan. measurement of molecular weight

and molecular weight dispersion by DOSY NMR. *Biomacromolecules.* **2006.** 8:2368-2376

23. Jansson, P.E.; Stenutz, R.; Widmalm, G. Sequence determination of oligosaccharides and regular polysaccharides using NMR spectroscopy and a novel Web-based version of the computer program CASPER. *Carbohydr Res.* **2006**. 341: 1003-1010.
24. Loss, A.; Stenutz, R.; Schwarzer, E.; von der Lieth, C.W. GlyNest and CASPER: two independent approaches to estimate ^{1}H and ^{13}C NMR shifts of glycans available through a common web-interface. *Nucleic Acids Res.* **2006**. 34: W733-W777.
25. Zaia, J. Mass spectrometry of oligosaccharides. *Mass Spectrom. Rev.* **2004.** 23: 161-277.
26. Harris, D.C. Gas chromatography. In: Quantitative chemistry analysis. Freeman and company (New York, USA). 1999: 675-711.
27. El-Aneed, A.; Cohen, A.; Banoub, J. Review of the Basics: Electrospray, MALDI, and commonly used mass analyzers. *Appl. Spectroc. Rev.* **2009**. 44: 210-230.
28. Harvey, D.J; Naven, T.J.P.; Kuster, B. Identification of oligosaccharides by matrix-assisted laser desorption ionization and electrospray MS. *Biochem. Soc. Trans.* **1996**. 24: 905-912.
29. Coimbra, M.A., Barros, A.; Rutledge, D.N.; Delgadillo, I. FTIR spectroscopy as a tool for the analysis of olive pulp cell-wall polysaccharide extracts. *Carbohydr. Res.***1999.** 317: 145-154
30. Chapman, D.; Jackson, M.; Haris, P.I. Investigation of membrane protein structure using Fourier Transform Infrared Spectroscopy. *Biochem Soc Trans.* **1989**. 17: 617-619.
31. Adt, I.; Toubas, D.; Pinon, J.M.; Manfai, M.; Sockalingum, G.D. FTIR spectroscopy as a potential tool to analyse structural modifications during morphogenesis of *Candida albicans*. *Arch Microbiol.* **2006**. 185: 277-285.

CHAPTER III

DIFFERENTIATION OF ISOMERIC LEWIS BLOOD GROUPS BY POSITIVE ION ELECTROSPRAY TANDEM MASS SPECTROMETRY

Analytical Biochemistry 397 (2010) 186–196

Contents lists available at ScienceDirect

Analytical Biochemistry

journal homepage: www.elsevier.com/locate/yabio

Differentiation of isomeric Lewis blood groups by positive ion electrospray tandem mass spectrometry

José A. Ferreira [a], M. Rosário M. Domingues [a], Ana Reis [a], Mario A. Monteiro [b], Manuel A. Coimbra [a,*]

[a] Departamento de Química, Universidade de Aveiro, 3810-193 Aveiro, Portugal
[b] Department of Chemistry, University of Guelph, Guelph, Ont., Canada N1G 2W1

ARTICLE INFO

Article history:
Received 8 June 2009
Received in revised form 7 October 2009
Accepted 16 October 2009
Available online 28 October 2009

Keywords:
Mass spectrometry
Lewis antigens
Oligosaccharides
Electrospray
Helicobacter pylori

ABSTRACT

Lewis histo-blood group antigens are one of the major classes of biologically active oligosaccharides. In this work, underivatized Lewis blood groups were studied by electrospray tandem mass spectrometry (ESI–MS^n) in the positive mode with three different mass analyzers: Q-TOF (quadrupole time-of-flight), QqQ (triple quadrupole), and LIT (linear ion trap). It was observed that, under collision-induced fragmentations, type 1 Lewis antigens (Le^a and Le^b) could be distinguished from type 2 (Le^x and Le^y) on the basis of specific fragmentations of the GlcNAc unit. Whereas *O*-4-linked sugars of the GlcNAc are lost as residues, the *O*-3-linked sugars undergo fragmentation both as sugar units and as sugar residues (unit −18 Da). Type 2 Lewis antigens also showed a characteristic cross-ring cleavage $^{0,2}A_2$ of the GlcNAc. As a result, the product ions at *m/z* 388 and 305, characteristic of Le^x, and *m/z* 372, characteristic of Le^a, are proposed to distinguish the trisaccharide isomers Le^x/Le^a. Also, the product ions at *m/z* 534 and 305, characteristic of Le^y, and *m/z* 372, characteristic of Le^b, are proposed to distinguish the tetrasaccharide isomers Le^b/Le^y. These diagnostic fragment ions were further applied in the identification of Lewis type 2 antigens (Le^x and Le^y) in the lipopolysaccharide of the human gastric pathogen, *Helicobacter pylori*.

Glycosylation is known to mediate and control various biological and physiological events such as modeling of protein conformational and functional properties, cellular recognition, and aiding in the processes of fertilization and inflammation, tumorigenesis, and metastases [1–4].

One of the major classes of biologically active oligosaccharide structures is the Lewis antigens (Le), structurally related to determinants of the ABO blood group system. The Lewis histo-blood group ABO system is composed of two major antigenic cores: type 1 chains, D-Gal-β-(1→3)-D-GlcNAc-β-(1→, and type 2 chains, D-Gal-β-(1→4)-D-GlcNAc-β-(1→. Fucosylation on type 1 core gives rise to Lewis a (Le^a)[1] and Lewis b (Le^b), and fucosylation on type 2 originates Lewis x (Le^x) and Lewis y (Le^y), the positional isomers of Le^a and Le^b, respectively, as shown in Fig. 1. Lewis antigens are commonly found as carbohydrate chains of heavily glycosylated proteins (mucins) in the cell membrane of human epithelial cells of mammary and salivary glands, digestive and respiratory tracts, kidney, bladder, prostate, uterus, and testis [5–8]. Alteration in the expression pattern of Lewis antigens, as well as their overexpression, is a characteristic event among neoplasic transformations [9–13]. The expression of Lewis blood group antigens by several Gram-negative bacteria has also been long postulated [14]. These antigens are of particular interest in the case of the human pathogenic bacterium *Helicobacter pylori*, a category 1 (definitive) carcinogenic, directly related to the development of gastric malignancies such as gastritis, gastric ulcers, and gastric cancer [15]. Lewis blood antigens can be found in *O*-chains of lipopolysaccharides (LPSs: *O*-chain-core oligosaccharide–lipid A~cell) at the bacteria cell surface [16,17], where they are thought to contribute to the persistence of infection and the mediation of adhesion to gastric cells [16]. Due to their key role, the Lewis profile has been taken into consideration in several virulence and epidemiologic studies. Moreover, results presented so far have led to the conclusion that the Lewis expression pattern in *H. pylori* can be a marker for human geographical distribution [18]. Evidence for the expression of blood group antigens in higher plants has also been reported [19], allowing one to conclude that they are widely and transversely expressed in nature.

Due to their key biological roles, the identification of Lewis glycoside structures is a challenging topic in modern cell biology where rapid and sensitive methods are required to determine oligosaccharide sequences that allow the establishment of the

* Corresponding author. Fax: +351 234370084.
E-mail address: mac@ua.pt (M.A. Coimbra).

[1] *Abbreviations used:* Le^a, Lewis a; Le^b, Lewis b; Le^x, Lewis x; Le^y, Lewis y; LPS, lipopolysaccharide; MS, mass spectrometry; MS^n, tandem mass spectrometry; ESI–MS^n, electrospray tandem mass spectrometry; Q-TOF, quadrupole time-of-flight; QqQ, triple quadrupole; LIT, linear ion trap; HPLC, high-performance liquid chromatography; CID, collision-induced dissociation; FWHM, full-width at half-maximum; PNA, peptide nucleic acid; GPC, gel permeation chromatography; ELISA, enzyme-linked immunosorbent assay.

0003-2697/$ - see front matter © 2009 Elsevier Inc. All rights reserved.
doi:10.1016/j.ab.2009.10.034

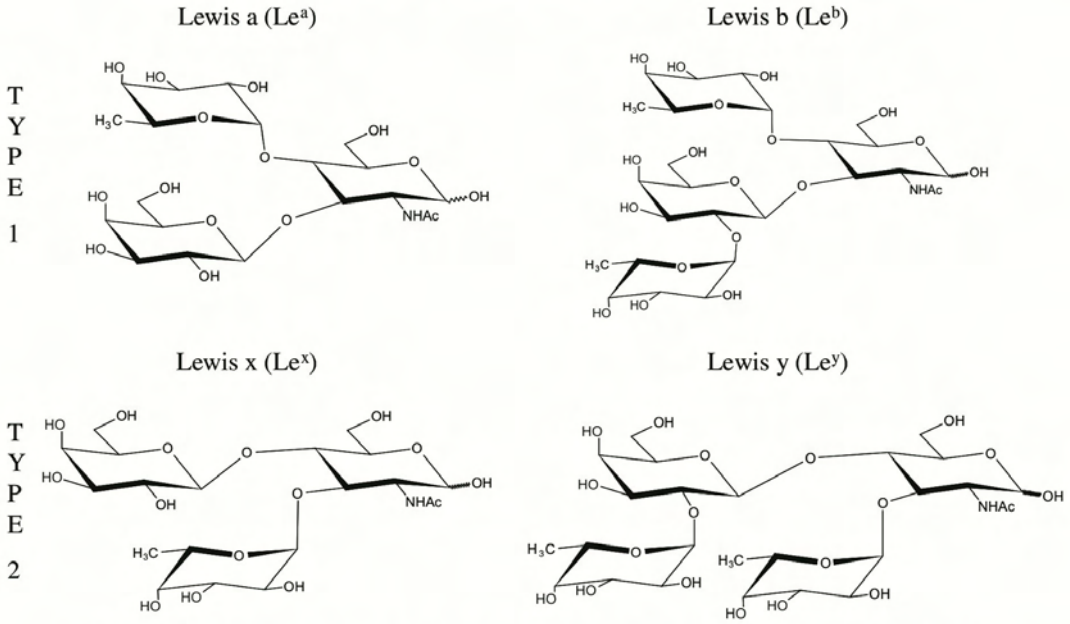

Fig. 1. Structures of the studied Lewis antigens. Type 1-derived structures: Le^a and Le^b; type 2-derived structures: Le^x and Le^y.

accurate structure/function relationships and the evaluation of potential cell malignancy during carcinogenesis. However, when dealing with biologic samples, the amount of oligosaccharides obtained for analysis is in most cases very low, on the order of picomoles or femtomoles. In this context, mass spectrometry (MS), and in particular tandem mass spectrometry (MS^n), is nowadays a powerful, highly sensitive, and well-established analytical technique for carbohydrate structural analysis [20–23].

Studies published so far concerning the analysis of underivatized Lewis antigens by electrospray tandem mass spectrometry (ESI–MS^n) have been made in negative mode conditions [24–26], reporting the fragmentation of the $[M-H]^-$ [24,26] and $[M+Cl]^-$ [25] oligosaccharides. The low chemical background noise [27] and the low level of cation adduct formation [28] in negative mode has been shown to be advantageous for oligosaccharide analysis. Furthermore, the negative ionization also has been preferred for the analysis of fucosylated oligosaccharides due to the higher stability of Fuc in negative mode when compared with the positive mode [29–31]. Chai and coworkers [24] demonstrated that MS^2 data of $[M-H]^-$ could be used to successfully distinguish Le^a/Le^x and Le^b/Le^y based on different glycosyl linkage fragmentations as well as cross-ring cleavages ($^{0,2}A$, nomenclature by Domon and Costello [32]) of the 4-linked GlcNAc. Conversely, there are also advantages in studying oligosaccharides by MS in positive mode. Their high affinity for alkali metal cations, namely sodium, lithium, and potassium, is known to facilitate ionization, thereby increasing sensitivity [33–35]. In particular, the sodium adducts, where fragmentation takes place mainly at the glycosidic linkages, have been studied in more detail [36–38]. Positive mode has also been shown to distinguish anomers and linkage types of nonderivatized Glc disaccharides based on the relative intensities of cross-ring fragmentations and glycosidic linkage cleavages [39]. Distinction of Lewis antigens based on cross-ring fragmentations obtained from MS^n experiments was also achieved in positive mode using 2-aminopyridine-labeled [40] and 4′-*N*,*N*-dimethylamino-4-aminoazobenzene-labeled [41] oligosaccharides. However, avoiding derivatization prior to MS studies makes the analysis easier and less time-consuming, decreasing considerably the risk of introducing contaminants and aberrations into the samples. So far as we know, no studies have yet been presented concerning the distinction of nonderivatized Lewis antigens using ESI–MS in positive mode.

In this work, we report the study of underivatized Lewis antigens by ESI–MS in positive mode. Because fragmentation may change with the analyzer used [22,39], analysis of Lewis antigens was performed using three mass spectrometers with different analyzers: Q-TOF (quadrupole time-of-flight), QqQ (triple quadrupole), and LIT (linear ion trap).

Materials and methods

Materials

Le^a, Le^x, Le^b, and Le^y were purchased from Dextra Laboratories (Reading, UK). Methanol was high-performance liquid chromatography (HPLC) grade. Water was of Milli-Q purity, filtered through a 0.22-μm filter (Millipore, Billerica, MA, USA). Each standard was diluted in water to a final concentration of 0.5 mg ml^{-1} and further diluted to 1:100 in methanol. Combined solutions of Le^a/Le^x and Le^b/Le^y were prepared from their initial aqueous solutions of 0.5 mg ml^{-1} in proportions of 1:9, 1:1, and 9:1 of each isomer. Each solution mixture was then diluted to 1:100 in methanol. Sodium borohydride (⩾96% pure) and glacial acetic acid were purchased from Sigma.

Preparation of Lewis alditols

Lewis alditols were prepared by the addition of 50 ml of sodium borohydride solution (15% in NH_4OH, 3 M) to 100 ml of the 0.5-mg ml^{-1} Lewis antigen solution using the procedure described by Reis and coworkers [42]. The mixture was left to react for 1 h at 30 °C in a screw cap tube. The excess of reducing agent was removed by the addition of 0.5-ml aliquots of glacial acetic

acid until no gas release was observed. The borate formed was removed by the successive addition of methanol followed by evaporation under reduced pressure. The material was further resuspended in Milli-Q high-purity water, and the excess of sodium was removed by exposing the solution to Dowex cation exchange resin.

MS analysis

The ESI–MS and ESI-MS^2 analyses were carried out on three mass spectrometers: an LIT LXQ (ThermoFinnigan, San Jose, CA, USA), a Q-TOF 2 instrument (Micromass, Manchester, UK), and a QqQ Quattro (Micromass). All MS spectra were obtained in triplicate. The collision energies used were optimized to reduce the relative abundances of precursor ions of approximately 50%. The relative abundance of each ion was calculated by comparing its intensity with the intensity of the base peak of each spectrum. The results presented correspond to the mathematical average of the three independent analyses.

Quadrupole time-of-flight

Samples were introduced into the electrospray source at a flow rate of 10 μl min^{-1}. The cone voltage was set at 35 V, and the capillary voltage was set at 3 kV. The source temperature was set at 80 °C, and the desolvation temperature was set at 150 °C. Tandem mass spectra (MS^2) were obtained by collision-induced dissociation (CID) using argon as the collision gas (measured pressure in the Penning gauge $\sim 6 \times 10^{-5}$ mbar). In MS and MS^2 experiments, TOF resolution was set to approximately 9000 FWHM (full-width at half-maximum). The collision energy used for sodium adducts was 30 eV for all studied compounds. Data acquisition was carried out with a MassLynx 4 data system.

Triple quadrupole

Samples were introduced into the electrospray source at a flow rate of 8 μl min^{-1}. The cone voltage was set at 35 V, and the capillary voltage was set at 3 kV. The source temperature was set at 80 °C, and the desolvation temperature was set at 150 °C. Tandem mass spectra were obtained using argon as the collision gas. The gas pressure in the Q2 collision cell was approximately 1.4×10^{-3} mbar. The collision energy used for sodium adducts was 35 eV for all studied compounds. Data acquisition was carried out with a MassLynx 4 data system.

Linear ion trap

Samples were introduced into the mass spectrometer at 10 μl min^{-1}. Electrospray conditions were as follows: nitrogen sheath gas was set at 30 psi along with spray voltage of 5.5 kV, heated capillary temperature of 350 °C, capillary voltage of 1 V, and tube lens voltage of 40 V. MS^n experiments were performed on mass selected precursor ions using standard isolation and excitation procedures (activation *q* value of 0.25 and activation time of 30 ms). The collision energy used for the sodium adducts was 20 arbitrary units for all studied compounds. Data acquisition was carried out with an Xcalibur data system.

Microbiology

Biological studies were carried out on *H. pylori* reference strain NCTC 11637 obtained from the National Collection of Type Cultures (London, UK).

Helicobacter pylori growth conditions

Helicobacter pylori cells were maintained as stock cultures in Trypticase Soy Broth with 20% glycerol, recovered on prewarmed Gelose Columbia solid medium supplemented with 5% horse blood (bioMérieux, Craponne, France), and incubated at 37 °C for 72 h on a microaerophilic atmosphere generated by a CampyGen gas pack (Oxoid, Basingstoke, UK). This strain was previously characterized, under the above-mentioned growth conditions, as producing approximately 40 μg of *O*-chain material/mg biomass of which approximately 7–10% corresponds to Lewis determinants [43].

Helicobacter pylori purity assessment

Helicobacter pylori purity was ensured by using a highly specific peptide nucleic acid probe (PNA) in a fluorescence in situ hybridization procedure according to the protocol described by Guimarães and coworkers [44]. For every experiment, a negative control was performed simultaneously, where all of the steps described above were carried out but no probe was added during the hybridization procedure. Microscopy visualization was performed using an Olympus BX51 epifluorescence microscope (Olympus Portugal, Porto, Portugal) equipped with one filter sensitive to the Alexa Fluor 594 signaling molecule attached to the PNA probe (excitation 530–550 nm, barrier 570 nm, and emission LP 591 nm).

Isolation of H. pylori cell surface Lewis determinants

Approximately 100 mg of *H. pylori* NCTC 11637 cells were subjected to hot phenol/water extraction according to Westphal and Jann [45] for extraction of cell surface glycans. The aqueous layer was dialyzed against distilled water using a 1000 Da cutoff membrane and lyophilized. This extract was then treated with 1% acetic acid at 100 °C for 1 h to cleave the lipid A moiety of the LPS through an acid-labile ketosidic linkage [17]. The insoluble lipid A was removed by gentle centrifugation, whereas oligosaccharides resulting from this treatment containing Lewis determinants were isolated by gel permeation chromatography (GPC) in the inclusion volume of polyacrylamide Bio-Gel P-2 column (0.65 m length and 1.14 cm diameter). Elution was performed using distilled water as the eluting solvent at a constant flow rate of 0.33 ml min^{-1}. The fraction with lower molecular weight included in the Bio-Gel column was used for ESI–MS analysis on the three mass spectrometers (Q-TOF, QqQ, and LIT).

Results

On ionization under electrospray conditions, all Lewis trisaccharides (Le^a and Le^x) and tetrasaccharides (Le^b and Le^y) ionized preferentially as sodium adducts, $[M+Na]^+$, with *m/z* 552 and 698, respectively. From the literature available on oligosaccharide structural characterization, the structural information obtained is intimately dependent on the instrumentation used, as described for hexose disaccharides [39]. In the following sections, the MS^n data obtained for the type 1 and type 2 oligosaccharides acquired in different mass instruments (Q-TOF, QqQ, and LIT) are described and discussed. The product ion spectra (MS^2) obtained for the trisaccharides, $[Le^a+Na]^+$ and $[Le^x+Na]^+$, using the three different mass spectrometers are shown in Figs. 2 and 3, respectively, and the product ion spectra obtained for the tetrasaccharides, $[Le^b+Na]^+$ and $[Le^y+Na]^+$, are shown in Figs. 4 and 5, respectively.

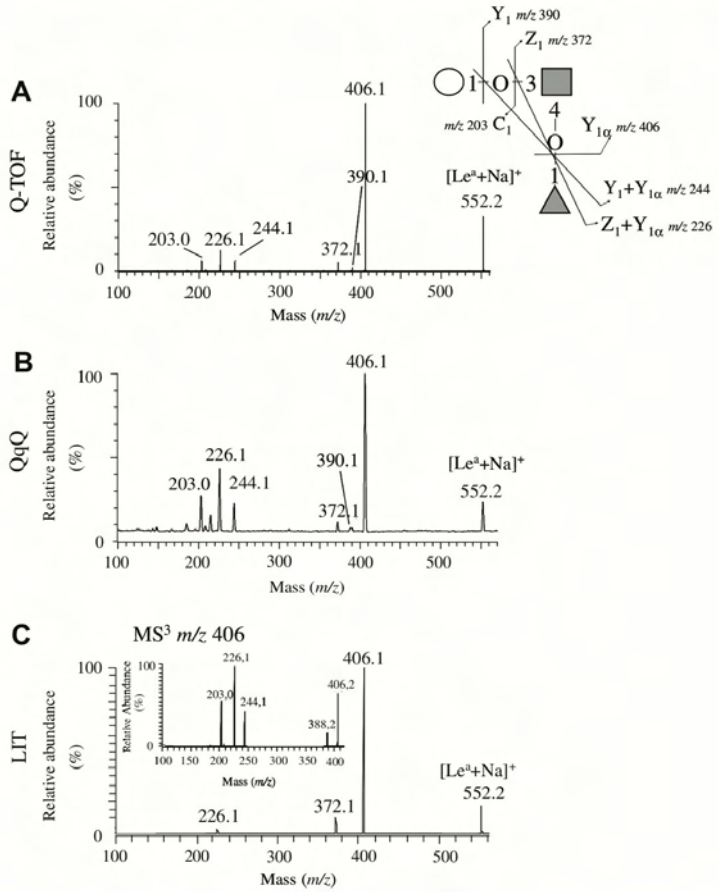

Fig. 2. ESI–MS^2 spectra of type 1 [Le^a+Na]$^+$ obtained in three mass spectrometers—Q-TOF (A), QqQ (B), and LIT (C)—and schematic presentation of the most relevant fragmentation pathways. ○, Gal; ■, GlcNAc; ▲, Fuc.

Fragmentation of Le^a

Fig. 2A shows the [M+Na]$^+$ product ion spectra of the type 1 trisaccharide, Le^a, at m/z 552 and detected using a Q-TOF instrument. When induced to fragmentation by collision with a gas, a major product ion was observed at m/z 406 ($Y_{1\alpha}$ fragmentation, according to Domon and Costello [32]), attributed to [Gal-GlcNAc+Na]$^+$, due to the loss of an *O*-4-linked fucose residue (−146 Da, Fuc_{res}). Other product ions of lower relative abundance were observed at m/z 372 (Z_1 fragmentation), attributed to [Fuc-GlcNAc$_{res}$+Na]$^+$, by loss of an *O*-3-linked Gal unit (−180 Da), at m/z 226 (Z_1+$Y_{1\alpha}$ fragmentations), attributed to [GlcNAc$_{res}$+Na]$^+$, due to the combined loss of $(Fuc+Gal)_{res}$ (−326 Da), at m/z 390 (Y_1 fragmentation), attributed to [Fuc-GlcNAc+Na]$^+$, by loss of *O*-3-linked Gal_{res} (−162 Da), at m/z 244 (Y_1+$Y_{1\alpha}$ fragmentations), attributed to [GlcNAc+Na]$^+$, by loss of *O*-4-linked Fuc_{res} (−146 Da) and *O*-3-linked Gal_{res} (−162 Da), and at m/z 203 (C_1 fragmentation), attributed to [Gal+Na]$^+$, by loss of Fuc-GlcNAc$_{res}$ (−372 Da).

The [M+Na]$^+$ product ion spectra of Le^a, at m/z 552, obtained with a QqQ instrument (Fig. 2B) showed the same product ions and relative intensities as those observed for the MS^2 spectra acquired in Q-TOF (Fig. 2A). However, when an LIT instrument was used, only the ions at m/z 406, 372, and 226 were detected (Fig. 2C). By performing ESI–MS^3 experiments involving the fragmentation of the ion at m/z 406 resultant from a loss of Fuc_{res} from the [Le^a+Na]$^+$ ion, it was also possible to observe the ions at m/z 244 and 203 (Fig. 2C, inset). In this fragmentation, a loss of water is also identified at m/z 388.

Fragmentation of Le^x

The [M+Na]$^+$ ion of the type 2 trisaccharide, Le^x, with m/z 552, when induced to fragmentation, gave origin to the major product ion at m/z 406 ($Y_{1\alpha}$ fragmentation), attributed to [Gal-GlcNAc+Na]$^+$, due to the loss of the *O*-3-linked Fuc_{res} (−146 Da) (Fig. 3). The product ion spectra obtained for the three instruments also showed a high relative abundance of a product ion at m/z 388, attributed to [Gal-GlcNAc$_{res}$+Na]$^+$, by loss of an *O*-3-linked Fuc (−164 Da), a fragment not observed in Le^a product ion spectra (Fig. 2). A small ion at m/z 390 (Y_1 fragmentation), corresponding to [Fuc-GlcNAc+Na]$^+$ by loss of *O*-4-linked Gal_{res} (−162 Da), was also observed in Le^x spectra of Q-TOF and LIT instruments. Product ions at m/z 305, resultant from the combined loss of Fuc_{res} (−146 Da) with a cross-ring cleavage $^{0,2}A_2$ (loss of $C_4H_7O_2N$, −101 Da) of the GlcNAc at the reducing end, at m/z 244 (Y_1+$Y_{1\alpha}$ fragmentations), attributed to [GlcNAc+Na]$^+$, by loss of *O*-3-linked Fuc_{res} (−146 Da) and *O*-4-linked Gal_{res} (−162 Da), at m/z 226 (Z_1+$Y_{1\alpha}$ fragmentations), attributed to [GlcNAc+Na]$^+$, due to the combined loss of $(Fuc+Gal)_{res}$ (−326 Da), and at m/z 203 (C_1 fragmentation), attributed to [Gal+Na]$^+$, by loss of

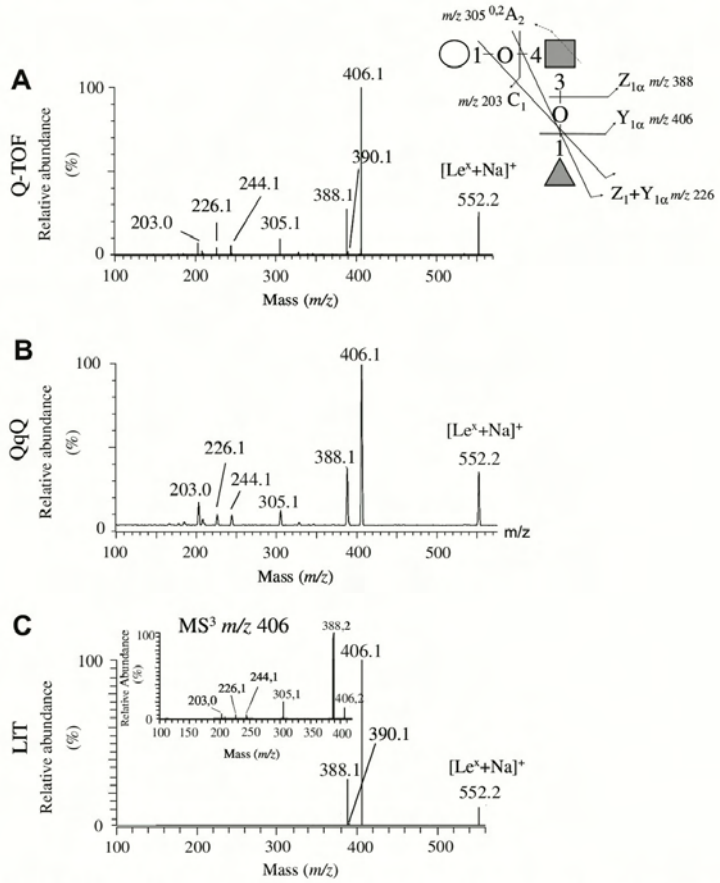

Fig. 3. ESI–MS^2 spectra of type 2 $[Le^x+Na]^+$ obtained in three mass spectrometers—Q-TOF (A), QqQ (B), and LIT (C)—and schematic presentation of the most relevant fragmentation pathways. ○, Gal; ■, GlcNAc; ▲, Fuc.

$Fuc\text{-}GlcNAc_{res}$ (−349 Da), were observed only in ESI–MS^2 obtained with Q-TOF and QqQ instruments (Fig. 3A and B). However, as was described for Le^a, all of these product ions can be further found in the ESI–MS^3 mass spectrum of the ion at m/z 406 obtained in the LIT analyzer (Fig. 3C, inset). From these, the product ion at m/z 305 was absent in Le^a product spectra from all instruments (Fig. 2).

Fragmentation of Le^b

The ESI–MS^2 spectra of $[M+Na]^+$ ion of the type 1 tetrasaccharide, Le^b, with m/z 698, when induced to fragment in Q-TOF (Fig. 4A) and QqQ (Fig. 4B) mass spectrometers, gave origin to two major product ions, at m/z 552 ($Y_{1\alpha}$ or $Y_{2\alpha}$ fragmentations), attributed to [(Fuc)Gal-GlcNAc+Na]$^+$ and [Gal-(Fuc)GlcNAc-+Na]$^+$, due to the combined loss of the *O*-2 or *O*-4-linked Fuc_{res} (−146 Da) from either the Gal or GlcNAc residue, and at m/z 406 ($Y_{1\alpha}+Y_{2\alpha}$ fragmentations), attributed to [Gal-GlcNAc+Na]$^+$, due to the loss of two Fuc_{res} (−292 Da). In the ESI–MS^2 spectrum obtained in an LIT instrument (Fig. 4C), however, the product ion at m/z 552 was the most abundant one.

The MS^2 acquired in the Q-TOF, QqQ, and LIT instruments all exhibited an additional less abundant ion at m/z 372 (Z_1 fragmentation), attributed to $[Fuc\text{-}GlcNAc_{res}+Na]^+$, due to the combined loss of Fuc_{res} (−146 Da) plus the Gal (−180 Da) *O*-3 linked to the GlcNAc. The loss of an *O*-3-linked Gal as a full unit originating the product ion at m/z 372 was also observed for type 1 trisaccharide Le^a (Fig. 3). Other small-intensity product ions were also present in Q-TOF and QqQ instruments at m/z 390 (Y_1 fragmentation), attributed to $[Fuc\text{-}GlcNAc+Na]^+$, by the combined loss of *O*-3-linked Gal_{res} (−162 Da) plus Fuc_{res} (−146 Da), at m/z 349 (C_1 fragmentation), attributed to [Fuc-Gal+Na]$^+$, by the combined loss of $GlcNAc_{res}$ (−203 Da) plus Fuc_{res} (−146 Da), at m/z 331 (B_1 fragmentation), attributed to $[Fuc\text{-}Gal_{res}+Na]^+$, by the combined loss of GlcNAc (−221 Da) plus Fuc_{res} (−146 Da), at m/z 244 ($Y_1+Y_{1\alpha}$ fragmentations), attributed to [GlcNAc+Na]$^+$, at m/z 226 ($Z_1+Y_{1\alpha}$ fragmentations), attributed to $[GlcNAc_{res}+Na]^+$, and at m/z 203 ($C_1+Y_{2\alpha}$ fragmentations), attributed to [Gal+Na]$^+$. In the MS^3 spectra of ion at m/z 552 obtained in the LIT instrument (Fig. 4C, inset), it was possible to further identify the ions at m/z 349 and 226. The MS^3 of the ion at m/z 406 for Le^b (data not shown) originated a spectrum equal to the one exhibited for type 1 trisaccharide Le^a (Fig. 2C, inset).

Fragmentation of Le^y

The ESI–MS^2 spectra of $[M+Na]^+$ of type 2 tetrasaccharide, Le^y, with m/z 698, when obtained from Q-TOF (Fig. 5A) and QqQ (Fig. 5B) analyzers, exhibit the same two major product ions

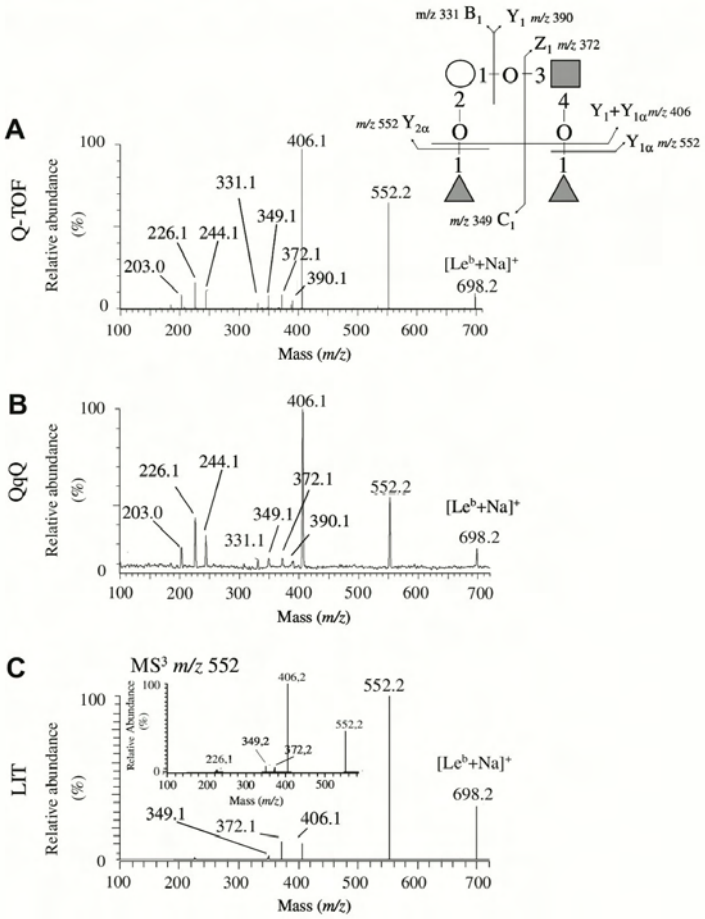

Fig. 4. ESI–MS^2 spectra of type 1 [Le^b+Na]$^+$ obtained in three mass spectrometers—Q-TOF (A), QqQ (B), and LIT (C)—and schematic presentation of the most relevant fragmentation pathways. ○, Gal; ■, GlcNAc; ▲, Fuc.

observed previously for Le^b: at *m/z* 552 ($Y_{1\alpha}$ or $Y_{2\alpha}$ fragmentations), attributed to [(Fuc)Gal-GlcNAc+Na]$^+$ and [Gal-(Fuc)GlcNAc+Na]$^+$, due to the loss of the *O*-2- or *O*-3-linked Fuc_{res} (−146 Da) from either the Gal or GlcNAc residue, and at *m/z* 406 ($Y_{1\alpha}$+$Y_{2\alpha}$ fragmentations), attributed to [Gal-GlcNAc+Na]$^+$, due to the combined loss of two Fuc_{res} (−292 Da). In an LIT analyzer, as observed previously for Le^b (Fig. 4C), only the product ion at *m/z* 552 was found to be the most abundant (Fig. 5C).

The Le^y MS^2 spectra obtained for the three instruments also presented high relative abundance of the product ion at *m/z* 534 ($Z_{2\alpha}$ fragmentation), attributed to [(Fuc)-Gal-$GlcNAc_{res}$+Na]$^+$, due to the loss of Fuc (−164 Da). The MS^3 fragmentation of this ion originated the product ions at *m/z* 388, attributed to [Gal-$GlcNAc_{res}$+Na]$^+$, at *m/z* 349 (C_1 fragmentation), attributed to [Fuc-Gal+Na]$^+$, and at *m/z* 331 (B_1 fragmentation), attributed to [Fuc-Gal_{res}+Na]$^+$ (Fig. 6). The absence of the ion at *m/z* 372 (Z_1 fragmentation), diagnostic of [Fuc-$GlcNAc_{res}$+Na]$^+$, unequivocally demonstrates that this fragmentation occurs only through the *O*-3-linked Fuc to GlcNAc. The loss of an *O*-3-linked Fuc unit had already been observed for the product ion spectra of Le^x (Fig. 3). Conversely, this specific fragmentation was not found in Le^a (Fig. 2) and Le^b (Fig. 4), where the Fuc is *O*-4 linked to the GlcNAc.

A less abundant product ion was also observed in all instruments at *m/z* 388 ($Y_{2\alpha}$+$Z_{1\alpha}$ fragmentations), attributed to [Gal-$GlcNAc_{res}$+Na]$^+$, due to the loss of an *O*-2 Fuc_{res} from the non-reducing Gal and an *O*-3 Fuc unit from the GlcNAc reducing end. This ion was also found in type 2 trisaccharide Le^x (Fig. 3), but it was absent in type 1 trisaccharides (Le^a, Fig. 2) and tetrasaccharides (Le^b, Fig. 4). This observation reinforces the previous statement that the loss of Fuc as a unit was observed only in type 2 structures, namely Le^x and Le^y, where this sugar is *O*-3 linked to GlcNAc.

All minor product ions observed in both Q-TOF and QqQ MS^2 spectra of Le^y were also observed in Le^b (Fig. 4A and B) with the exception of the product ion at *m/z* 305. This ion, also observed previously in Le^x MS^2 spectra (Fig. 3A and B), is the result, in Le^y, of a combined loss of two Fuc_{res} (−146 Da) plus a cross-ring cleavage $^{0,2}A_2$ (loss of $C_4H_7O_2N$, −101 Da) of the GlcNAc at the reducing end.

The MS^3 product ion spectrum of [Le^y+Na]$^+$ at *m/z* 552, resultant from a loss of Fuc_{res}, acquired in an LIT instrument (Fig. 5C, inset), exhibited the product ions at *m/z* 406 (−146 Da, Fuc_{res}) and *m/z* 388 (−164 Da, Fuc). In this fragmentation, a loss of water was also identified at *m/z* 534. The MS^3 of the ion at *m/z* 406 for Le^y (data

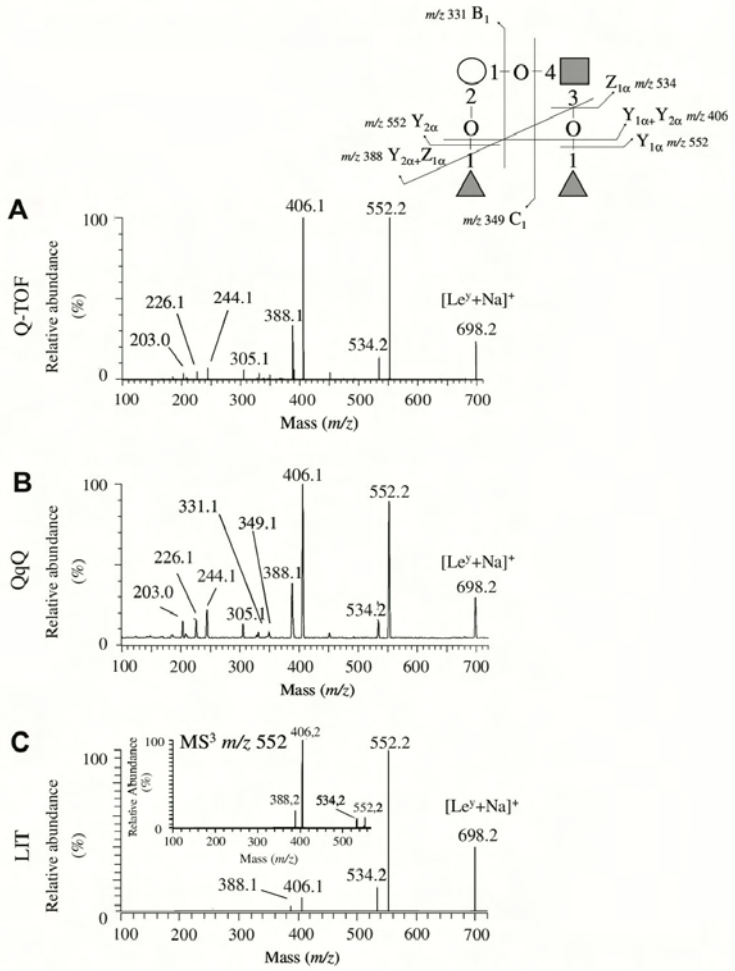

Fig. 5. ESI–MS^2 spectra of type 2 [Le^y+Na]$^+$ obtained in three mass spectrometers—Q-TOF (A), QqQ (B), and LIT (C)—and schematic presentation of the most relevant fragmentation pathways. ○, Gal; ■, GlcNAc; ▲, Fuc.

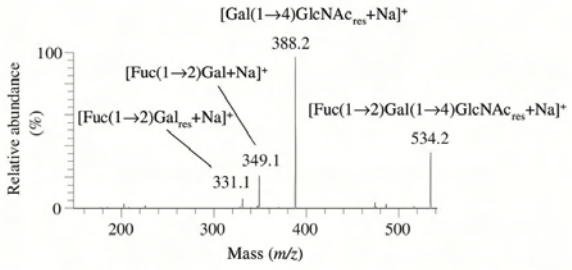

Fig. 6. ESI–MS^3 spectra of product ion at m/z 534 from type 2 [Le^y+Na]$^+$.

not shown) originated a spectrum equal to the one exhibited for type 1 trisaccharide Le^x (Fig. 3C, inset), where the ion at m/z 305 was observed.

Identification of Lewis antigens in the LPS of H. pylori NCTC 11637

To observe the feasibility of the described MS^n fragmentation specificities of Lewis blood groups, an experiment was designed for the identification of Lewis blood groups arising from the LPS of gram-negative bacterium *H. pylori* NCTC 11637.

Cell surface glycan-rich, low-molecular-weight fractions isolated on a Bio-Gel P2 column, when screened by ESI–MS, revealed the presence of cell surface oligosaccharides belonging to the core and to the *O*-chain of the LPS. The presence of α-glucans was also detected [43]. A detailed list of the ions identified and their assignments is presented in Table 1, organized according to their origin. This approach allowed the identification in the ESI–MS spectra of the ions at m/z 552 and 698 (Fig. 7A), previously recognized as corresponding to the Lewis blood groups. These Lewis oligosaccharides were further induced to fragmentation so as to obtain their identification (Figs. 7B–F). The product ion spectrum (ESI–MS^2) of the ion at m/z 552 (Fig. 7B) exhibited the product ion at m/z 406 (Fig. 7C). The ESI–MS^3 data obtained for the m/z 406 product ion gave origin to the product ion spectrum characteristic of the trisaccharide Le^x (Fig. 3). The ESI–MS^2 product ion spectrum of the ion at m/z 698 (Fig. 7D) showed two major ions with m/z 552 and 406. The ESI–MS^3 data obtained for the product ion at m/z 552 (Fig. 7E) and 406 (Fig. 7F) gave origin to the product ion spectra characteristic of the tetrasaccharide Le^y (Fig. 4). All of the identified

Table 1
Identified ions in the ESI–MS spectra of low-molecular-weight glycan-rich fractions from *H. pylori* NCTC 11637.

Assignment	$[M+Na]^+$ (m/z)
LPS	
Core	
Hep-Hep	425
Hep(P)-Kdo	533
Hep-Hep(EAP)	535
Hep(EAP)-Kdo	563
Hex-Hex-Hep	557
Hep-Hep-Kdo	645
Hex-Hex-Hep-Hep	749
Hep-Hep(EAP)	755
Hep-Hep-Hep(EAP)-Kdo	947
O-antigen chain	
LacNAc	406
Le^x	552
Le^y	698
Le^x-Gal	714
α-Glucan	
Glc-Glc	365
Glc-Glc-Glc	527
Glc-Glc-Glc-Glc	689
Glc-Glc-Glc-Glc-Glc	851
Glc-Glc-Glc-Glc-Glc-Glc	1013
Glc-Glc-Glc-Glc-Glc-Glc-Glc	1175

Note: Hep, heptose; P, phosphate; Kdo, 3-deoxy-D-*manno*-octulosonic acid; AEP, 2-aminoethylphosphate; LacNAc, Gal(1→4)GlcNAc.

structures were in agreement with what was previously described to be the Lewis expression pattern for this strain [46,47].

Discussion

The main product ions resulting from fragmentation of type 1 $[Le^a+Na]^+$ (Fig. 2) and $[Le^b+Na]^+$ (Fig. 4) and of type 2 $[Le^x+Na]^+$ (Fig. 3) and $[Le^y+Na]^+$ (Fig. 5) are summarized graphically in Fig. 8. Graphical observation highlights that the ion at m/z 406, attributed to [Gal-GlcNAc+Na]$^+$, is common to all tri- and tetrasaccharide Lewis antigens in all mass spectrometers used (Fig. 9). The same observation is valid for the ion at m/z 552, attributed to [(Fuc)-Gal-GlcNAc+Na]$^+$, in the case of Le^b and Le^y tetrasaccharides. The ions at m/z 390, attributed to [Fuc-GlcNAc+Na]$^+$, at m/z 349, attributed to [Fuc-Gal+Na]$^+$, at m/z 244, attributed to [GlcNAc+Na]$^+$, at m/z 226, attributed to [$GlcNAc_{res}$+Na]$^+$, and at m/z 203, attributed to [Gal+Na]$^+$, are commonly found in all antigens (Figs. 2–5). Therefore, these product ions, although diagnostic for the presence of these Lewis structures, cannot be used for the distinction of their type.

Type 1 oligosaccharides are specifically characterized by the ion at m/z 372, attributed to [Fuc-$GlcNAc_{res}$+Na]$^+$, resultant of the loss, from the GlcNAc residue, of an *O*-3-linked Gal as a sugar unit. Conversely, type 2 oligosaccharides are specifically characterized by the ion at m/z 388, attributed to [Gal-$GlcNAc_{res}$+Na]$^+$, resultant of the loss, from the GlcNAc residue, of an *O*-3-linked Fuc as a sugar unit. The product ion at m/z 534, attributed to

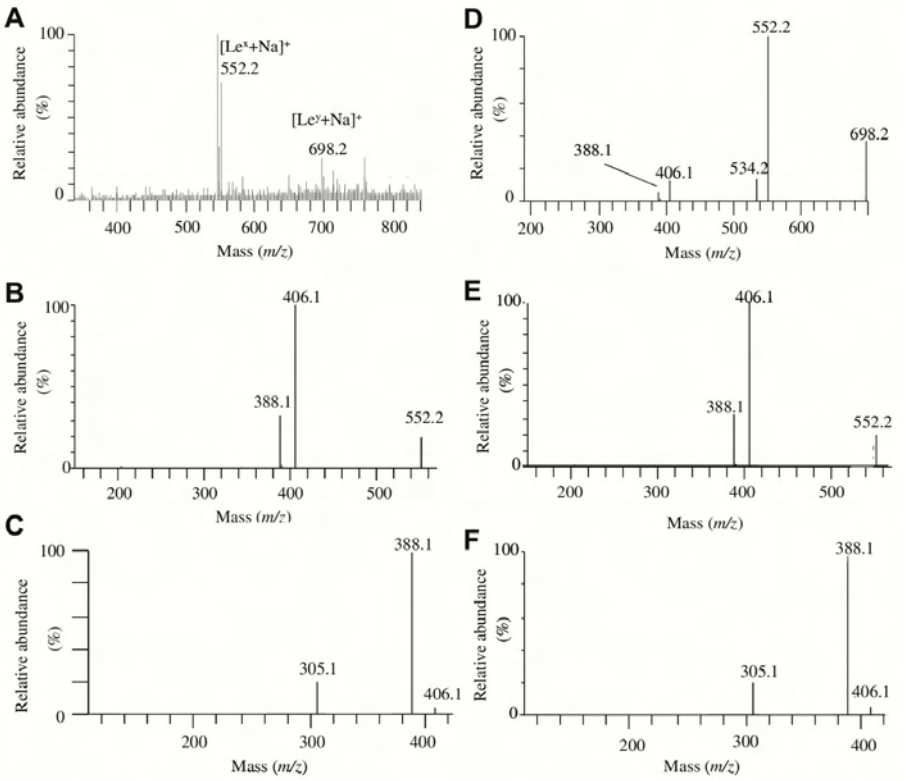

Fig. 7. MS spectra of *H. pylori* glycan-rich fraction isolated by GPC on a Bio-Gel P2 yielding type 2 Le^x and Le^y antigens: (A) ESI–MS; (B) ESI–MS^2 of the ion at m/z 552; (C) ESI–MS^3 of the ion at m/z 406 from the ion at m/z 552; (D) ESI–MS^2 of the ion at m/z 698; (E) ESI–MS^3 of the ion at m/z 552 from the ion at m/z 698; (F) ESI–MS^4 of the ion at m/z 406 from the ion at m/z 552 derived from the ion at m/z 698.

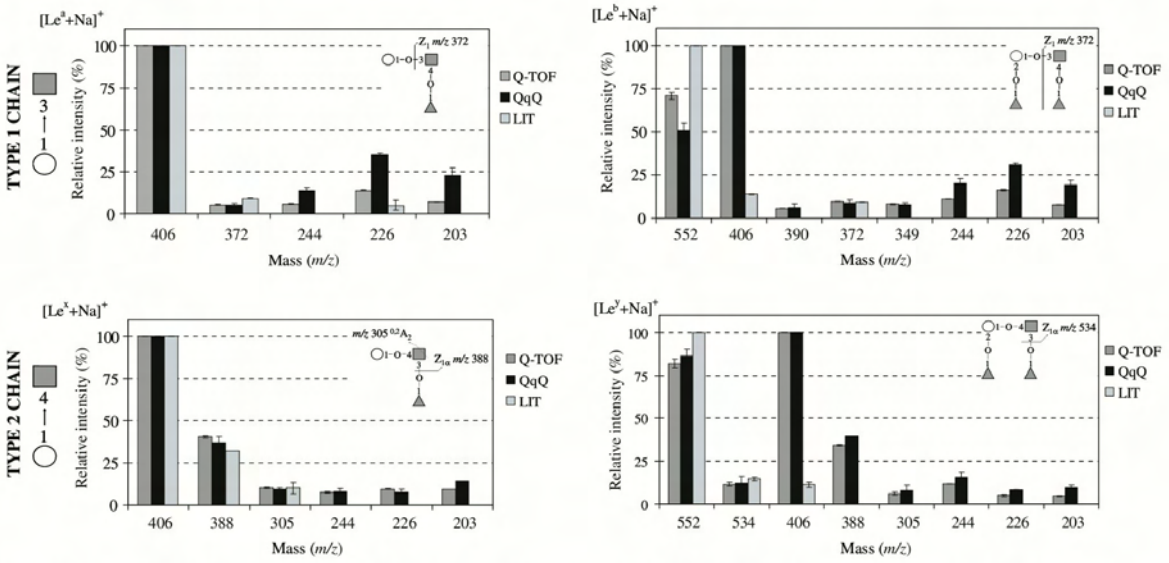

Fig. 8. Graphical summary of the ions obtained from the fragmentation of $[M+Na]^+$ of type 1 (Le^a and Le^b) and type 2 (Le^x and Le^y) Lewis antigens in three mass spectrometers (Q-TOF, QqQ, and LIT). Relative intensities are calculated by comparison with the base peak. Only ions with a relative abundance higher than 5% are considered in this figure. ○, Gal; ■, GlcNAc; ▲, Fuc.

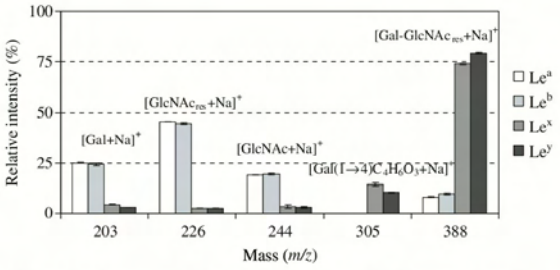

Fig. 9. Graphical summary of the ions obtained from MS^n fragmentation of the ion at m/z 406 of type 1 (Le^a and Le^b) and type 2 (Le^x and Le^y) Lewis antigens. Relative intensities are calculated by comparison with the base peak. Only ions with a relative abundance higher than 5% are considered in this figure.

$[Fuc\text{-}Gal\text{-}GlcNAc_{res}+Na]^+$, resultant of the loss, from the GlcNAc residue, of an *O*-3-linked Fuc as a sugar unit, was found exclusively in type 2 Lewis tetrasaccharides. Conversely, type 2 Lewis tetrasaccharides do not present this fragmentation. Therefore, it can be stated that the sugars *O*-3 linked to the GlcNAc are susceptible to being lost as sugar residues as well as sugar units, whereas the sugars *O*-4 linked to the GlcNAc are lost only as sugar residues, giving fragment ions with less −18 Da. This different behavior is responsible for the origin of diagnostic ions that can be used to distinguish type 1 from type 2 oligosaccharides and, as a result, of the trisaccharide isomers Le^a/Le^x based on the pair of fragment ions at m/z 372/388 and the tetrasaccharide isomers Le^b/Le^y based on the pair of fragment ions at m/z 372/534.

To evaluate the influence of the anomeric carbon of GlcNAc on the different fragmentation behavior demonstrated by *O*-3-linked Lewis sugar residues, the aldehyde group of all four Lewis oligosaccharides under study was reduced with sodium borohydride [42]. Under these conditions, type 1 and type 2 Lewis alditols showed similar fragmentation behavior with no observed losses as sugar units (results not shown). This experiment demonstrates that the presence of an aldehyde or its linkage forms of hemiacetal/acetal in GlcNAc strongly influences the observed fragmentation. Also, according to the literature [25], the presence of an acetoamide group in the *O*-2 position of GlcNAc might induce a deprotection effect on the neighboring protons. Such an effect might promote the fragmentation of the *O*-3-linked sugar residue as sugar unit as well as a sugar residue.

The fragment ion at m/z 305, resultant from the combined loss of Fuc_{res} plus a $^{0,2}A_2$ ring cleavage at the reducing end of the GlcNAc residue, was also found to be present only among type 2 Lewis structures, being a further aid in structural assignments.

Taking advantage of an LIT instrument to perform successive MS experiments (MS^n), further fragmentation of the ion at m/z 406, attributed to $[Gal\text{-}GlcNAc+Na]^+$, was induced. As a result of their distinct linkage pattern, type 1 and type 2 also exhibit differentiated product ion spectra of the ion at m/z 406. The graph in Fig. 8 shows that the ESI–MS^3 fragmentation of $[Gal\text{-}(1\rightarrow3)\text{-}GlcNAc+Na]^+$, present in type 1, gave ions at m/z 203, 226, and 244 that showed higher relative abundance (>20% vs. the base peak) than those obtained by the fragmentation of $[Gal\text{-}(1\rightarrow4)\text{-}GlcNAc+Na]^+$ (<5% of the base peak), present in type 2. Conversely, the product ion at m/z 388 is much less abundant in type 1 structures (<15%) than in type 2 structures (>75%). Also, the ion at m/z 305 is found only in type 2 product ion spectra. Relying on these characteristics, it is possible, taking advantage of LIT capability of performing MS^n experiments, to identify the isomeric core structure base on the fragmentation of the product ion disaccharide sodium adducts at m/z 406.

To evaluate the possibility of identifying Lewis isomers within a mixture, the Le^a/Le^x trisaccharides and Le^b/Le^y tetrasaccharides were combined in different proportions (1:9, 1:1, and 9:1). The resulting product ion spectra arising from the ions at m/z 552 and 698 revealed the common fragments to both isomers and allowed the corresponding diagnostic ions to be observed (data not shown). However, independent of the proportion of each isomer in the mixture, type 2 diagnostic ions at m/z 388 and 305, as well as at m/z 534 in the case of Le^y, are always more abundant than type 1 diagnostic ion at m/z 372. These results show that the distinction between isomers within a mixture is possible without

the requirement for more purification steps such as chromatographic approaches, gel electrophoresis, and immunoseparation-based assays.

In the current work, we have demonstrated that all commonly used ESI–MS analyzers were found to be suitable for distinguishing Lewis blood group isomers, namely the trisaccharides Le^a/Le^x and the tetrasaccharides Le^b/Le^y, in positive mode based on the characteristic fragmentation of their $[M+Na]^+$ ions. This observation reveals itself to be of primary importance given that the analysis time scales and energy deposition methods differ among these tandem MS instruments, originating differences between their MS^2 spectra. Thus, the comparison performed in this study was important by showing that analysis of Lewis determinants using ESI–MS in positive mode approach can be generally applicable on a variety of instrumental platforms. However, as can be seen, the product ion spectra obtained for the tri- and tetrasaccharides in each mass spectrometer exhibited slight differences when compared with each other. These differences are not unusual and have been found for other biomolecules [39,48], and they further corroborate the need to evaluate the MS^2 behavior under different instrumental conditions. Thus, in the LIT MS^2, the precursor ion is specifically activated via resonant excitation, usually resulting in only primary fragments. By contrast, QqQ and Q-TOF MS^2 involves relatively nonspecific activation whereby all precursor ions are accelerated through a potential difference. In this way, primary fragments can experience further activation, leading to secondary fragmentation products.

To demonstrate the effectiveness of ESI–MS^2 and MS^n in positive mode in providing successful identification of the Lewis expression pattern of the Gram-negative human pathogenic bacteria *H. pylori*, analyses were carried out in glycan-rich water extracts from *H. pylori* reference strains NCTC 11637 containing vestigial amounts of free Lewis antigens (nmol to fmol range) in a partially purified complex biological matrix. The results shown in Fig. 6 allowed the identification of type 2 Lewis structures, namely the trisaccharide Le^x and the tetrasaccharide Le^y, in accordance with what was described previously for this strain [45,46]. All three instruments were shown to be suitable to fulfill this task.

Until now, serological methods such as hemagglutination inhibition assays [49], serodot [50,51], enzyme-linked immunosorbent assay (ELISA) [50–53], and Western blotting [50,54] have been used routinely to assess the Lewis antigen expression on *H. pylori*. A comparative study performed by Hynes and Moran [50] on several *H. pylori* strains showed that the use of only one of these methods may fail to detect Lewis antigens, further suggesting that the combination of at least two methods would be required to achieve unequivocal results. In addition, whenever considering serological approaches, it should be accounted that complex biological matrices can hinder antigenic responses or lead to erroneous outputs. Chemical analysis has already demonstrated the Lewis antigen expression in strains initially considered by serology as Lewis negative [55]. Furthermore, differences between Lewis antigen expression detected by chemical and serological analyses have been noted [56]. Thus, chemical and instrumental methods are regarded as more precise and direct approaches because they base detection directly on the molecule. In the current work, it was demonstrated that the use of two simple isolation/prepurification steps, such as phenol/water extraction and gel permeation chromatography, allows one to generate reliable results based on spectral output from a complex matrix when using MS.

Mass spectrometers are commonly present in modern laboratories and part of a day-to-day routine fulfilling a broad range of applications far beyond the scope of Lewis analysis. If that is the case, the determination of Lewis profiles can be easily performed without the need for further considerable investment. Conversely, in the case of serological methods, continuous investment in monoclonal antibodies is to be considered whenever a set of analyses is required. In conclusion, the MS approach described here can be employed as a highly sensitive and reliable method to analyze Lewis antigens.

Acknowledgments

The authors gratefully acknowledge the financial support provided by the project POCI/QUI/59337/2004 and Research Units 62/94-QOPNA, Fundação para a Ciência e a Tecnologia (FCT)-financed project Pylori E&LPS POCI/QUI/56393/2004, PhD Grant SFRH/BD/19929/2004, and the Natural Sciences and Engineering Research Council of Canada (NSERC).

References

[1] A. Varki, Biological roles of oligosaccharides: all of the theories are correct, Glycobiology 3 (1993) 97–130.
[2] R.A. Dwek, T.D. Butters, Glycobiology: understanding the language and meaning of carbohydrates, Chem. Rev. 102 (2002) 283–284.
[3] F. Dall'Olio, Protein glycosylation in cancer biology: an overview, J. Clin. Pathol. 49 (1996) 126–135.
[4] C. Couldrey, J.E. Green, Metastases: the glycan connection, Breast Cancer Res. 2 (2000) 321–323.
[5] T. Feize, Carbohydrate-mediated recognition systems in innate immunity, Immunol. Rev. 173 (2002) 79–88.
[6] C. Garcher, J. Bara, A. Bron, R. Oriol, Expression of mucin peptide and blood group ABH- and Lewis-related carbohydrate antigens in normal human conjunctiva, Invest. Ophthalmol. Vis. Sci. 35 (1994) 1184–1191.
[7] M.V. Croce, M. Isla-Larrain, M.E. Rabassam, S. Demichelis, A.G. Colussi, M. Crespo, E. Lacunza, A. Segal-Eiras, Lewis x is highly expressed in normal tissues: a comparative immunohistochemical study and literature revision, Pathol. Oncol. Res. 13 (2007) 130–138.
[8] R. Oriol, J.L. Pendu, R. Mollicone, Genetics of ABO, H, Lewis, X, and related antigens, Vox Sang. 51 (1986) 161–171.
[9] J.L. Pendu, S. Marionneau, A. Cailleau-Thomas, J. Rocher, B. Le Moullac-Vaidye, M. Clément, ABH and Lewis histo-blood group antigens in cancer, Acta Pathol. Microbiol. Immunol. Scand. 109 (2001) 9–31.
[10] H. Kimura, T. Kitamori, T. Sawada, Critical increment of Lewis blood group antigen in serum by cancer found by photothermal immunoassay, Anal. Biochem. 274 (1999) 98–103.
[11] R. Kannagi, Molecular mechanism for cancer-associated induction of sialyl Lewis X and sialyl Lewis A expression: the Warburg effect revisited, Glycoconj. J. 20 (2004) 353–364.
[12] I.M. Brockhausen, Mucin-type *O*-glycans in human colon and breast cancer: glycodynamics and functions, EMBO Rep. 7 (2006) 599–604.
[13] F. Carvalho, L. David, J.P. Aubert, A. López-Ferrer, C.D. Bolos, C. Reis, F. Gärtner, A. Peixoto, P. Alves, M. Sobrinho-Simões, Mucins and mucin-associated carbohydrate antigens expression in gastric carcinoma cell lines, Virchows Arch. 435 (1999) 479–485.
[14] G.F. Springer, P. Williamson, W.C. Brandes, Blood group activity of gram-negative bacteria, J. Exp. Med. 113 (1961) 1077–1093.
[15] B.E. Dunn, H. Cohen, M.J. Blaser, *Helicobacter pylori*, Clin. Microbiol. Rev. 10 (1997) 720–741.
[16] B.J. Appelmelk, M.A. Monteiro, S.L. Martin, A.P. Moran, C.M.J.E. Vandenbroucke-Grauls, Why *Helicobacter pylori* has Lewis antigens, Trends Microbiol. 8 (2000) 565–570.
[17] M.A. Monteiro, *Helicobacter pylori*—a wolf in sheep's clothing: the glycotype families of *Helicobacter pylori* lipopolysaccharides expressing histo-blood groups: structure, biosynthesis, and role in pathogenesis, Adv. Carbohydr. Chem. Biochem. 57 (2001) 99–158.
[18] B.S. Sheu, J.J. Wu, Type 1 and type 2 antigens of *Helicobacter pylori:* a potential marker of human geographical distribution, J. Med. Microbiol. 57 (2008) 543–544.
[19] G.F. Springer, P. Williamson, B.L. Readler, Blood group active gram-negative bacteria and higher plants, Ann. NY Acad. Sci. 97 (2006) 104–110.
[20] D.J. Harvey, Matrix-assisted laser desorption/ionization mass spectrometry of carbohydrates, Mass Spectrom. Rev. 18 (1999) 349–450.
[21] A. Dell, H.R. Morris, Glycoprotein structure determination by mass spectrometry, Science 291 (2001) 2351–2356.
[22] J. Zaia, Mass spectrometry of oligosaccharides, Mass Spectrom. Rev. 23 (2004) 161–277.
[23] A. Reis, P. Domingues, M.A. Coimbra, M.R.D. Domingues, Positive and negative electrospray ionisation tandem mass spectrometry as a tool for structural characterisation of acid released oligosaccharides from olive pulp glucuronoxylans, Carboydr. Res. 338 (2003) 1497–1505.
[24] W. Chai, V. Piskarev, A.M. Lawson, Negative-ion electrospray mass spectrometry of neutral underivatized oligosaccharides, Anal. Chem. 73 (2001) 651–657.

[25] H. Suzuki, T. Yamagaki, K. Tachibana, F. Fukui, Fragmentation of Lewis-type trisaccharides in the gas phase: experimental and theoretical studies, Int. J. Mass Spectrom. 278 (2008) 1–9.
[26] A. Pfenninger, M. Karas, B. Finke, B. Stahl, Structural analysis of underivatized neutral human milk oligosaccharides in the negative ion mode by nano-electrospray MS^n (part 1), J. Am. Soc. Mass Spectrom. 13 (2002) 1331–1340.
[27] A.M. Lawson, W. Chai, G.C. Cashmore, M.S. Stoll, E.F. Hounsell, T. Feizi, High-sensitivity structural analyses of oligosaccharide probes (neoglycolipids) by liquid–secondary–ion mass spectrometry, Carbohydr. Res. 200 (1990) 47–57.
[28] W. Chai, J. Luo, C.K. Lim, A.M. Lawson, Characterization of heparin oligosaccharide mixtures as ammonium salts using electrospray mass spectrometry, Anal. Chem. 70 (1998) 2060–2066.
[29] S.G. Penn, M.T. Cancilla, C.B. Lebrilla, Collision-induced dissociation of branched oligosaccharide ions with analysis and calculation of relative dissociation thresholds, Anal. Chem. 68 (1996) 2331–2339.
[30] D.J. Harvey, T.S. Mattu, M.R. Wormald, L. Royle, R.A. Dwek, P.M. Rudd, Internal residue loss: rearrangements occurring during the fragmentation of carbohydrates derivatized at the reducing terminus, Anal. Chem. 74 (2002) 734–740.
[31] P.B. O'Connor, E. Mirgorodskaya, C.E. Costello, High pressure matrix-assisted laser desorption/ionization Fourier transform mass spectrometry for minimization of ganglioside fragmentation, J. Am. Soc. Mass Spectrom. 13 (2002) 402–407.
[32] B. Domon, C.E. Costello, A systematic nomenclature for carbohydrate fragmentations in FAB–MS/MS spectra of glycoconjugates, Glycoconj. J. 5 (1988) 397–409.
[33] M.D. Mohr, K.O. Bornsen, H.M. Widmer, Matrix-assisted laser desorption/ionization mass spectrometry: improved matrix for oligosaccharides, Rapid Commun. Mass Spectrom. 9 (1995) 809.
[34] M.T. Cancilla, S.G. Penn, J.A. Carrol, C.B. Lebrilla, Coordination of alkali metals to oligosaccharides dictates fragmentation behavior in matrix assisted laser desorption ionization/Fourier transform mass spectrometry, J. Am. Chem. Soc. 18 (1996) 6736–6745.
[35] U. Boesl, R. Weinkauf, E.W. Schlag, Reflectron time-of-flight mass spectrometry and laser excitation for the analysis of neutrals, ionized molecules, and secondary fragments, Int. J. Mass Spectrom. Ion Process. 112 (1992) 121–166.
[36] F.M. Nunes, A. Reis, A.M.S. Silva, M.R.M. Domingues, M.A. Coimbra, Rhamnoarabinosyl and rhamnoarabinoarabinosyl side chains as structural features of coffee arabinogalactans, Phytochemistry 69 (2008) 1573–1585.
[37] F.M. Nunes, A. Reis, M.R.M. Domingues, M.A. Coimbra, Characterization of galactomannan derivatives in roasted coffee beverages, J. Agric. Food Chem. 54 (2006) 3428–3439.
[38] A. Reis, P. Pinto, D.V. Evtuguin, C.P. Neto, P. Domingues, A.J. Ferrer-Correia, M.R. Domingues, Electrospray tandem mass spectrometry of underivatised acetylated xylo-oligosaccharides, Rapid Commun. Mass Spectrom. 19 (2005) 3589–3599.
[39] J. Simões, P. Domingues, A. Reis, F.M. Nunes, M.A. Coimbra, M.R.M. Domingues, Identification of anomeric configuration of underivatized reducing glucopyranosylglucose disaccharides by tandem mass spectrometry and multivariate analysis, Anal. Chem. 79 (2007) 5896–5905.
[40] N. Hashii, N. Kawasaki, S. Ithoh, A. Harazono, Y. Matsuishi, T. Hayakawa, T. Kawanishi, Specific detection of Lewis x-carbohydrates in biological samples using liquid chromatography/multiple-stage tandem mass spectrometry, Rapid Commun. Mass Spectrom. 19 (2005) 3315–3321.
[41] H. Towbin, C. Schoenenberger, D.G. Braun, G. Rosenfelder, Chromogenic labelling of milk oligosaccharides: purification by affinity chromatography and structure determination, Anal. Biochem. 173 (1988) 1–9.
[42] A. Reis, M.A. Coimbra, P. Domingues, A.J. Ferrer-Correia, M.R.M. Domingues, Fragmentation pattern of underivatised xylo-oligosaccharides and their alditol derivatives by electrospray tandem mass spectrometry, Carbohydr. Polym. 55 (2004) 401–409.
[43] J.A. Ferreira, C. Pires, M. Paulo, N.F. Azevedo, M.R. Domingues, M.J. Vieira, M.A. Monteiro, M.A. Coimbra, Bioaccumulation of amylose-like glycans by Helicobacter pylori, Helicobacter 14 (2009) 559–570.
[44] N. Guimarães, N.F. Azevedo, C. Figueiredo, C.W. Keevil, M.J. Vieira, Development and application of a novel peptide nucleic acid probe for the specific detection of *Helicobacter pylori* in gastric biopsy specimens, J. Clin. Microbiol. 45 (2007) 3089–3094.
[45] O. Westphal, K. Jann, Bacterial lipopolysaccharides: extraction with phenol–water and further applications of the procedure, Methods Carbohydr. Chem. 5 (1965) 83–91.
[46] G.O. Aspinall, M.A. Monteiro, H. Pang, E.J. Walsh, A.P. Moran, Lipopolysaccharide of the *Helicobacter pylori* type strain NCTC 11637 (ATCC 43504): structure of the *O* antigen chain and core oligosaccharide regions, Biochemistry 35 (1996) 2489–2497.
[47] B.J. Appelmelk, S.L. Martin, M.A. Monteiro, C.A. Clayton, A.A. McColm, P. Zheng, T. Verboom, J.J. Maaskant, D.H. van den Eijnden, C.H. Hokke, M.B. Perry, C.M.J.E. Vandenbroucke-Grauls, J.G. Kusters, Phase variation in *Helicobacter pylori* lipopolysaccharide, Infect. Immun. 66 (1998) 70–76.
[48] C. Simões, V. Simões, A. Reis, P. Domingues, M.R.M. Domingues, Determination of the fatty acyl profiles of phosphatidylethanolamines by tandem mass spectrometry of sodium adducts, Rapid Commun. Mass Spectrom. 22 (2008) 3238–3244.
[49] H.P. Wirth, M. Yang, E. Sanabria-Valentín, D.E. Berg, A. Dubois, M.J. Blaser, Host Lewis phenotype-dependent *Helicobacter pylori* Lewis antigen expression in rhesus monkeys, FASEB J. 20 (2006) 1534–1536.
[50] S.O. Hynes, A.P. Moran, Comparison of three serological methods for detection of Lewis antigens on the surface of *Helicobacter pylori*, FEMS Microbiol. Lett. 190 (2000) 62–67.
[51] N. Broutet, A.P. Moran, S. Hynes, C. Sakarovitch, F. Me'graud, Lewis antigen expression and other pathogenic factors in the presence of atrophic chronic gastritis in a European population, J. Infect. Dis. 185 (2002) 503–512.
[52] L. Muñoz, G. Gonzáles-Valencia, G.I. Pérez-Pérez, S. Giono-Cerezo, O. Muñoz, J. Torres, A comparison of Lewis X and Lewis Y expression in *Helicobacter pylori* obtained from children and adults, J. Infect. Dis. 183 (2001) 1147–1151.
[53] E. Altman, H. Fernández, V. Chandan, B.A. Harrison, M.W. Schuster, L.O. Rademacher, C. Toledo, Analysis of *Helicobacter pylori* isolates from Chile: occurrence of selective type 1 Lewis b antigen expression in lipopolysaccharide, J. Med. Microbiol. 57 (2008) 585–591.
[54] K.I. Amano, S. Hayashi, T. Kubota, N. Fujii, S.I. Yokota, Reactivities of Lewis antigen monoclonal antibodies with lipopolysaccharides of *Helicobacter pylori* strains isolated from patients with gastroduodenal diseases in Japan, Clin. Diagn. Lab. Immunol. 4 (1997) 540–544.
[55] Y.A. Knirel, N.A. Kocharova, S.O. Hynes, G. Widmalm, L.P. Andersen, P.E. Janson, A.P. Moran, Structural studies on lipopolysaccharides of serologically non-typable strains of *Helicobacter pylori* AF1 and 007, expressing Lewis antigenic determinants, Eur. J. Biochem. 26 (1999) 123–131.
[56] M.A. Monteiro, K.H.N. Chan, D.A. Rasko, D.E. Taylor, P.Y. Zheng, B.J. Appelmelk, H.P. Wirth, M. Yang, M.J. Blaser, S.O. Hynes, A.P. Moran, M.B. Perry, Simultaneous expression of type 1 and type 2 Lewis blood group antigens by *Helicobacter pylori* lipopolysaccharides: molecular mimicry between *H. pylori* lipopolysaccharides and human gastric epithelial cell surface glycoforms, J. Biol. Chem. 273 (1998) 11533–11543.

CHAPTER IV

BIOACCUMULATION OF AMYLOSE-LIKE GLYCANS BY *HELICOBACTER PYLORI*

Helicobacter

Helicobacter ISSN 1523-5378

Bioaccumulation of Amylose-Like Glycans by *Helicobacter pylori*

José A. Ferreira,* Cristiana Pires,* Marina Paulo,* Nuno F. Azevedo,† M. Rosário Domingues,* Maria João Vieira,† Mario A. Monteiro‡ and Manuel A. Coimbra*

*Departamento de Química da Universidade de Aveiro, Campus de Santiago, Aveiro, Portugal, †Centro de Engenharia Biológica, Universidade do Minho, Campus de Gualtar, Braga, Portugal, ‡Department of Chemistry, University of Guelph, Guelph, Canada

Keywords
Helicobacter pylori, cell-surface polysaccharide, glucan, environmental pressure.

Reprint requests to: Manuel A. Coimbra, Departamento de Química da Universidade de Aveiro, Campus de Santiago, 3810-193 Aveiro, Portugal. E-mail: mac@ua.pt

Abstract

Background: *Helicobacter pylori* cell surface is composed of lipopolysaccharides (LPSs) yielding structures homologous to mammalian Lewis *O*-chains blood group antigens. These structures are key mediators in the definition of host-microbial interactions and known to change their expression pattern in response to environmental pressure.

Aims: The present work is focused on the identification of new *H. pylori* cell-surface glycosides. Special attention is further devoted to provide insights on the impact of *in vitro* subcultivation on *H. pylori* cell-surface phenotypes.

Methods: Cell-surface glycans from *H. pylori* NCTC 11637 and two clinical isolates were recovered from the aqueous phase resulting from phenol:water extraction of intact bacteria. They were evaluated in relation to their sugars and glycosidic-linkages composition by CG-MS, size-exclusion chromatography, NMR, and Mass Spectrometry. *H. pylori* glycan profile was also monitored during subcultivation *in vitro* in agar and F12 liquid medium.

Results: All three studied strains produce LPS expressing Lewis epitopes and express bioaccumulate amylose-like glycans. Bioaccumulation of amylose was found to be enhanced with the subcultivation of the bacterium on agar medium and accompanied by a decrease in the expression of LPS *O*-chains. In contrast, during exponential growth in F12 liquid medium, an opposite behavior is observed, that is, there is an increase in the overall amount of LPS and decrease in amylose content.

Conclusions: This work shows that under specific environmental conditions, *H. pylori* expresses a phase-variable cell-surface α-(1→4)-glucose moiety.

Helicobacter pylori is a widespread Gram-negative bacterium that infects the gastric mucosa of humans leading to the onset of several gastric disorders, such as gastritis, gastric ulcers, and cancers [1,2]. Moreover, persistent infection with *H. pylori* is strongly associated with the risk of developing gastric cancer [2,3]. Therefore, the microorganism is recognized as a category (definitive) human carcinogen [4].

H. pylori is regarded as a highly fastidious organism, typically requiring 3 days of growth on complex media containing blood or serum in a low-oxygen atmosphere at 35–37 °C [5–7]. The fastidious nature of *H. pylori* has hampered the initial isolation of the microorganism from the human stomach and continues to be one of the major drawbacks in research progresses since its discovery. In fact, studies reporting the growth of the microorganism in broth, particularly in chemically defined liquid medium, are relatively scarce. A possible and most likely explanation for the difficulties encountered in the cultivation of *H. pylori* in vitro may reside on the inability to mimic special conditions encountered by this microorganism gastric niche. Thus, it can be considered that during growth outside the human reservoir *H. pylori* is submitted to a different environmental pressure.

As a Gram-negative bacterium, *H. pylori* expresses at its cell surface lipopolysaccharides (LPSs) that comprise, when biosynthetically complete, three structural domains: a polysaccharide (PS) known as *O*-chain, an oligosaccharide termed core, and a fatty-acid-rich endotoxin moiety named lipid A (LPS: *O*-chain → Core→Lipid A∼cell). Commonly found *O*-chains yield fucosylated glycoside structures analogous to some mammalian histo-blood-group antigens, such as Lewis

determinants (Le^a, Le^b, Le^x, sialyl Le^x, Le^y) [8]. By mimicking the human cell-surface glycosylation in the stomach they act as molecular decoys for the immune system and therefore contribute to the persistence of the infection [9,10]. Another feature of some *H. pylori* strains is the presence of an additional chain of D-*glycero*-D-*manno*-heptose (DD-Hep), which has been reported to connect the *O*-chain to the LPS core [11]. Also, some LPS strains have been shown to express elongated α-glucan chains linked to the core [8,12,13]. LPS α-glucans can be either found *O*-6-linked [8,12] or, as recently observed for *H. pylori* serotype O:2, as an elongated *O-chain* composed of alternating *O*-2- and *O*-3-linked α-D-glucopyranose (α-D-Glc*p*) residues [→2)-α-D-Glc*p*-(1→3)-α-D-Glc*p*-(1→]$_n$ [13]. Proof have also been presented for the expression of a highly branched cell-surface α-mannan composed of terminal, *O*-2-, *O*-6-, and *O*-2,6-substituted mannose (Man) residues [14].

Cell-surface glycosylation is known to be involved in the control of various biologic and physiologic events such the modulation of protein conformational and functional properties [15,16], mediation of cell–cell adhesion and cell–host interaction [16,17], regulatory [16,18] and immunologic [16,19,20] phenomena. Alteration of the cell-surface glycosylation patterns often occurs as a result of the adaptive responses to environmental changes comprising events such as the expression of capsular polysaccharides as well as excretion of polysaccharides to the surrounding media as exopolysaccharides [21]. These events are thought to confer extra protection against harsh environments and external aggressions. Production of exopolysaccharides is strongly correlated with the formation of biofilms responsible for the colonization of unfriendly environments and the promotion of bacterial life on community [22].

In this work, we devote our attention to the identification and structural characterization of novel *H. pylori* cell-surface glycosides mainly produced as a result of environmental adaptation to growth in vitro solid and liquid media. Such insight can provide some enlightenment on the bacterial colonization strategies outside the human host, namely through the production of exopolysaccharides involved in the formation of biofilms or expression of capsular polysaccharides under very specific environmental conditions.

Materials and Methods

Bacterial Cultures

Reference strain *H. pylori* NCTC 11637 was obtained from the National Collection of Type Cultures (London, UK), clinical isolate 968 was provided by the Centre of Biological Engineering of the University of Minho (Braga, Portugal), and clinical isolate 14255 was provided by IPATIMUP (Porto, Portugal).

Bacterial Growth in CBA

H. pylori cells were maintained as stock cultures in trypticase soy broth with 20% glycerol, recovered on prewarmed Gelose Columbia solid media supplemented with 5% horse blood (bioMérieux, France) and incubated at 37 °C for 72 hours, on a microaerophilic atmosphere generated by a CampyGen gas pack (Oxoid, Basingstoke, UK). Cells were subcultivated after 48-hour incubation periods in the conditions described before. The resulting biomass was harvested to sterile and filtered (0.22 μm) distilled water.

Bacterial Growth in F12 Liquid Media

H. pylori reference strain NCTC 11637 and clinical isolate 968 were grown on Ham's F12 defined liquid media without the addition of enhancing growth factors. The medium was inoculated with cellular extracts obtained from Columbia blood agar (CBA) growth media. Cells were allowed to grow for 24 hours in a glass flask under microaerophilic atmosphere by gentile stirring at 37 °C as described by Testerman et al. [6].

Purity Assessment of Bacterial Growth

Purity assessment was assured by using a highly specific peptide nucleic acid probe in a fluorescence in situ hybridization procedure, according to the protocol described by Guimaraes et al. [23]. For every experiment, a negative control was performed simultaneously where all the steps described before were carried out but where no probe was added during the hybridization procedure. Microscopy visualization was performed using an Olympus BX51 (OLYMPUS Portugal SA, Porto, Portugal) epifluorescence microscope equipped with one filter sensitive to the Alexa fluor 594 signaling molecule attached to the PNA probe (excitation 530–550 nm; barrier 570 nm; emission LP 591 nm).

Extraction and Purification of Cell-Surface Glycans

Cell-surface glycans were isolated from cells using the hot phenol : water extraction according to Westphal and Jann [24]. The aqueous layer was dialyzed against distilled water using a 1000 Da cut-off membrane and lyophilized. The resulting material was fractioned by gel permeation/adsorption chromatography (GPC) on a

polyacrylamide Bio-Gel P-6 (Bio-Rad Laboratories, Hercules, CA, USA) (0.6 m in length and 1.0 cm in diameter) column using distilled water as the eluting solvent at a constant flow rate of 0.33 mL/minute. The initial material (~2.5 mg) was suspended in 400 μL of degassed distilled water and introduced in the column. Fractions of 2.8 mL were collected. The mass content in the fractions was estimated on evaporative light scattering detector SEDEX55 (SEDERE, Alfortville, France) and further assayed for total sugars with the phenol–H_2SO_4 method [25]. Exclusion and total volume were calibrated with blue dextran and glucose, respectively.

Sugars Composition and Linkage Analysis

Sugars composition analysis was performed by the alditol acetate method as described by Harris et al. [26]. The hydrolysis was done in 4 mol/L of trifluoroacetic acid (TFA) at 100 °C for 3 hours, followed by reduction with $NaBH_4$ and subsequent acetylation with acetic anhydride in the presence of 1-methylimidazole. Alditol acetates derivatives were analyzed by gas chromatography-mass spectrometry (GC-MS), performed in an Agilent Technologies (Santa Clara, CA, USA) 6890N Network Gas Chromatograph connected to an Agilent 5973 Selective Mass Detector. The GC was equipped with a DB-1 capillary column (30 m in length, 0.32 mm in internal diameter, and 0.25 μm film thicknesses). The samples were injected in splitless mode (splitless time is 1.00 minute), with the injector and detector operating at 220 and 230 °C, respectively, using the following temperature program: 100 °C (1 minute) → 150 °C at 5 °C/minute (8 minutes) → 159 °C at 0.5 °C/minute (5 minutes) → 250 °C at 5 °C/minute (2 minutes) → 320 °C at 2 °C/minute (2 minutes). The carrier gas (He) had a flow of 1.7 mL/minute, with an average linear velocity of 47 cm/second, and a solvent delay of 9 minutes. The column head pressure was 5.34 psi. The mass spectrometer was operated in the electron impact mode at 70 eV, scanning the mass range m/z 40–500 and performing 3.18 scans per second.

Linkage analysis was carried out by methylation with $NaOH/Me_2SO/CH_3I$, as described by Ref. [27]. The methylated polysaccharides were hydrolyzed with 2 mol/L of TFA at 121 °C for 1 hour, reduced by $NaBD_4$, and acetylated with acetic anhydride in the presence of 1-methylimidazole. The partially methylated alditol acetates were analyzed by GC-MS using the chromatographic conditions previously described, using the following temperature program: 45 °C (5 minutes) → 140 °C at 10 °C/minute (5 minutes) → 170 °C at 0.5 °C/minute (1 minute) → 280 °C at 15 °C/minute (5 minutes).

Iodine Test

A thin layer of fresh bacterial cells grown on solid medium was fixed on a cleaned sterile glass slide. Cells were then covered with Gram's iodine solution (0.33% (w/v) I_2 in 0.66% (w/v) KI aqueous solution; Sigma-Aldrich Química S.A., Sintra, Portugal) and incubated for 1 minute at room temperature. After incubation, the cells were washed with water to remove the excess of staining agent and observed by light microscopy.

Enzymatic Assays

Digestion with α-amylase from human saliva (Type IX-A, lyophilized powder, 1000–3000 units/mg protein; Sigma Aldrich) was performed in 50 mmol/L phosphate buffer at pH 6.8 for 3 hours at 20 °C. The enzyme was denatured by heating the solution for 15 minutes at 100 °C and the precipitate material was removed by centrifugation.

The enzyme-treated material was separated on a polyacrilamide Bio-Gel P-4 column (0.6 m in length and 1.0 cm in diameter) using water as an eluent in the conditions previously mentioned for the separation on the Bio-Gel P6 column.

NMR Spectroscopy

^1H spectra were recorded on a Bruker (Bruker BioSpin GmbH, Rheinstetten, Germany) AMX 400 spectrometer at 295 K using standard Bruker software. Prior to performing the nuclear magnetic resonance (NMR) experiments, the samples were lyophilized thrice with D_2O (99.9%). The HDO peak was used as the internal reference at δ_H of 4.76 ppm.

Mass Spectrometry

MS assays were performed in a linear ion trap (LIT) electrospray (ESI) spectrometer in positive mode. Samples were dissolved in 1 : 200 of water : methanol and introduced into the MS at 10 μL/min. Typical ESI conditions were as follows: nitrogen sheath gas 30 psi, spray voltage 5.5 kV, heated capillary temperature 350 °C, capillary voltage 1 V, and tube lens voltage 40 V. Collision-Induced Dissociation-Mass Spectrometry (CID-MS/MS) experiments were performed on mass-selected precursor ions using standard isolation and excitation procedures (activation q value of 0.25, activation time of 30 ms). The spectra were collected in the positive mode and collision energy used was 32 (arbitrary units). Data acquisition was carried out with Xcalibur data system (Thermo Fisher Scientific Inc., Waltham, MA, USA).

Statistics

Statistical significance was determined using paired Student's *t*-tests ($p = .05$). Between- and within-sample variances were determined by one-way ANOVA and comparison between standard deviations performed using an *F*-test ($p = .05$). Correlation between samples was determined by linear regression method.

Results

Carbohydrate Profile of Glycan-Rich Extracts from *Helicobacter pylori* Cells Grown in Solid Media

In this study, *H. pylori* reference strain NCTC 11637 and clinical isolates 968 and 14255 were evaluated in relation to their cell-surface glycan profile. The first step in the identification and structural characterization of cell-surface polysaccharides comprised the recovery of glycan-rich aqueous phase resulting from hot phenol : water extraction performed on intact bacterial cells. The overall sugars composition of such extracts is presented in Table 1. The different strains present distinct sugars composition. NCTC 11637 contains a large amount of Rib, possibly a contamination from RNA, glucose (Glc), and galactose (Gal) whereas 968 presents also Gal and Glc but is richer in *N*-acetylglucosamine (GlcNAc) and D-*glycero*-D-*manno*-heptose (DD-Hep) and 14255 is richer in Gal and GlcNAc. Lower amounts of fucose (Fuc), arabinose (Ara), Man, and L-*glycero*-D-*manno*-heptose (LD-Hep) have also been observed in all strains. The occurrence of Ara has never been reported to occur in *H. pylori*. The different sugar contents might reflect both strain-to-strain variability and biosynthetic microheterogeneity.

To highlight the structural features of these polymers, the linkage profile held by the identified sugars was further evaluated by GC-MS of the permethylated alditol acetate derivatives released after hydrolysis of the original glycans.

Linkage analysis has revealed, in all CBA grown strains, a prevalence of *O*-3-linked Gal and *O*-4-linked GlcNAc residues in proportions of approximately 1 : 1. Based on previous knowledge on *H. pylori* cell-surface glycans [8], these structures belong to *N*-acetyllactosamine (LacNAc) moieties [→3)Gal(1→4)GlcNAc(1→] characteristic of LPS *O*-chains. The identification of terminal Fuc residues and *O*-3,4-linked GlcNAc residues in proportions of approximately 1 : 1 further suggests the expression of Type 1 Le^a or Type 2 Le^x blood group determinants. The existence of residual amounts (<1%) of *O*-2,3-linked Gal indicates the expression of small amounts of Type 1 Le^b or Type 2 Le^y blood group determinants. This linkage composition is in accordance with what has been described for reference strain NCTC 11637 that is known to have *O*-chains containing LacNAc and Type 2 Le^x and Le^y [28]. The clinical isolate 968 presents a high percentage of *O*-7-linked DD-*manno*-Hep, suggesting the expression of an elongated heptoglycan usually found linking the core to the *O*-chains [8]. Low amounts (<5%) of other *O*-chain and core-related residues have also been identified and assigned as shown in Table 2.

Man was observed in all extracts in percentages that span from 5 to 11% of total sugars (Table 1). These residues are essentially found as terminal, *O*-2-, *O*-6-, and *O*-2,6-linked (Table 2). Monteiro et al. [14] have shown the occurrence of a mannan containing these characteristic linkages when studying a *H. pylori* mutant strain. Methylation analysis shows that the Ara residues occur mainly as *O*-2-substituted even though trace amounts of terminal and *O*-5-linked residues could also be observed.

In addition to LPS sugars, Man and Ara, high amounts of *O*-4-linked Glc residues [→4)-Glc*p*-(1→] were also common to all extracts (Table 2). The total amount of

Table 1 Relative sugar composition of glycan-rich water extracts of the *Helicobacter pylori* studied strains

	Molar ratio (%)								
H. pylori strains	Rib	Fuc	Ara	Man	Glc	Gal	GlcNAc	DD-Hep	LD-Hep
Growth in CBA									
NCTC 11637	39	5	1	11	19	18	4	2	1
968	2	3	1	7	13	20	24	20	10
14 255	4	9	2	5	7	31	32	7	3
Growth in F12 broth									
NCTC 11637	5	5	2	22	25	23	9	6	3
968	5	2	1	27	33	15	14	2	1

Rib, ribose; Fuc, fucose; Ara, arabinose; Man, mannose; Glc, glucose; Gal, galactose; GlcNAc, *N*-acetylglucosamine; DD-Hep, D-*glycero*-D-*manno*-heptose; LD-Hep, L-*glycero*-D-*manno*-heptose; CBA, Columbia blood agar.

Table 2 Sugar linkage profile of the sugars in glycan-rich extracts from the *Helicobacter pylori* studied strains

	Relative molar ratio (%)				
	Growth in CBA			Growth in F12 broth	
Linkage type	NCTC 11637	968	14255	NCTC 11637	968
LPS *O*-chain					
T-Fuc	5	4	8	4	7
→3)Fuc	–	tr	1	–	3
→6)Glc	1	–	tr	5	4
T-Gal	2	1	2	1	1
→3)Gal	18	15	20	9	12
→2,3)Gal	1	1	tr	tr	1
→2,4)Gal	–	tr	tr	–	–
→3,4)Gal	–	tr	tr	–	–
→3,6)Gal	–	1	tr	–	–
T-GlcNAc	tr	1	–	2	–
→4) GlcNAc	10	11	16	9	5
→3) GlcNAc	tr	1	1	tr	1
→3,4)GlcNAc	5	5	14	2	8
→3,6)GlcNAc	–	tr	–	–	–
→4,6)GlcNAc	–	tr	–	–	–
LPS Core					
*T-Glc	6	3	2	3	2
→3)Glc	tr	v	2	tr	tr
→4)Gal	4	3	2	2	tr
T-DD-*manno*-Hep	–	–	–	1	tr
T-LD-*manno*-Hep	–	–	–	tr	–
→2)DD-*manno*-Hep	tr	5	3	4	1
→2)LD-*manno*-Hep	2	3	3	tr	1
→3)LD-*manno*-Hep	1	5	tr	tr	tr
→7)DD-*manno*-Hep	1	14	5	3	1
→7)LD-*manno*-Hep	–	7	tr	tr	1
→2,7)DD-*manno*-Hep	1	1	1	4	2
LPS Lipid A					
→6) GlcNAc	tr	3	4	4	1
Man-rich glycans					
T-Man	3	1	1	6	9
→2)Man	3	4	2	7	11
→6)Man	5	tr	1	4	5
→2,6)Man	4	1	tr	5	8
Amylose-like glycans					
→4)Glc	26	9	5	13	7
→4,6)Glc	1	tr	tr	–	–
Unassigned sugars					
T-Ara	tr	–	tr	tr	1
→2)Ara	1	1	6	1	3
→5)Ara	tr	tr	1	–	1
→2,3,5)Ara	–	–	–	–	–
→6)Gal	1	tr	tr	11	4

*Terminal Glc residues can also be addressed to the (1→4)-glucan or the (1→6)-dextran antenna in the lipopolysaccharides (LPS).
tr, vestigial amounts (> 0.5%); CBA, Columbia blood agar.

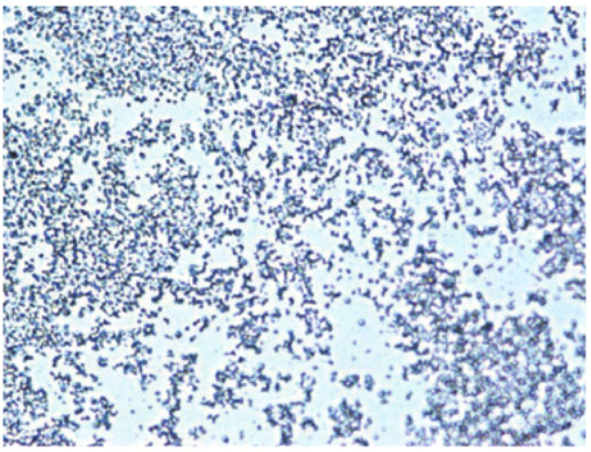

Figure 1 *Helicobacter pylori* cells stained with iodine. Characteristic blue color is indicative of the presence of α-(1→4)-D-Glc polysaccharides.

O-4-substituted Glc was found to vary from 5 to 26% of total sugars and its presence in glycan-rich water extracts is now being described for the first time for *H. pylori*. To confirm the presence of amylose-like glycans, *H. pylori* cells were treated with Lugol iodine solution. The blue-stained cells shown in Fig. 1 demonstrate the presence of amylose, with (1→4)-D-Glc in α configuration. Trace amounts of *O*-4,6-linked Glc residues were also identified in all samples, suggesting the existence of residual branching points in the glucan chain. Because the CBA culture medium contains starch, it is not possible to identify the origin of this material, if produced by the bacterium or uptaken from the medium.

Carbohydrate Profile of Glycan-Rich Extracts from *Helicobacter pylori* Cells Grown on Liquid Media

To determine if *H. pylori* was capable of biosynthesizing amylose-like glycans, the reference strain NCTC 11637 and the clinical isolate 968 were grown in Ham's F12 defined liquid media, which is devoid of polysaccharides in its composition. Cellular growth was promoted in the absence of external growth enhancers such as FBS, BSA, or cyclodextrin further fulfilling the requirement for a glycan-depleted environment. As it can be observed from sugars (Table 1) and linkage (Table 2) analysis, growth in liquid medium resulted, in both strains, in an increase percentage of Man and sugars belonging to the LPS moiety (Glc, Gal, GlcNAc, and Hep). The two strains also retrieved positive for the presence of amylose in liquid medium thus demonstrating the capability of those strains to synthesize amylose-like glycans in a polysaccharide-depleted medium.

To fully access the structural organization of the *O*-4-linked glucan, the water extracts from *H. pylori* reference strain NCTC 11637 was fractionated by size-exclusion chromatography on a Bio-Gel P6 medium.

Purification and Characterization of *Helicobacter pylori* Amylose-Like Glycans

Fractionation of the glycan-rich material in a Bio-Gel P6 resulted in the elution profile presented in Fig. 2, from which six fractions were identified and labeled from A to F.

The high-molecular weight fractions (A–C) were composed mainly of Gal (31–36%), Man (24–30%), Glc (17–25%), and also contained Rib (~7%). Lower amounts of GlcNAc (2–5%), Fuc (~3%), DD- and LD-Hep (1–3%), and Ara (~2%) have also been observed (Table 3). Linkage analysis allowed assigning the Fuc, Gal, GlcNAc, DD- and LD-Hep to the LPS moiety (Table 4) [8]. The Ara residues in fractions A–C were almost exclusively found *O*-2,3,5-linked (Table 4), a very uncommon substitution pattern in nature, although reported to occur in some seeds [29]. Residual amounts of terminal, *O*-2-, and *O*-5-linked Ara residues were also identified. Their presence throughout all fractions points towards that variously linked Ara residues are structural motifs of *H. pylori* strains.

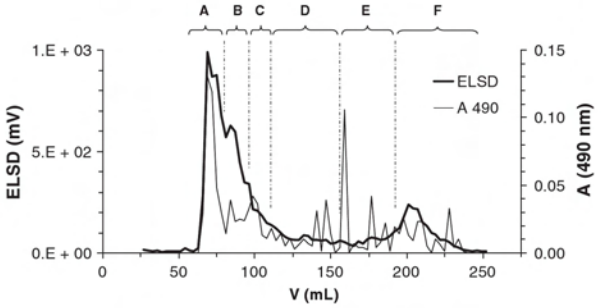

Figure 2 *Helicobacter pylori* NCTC 11637 glycan-rich extract elution profile on a Bio-Gel P6 column. Letters A–F correspond to isolated fractions.

The percentage of *O*-4-linked Glc residues increased from fractions A to F (Table 4). Glc was found to be the second major component of fractions A–C, and predominantly identified as being *O*-4-linked (~66–79% of the total Glc) The remaining Glc was either found in the *O*-3-linked form (7–14% of total Glc), assigned to the LPS, or *O*-6-linked form, assigned to dextran antenna in the LPS [12]. Terminal Glc was also present in percentages that span from 5% (fraction C) to 11% (fraction A) of total Glc and can either be found in the terminal ends of LPS core and dextran antenna as well as in the *O*-4-substituted glucan. Such structural diversity makes impossible the determination of the exact percentage of terminal Glc belonging to the glucan chain thus hindering the estimation of the molecular weight based on *O*-4-linked Glc/terminal Glc ratio. Linkage analysis on fractions A–C also showed residual amounts of *O*-4,6-disubstituted Glc (~2%) thus reinforcing that, even though almost exclusively linear, the glucan might exhibit vestigial branching. In fraction D, the *O*-4-linked Glc was the most abundant linkage. Still, it contains significant amounts of Man and Gal (16 and 19% of total sugars, respectively) and, in lower percentages, Rib (9%), Fuc (5%), Ara (4%), GlcNAc (2%), DD-Hep (3%), and LD-Hep (4%). Fractions E and F were composed almost exclusively of *O*-4-linked Glc (83 and 78%, respectively). Assuming a linear structure, the (1→4)/terminally linked Glc ratio allows inferring that the average length of these polymers can vary from 42 (7 kDa, fraction E) up to 28 residues (4 kDa, fraction F) Glc residues.

The polyacrylamide Bio-Gel P6 is expected to separate molecules based on their molecular weight, from 6 kDa (void volume) to 1 kDa (inclusion volume). These conditions are valid when no interactions occur between the stationary phase and the eluted sample. In

Table 3 Sugar composition of *Helicobacter pylori* NCTC 11637 glycan-rich extract fractions collected from a Bio-Gel P6 column (A–F)

	Molar ratio (%)								
Fraction	Rib	Fuc	Ara	Man	Glc	Gal	GlcNAc	DD-Hep	LD-Hep
A	8	3	2	30	17	36	2	1	1
B	7	4	1	30	19	31	5	2	1
C	6	3	2	24	25	32	4	1	3
D	9	5	4	16	38	19	2	3	4
E	3	6	6	2	78	2	–	1	2
F	59	1	4	1	34	1	–	–	–

Rib, ribose; Fuc, fucose; Ara, arabinose; Man, mannose; Glc, glucose; Gal, galactose; GlcNAc, *N*-acetylglucosamine; DD-Hep, D-*glycero*-D-*manno*-heptose; LD-Hep, L-*glycero*-D-*manno*-heptose.

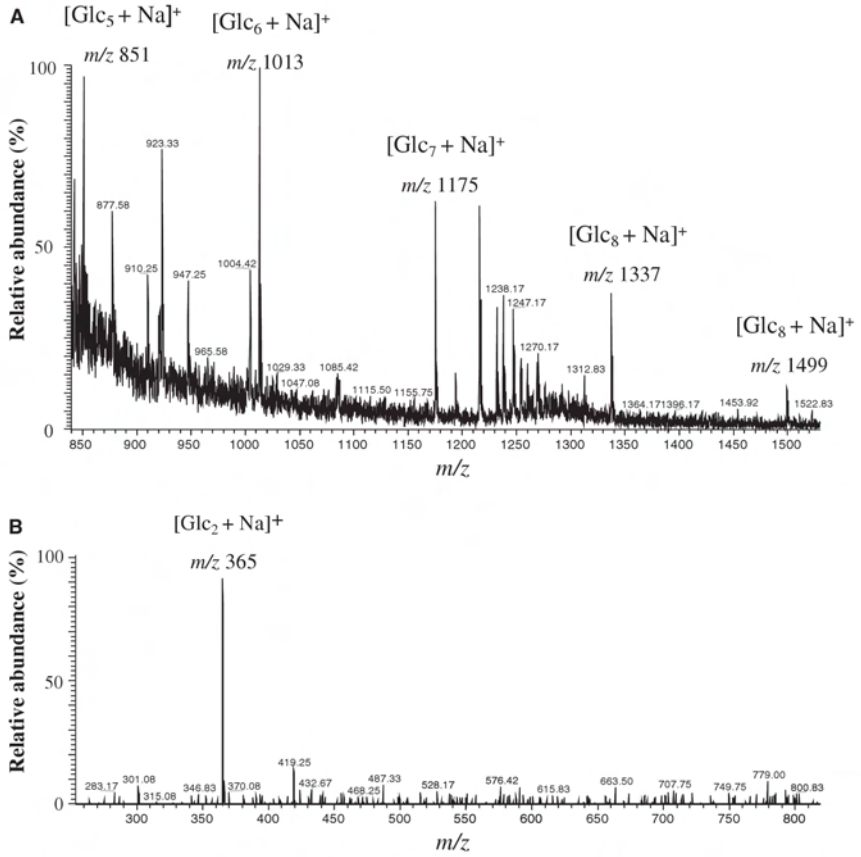

Figure 4 Electrospray-mass spectrometry spectra of (*A*) fraction E and (*B*) material recovered after digestion with α-amylase.

fractions, one corresponding to the void volume and another to nonincluded material (data not shown). The ^{1}H NMR spectrum of the material recovered from the void volume showed the disappearance of the α-anomeric signal, demonstrating the effectiveness of the enzymatic treatment (Fig. 3B). The nonretained material was composed exclusively of disaccharides resulting from the enzymatic hydrolysis of the oligomeric glucan as demonstrated by the ion at *m/z* 365 observed in the ESI-MS spectrum (Fig. 4B).

Bioaccumulation of Amylose under Subcultivation in Solid Medium

After having shown the expression of an amylose-like polysaccharide by *H. pylori* in both solid and liquid media, the impact of successive subcultivation on cell-surface glycans (LPS and amylose-type glycans) was evaluated. The reference strain NCTC 11637 and the clinical isolates 968 and 14255 were subcultivated in CBA. The impact of successive subcultivation on cell-surface glycans was determined by the analysis of the sugars carried out on the freeze-dried biomass of intact cells. The total LPS (Fig. 5A), given by the amount of Fuc, Glc, Gal, GlcNAc, and Hep, LPS *O*-chain (Fig. 5C), given by the amount of Fuc, Gal, and GlcNAc, were quantified independently based on the output from sugar analysis. The results are expressed in terms of concentration (w/w) for six passages in CBA comprising a total of 13 days in solid media. Between- and within-sample variance was estimated by one-way ANOVA for each component (LPS, LPS *O*-chain, and amylose-type glycans) for the three strains during the subcultivation period. *F*-test ($p = .05$) performed on those estimates retrieved that between-measurements variance was more significant than random errors expressed by within-sample variance for all cases.

For LPS (Fig. 5A), an initial increase in the overall amount of the material was observed in all strains, possibly because of an initial adaptation of the bacteria when passing from a vegetative state in the glycerol inoculums to the solid media. However, this tendency is reversed after the third and the fourth passages after which the amount of total LPS expressed decreases.

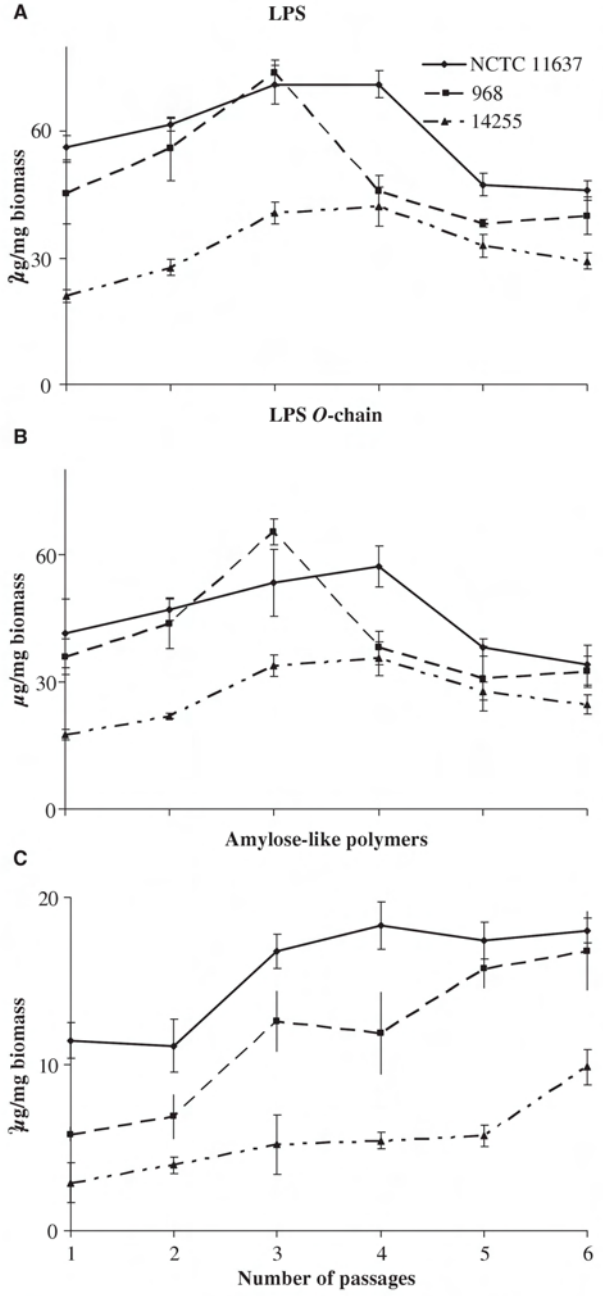

Figure 5 Variation in (*A*) lipopolysaccharides (LPS), (*B*) LPS *O*-chains, and (*C*) amylose-like polymer content in *Helicobacter pylori* cells during subcultivation in Columbia blood agar.

Variations in *O*-chain sugars, presented graphically in Fig. 6B, show the same tendency of the overall LPS. Amylose, in opposition to what has been observed for the LPS, is seen to increase continuously with the incubation time (Fig. 5C). This effect was observed for all strains and demonstrates that *H. pylori* bioaccumulates amylose during the subcultivation period.

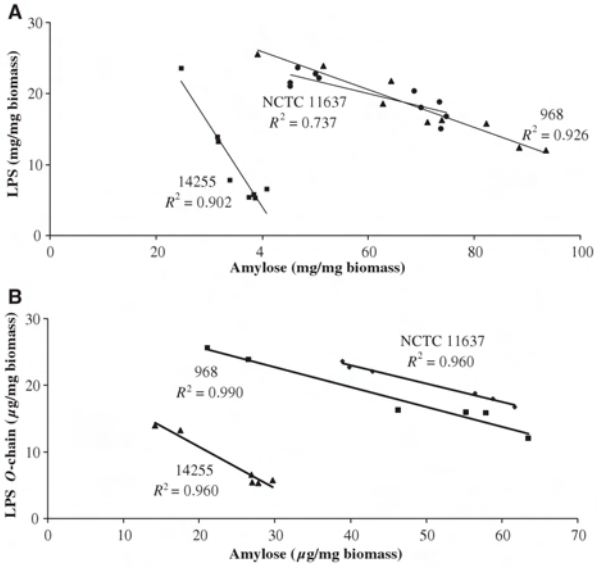

Figure 6 (*A*) Lipopolysaccharides (LPS) versus amylose and (*B*) LPS *O*-chain versus amylose content during subcultivation in Columbia blood agar.

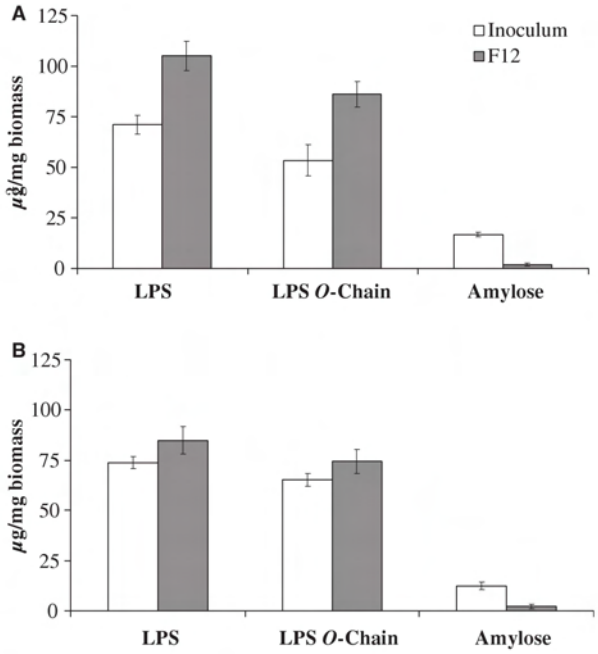

Figure 7 Lipopolysaccharides (LPS), LPS *O*-chains, and amylose content in *Helicobacter pylori* cells present in the initial inoculum and after F12 growth for: (*A*) reference strain NCTC 11 637 and (*B*) clinical isolate 968.

The plot of the total amount of LPS and LPS *O*-chain sugars versus the total amount of amylose throughout the incubation period (Fig. 6) suggests a correlation

between the expression of LPS/LPS *O*-chains and amylose. However, this correlation could only be observed when the data from the first and second passages are not included. This seems to be most likely correlated with an initial adaptation period of the bacteria to solid medium upon recovery from a latent stage resulting from cryostorage.

Amylose Expression in F12 Liquid Media

The *H. pylori* reference strain NCTC 11637 and the clinical isolate 968 obtained after three passages in solid media (day 7) were further recovered to a F12 liquid media.

The glycan profile for each inoculum and F12 material are presented graphically in Fig. 7. In both strains, a statistically significant (Student's *t*-test; $p = .05$) increase was observed in LPS content in the passage from solid to liquid media. This phenomenon was more pronounced in strain NCTC 11637 (48%) than in 968 (12%) and was caused almost exclusively by an increase in the concentration of *O*-chain sugars (62% for NCTC 11637 and 12% for 968). Conversely, the amount of amylose decreased significantly in the passage from solid to liquid media where only residual amounts were observed.

Discussion

In the present work, we describe that *H. pylori* is capable of producing an amylose-like α-(1→4)-D-glucan and further bioaccumulates this polysaccharide under selective pressure induced by subcultivation in the agar medium. Gathered information also suggests that *H. pylori* cell surface is composed of a mixed population of glycans comprising LPS, mannose-rich glycosides as well as capsular/exopolysaccharide α-glucans. The now observed amylose belongs to the class of biomolecules generally referred to as ''bacterial glycogen'' and considered to be a source of readily available glucose [30]. However, unlike most bacteria that indeed produce 8–12% branching in the *O*-6 Glc residues in glycogen [30], in *H. pylori* only vestigial branching was observed (<1%).

Glycogen-like metabolism in bacteria is strongly correlated with the mobilization of ADP-Glc mostly by intracellular synthetic and degradative enzymes belonging to clearly identified families of glycosyltransferases (GT) and of glycosidases/transglycosidases. In a study carried out by Henrissat et al. [31], 55 currently sequenced bacterial genomes were screened for members of the most relevant families of GT (GT5, GT35, GH13, and GH15). The authors concluded that a significant proportion of those microorganisms, including *H. pylori* 26695 and J99 and *Campylobacter jejuni* NCTC 11168, lacked the necessary enzymatic machinery to metabolize glycogen-like molecules. Interestingly, all of them were parasitic, symbiotic, or fastidious thus suggesting that such genotype resulted from a trait associated with the parasitic behavior of the microorganisms. Our results now point in a different direction. Here, it is demonstrated that *H. pylori*, even though being recognized as extremely fastidious, indeed produces α-(1→4)-D-glucans *in vitro*. This finding is in agreement with the recently reported capability of *C. jejuni* 81-176, a virulent model strain used in the study of mechanisms and pathogenesis of *C. jejuni* infection, of also producing a α-(1→4) glucan [32]. Another example of a generally regarded as nonproducing glycogen Gram-negative bacteria is *Neisseria meningitidis* [31,33]. Again, in this case, evidences of strains producing glycogen-like molecules have been presented, as demonstrated by the identification of a genetic *loci* encoding amylosucrase in *N. meningitidis* 93246, responsible for the production of amylose from sucrose [33].

The events triggering the overexpression of α-(1→4)-D-glucans have been correlated with the responses of the organism to environmental pressure or long-term survival strategies. The bioaccumulation phenomenon has been previously observed in microorganisms facing limiting growth conditions [34] as well as in grapevine plants as a nonspecific response to biotic and abiotic stresses [35]. This stress-related strategy based on the production of α-glucan seems to be common to microorganisms and plants. In bacteria, environmental pressure resulting from shortage of a nutrient such as nitrogen in the presence of excess of carbon has also been reported as responsible for the intracellular accumulation of this polysaccharide [31,34,36]. Some bacteria, however, accumulate them in the exponential growth phase [37]. In line with this observation, a recent report concerning the pathogenic Gram-negative bacteria *Vibrio cholerae* states that the capacity of this bacteria to store carbon as glycogen facilitates bacterial fitness when passing both from nutrient-rich human intestinal tract and nutrient-poor aquatic environments, facilitating the transmission to a new host [38]. Thus, it can be inferred that different organisms can trigger at some point of their life cycle the pathways leading to the expression of α-(1→4)-D-glucans as a result of specific environmental pressure.

In this work, aware of *H. pylori* high fastidiousness, we further devoted our attention to fully understanding the influence of environmental pressure resulting from subcultivation in solid agar medium and recovery to liquid medium in the bacterium cell-surface polysaccharides. The results suggest that *H. pylori* cells facing a lag stage resulting from subcultivation in agar medium

bioaccumulate amylose-like polymers over time. The observation of the decrease of cell-surface LPS, namely the *O*-chain, during subcultivation in solid medium is in accordance with previous reports [8,39,40]. A more up-to-date work carried out by Nilson et al. [41] further reinforced that the absence of high-molecular weight *O*-chains was a common feature in two clinical isolates after a number of experimentally passages both in vitro and in mice models. However, this phenotype was not evident in fresh human clinical isolates, where all cells expressed high-molecular weight *O*-chains [41]. In contrast, when *H. pylori* was in an exponential growth phase resulting from cultivation in F12 liquid medium, the amount of expressed amylose-like polymers decreased considerably. This decrease was accompanied by an increase in the overall amount of LPS mainly because of an *O*-chain increment. The observed overexpression of *O*-chain material upon recovery to the liquid medium was in agreement with previous reports [8]. Anyway, F12 has been shown to be able to overcome some of the lower growth rates exhibited by the solid media [6] and to be ideal for the rapid isolation, cultivation, and identification of *H. pylori* from biopsy specimens [42], suggesting its success in mimicking in vivo growth conditions. Furthermore, LPS with high-molecular weight *O*-chains can be considered a characteristic in vivo phenotype during colonization of the human gastric mucosa.

Facing these considerations, it can be stated that phenotypes resulting from F12 growth may resemble in vivo cell-surface patterns. Thus, in vivo cells are led to produce elongated *O*-chains bearing Lewis antigens that are recognized as a prerequisite in the modulation of host–cell interaction and evasion to immune response. Silencing of *O*-chain expression accompanied by bioaccumulation of amylose-like polymers in solid media suggests a redirection in metabolic efforts in response to the no-longer need for interaction with the host and a response to a new environment. Moreover, the expression of elongated *O*-chains might be considered a favorable phenotype among planktonic free-swimming bacteria like the ones encountered during F12 growth. Its substitution by amylose-like polymers upon cultivation in solid medium may be because of a swift toward life on community and formation of biofilm frameworks that render the bacteria protection in certain specific microenvironments.

Based on these considerations, we are also led to think that *H. pylori* cell-surface polysaccharides undergo phase variation in response to different growth stages and environmental pressures. Even though at this stage the biologic role resulting from the decoration of *H. pylori* cell surface with α-glucans is still unclear, the expression of such structures in other bacteria reveals its key importance. Recent studies have highlighted that this class of polysaccharides do not restrict their function just to provide the microorganisms with resources to resist food depletion and long starvation periods. They have been shown to protect against phagocytosis [43] and modulate the host immune response [44,45]. For example, inducing monocytes to differentiate into altered dendritic cells that fail to upregulate CD80 and to present lipid antigens to CD1-restricted T cells, and produce interleukin (IL)-10 but not IL-12 [45]. Thus, the expression/bioaccumulation of α-glucans can be thought to also contribute to the pathogenicity of the bacteria by aiding in the evasion/modulation of immune responses and conferring extra protection against external aggression and unfavorable environments.

Facing all these considerations, further work is being conducted to clarify the biosynthetic pathways behind the expression of α-glucans by *H. pylori*, to clarify the impact of specific environmental factors in amylose bioaccumulation, and to understand its biologic role.

Acknowledgements and Disclosures

This work was supported by Fundação para a Ciência a e Tecnologia (FCT) found project Pylori E&LPS POCI/QUI/56393/2004, PhD grant SFRH/BD/19929/2004, and Natural Sciences and Engineering Research Council of Canada (NSERC). The authors also thank Dr Maria de Lurdes Monteiro (Instituto Nacional de Saúde Dr Ricardo Jorge, Lisbon) and Dr Céu Figueiredo (IPATIMUP, Porto) for kindly providing the clinical isolates used in this study.

References

1 Forman D, Graham DY. Impact of *Helicobacter pylori* on society-role for a strategy of ''search and eradicate''. *Aliment Pharmacol Ther* 2004;19:17–21.
2 Ferreira AC, Isomoto H, Moriyama M, Fujioka T, Machado JC, Yamaoka Y. *Helicobacter* and gastric malignancies. *Helicobacter* 2008;13:28–34.
3 Sugiyama T. Development of gastric cancer associated with *Helicobacter pylori* infection. *Cancer Chemother Pharmacol* 2004;54:S12–20.
4 Labigne A, De Reuse H. Determinants of *Helicobacter pylori* pathogenicity. *Infect Agents Dis* 1996;5:191–202.
5 Stevenson TH, Castillo A, Lucia LM, Acuff GR. Growth of *Helicobacter pylori* in various liquid and plating media. *Lett Appl Microbiol* 2000;30:192–6.
6 Testerman TL, McGee DJ, Mobley HLT. *Helicobacter pylori* growth and urease detection in the chemical defined medium Ham's F-12 nutrient mixture. *J Clin Microbiol* 2001;39:3842–50.
7 Azevedo NF, Pacheco AP, Keevil CW, Vieira MJ. Nutrient shock and incubation atmosphere influence the recovery of viable *Helicobacter pylori* from water. *Appl Environ Microbiol* 2004;70:490–3.
8 Monteiro MA. *Helicobacter pylori*: a wolf in sheep's clothing: the glycotype families of *Helicobacter pylori* lipopolysaccharides expressing histo-blood groups: structure, biosynthesis, and

CHAPTER V

IDENTIFICATION OF MANNOSE-RICH HETEROPOLYMERIC GLYCANS IN THE CELL-SURFACE OF A VIRULENT *HELICOBACTER PYLORI* WILD TYPE STRAIN

Identification of mannose-rich heteropolymeric glycans in the cell-surface of a virulent *Helicobacter pylori* wild type strain

José A. Ferreira[a], Nuno F. Azevedo[b,c], Maria J. Vieira[c], Céu Figueiredo[d,e], Brian J. Goodfellow[a,f], Rui Vitorino[a], Mario A. Monteiro[g], Manuel A. Coimbra [a,*]

[a] Departamento de Química, Universidade de Aveiro, 3810-193 Aveiro, Portugal, [b] LEPAE, Department of Chemical Engineering, Faculty of Engineering, University of Porto, Porto, Portugal, [c]Centro de Engenharia Biológica, Universidade do Minho, Campus de Gualtar, Braga, Portugal, [d]Institute of Molecular Pathology and Immunology, University of Porto, Portugal, [e]Medical Faculty of Porto, Porto, Portugal, [f]CICECO, University of Aveiro, Aveiro, Portugal, [g]Department of Chemistry, University of Guelph, Guelph, ON, Canada

Abstract

With the intent of contributing for a carbohydrate-based vaccine against the gastroduodenal pathogen *Helicobacter pylori*, we report the structural characterization of a cell-surface mannose-rich glycans isolated from a virulent strain *H. pylori* 968. Sugars and linkage analysis and 1D and 2D ^{1}H NMR revealed that this strains expresses a highly branched mannan formed by a backbone of α-(1→6)-linked mannopyranosyl residues showing up to 80% substitution in the *O*-2 position. The side chains were found to contain *O*-2 linked Man residues both in α- and β- configurations, as follows:

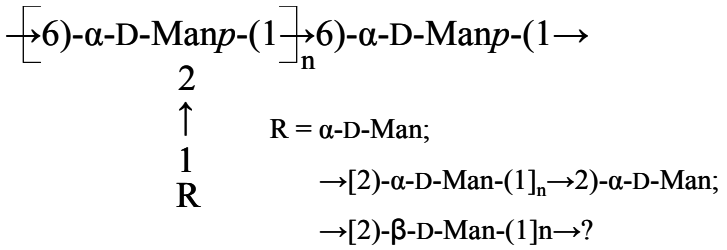

In addition, this strain also expresses cell-surface lipopolysaccharides (LPS) yielding partially fucosylated polyLacNAc *O*-chains. However, affinity assays with Polymyxin-B, Concanavalin A, as well as SDS-PAGE and DOSY NMR experiments, revealed no association between the mannan and the LPS moieties. Furthermore, they demonstrated that the expressed mannan is part of a much more complex heteropolymeric structure containing Glc, Gal, and GlcNAc connected to a protein domain. *H. pylori* cell-surface mannans seem to be directly implicated in the mediation of host-microbial interactions and immunological modulation. This is the first report of their expression by a Gram-negative bacterium.

Keywords: Cell-surface glycans; *Helicobacter pylori*; lipopolysaccharide; mannan; vaccine.

1. Introduction

Helicobacter pylori is a widespread Gram-negative bacteria that colonizes the gastric mucosa of about 50% of the global human population[1,2]. *H. pylori* infection is currently recognized to be a crucial event in the induction of gastric malignancies such as gastritis, gastric atrophy, and peptic and duodenal ulcers[3,4]. It is also directly correlated with an increased risk of developing gastric cancer[5], the reason why it is classified as a class I (definitive) human carcinogen[6]. As of yet, there is no vaccine against this bacteria and control of infection is accomplished by various combinations of antibiotic regimes[7]. However, this treatment is gradually losing effectiveness due to the rise of antibiotic resistant strains[8] urging the need for new eradication strategies. Based on the proven success of carbohydrate based-vaccines against several pathogenic bacteria[9,10], much attention has been drawn towards the identification and structural characterization of *H. pylori* cell-surface glycans.

Like other Gram-negative bacteria, *H. pylori* expresses cell-surface lipopolysaccharides (LPS) that exert much influence in the mediation of host-pathogen interactions, namely the adhesion to gastric cells and modulation of the host immune response[11,12]. It is now well established that *H. pylori* LPS comprise three distinct structural domains constituted by an elongated *O*-antigenic chain (*O*-chain), an oligosaccharide core, and a fatty-acid rich endotoxin moiety, the Lipid A (*O*-chain→core→Lipid A ~ cell)[13]. *H. pylori O*-chains are known to mimic the glycosylation in the gastric niche[13] by expressing fucosylated glycosides analogous to some mammalian histo-blood-group antigens, namely, the Lewis determinants (Le^a, Le^b, Le^x, sialyl Le^x, Le^y) and the blood groups A and linear B[14]. *H. pylori* serotypes O:3 and O:6 further present an heptoglycan (D-glycero-α-D-manno-heptoses) domain between the Le *O*-chain and the core region (*O*-Chain→Heptoglycan→Core→Lipid A ~ cell)[14-16]. Also, some strains have shown elongated α-(1→6)-Glc chains linked to the core[14,17] or, as recently observed for *H. pylori* serotype O:2, an *O*-chain composed of alternating *O*-2- and *O*-3-linked α-D-glucopyranose residues [→2)-α-D-Glc*p*-(1→3)-α-D-Glc*p*-(1→]$_n$[16].

In addition to the LPS, it has been recently demonstrated that *H. pylori* bioaccumulates considerable amounts of amylose-like glycans under specific environmental pressures such as subcultivation in solid medium[18]. The same study points out the existence of terminal, *O*-2, *O*-6 and *O*-2,6 linked Man residues in the cell-surface

glycan rich extracts of *H. pylori* strains NCTC 11637 and clinical isolates 968 and 14255[18]. Furthermore, it was suggested that growing *H. pylori* in Ham's F12 liquid medium enhances the expression of Man[18]. Further reinforcing the evidences of cell-surface mannose containing molecules, both *H. pylori* coccoid and spiral cellular forms have shown to agglutinate with the α-Man specific lectin of *Pisum sativum*[19]. In addition, coccoid cells have also demonstrated to agglutinate with the α-Man specific lectins of *Lens culinaris* and *Narcissus pseudonarcissus*[19]. Despite these evidences, up to now only one report has been presented addressing the origin and structural organization of *H. pylori* cell-surface mannose-rich polysaccharides (mannans)[20]. However, this polysaccharide was isolated from *H. pylori* mutant strain NCTC 11637 *pgm* having a know-out of the phosphomannomutase gene[20]. Silencing of phosphomannomutase was described as responsible for the reduction of the overall amount of expressed polysaccharides thus facilitating the extraction and purification of external glycocalyx material regarded as yielding Man-rich polysaccharides[20]. In the mentioned report, Monteiro et al.[20] described an immunogenic formulation against *H. pylori* comprising a highly branched polymeric mannan formed by trisaccharide repeating units composed of terminal, *O*-2 and *O*-2,6 Man residues[20]. Still, no structural studies have been conducted in wild type strains casting some doubt on the expression of the mutant-originated mannan by normal cells. In order to clarify this matter, the present study engages in the structural characterization of mannose-rich glycans isolated from *H. pylori* clinical isolate 968 previously recognized as expressing high amounts of Man[18].

2. Experimental

2.1. Bacterial cultures

H. pylori 968 was isolated from a gastric biopsy of a patient diagnosed with a peptic ulcer was provided by the Centre of Biological Engineering of the University of Minho (Braga, Portugal).

2.2. Definition of virulence profile

H. pylori virulence determinants cytotoxin-associated protein (*cagA*) and vacuolating cytotoxin (*vacA*) encoded by the *cagA* and *vacA* genes were accessed by

polymerase chain reaction (PCR). Primers VA1F and VA1xR were used to amplify *vacA* s region, resulting in a fragment of 176 bp for type s1 variants and a fragment of 203 bp for type s2 variants[21]. To amplify the *vacA* m region, a mixture of forward primers MF1.1, MF1.2, MF1.3, and MF1.4 and reverse primer MR1 was used, resulting in the amplification of fragments of 107 and 182 bp for m1 and m2 strains, respectively[22]. The presence of *cagA* was detected with primers *CagA*F and *CagA*R, yielding a product of 183 bp[21]. PCR primers and conditions were as previously described[21,22]. PCR products were visualized by electrophoresis on 2% agarose gels as described by Sambrook et al.[23].

2.3. Bacterial growth in Columbia blood agar

H. pylori cells isolated from gastric biopsies by recovery to pre-warmed Gelose Columbia solid media supplemented with 5% horse blood (bioMérieux, France) and incubated at 37ºC for 72 h, on a microaerophilic atmosphere generated by a CampyGen gas pack (Oxoid, United Kingdom). Cells were subcultivated after 48 h incubation periods in the conditions described above.

2.4. Bacterial growth in F12 liquid media

Cells were grown on Ham's F12 defined liquid media without the addition of enhancing growth factors. The medium was inoculated with cellular extracts obtained from CBA growth media. Cells were allowed to grow for 24 h in a glass flask under microaerophilic atmosphere under gentle stirring at 37ºC.

2.5. Purity assessment of bacterial growth

Purity assessment was assured by using a highly specific peptide nucleic acid probe in a fluorescence *in situ* hybridization procedure, according to the protocol described by Guimaraes et al.[24]. For every experiment a negative control was performed simultaneously where all the steps described above were carried out but where no probe was added during the hybridization procedure. Microscopy visualization was performed using an Olympus BX51 (OLYMPUS Portugal SA, Porto, Portugal) epifluorescence microscope equipped with one filter sensitive to the Alexa fluor 594 signalling molecule attached to the PNA probe (Excitation 530 to 550 nm; Barrier 570 nm; Emission LP 591 nm).

2.6. Extraction and purification of cell-surface glycans

Cell-surface glycans were isolated from cells using the hot phenol:water extraction, according to Westphal and Jann[25]. The aqueous layer was dialyzed against distilled water using a 1,000 Da cut-off membrane and lyophilized. The resulting material was fractioned by Gel Permeation/Adsorption Chromatography (GPC) on a polyacrylamide Bio-Gel P-6 (Bio-Rad) (fractionation range: 1,000-6,000 Da) (1.0 m length and 1.0 cm diameter) column using distilled water as the eluting solvent at constant flow rate of 0.33 mL/min. A portion of the initial material was suspended in degassed distilled water and introduced in to the column. Fractions of 2.8 mL were collected. The mass content in the fractions was estimated on evaporative light scattering detector SEDEX55 (SEDERE France) and further assayed for total sugars with the phenol-H_2SO_4 method[26]. Exclusion and total volume were calibrated with blue dextran 2,000 kDa and glucose, respectively.

2.7. Sugars composition and linkage analysis

Sugars composition analysis was performed by the alditol acetate method as described by Harris et al.[27]. The hydrolysis was done in 4 M trifluoroacetic acid (TFA) at 100ºC for 3 h, followed by reduction with $NaBH_4$ and subsequent acetylation with acetic anhydride in the presence of 1-methylimidazole. Alditol acetates derivatives were analyzed by gas chromatography mass spectrometry (GC-MS), performed in an Agilent Technologies 6890N Network Gas Chromatograph connected to an Agilent 5973 Selective Mass Detector. The GC was equipped with a DB-1 capillary column (30 m length, 0.32 mm internal diameter, and 0.25 μm film thicknesses). The samples were injected in splitless mode (time of splitless 1.00 min), with the injector and detector operating at 220 and 230ºC, respectively, using the following temperature program: 100ºC (1 min) → 150ºC at 5ºC min^{-1} (8 min) → 159ºC at 0.5ºC min^{-1} (5 min) → 250ºC at 5ºC min^{-1} (2 min) → 320ºC at 2ºC min^{-1} (2 min). The carrier gas (He) had a flow of 1.7 mL min^{-1}, with an average linear velocity of 47 $cm.s^{-1}$ and a solvent delay of 9 min. The column head pressure was 5.34 psi. The mass spectrometer was operated in the electron impact mode at 70 eV, scanning the mass range *m*/*z* 40–500 and performing 3.18 scans s^{-1}.

Linkage analysis was carried out by methylation with $NaOH/CH_2SO/CH_3I$, as described by Ciucanu and Kerek[28]. The methylated polysaccharides were hydrolyzed with TFA 2M at 121ºC for 1 h, reduced by $NaBD_4$, and acetylated with acetic anhydride in the

presence of 1-methylimidazole. The partially methylated alditol acetates were analyzed by GC-MS using the chromatographic conditions described previously, using the following temperature program: 45ºC (5 min) → 140ºC at 10ºC min^{-1} (5 min) → 170ºC at 0.5 ºC min^{-1} (1 min) → 280ºC at 15ºC min^{-1} (5 min)

2.8. Protein quantification

Total protein content was estimated by the bicinchoninic acid (BCA) method using bovine serum albumin (BSA) as standard, according Smith et al.[29].

2.9. Affinity chromatography using Polymyxin-B

Mannose-rich material isolated on the void volume of the Bio-Gel P6 column was fractionated based on its affinity to Polymyxin-B. Fractionation was performed according to Arafat et al.[30] in a Polymyxin B-agarose (Sigma Chemical Co.) column with 0.5 cm length and 0.25 cm diameter, operated at 5ºC a constant flow rate of 0.2 $mL.min^{-1}$. The resin was equilibrated with an endotoxin-free 0.1 M ammonium bicarbonate buffer pH 8.0. The sample was dissolved in the buffer to a final concentration of 0.5 $mg.mL^{-1}$, centrifuged to remove suspended particles and the resulting supernatant was loaded into the column. Non-retained material was recovered by elution with with endotoxin-free buffer and the retained material recovered by elution with 1% sodium deoxycholate in buffer endotoxin-free solution.

2.10. Affinity chromatography using a Concanavalin-A

Mannose-rich material isolated on the void volume of the Bio-Gel P6 column was fractionated based on its affinity to the Concanavalin A lectin. Fractionation was performed on a *Concanavalin A* (Conc A) *from Canavalia ensiformis* (Jack Bean) agarose conjugate (Sigma) column with 0.5 cm length and 0.25 cm diameter, operated at 5ºC a constant flow rate of 0.33 mL/min. Prior to elution the column was pre-washed with a wash solution composed of 1 M NaCl, 5 mM $MgCl_2$, 5 mM $MnCl_2$, and 5 mM $CaCl_2$ and equilibrated with a buffer solution of 20 mM Tris 0.5 M NaCl at pH 7.4. The sample was dissolved in the buffer to a final concentration of 1 $mg.mL^{-1}$, centrifuged to remove suspended particles and the resulting supernatant was loaded into the column. Non-retained material was recovered by elution with the buffer and retained material was recovered in a

stepwise elution using 5 mM, 25 mM and 100 mM of methyl-α-D-mannopyranoside in buffer solution.

2.11. Gel electrophoresis

Mannose-rich material isolated on the void volume of the Bio-Gel P6 column was fractionated under SDS-PAGE conditions using a 12.5% polyacryamide gel. Following protein separation, the gels were stained PAS (periodic acid Schiff) according to Doerner and White[31] to detect the glycoproteins and coomassie for general protein detection. Gel images were collected using Gel Doc Transllluminator (Gel DOC XR, BioRad). Following this, the gel bands were recovered for sugars analysis.

2.12. NMR experiments

^{1}H, ^{13}C and ^{31}P NMR spectra were recorded on a Bruker AMX 600 spectrometer equipped with a TXI probe at 310 K and a Varian vnmrs 600 equipped with triple-resonance (^{1}H, ^{13}C, ^{15}N) cryoprobe and recorded at 310 K. Two-dimensional (2D) NMR correlation spectroscopy (COSY), total correlation spectroscopy (TOCSY), nuclear Overhauser effect spectroscopy (NOESY) and heteronuclear spin quantum correlation (HSQC) spectroscopy were performed using the instrument's Bruker software. Prior to performing the NMR experiments, the samples were lyophilized three times with D_2O (99.9%). The HOD peak was used as the internal reference at δ_H 4.761 for ^{1}H NMR spectroscopy, and orthophosphoric acid (δ_P 0.0) as the external reference for ^{31}P NMR experiments. Just before the NMR experiments were carried out, a D_2O sample containing TMS (δ_H 0.00) was run to aid in the reference the HOD signal. The DOSY experiment was recorded on a Bruker AMX 500 equipped with a BBI probe at 310 K.

3. Results and discussion

3.1. *H. pylori* 968 clinicopathological and virulence characterization

H. pylori strain 968 was recovered from a gastric biopsy specimen of a patient with peptic ulcer. Polymerase chain reaction (PCR) characterization of this strain virulence profile highlighted the presence of *cagA*, the terminal gene of the *cag* pathogenicity island (PAI). The *cag* PAI encodes a type IV secretion system through which the CagA protein is

injected into host epithelial cells[32]. *H. pylori* strains containing *cagA* are associated with increased risk of peptic ulcer disease and gastric carcinoma[2,33]. In addition, *H. pylori* 968 was also found to carry the s1/m1 type *vacA* gene. *vacA* encodes the VacA cytotoxin, a protein that induces vacuolization in cultured epithelial cells. *H. pylori* strains containing the s1/m1 genotype, meaning that the signal-region comprises allelic variant s1 and the middle-region comprises allelic variant m1, are frequently associated with peptic ulceration and gastric carcinoma[2,33].

3.2. Pre-characterization of *H. pylori* 968 glycan-rich water extracts

H. pylori 968 was grown in CBA solid medium and Ham's F12 liquid medium, both without the addition of growth enhancing factors that could constitute external sources of polysaccharides. For example, the frequently used fetal bovine serum[34] contains significant amounts of polymeric Man in its composition (data not shown). Cell-surface glycans were isolated in the aqueous phase resulting from hot phenol:water extraction performed on intact bacterial cells. The sugars composition of these extracts are presented in Fig. 1 in terms of μg per mg of dry biomass and correspond to the mean value from three independent growth batches. The results show that CBA glycan-rich extracts were mainly composed by Gal (2.5 μg/mg), Glc (1.8 μg/mg), GlcNAc (1.7 μg/mg), and Rib (1.0 μg/mg). Lower amounts (<1 μg/mg) of DD- (0.8 μg/mg) and LD-Hep (0.7 μg/mg), Man (0.6 μg/mg), Fuc (0.4 μg/mg), Rha (0.1 μg/mg), and traces of Ara were also detected. Rib indicates the presence of ribonucleic acids while Fuc, Glc, Gal, GlcNAc, and DD- and LD-Hep are normally found in *H. pylori* LPS[14] forming what appears to be a highly heterogeneous fraction. As observed for the solid CBA medium, the carbohydrate material present in the Ham's F12 liquid medium also yield considerable amounts of Rib (3.3 μg/mg), Gal (2.3 μg/mg), GlcNAc (2.2 μg/mg), and Glc (1.1 μg/mg), and lower content of Fuc (0.8 μg/mg), DD- (0.6 μg/mg) and LD-Hep (0.6 μg/mg), Rha (0.2 μg/mg), and Ara (0.1 μg/mg). However, in this case, the major sugar after Rib was Man (2.6 μg/mg) in a concentration approximately five times higher than what was observed in the cells recovered from routinely used culture media CBA. The enhanced expression of Man upon growth in Ham's F12 liquid media thus suggests the production of Man-rich glycans.

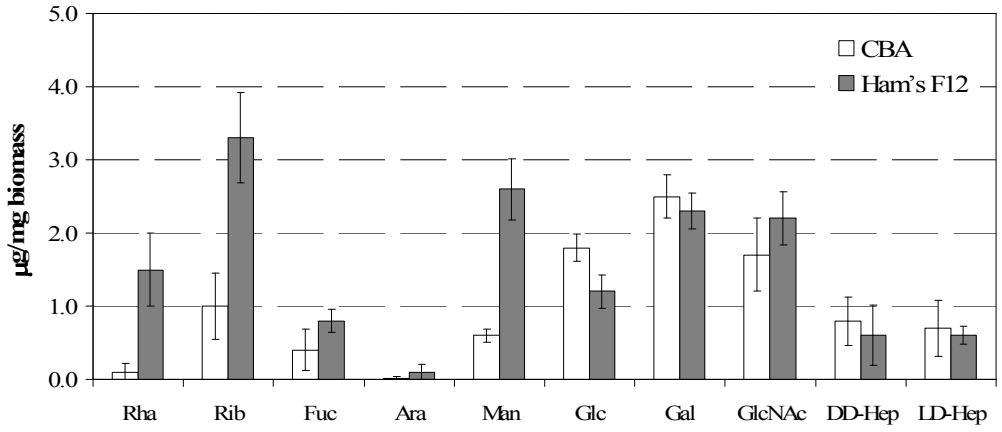

Figure 1. Sugars composition of *H. pylori* 968 glycan-rich water extracts resulting from growth in solid medium (CBA) and Ham's F12 liquid medium.

Linkage analysis (Table 1) confirmed that the F12 material was mainly composed by mannopyranosyl residues consisting of terminal (10.3%), *O*-2 linked (12.0%), *O*-2,6 linked (9.0%) units, and *O*-6 Man (4.3%). Considerable amounts of *O*-4 linked Glc (9.6%) arising from amylose-like glycans[18] and *O*-3 linked Gal (10.1%) and *O*-4 linked GlcNAc (8.5%), recognized as LPS *O*-chain sugars[14], were also present. The similar proportion of *O*-3 linked Gal and *O*-4 linked GlcNAc indicates *O*-chains exhibiting *N*-acetyllactosamine (LacNAc) moieties [→3)Gal(1→4)GlcNAc(1→]. Equal amounts of terminal Fuc (3.4%) and *O*-3,4 linked GlcNAc (4.0%) residues and the absence of branched Gal residues, also suggest the expression of Type 1 Le^a and/or Type 2 Le^x blood group determinants[14]. The presence of LPS was further confirmed by the identification of terminal and *O*-3 linked Glc, *O*-4 linked Gal, *O*-7 DD-Hep, and *O*-2, *O*-2,7 and *O*-3,7 linked LD Hep, normally observed in the core, and *O*-6 linked GlcNAc from Lipid A[14].

The Ham's F12 Man-rich material was then eluted in a Bio-Gel P6 column originating a major peak corresponding to the void volume (Mw > 6,000 Da). Linkage analysis performed on this partially purified material (Table 1) revealed a slightly Man-enriched material, mainly resulting from an increase in the percentage of *O*-2 linked Man. Conversely, the overall amounts of *O*-4 linked Glc decreased significantly, from 10.2% to 3.5%, denoting that the amylose-like glycans in the original water extracts had a Mw lower to 6,000 Da. The percentage of LPS assigned sugars remained mostly unchanged when compared with the non-purified material, showing the presence of semi-rough (oligomeric *O*-chain-core-Lipid A) and smooth phenotypes (polymeric *O*-chain-core-Lipid A).

Table 1. Linkage profile of the sugars in glycan-rich extracts from the *H. pylori* 968 non-purified material and partially purified material recovered in the void volume of a P6 column (Mw > 6,000 Da).

Linkage Type	Relative Molar Ratio (%)	
	non-purified	partially-purified
LPS		
***O*–Chain**		
T-Fuc	3.4	2.8
→6) Glc	4.2	7.9
T-Gal	1.7	3.4
→3) Gal	10.1	11.9
T-GlcNAc	1.8	2.5
→4) GlcNAc	8.5	7.1
→3,4) GlcNAc	4.0	3.1
Core		
*T-Glc	2.8	3.9
→3) Glc	1.1	2.2
→4) Gal	5.9	2.6
T-DD-*manno*-Hep	0.2	v
T-LD-*manno*-Hep	0.3	v
→2) DD-*manno*-Hep	0.5	0.4
→2) LD-*manno*-Hep	0.9	0.5
→3) LD-*manno*-Hep	0.6	0.4
→7) DD-*manno*-Hep	1.0	0.4
→7) LD-*manno*-Hep	0.5	0.6
→3,7) LD-*manno*-Hep	0.8	0.5
→2,7) DD-*manno*-Hep	1.4	0.9
Lipid A		
→6) GlcNAc	0.7	0.3
Mannose-rich glycans		
T-Man	10.3	10.8
→2) Man	12.0	19.2
→6) Man	4.3	3.8
→2,6) Man	9.0	9.5
Amylose-like glycans		
T-Glc*		
→4)Glc	9.6	3.5
→4,6)Glc	0.6	-
Unassigned Sugars		
→2) Ara	0.6	-
→6) Gal	3.2	2.8

Terminal Glc residues can either be addressed to amylose-like polymers or to non-reducing ends of the LPS core. v – Vestigial amounts; > 0.5% total sugars.

3.3 NMR studies on partially purified Man-rich glycans

The ^{1}H Nuclear Magnetic Resonance (NMR) spectrum of the Man-rich fraction recovered from the P6 Bio-Gel column (Fig. 2) exhibited several resonances in the anomeric region δ_{1H} 4.9 to 5.4 ppm thus reflecting the sample high heterogeneity shown by linkage analysis (Table 1).

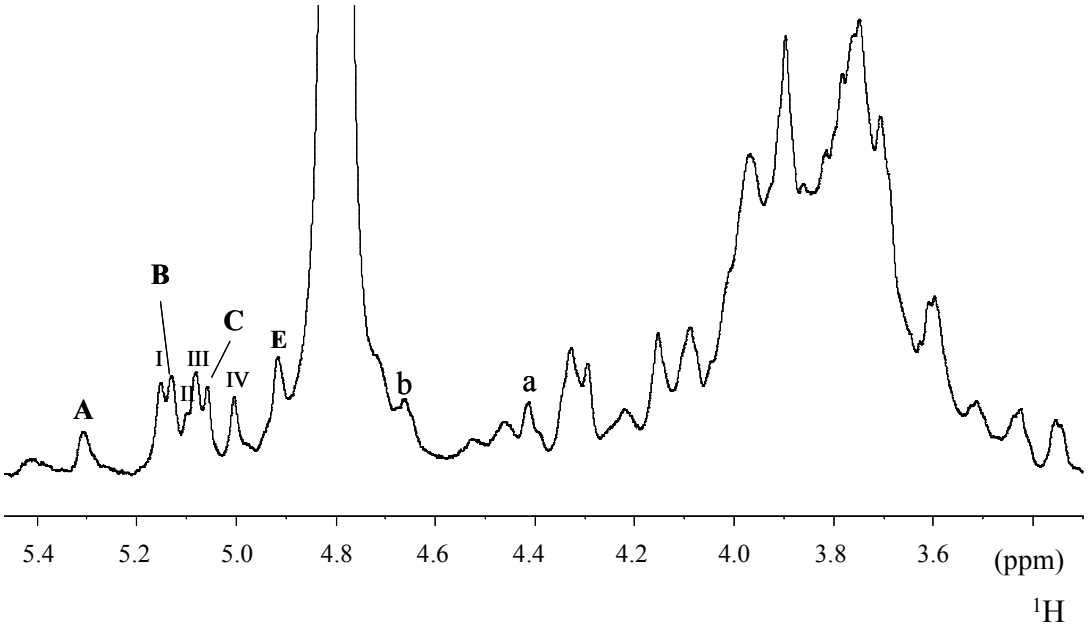

Figure 2. ^{1}H NMR spectrum of the Man-rich material recovered in the void volume of a P6 column (Mw > 6,000 Da).

Combined data from 2D ^{1}H-^{13}C HSQC experiments (Fig. 3), linkage analysis (Table 1), and available literature[35-38] resulted in the assignment of the resonances at $\delta_{1H/13C}$ 5.31/101.90 (residue A), 5.12/99.71 (residue B), and 5.05/103.20 (residue C), respectively to *O*-2 Man, *O*-2,6 Man, and terminal Man, all in α configuration. A weak resonance at $\delta_{1H\text{-}1}$ 4.88 (Residue D in Table 2), resulting from vestigial amounts of α-*O*-6 Man residues (>5%, Table 1), in α configuration[35], was also observed. Sequential assignment of proton signals for spin systems A-D were obtained from the 2D ^{1}H-^{1}H COSY (results not shown) and TOCSY (Fig. 4).

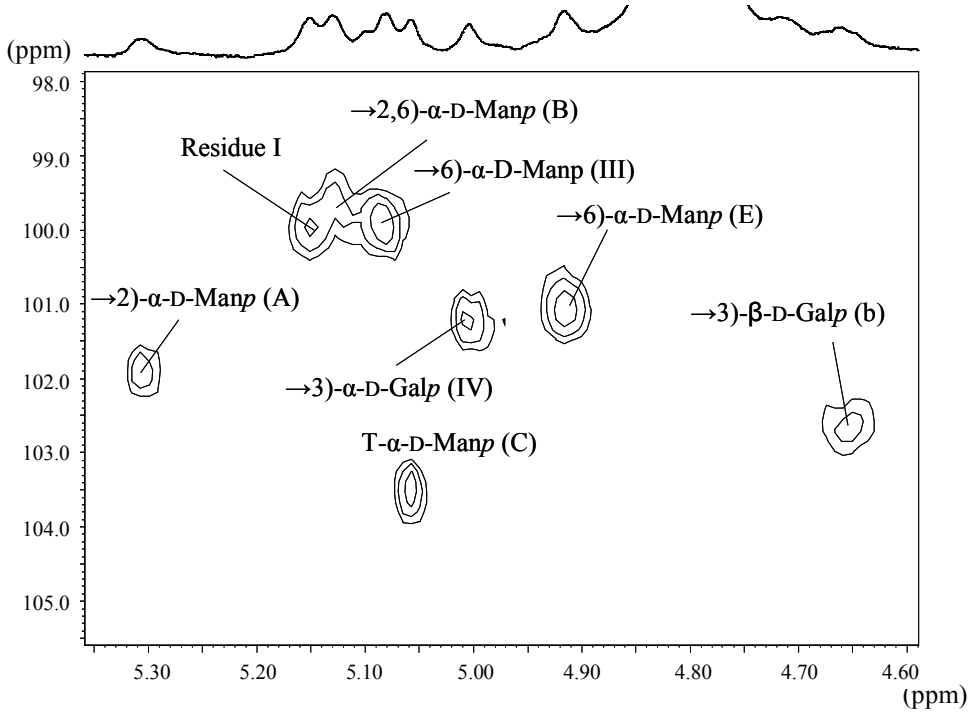

Figure 3. Anomeric region of the 2D ^{1}H–^{13}C HSQC spectrum of the Man-rich material recovered in the void volume of a P6 column (Mw >6,000 Da).

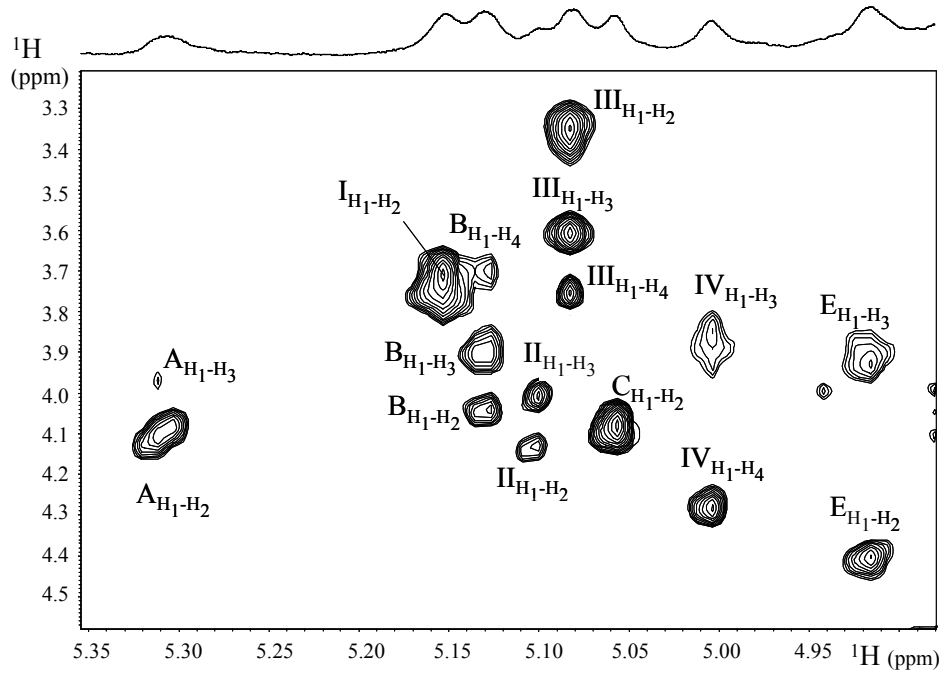

Figure 4 Anomeric region of the 2D ^{1}H-^{1}H TOCSY spectrum of the Man-rich material recovered in the void volume of a P6 column (Mw > 6,000 Da).

The H-6 protons of *O*-2,6 Man residues have also been assigned from the HSQC spectrum (Table 2) based on characteristic downfield shift of Man residues at $\delta_{^{13}C}$ 62.30 to 68.00 ppm upon substitution at the *O*-6 position[35,38]. The identified resonances have been summarized in Table 2 and were found to be in accordance with previous reports[35,36].

Table 2. ^{1}H NMR chemical shifts (ppm) from 2D COSY and 2D TOCSY and 13C chemical shifts from HSQC spectra of Man-rich fraction

Residue	H-1/C-1	H-2/C-2	H-3/C-3	H-4/C-4	H-5/C-5	H-6/C-6	NOE with anomeric
LPS *O*-chain							
a →3)-β-D-Gal	4.45 103.03	3.52 -	3.68 -	-	-	-	-
b →4)-β-D-GlcNAc	4.65 102.56	3.84 -	-	-	-	-	-
Mannose moiety							
A →2)-α-D-Man	5.31 101.99	4.12 79.42	3.98 71.15	-	-	-	A1 (M); B2 (W)
B →2,6)-α-D-Man	5.12 99.71	4.05 -	3.71 71.02	3.91 72.90	-	3.91, 3.70 68.00	B2 (M); B6 (S)
C T- α-D-Man	5.05 103.4	4.08 -	3.85 71.73	-	-	3.90, 3.77 62.30	C2 (S); A2 (W)
D →6)-α-D-Man	4.88 -	3.98 -	-	-	-	-	-
E →2)-β-D-Man	4.92 101.20	4.41 79.33	3.91 71.70	-	-	-	D2 (S); D3 (S); B2 (VW)
Other structural motifs							
I Unassigned Residue	5.15 99.99	3.69 70.70	- -	-	-	-	I2 (S); III6 (S)
II Unassigned Residue	5.10 108.7	4.13 82.41	4.00 84.50	-	-	-	-
III →6)-α-D-Glc	5.08 99.8	3.36 72.71	3.62 73.81	- -	-	3.92, 3.68 68.01	III2 (M); IV3 (VW)
IV →3)-α-D-Gal	5.00 101.1	4.27 70.78	3.86 74.20	-	-	-	IV2 (S); IV3 (S)

Legend: S - strong NOE; M – medium NOE; W – weak NOE; VW – very weak NOE.

Additionally, NOESY experiments (Fig. 5) confirmed the α-configuration of spin system A assigned to *O*-2 Man residue by showing a medium intensity NOE (Nuclear Overhauser Effect) between the anomeric proton at 5.31 ppm and its H-2 at 4.12 ppm.

Residue A also exhibited a low intensity inter NOE between its H-1 and the H-2 of residue B at 4.05 ppm demonstrating that *O*-2 linked Man are linked to the *O*-2 position of *O*-6 Man residues. It further revealed connectivity between the anomeric proton of residue B at 5.12 and its H-6 protons at 3.70 and 3.91 ppm highlighting the presence of sequential *O*-6 linked B residues. The spin-system C corresponding to terminal Man residues showed a single medium intensity inner NOE between its anomeric proton at 5.05 ppm and the H-2 at 4.08 ppm confirming its α configuration. A NOESY spectrum acquired with a longer mixing time (data not shown), even though resulting in strong signal overlapping, allowed to detect a very weak connectivity between H-1 and the H-2 of residue A and of residue B. This observation led to conclude that *O*-2 linked α-Man side chains are terminated by α-Man residues and that some branches exhibit just one terminal residue. Combined information from NMR and linkage analysis thus suggest that *H. pylori* 968 expresses a mannan consisting of α-(1→6)-linked mannopyranose units with approximately 80% of *O*-2 substituted residues. Side chains were found to be composed by terminal and *O*-2 linked α-Man residues.

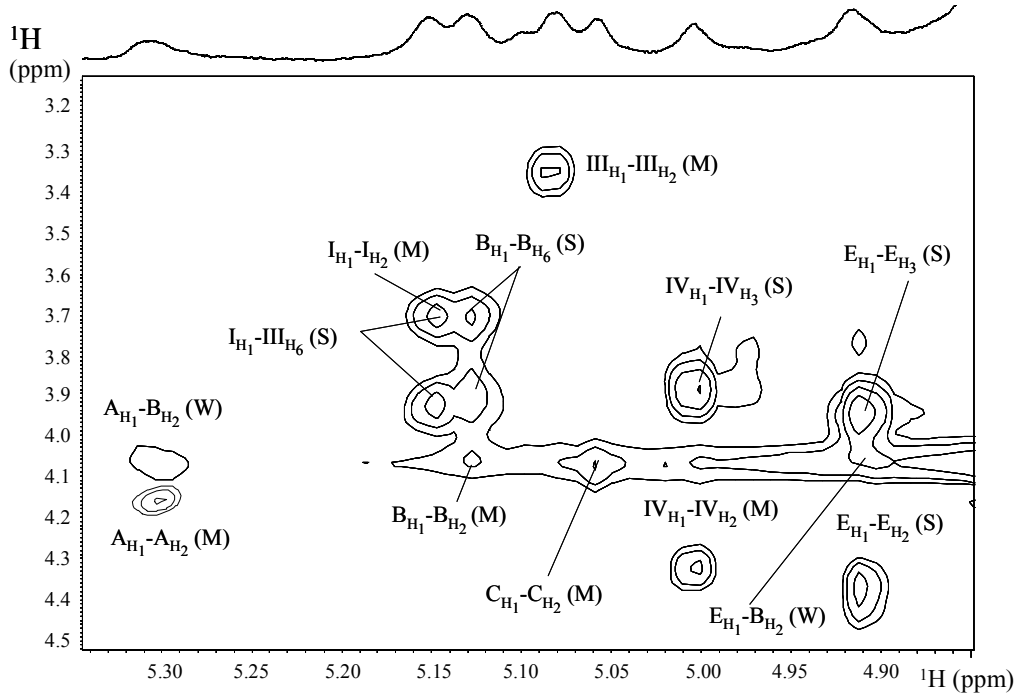

Figure 5. Anomeric region of the 2D ^{1}H-^{1}H NOESY spectrum of the Man-rich material recovered in the void volume of a P6 column (Mw > 6,000 Da). The intensity of the observed NOEs are labelled as follows: S: strong; M: medium; W: weak.

The integration of A-C anomeric resonances in the ^{1}H NMR spectrum retrieved a proportion of *O*-2, *O*-2,6, and terminal Man of approximately 1:1:1 suggesting the existence of a repetitive unit in this mannan. However, the proportion between α-Man residues calculated from the ^{1}H NMR spectrum revealed significantly lower amounts of *O*-2 linked Man residues than that shown by linkage analysis (Table 1). A residue E could also be assigned to the resonances at $\delta_{H1/13C}$ 4.92/101.25 ppm and showed in the TOCSY/HSQC spectra δ_{H_2/C_2} at 4.41/79.33 ppm and $\delta_{H3/C3}$ at 3.91/71.71 ppm. Furthermore, the NOESY spectrum (Fig. 5) exhibited a strong H-1/H-2 inner and inner NOE and a strong H-1/H-3 inner NOE. These assignments are consistent with previous reports for inner chain *O*-2 linked Man residues in β configuration[39,40]. The NOESY spectrum of residue E highlighted the connectivity between its anomeric proton and the H-2 of residue B, revealing that some of the *O*-6 mannose side chains had *O*-2 linked β-Man residues.

The NMR studies also showed an array of low intensity signals from 5.50 to 5.34 ppm assigned to α-Hep from the LPS as well as *O*-3 and *O*-4 linked α-Glc residues and signals at 4.4 to 4.7 ppm assigned to *O*-3 linked Gal and *O*-4 linked GlcNAc residues in β configuration, characteristic of *O*-chains[14,41].

Other resonances were observed in the α-anomeric region of the ^{1}H spectrum (Fig. 1), namely at 5.15 ppm (residue I) exhibiting a carbon chemical shift of 99.95 ppm (Fig. 3). However, the anomeric region of the COSY and TOCSY (Fig. 2) spectra showed for this residue a single cross-peak with the H-2 proton at 3.69 ppm. The strong signal overlapping observed in the ring region prevented the identification of other inner-ring protons and the absence of other cross-peak further compromised its identification. Another unassigned low intensity resonance was detected at 5.10 ppm (Residue II in Table 2) and revealed a highly deshielded C1 chemical shift at 108.7 ppm (data not shown). Two additional strong resonances were detected at δ 5.19 ppm and 5.00 ppm and assigned, based on its anomeric chemical shifts and linkage analysis, to α-*O*-6 linked Glc (residue III) and α-*O*-3 linked Gal (residue IV) respectively. Still, it should be pointed out the considerable shift upfield exhibited by the H-2 proton of residue *O*-6 in relation to a linear *O*-6 linked structure[42]. Additionally, the NOESY spectrum (Fig. 4) exhibited a cross-peak between the anomeric proton of residue I and H-6 protons of residue II at 3.92 ppm and 3.68 ppm confirming both the assignment of residue II to *O*-6 Glc and the connectivity

between the two residues. It also showed a weak intra-residue NOE between the H-1 of residue II and the H-3 of residue III (Table 2) therefore confirming the assignment of residue III to *O*-3 Gal and revealing that residue II is linked to the *O*-3 position of residue III. In addition, the NOESY also highlighted the existence of contiguous *O*-3 linked α-Gal residues by showing a strong H-1/H-3 NOE at 5.00/3.85 ppm in addition to the H-1/H-2 inner NOE at 5.00/4.27 ppm (Fig. 5). Interestingly, the integration of the anomeric protons of residues I, II, and III in the ^{1}H NMR spectrum (Fig. 2) revealed a proportion of 1.0:1.0:1.5, thus consistent with the observation of sequential *O*-3 linked α-Gal residues, also seen by linkage analysis (Table 2). These observations thus suggest the following structural motif: α-Residue I-(1→6)-α-D-Glc-(1→3)-α-D-Gal-(1→3)-α-D-Gal-(1→. The experimental proton and carbon chemical shifts recovered from the COSY, TOCSY, and HSQC spectra for residues II and III (Table 2) matched the theoretical simulation for the oligosaccharide sequence →6)-α-D-Glc-(1→3)-α-D-Gal-(1→3)-α-D-Gal-(1→ using CASPER[45]. This calculation revealed a low overall error of 6.38 ppm between the predicted and experimental data further confirming the mentioned assignment. However, the NOESY spectrum revealed no connectivity between the described structural motif and the mannan moiety or LPS related signals.

3.4. Purification of mannose-rich glycans using polymyxin-B

The *H. pylori* 968 Man-rich fraction isolated in the void volume of the Bio-Gel P6 column was fractionated according to its ability to bind to the amphiphilic polypeptide polymyxin-B, an antibiotic recognized for its affinity for LPS[43,44]. The starting material (Table 3) contained 24% of proteins and 36% of sugars. Its sugars composition was in accordance with linkage analysis (Table 1) by revealing a high percentage of Man (40% of Man) and lower amounts of LPS (19% of Gal, 13% of GlcNAc, and 2% of Fuc, DD-Hep, and LD-Hep), amylose-like glycans (15% Glc), and ribonucleic acids (6% Rib). This material was then loaded into an agarose immobilized polymyxin-B column and approximately half, composed of 33% of proteins and 28% of sugars, showed no affinity to the column. The non-retained fraction (Table 3) was found mainly composed of Man (46%), although other sugars were present. The absence of Fuc, DD- and LD-Hep residues was indicative that the polymyxin B column successfully retained the LPS moiety. The non-retained material was found not significantly enriched in Man when compared with

the starting material, which shows that some Man containing molecules interacted with the column. Conversely, the material recovered from the column using sodium deoxycholate (Table 3) was mainly composed by LPS (22% Gal, 23% GlcNAc and ~4% of Fuc, DD- and LD-Hep). However, both the 1% and 5% sodium deoxycholate eluted material still yielding considerable percentages of Man (16-27%), Glc (13-23%), and Rib (3-10%). Therefore, even though the bulk of Man containing molecules revealed no affinity to polymyxin-B, these results demonstrate its presence among LPS-rich material. Such behaviour shows the amphiphilic behaviour of some of the Man-rich molecules and raises the doubt about of the existence of a Man moiety in the LPS. In addition, the detection of proteins in all fractions may result from a possible protein-carbohydrate association.

3.5. Purification of mannose-rich glycans using concanavalin A

H. pylori mannose-rich fraction isolated in the void volume of the Bio-Gel P6 column (Table 1) was fractionated according to its ability to bind concanavalin A, a lectin recognized to bind to terminal α-D-mannosyl and α-D-glucosyl[45] residues.

The starting material for this experience was found to have a similar composition to the one used for polymyxin-B essays (Table 3), however it contained a lower percentage of sugars (21%) and higher protein content (32%). Elution through the agarose immobilized concanavalin A column originated a sugars-poor (7% of sugars) non-retained fraction yielding 23% of proteins. Sugars analysis highlighted that the sugars moiety was almost exclusively composed of ribonucleic acid (60% Rib) and residual amounts of Man (11%), Gal (13%), and GlcNAc (9%). Moreover, the non-retained fraction yielded approximately 39% of the starting material thus demonstrating that the bulk material showed affinity to concanavalin A.

The retained fraction was recovered in a stepwise elution using 5 mM, 25 mM, and 100 mM methyl-α-D-mannopyranoside. The main retained fraction yielding 27% of the initial material. It revealed a high percentage of proteins (31%) and low amount of sugars (17%), mainly Man-rich material (39%) but also LPS (25% Gal, 9% GlcNAc, 4% Fuc, 3% LD-Hep, and 2% DD-Hep) and amylose-like glycans (18% Glc). Conversely, the 25 mM methyl-α-D-mannopyranoside fraction (19% of the starting material) showed 26% of proteins and a high percentage of sugars (45%), 55% of which Man and 21% of Glc, 17% of Gal, and 7% of GlcNAc. The absence of Fuc and traces of Hep revealed a LPS free

material implying a lack of connectivity between the Man-rich glycans and the LPS, as previously suggested upon fractionation in the polymyxin B column. Interestingly, this fraction showed a proportion between Man:Glc:Gal:GlcNAc of approximate 4:2:2:1 thus similar to the one observed in the LPS-free material non-retained by polymyxin-B (Table 3). This observation suggests a common structural origin for these sugars. The remaining material was recovered with 100 mM methyl-α-D-mannopyranoside and resulted in a fraction with 32% of sugars and 19% of proteins. Contrasting with the 25 mM obtained material, it showed to be mainly composed of LPS and low amounts of Man (9%). Furthermore, it contained significant amounts of Fuc (9%) which denotes a high expression of Le determinants as well as DD- (9%) and LD-Hep (11%) residues, suggesting a prevalence of semi-rough LPS phenotypes. The strong interaction of this LPS forms with concanavalin A can be most likely explained by the existence of terminal α-Glc and Hep residues in a *manno* configuration at the LPS core[14].

3.6. SDS-PAGE/GC-MS evaluation of protein-carbohydrate associations

A portion of the Man-rich material isolated in the void volume of the Bio-Gel P6 column and used as starting material for polymyxin-B essays was fractionated under SDS-PAGE conditions. To evaluate possible protein-carbohydrate associations, the gels were stained with coomassie for general protein detection and periodic acid Schiff (PAS) to detect the glycosidic moiety[46]. Both stainers allowed the distinction of five bands (Fig. 6), corresponding to the non-migrated material (>100 kDa), 36 kDa, 32 kDa, 16 kDa, and 12 kDa, thereby showing that all fractions exhibit proteins with carbohydrate domains. These bands were then removed from the gel and were submitted to sugars analysis (Table 3). To our knowledge, this is the first report demonstrating the feasibility of performing neutral sugars analysis directly in SDS-PAGE bands, although colorimetric methods for detection of uronic acids and total sugars have been already performed[47]. Sugars analysis of the non-migrated material showed high amounts of GlcNAc (28%), Gal (26%), 9% of Fuc and 6% of DD- plus LD-Hep, leading to conclude that it was mainly composed of high-molecular weight smooth-type LPS. In addition, the presence of 20% of Glc might be indicative of polymeric amylose-like glycans while the 5% of Rib residues has its origin in bacterial RNA. However, the amount of Man in this band was 5%, thus considerably low, suggesting that the bulk of the Man-rich material has a molecular weight lower than 100

kDa. Conversely, the 36 kDa band presented Man as its main sugar (37%), even though also yielding 45% of sugars from LPS. These results also highlight that both the non-migrated material and the 36 kDa fraction are a heterogeneous mixture of Man-rich glycans, LPS, and proteins. As it was previously observed in the 36 kDa band, the nearby fraction at 32 kDa also presented Man as main sugar (44%) but it was found devoid of LPS. Furthermore, it also contained approximately 24% of Glc and Gal as well as 9% of GlcNAc revealing a proportion of 4:2:2:1 of Man:Glc:Gal:GlcNAc. Interestingly, similar proportions of these sugars have been also observed in other Man-rich LPS-free fractions, namely the non-retained material from polymyxin-B and 25 mM methyl-α-D-mannopyranoside eluted material from concanavalin A columns (Table 3). These observations further reinforce the existence of a mannose-rich glycan containing a proteic domain and lower amounts of Glc, Gal, and GlcNAc in its composition. Furthermore, the lower molecular weight material in the band at 16 kDa also corresponded to a mixture of Man-rich material and LPS. However, its sugars composition revealed high percentages core-belonging DD- (12%) and LD-Hep (14%) indicating the presence of semi-rough LPS. Like the band at 36 kDa, the band at 12 kDa also did not exhibit LPS. However in this case the main sugars were Glc (40%) and Gal (46%) while Man corresponded only to 10% of the total sugars.

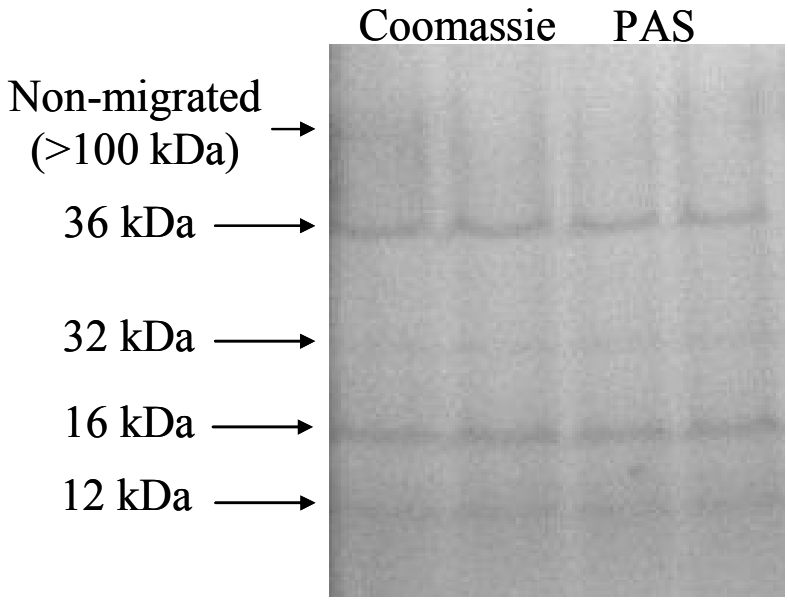

Figure 6. SDS-PAGE of *H. pylori* 968 partially purified material recovered in the void volume of a P6 column (Mw >6,000 Da). Two of the replicates were revealed with coomassie and two with PAS

Table 3. Sugars analysis and protein content of the material resulting from fractionation of the *H. pylori* 968 Man-rich in polymyxin B and concanavalin A columns and under SDS-PAGE conditions.

Fraction	Yield (%)	Molar Ratio (%)										Total Sugars (%)	Total Protein (%)
		Rha	Rib	Fuc	Ara	Man	Glc	Gal	GlcNAc	DD-Hep	LD-Hep		
Polymyxin B													
Starting Material	-	v	6	2	v	40	15	19	13	2	3	36	24
Non-retained	49	-	14	-	-	46	18	17	5	-	-	28	33
Retained													
1% sodium deoxycholate	30	-	10	4	-	27	13	20	22	2	2	35	9
5% sodium deoxycholate	4	-	3	3	-	16	23	22	22	5	6	7	17
Concanavalin A													
Starting Material	-	1	6	4	1	44	16	14	9	2	4	21	32
Non-retained	39	1	60	2	2	11	2	13	9	1	1	7	23
Retained													
5 mM methyl-mannopyranoside	27	-	-	4	-	39	18	25	9	2	3	17	31
25 mM methyl-mannopyranoside	19	-	-	-	-	55	21	17	7	v	v	45	26
100 mM methyl-mannopyranoside	17	-	-	9	-	9	12	22	28	9	11	32	19
SDS-PAGE[a]													
Non-migrated (> 100 kDa)	-	-	5	9	1	7	20	26	28	2	4	-	-
36 kDa	-	-	-	5	-	37	16	18	19	2	3	-	-
32 kDa	-	-	-	-	-	44	23	24	9	-	-	-	-
16 kDa	-	-	-	-	-	10	20	19	25	12	14	-	-
12 kDa	-	-	-	-	-	14	40	46	-	-	-	-	-

v – Vestigial amounts; > 0.5% total sugars.

[a] The impossibility to determine the mass of each fraction did not allow the presentation of total sugars and total protein content

3.7. Linkage analysis on concanavalin A Man-rich fractions

The Man-rich fractions recovered from the concanavalin-A column were evaluated in relation to their glycosidic linkage profile (Table 4). The linkage pattern observed for the 5 mM methyl-α-mannopyranoside eluted fractions confirmed a heterogeneous mixture of Man-rich material, LPS, and amylose-like glycans previously suggested by sugars analysis (Table 3). However, it showed a lower percentage of *O*-2 linked Man (8.0%) residues when compared with the starting material (19.2%, Table 1) while the percentage of the other residues remained mostly unchanged. This observation further suggests that some of the mannan branches are single Man residues. In addition, the *O*-6 mannan backbone in this fraction exhibited a mean percentage of branching residues of 70%, thus lower than what was found in the starting material (80%). The LPS moiety in this fraction was composed by more than 62% of *O*-chain sugars; in particular *O*-3 linked Gal and *O*-4 GlcNAc. Like in the previous fraction, the 25 mM methyl-α-mannopyranoside eluted fraction also presented Man as main sugar. However, its mannans showed higher percentages of terminal and *O*-2,6 Man residues (~22%) and similar amounts of *O*-6 (5.1%) Man residues, therefore showing a higher branching degree, around 80%. It should also be pointed out that the high degree of *O*-6 substituted D-mannopyranosyl residues (26.7%) is known to inhibit the interaction with concanavalin A[48]. However, this effect is thought to be strongly compensated by the high percentage of α-terminal residues (22.4%) thus explaining the affinity of these mannans to concanavalin A. In addition, this fraction contained 7-10% of terminal and *O*-6 linked Glc and *O*-3 Gal and lower percentages (<5%) of *O*-3 and *O*-4 Glc, terminal and *O*-6 linked Gal and terminal and O-4 linked GlcNAc that had been assigned to the LPS moiety in LPS-containing fractions. Due to the absence of LPS in this fraction these sugars should be referred as unassigned (Table 4) and a possible association with the mannan moiety may be though to occur. Contrasting with the previous two fractions, the material with higher affinity to Concanavalin A was found to be composed mainly by LPS, thus confirming what had been suggested upon sugars analysis (Table 3). The LPS moiety contained over 40% of core material, in particular DD- and LD-Hep residues as well as terminal Glc (5.8%), *O*-3 Glc (4.6%), and *O*-4 Gal (4.8%), revealing low molecular weight LPS. The high percentage of terminal Glc (5.8%) and the presence of Hep residues in a *manno* configuration is though to be responsible by the observed high affinity to Concanavalin A.

Table 4. Linkage profile of the sugars observed in *H. pylori* 968 fractions showing affinity to concanavalin A.

Linkage Type	Relative Molar Ratio (%) [methyl-α-D-mannopyranoside]		
	5 mM	25 mM	100 mM
LPS			
***O*–Chain**			
T-Fuc	3.0	-	7.0
→6) Glc	9.0	-	2.4
T-Gal	1.9	-	3.5
→3) Gal	10.7	-	17.3
T-GlcNAc	0.3	-	4.5
→4) GlcNAc	5.0	-	8.9
→3,4) GlcNAc	1.5	-	5.4
Core			
*T-Glc	6.2	-	5.8
→3) Glc	1.1	-	4.6
→4) Gal	6.3	-	4.8
T-DD-*manno*-Hep	v	-	0.7
T-LD-*manno*-Hep	v		0.9
→2) DD-*manno*-Hep	0.3	-	1.2
→2) LD-*manno*-Hep	0.9	-	6.0
→3) LD-*manno*-Hep	0.6	-	2.8
→7) DD-*manno*-Hep	0.9	-	3.9
→7) LD-*manno*-Hep	0.8	-	2.9
→3,7) LD-*manno*-Hep	0.8	-	2.2
→2,7) DD-*manno*-Hep	1.2	-	2.5
Lipid A			
→6) GlcNAc	1.0	-	-
Mannose-rich glycans			
T-Man	11.4	22.4	1.4
→2) Man	8.0	10.2	10.9
→6) Man	4.8	5.1	-
→2,6) Man	11.5	21.6	1.2
Amylose-like glycans			
T-Glc*	-	9.1	-
→4)Glc	8.1	4.2	0.3
→4,6)Glc	-	-	-
Unassigned Sugars			
→3) Glc	-	2.5	-
→6) Glc	-	6.8	-
T-Gal		2.3	
→4) Gal	-	0.8	-
→3) Gal	-	10.1	-
→6) Gal	4.7	2.0	-
T-GlcNAc	-	1.5	-
→4) GlcNAc	-	1.4	-

* Terminal Glc residues can either be addressed to amylose-like polymers or to non-reducing ends of the LPS core.v – Vestigial amounts; > 0.5% total sugars.

In addition, the *O*-chain moiety, formed by LacNAc units (17.3% of *O*-3 Gal and 8.9% of *O*-4 GlcNAc), exhibited the highest degree of fucosylation (7.0% of Fuc and 5.4% of *O*-3,4 GlcNAc) among the three fractions. Conversely, the Man content in this fraction did not exceeded 15% (Table 3 and Table 4), prevailing *O*-2 linked Man (~80% of the total Man) in relation to the other Man residues. Also, no *O*-6 residues were detected, revealing a 100% substituted *O*-6 mannan exhibiting elongated side chains of *O*-2 Man residues.

The structural diversity observed for the mannan moiety throughout the three studied fractions further suggests the absence of a structure formed by repeating blocks but rather a random organization showing different branching degrees and side chain extensions and even substitution.

3.8. Diffusion Ordered Spectroscopy and ^{31}P NMR studies on concanavalin A Man-rich fractions

The Man-rich fractions recovered from the concanavalin A column with 5 mM and 25 mM methyl-α-mannopyranoside were studied by Diffusion Ordered Spectroscopy (DOSY) to evaluate a possible association between the mannan moiety and other structural motifs. The DOSY spectra (Fig. 7) exhibits in the *x*-axis the ^{1}H NMR signals pointing out the anomeric resonances of Man residues A-C and E (Table 2) and in the *y*-axis the diffusion coefficient. The spectrum of the 5 mM fraction (Fig. 7a) was characterized by a significant dispersion of the proton signals along the *y*-axis (0.1 to 3.0 μm/s) highlighting the structural heterogeneity suggested by sugars (Table 2) and linkage analysis (Table 4). Even tough the spectrum in Fig. 7a exhibited strong signal overlapping in the anomeric and ring regions, it was still possible to observe that the signals from residues A-C and E exhibited the same diffusion coefficient (~0.3 μm/s). However, other resonances in the α-anomeric region from 5.13-4.88 ppm have also shown similar diffusion coefficients suggesting a possible association with the Man moiety. Conversely, the DOSY spectrum of the 25 mM fraction (Fig. 7b) revealed for all the ^{1}H NMR signals a similar diffusion coefficient around 2.5 μm/s. This value also demonstrated that the Man-rich glycans in this fraction have a lower Mw than the ones observed in the material with lower affinity to concanavalin A. The existence of proteins (Table 3) and also considerable amounts of Glc and Gal as well as GlcNAc (Table 3 and Table 4) in this fraction reinforces the thesis of a heteropolymeric Man-rich glycan, possibly containing a protein domain.

Both fractions were also screened for phosphorous content by ^{31}P NMR but revealed no signs of phosphorylation.

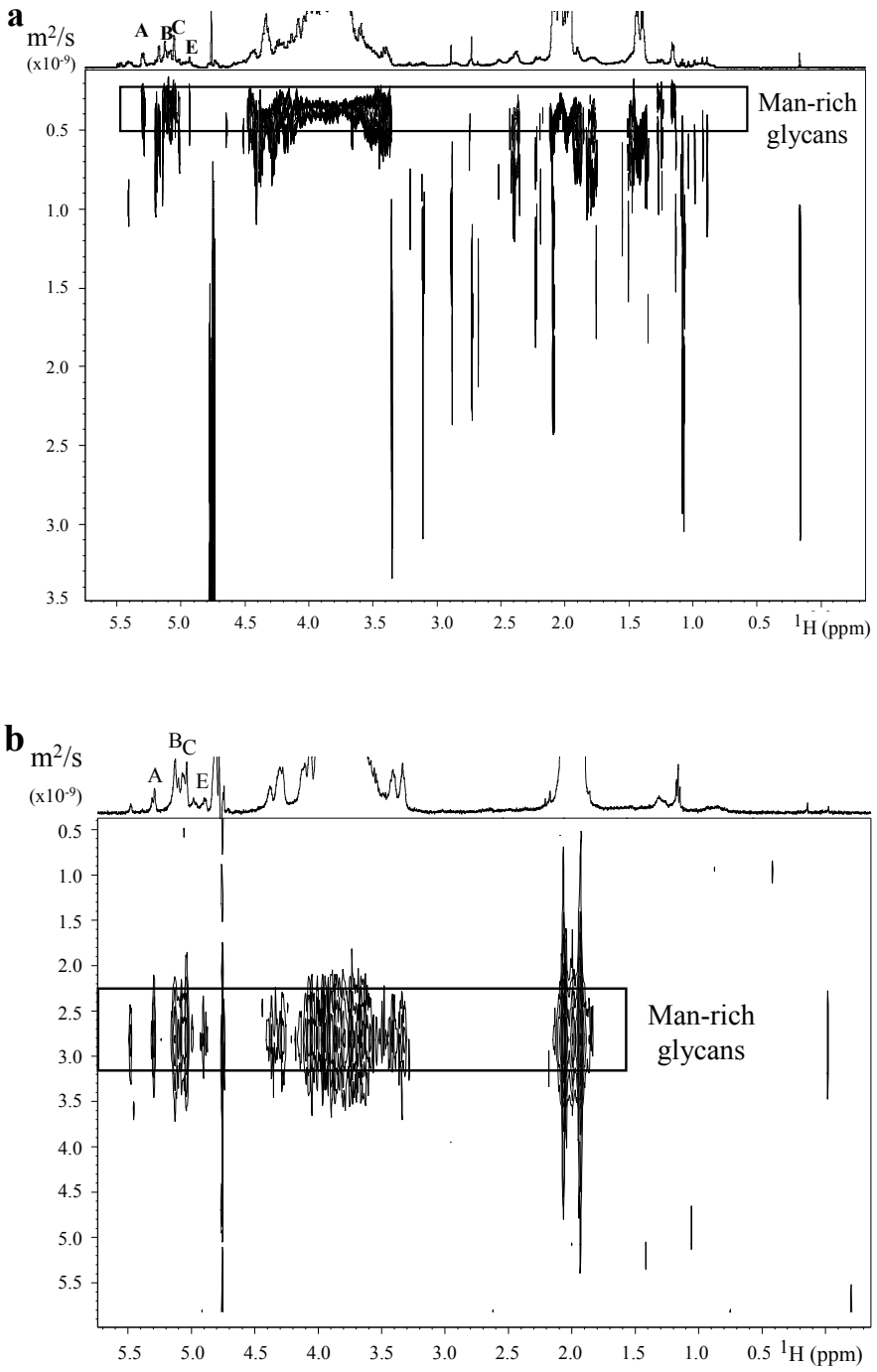

Figure 7. DOSY analysis of the Man-rich concavalin A retained material eluted with a) 5 mM and b) 25 mM methyl-α-D-mannopyranoside.

4. Discussion

The expression of vestigial amounts of Man at *H. pylori* cell-surface has been long postulated[16,19] and found widespread among several strains[18,19,55]. Despite these observations, the structural assignment of *H. pylori* cell-surface Man has remained overlooked, most likely due by its low biological abundance. Based on these considerations, the present work engaged in the structural characterization of *H. pylori* Man-rich glycans from wild type strain *H. pylori* 968 previously recognized by over-expressing Man[18]. *H. pylori* 968 was recovered from the gastric biopsy of a Portuguese patient diagnosed with a peptic ulcer and characterized as carrying virulence markers *cagA*$^+$ and *vacA*$^+$. This virulent strain was cultivated in routinely used CBA[17] and also in Ham's F12 liquid medium, a medium known by its capability to overcome *H. pylori* high fastidiousness[34,54], i.e. difficult to culture outside the human reservoir[56]. Cultivation in F12 liquid medium has been shown to promote the expression *in vitro* of cell-surface phenotypes similar to those observed *in vivo*[18]. Our work also shows that this medium also enhances the production of Man by *H. pylori* cells when compared with CBA. This observation suggests that the expression of Man by *H. pylori* may be considerably higher *in vivo* when compared with long-term laboratory maintained strains.

The high amounts of Man observed in Ham's F12 grown cells might be also explained by pH changes in the culture medium from an initial pH 6.5 to approximately 5.0. These variations exert strong influence in gene expression and modulation of the activity of the enzymes related with the biosynthesis of GDP-D-Man[52,53]. In *H. pylori*, GDP-D-Man is mainly produced from D-fructose-6-phosphate in a three step pathway[53-55] and the first and third steps are catalyzed by a bifunctional phophomannose isomerase/GDP-D-mannose phosphorylase, an enzyme only found in bacteria and involved in the expression of capsular polysaccharides[55]. GDP-D-Man is the main precursor of GDP-L-Fuc used by *H. pylori* in the fucosylation of LPS *O*-chains[56] using a pathway with three additional steps[61]. A decrease in pH from 6.5 to 5.0 has been recognized to enhance the expression of the *wbcJ* gene, encoding a protein homolog involved in the conversion of GDP-Man to GDP-Fuc[53]. Thus, pH conditions encountered in *H. pylori* 968 culture medium may be considered to favour the fucosylation of LPS *O*-chains. However, the enzymes involved in the conversion of GDP-D-Man into GDP-L-Fuc have been described to have optimal pH activities at 6.5 and 8.0, respectively[59], which may contribute to an

increase in the pool of GDP-D-Man residues available for the production of Man-rich glycans. It should also be pointed out that GDP-D-Man is also the precursor of other activated nucleotides, namely GDP-6-deoxy-D-talose and GDP-D-Rha[60], which that might explain the trace amounts of Rha detected in glycan-rich water extracts.

Structural studies conducted on the Man-rich glycans recovered from Ham's F12 liquid medium led to conclude that *H. pylori* 968 co-expressed at its cell-surface complex Man-rich heteropolymers, LPS yielding partially fucosylated polyLacNAc *O*-chains units, and low amounts of amylose-like glycans. The structural heterogeneity of cell-surface water extracts was found to be the major drawback for the characterization of *H. pylori* Man-rich glycans. Moreover, the assignment of lower amounts of Glc, Gal, and GlcNAc to this mannan was only possible by combining information from affinity to polymyxin-B and concanavalin A, SDS-PAGE and DOSY experiments. In addition, these experiences strongly suggest that the mannan moiety is part of a hetepolimeric glycan containing a protein domain. However, the low amount of material available resulting from the reduced growth rates exhibited by *H. pylori* hampered a full structural characterization. Still, NMR experiments demonstrate that Man-rich glycans are formed by a sugar backbone consisting of α-(1→6)-linked mannopyranose units exhibiting up to 80% branching at the *O*-2 position and side chains composed of *O*-2 linked residues. Interestingly, the *O*-2 side chain residues were found to be either in α- or in β-anomeric configuration. Similar mannans has been observed in cell-surface of several other microorganisms, namely in the cell wall of yeasts such as *Candida albicans*[56], *Candida catenulate*[57], and *Candida sojae*[37], and fungi such as *Cryphonectria parasitica*[36], or in the form of phosphorylated mannans and arabinomannans in mycobacteria[58]. They have further been detected at the cell-surface of Gram-positive bacteria like *Corynebacterium diphtheriae*[38] and those belonging to the genus *Kribbella*[59], as well as in exopolysaccharides from Gram-negative *Pseudomonas syringae* pv. *ciccaronei*[35] and *Porphyromonas gingivalis*[61]. However, some structural variability was observed mainly in the percentage of branching of the backbone and substitution pattern of its side chains. Mannan side-chains similar to the ones of *H. pylori* 968, exhibiting both terminal and/or *O*-2 linked Man in α and/or β configurations have also been described in yeasts[39,57] and Gram-positive[38] bacteria. However, this is the first report of their expression by a Gram-negative bacterium. Moreover, the microorganism mannans may present *O*-3 linked Man, terminal Glc[35], and α-D-Ara[38,59] as side chains. The structural

diversity observed may be thought to also occur in *H. pylori* 968 where considerable amounts of unassigned terminal and *O*-6-Glc and *O*-3-Gal were systematically found in Man-rich extracts.

Alpha mannans were also observable as *O*-chains in the LPS of Gram-negative enterobacteria *Hafnia alvei* strain PCM 1223[60], *Citrobacter braakii*[62], *Escherichia coli* serotype O8[63], and O9[64] and *Klebsiella* pneumoniae serotype O5[75]. However, in *H. pylori 968*, experimental evidences point towards an association not with lipids but with proteins. Furthermore, in the mentioned cases, the mannan backbone was formed by *O*-2 and *O*-3 linked Man residues whereas in *H. pylori* 968 the backbone is formed by *O*-6 and *O*-2,6 linked Man.

H. pylori cell-surface mannans seem to be directly implicated in the mediation of host-microbial interactions and immunological modulation. In agreement with these considerations, proves have been presented that *H. pylori* cells can interact with the mannose-binding lectin (MBL) protein[65], coded by the *MBL-2* human gene, a key component in systemic and mucosal innate immunity[66-68]. MBL was found to induce bacterial elimination[69,70] by activating the complement system and to promote complement-independent opsonophagocytosis[71]. Besides activating local immune responses against the bacteria, the interaction between *H. pylori* mannans and the MBL protein may also exert much influence in the clinical outcome resulting from infection. Differences have been extensively explained by a conjugation of aspects, namely bacterial virulence markers[72], host genetic factors[73], and environmental pressure. Among these, mammalian Le blood groups expressed at *H. pylori* cell surface are recognized has the main glycan mediators in the interaction with the host's immune system. Several studies have been pointing out that abnormalities in the MBL protein in *H. pylori*-positive hosts potentiate gastric pathologies such as severe gastric mucosal atrophy[74], chronic gastritis, and gastric cancer[75,76]. MBL deficiencies[77] are common among many human populations[73,78]. By correlating genotypic variations in MBL proteins and particular clinical presentations, the mentioned studies highlight the importance of mannose-mediated phenomena in pathogenesis. Furthermore, they demonstrate the existence of other cell-surface glycans in addition to Le determinants acting as players in bacteria-host interactions turning the spotlight towards the up until now overlooked *H. pylori* cell-surface mannans.

H. pylori mannans are also thought to have an antigenic potential resulting from their capability of activating and triggering immune responses[73] making then potential candidates to include in a carbohydrate-based vaccine. Furthermore, they overcome some of the limitations shown by other glycans found in *H. pylori* cell-surface, namely amylose-like polysaccharides widespread through nature and LPS that are known to express mammalian Lewis histo-blood group determinants[14].

Acknowledgments

The authors gratefully acknowledge the financial support provided by the project POCI/QUI/59337/2004, and Research Units 62/94 – QOPNA, Fundação para a Ciência e a Tecnologia (FCT) financed project Pylori E&LPS POCI/QUI/56393/2004, PhD grant SFRH/BD/19929/2004 and Natural Sciences and Engineering Research Council of Canada (NSERC). The authors also gratefully acknowledge the access to research infrastructures within the 6th Framework Programme of the EC (Contract # RII3-026145, EU-NMR) and the opportunity to conduct experiments at the RALF-NMR facility. The authors further thank Dr. Adrien Favier (RALF-NMR facility) for conducting NMR experiments.

References

1. Farinha, P.; Gascoyne, R.D. Gastroenterology. **2005**, 128, 1579-1605.
2. Kusters, J.G.; van Vliet, A.H.M., Kuipers, E.J. Clin. Microbiol. Rev. **2006**, 19, 449-490.
3. Kandulski, A.; Selgrad, M.; Malfertheiner, P. Dig. Liver. Dis. **2008**, 40, 619-626
4. Ferreira, A.C.; Isomoto, H.; Moriyama, M.; Fujioka, T.;Machado, J.C.; Yamaoka, Y. Helicobacter. **2008**, 13, 28-34.
5. Wen S.; Moss S.F. Cancer Lett. **2009**, 282, 1-8.
6. I.A.R.C., Working Group on the Evaluation of Carcinogenic Risks to Humans, 1994.IARC Monogr. Eval. Carcinog. Risk. Hum. **1994**, 61, 1-214.
7. Campo, S.M.; Zullo, A.; Hassan, C.; Morini, S. Recent. Pat. Antiinfect. Drug Discov. **2007,** 2, 11-17.
8. Vakil, N. Rev. Gastroenterol. Disord. **2008**, 8, 77-82.
9. Vliegenthart, J.F.G. FEBS Lett. **2006**, 580, 2945-2950.
10. Monteiro, M.A.; Baqar, S.; Hall, E.R.; Chen, Y.H.; Porter, C.K.; Bentzel, D.E.; Applebee, L.; Guerry, P. Infect. Immun. **2009**, 77, 1128-1136.

11. Hooper L.V.; Gordon, JI. 2001. *Glycobiology*. **2001**, 11, 1R-10R.
12. Erridge, C; Bennett-Guerrero, E.; Poxton, I.R. Microbes Infect**. 2002**, 4, 837-451.
13. Moran, A.P. Carbohydr. Res. **2008**, 343, 1952-1965.
14. Monteiro, M.A. Adv. Carbohydr. Chem. Biochem**. 2001**, 57, 99-158.
15. Monteiro M.A.; Michael, F.S.T.; Rasko, D.A.; Taylor, D.E.; Conlan, J.W.; Chan, K.H.; Logan, S.M.; Appelmelk, B.J.; Perry, M.B. Biochem. Cell. **2001**, 79, 449-459.
16. Britton, S.; Papp-Szabo, E.; Simala-Grant, J.; Morrison, L.; Taylor, D.E.; Monteiro, M.A.. Carbohydr. Res. **2005**, 340, 1605-1611.
17. Altman, E.; Smirnova, N.; Li, J.; Aubry, A.; Logan, S.M. Glycobiology. **2003**, 13, 777-783.
18. Ferreira, J.A.; Pires, C.; Paulo, M.; Azevedo, N.F.; Domingues, M.R.; Vieira, M.J.; Monteiro, M.A.; Coimbra, M.A. Helicobacter. **2009**.14, 559-570.
19. Khin, M.M.; Hua, J.S.; Ng, H.C.; Wadstrm, T.; Ho, B. World. J. Gastroentero. **2000**, 6, 202-209.
20. Monteiro, M.A.; Fulginiti, J.; Dilts, D.A. U.S. Patent US 0118197 A1, **2005**.
21. van Doorn, L.J.; Figueiredo, C.; Rossau, R.; Jannes, G.; van Asbroek, M.; Sousa, J.C.; Carneiro, F.; Quint, W.G. J. Clin Microbiol. **1988**. 36, 1271-1276.
22. van Doorn, L.J.; Figueiredo, C.; Sanna, R.; Pena, S.; Midolo, P.; Ng, E.K.; Atherton, J.C.; Blaser, M.J.; Quint, W.G. J Clin Microbiol. **1998**. 36: 2597-2603.
23. Sambrook, J.; Fritsch, E.F.; Maniatis. Gel electrophoresis of DNA. T. In *Molecular cloning, a laboratory manual*. 2nd ed.; Cold Spring Harbor Laboratory Press: New York, 1989.
24. Guimarães, N.; Azevedo, N.F.; Figueiredo, C.; Keevil, C.W.; Vieira, M.J. J Clin Microbiol **2007**, 45, 3089-3094.
25. Westphal, O.; Jann, K. Methods Carbohydr. Chem. **1965**, 5, 83–91.
26. Dubois, M.; Gilles, D.A.; Hamilton, J.K.; Rebers, P.A.; Smith, F. Anal. Chem. **1956**, 8, 350–856.
27. Harris, P.J.; Blakeney, A.B.; Henry, R.J.; Stone, B.A. J AOAC Int. **1988**;71, 272–275.
28. Ciucanu, I.; Kerek, F. Carbohydr. Res. **1984**, 131, 209–217.
29. Smith, K.; Krohn, R.I.; Hermanson, G.T.; Mallia, A.K.; Gartner, F.H.; Provenzano, M.D.; Fujimoto, E. K.; Goeke, N.M.; Olson, B.J.; Klenk, D.C. Anal. Biochem. **1985**, 150, 76-85.

30. Arafat, H.H.; Sawada, H.; Tanaka, K.; Suzuki, K. Plant Pathol. **2009**, 8, 1-8.

31. Doerner, K.C.; White, B.A. Anal. Biochem. **1990**. 187: 147-150.

32. Backert, S.; Selbach, M. Cell. Microbiol. **2008**, 10, 1573-1581.

33. Figueiredo, C.; Machado, J.C.; Pharoah, P.; Seruca, R.; Sousa, S.; Carvalho, R.; Capelinha, A.F.; Quint, W.; Caldas, C.; van Doorn, L.J.; Carneiro, F.; Sobrinho-Simões M. J. Natl. Cancer Inst. **2002**, 94, 1680-1687.

34. Testerman, T.L.; McGee, D.J.; Mobley, H.L.T. J. Clin. Microbiol. **2001**, 39, 3842-3850.

35. Corsaro, M.M.; Evidente, A.; Lanzetta, R.; Lavermicocca, P.; Molinaro, A. Carbohydr. Res. **2001**, 330, 271-277.

36. Molinaro, A.; Piscopo, V.; Lanzetta, R.; Parrilli M. Carbohydr. Res. **2002**, 337, 1707-1713.

37. Oyamada, H.; Ogawa, Y.; Shibata, N.; Okawa, Y.; Suzuki, S.; Kobayashi, H. Arch Microbiol. **2008**, 189, 483-490.

38. Moreira, L.O.; Mattos-Guaraldi, A.L.; Andrade, A.F.B. Arch. Microbiol. **2008**, 190, 521–530.

39. Stenutz, R., Jansson, P.E., Widmalm, G. Carbohydr Res. **1998**, 306,11-17.

40. Shibata, N.; Suzuki, A.; Kobayashi, H.; Okawa, Y. Biochem. J. **2007**, 404, 365-372.

41. Aspinall, G.O.; Mainkar, A.S; Moran, A.P. Glycobiology. **1999**, 9, 1235-1245.

42. Colson, P.; Jennings, H.J.; Smith, I.C.P. J. Am. Chem. Soc. **1974**, 96, 8081-8087.

43. Issekutz, A.C. J. Immunol. Methods. **1983**. 61, 275-281.

44. Molvig, H.; Baek, L. Scand. J. Immunol. **1987**. 26, 611-619.

45. Goldstein, I.J.; Hollerman, C.E.; Smith, E.E. Biochemistry. **1965**, 4, 876-883.

46. Doerner, K.C.; White, B. Anal. Biochem. **1990**, 187, 147-150.

47. Saraiva, J.; Nunes, C.; Coimbra, M.A. Food Chem., **2007**, 101, 1594-1602.

48. Yahara, I.; Edelman, G.M. Proc. Nat. Acad. Sci. **1972**, 69, 608-612.

49. Moran, A.P; Helander, I.M.; Kosunten, T.U. J. Bacteriol. **1992**, 1370-1377.

50. Stevenson, T.H.; Castillo, A.; Lucia, L.M.; Acuff, G.R. Lett Appl Microbiol. **2000**, 30, 192-196.

51. Sainsus, N.; Cattori, V.; Lepadatu, C.; Hofmann-Lehmann, R. Eur. J. Clin. Microbiol. Infect. Dis. **2008**, 27, 1209-1217.

52. McGowa, C.C.; Nechev, A.; Thompso, S.A.; Cove, T.L.; Blasé, M.J. Mol. Microbiol. 1998, 30, 19-31.

53. Wu, B.; Zhang, Y.; Wang, P.G. Biochem. Biophys. Res. Commun. **2001**, 285, 364-371.

54. Wu, B.; Zhang, Y.; Zheng, R.; Guo, C.; Wang, P.G. FEBS Lett. **2002**, 519, 87-92.

55. Mäki, M; Renkonen, R. Glycobiology. **2004**, 14, 1R-15R.

56. Shibata, N.; Suzuki, A.; Kobayashi, H.; Okawa, Y. Biochem. J. **2007**, 404, 365-372.

57. Kobayashi, H.; Suzuki, J.; Tanaka, S.; Kiuchi, Y.; Oyamada, H.; Iwadate, N.; Suzuki, H.; Shibata, N.; Suzuki, S.; Okawa, Y. Arch. Biochem. Biophys. **1997**, 341, 70-74.

58. Maes, E.; Coddville, B.; Kremer, L.; Guérardel, Y. Glycoconj. J**.2007**, 24, 349-448.

59. Shashkov, A.S.; Tul'skaya, E.M.; Streshinskaya, G.M.; Senchenkova, S.N.; Avtukh, A.N.; Evtushenko, L.I. Carbohydr Res. **2009**, 344, 2255-2262.

60. Katzenellenbogen, E.; Kocharova, N.A; Zatonsky, G.V.; Kübler-KieIb, J.; Gamian, A.; Shashkov, A.S.; Knirel, Y.A.; Romanowska, E. FEMS Immunol. Med. Microbiol. **2001**, 30, 223-227.

61. Rangarajan, M.; Opoku, J.A.; Paramonov, N.; Hashim, A.; Bostanci, N.; Fraser, O.P.; Tarelli, E.; Curtis, M.A. J. Bacteriol. **2008**, 190, 2920-2932.

62. Kocharova, N.A.; Zatonsky, G.V.; Bystrova, O.V.; Shashkov, A.S.; Knirel, Y.A.; Kholodkova, E.V.; Stanislavsky, E.S. Carbohydr Res. **2001**, 333, 335-338.

63. Jansson, P.E.; Lönngren, J.; Widmalm, G.; Leontein, K.; Slettengren, K.; Svenson, S.B.; Wrangsell, G.; Dell, A.; Tiller, P.R. Carbohydr Res. **1985**, 145, 59-66.

64. Tada, R.; Nagi-Miura, N.; Adachi, Y.; Ohno, N. Chem. Pharm. Bull. **2007**, 55, 992-995.

65. Holmskov, U.; Thiel, S.; Jensenius, J.C.; Annu. Rev. Immunol. **2003**, 21, 547-578.

66. Jack, D.L.; Klein, B.J.; Turner, M.W. Immunol. Rev. **2001**, 180, 86-99.

67. Garred, P.; Larsen, F.; Madsen, H.O.; Kock, C., Mol. Immunol. **2003**, 40, 73-84.

68. Baccarelli, A.; Hou ,L.; Chen, J.; Lissowska, J.; El-Omar, E.M.; Grillo, P.; Giacomini, S.M.; Yaeger, M.; Bernig, T.; Zatonski, W.; Fraumeni, J.F.Jr.; Chanock, S.J.; Chow, W.H. Int. J. Cancer. **2006**, 119,1970-1975.

69. Kilpatrick, D.C. Biochim. Biophys. Acta. **2002**, 1572, 401-413.

70. Jack, D.L.; Turner, M.W.Biochem. Soc. Trans., **2003**, 31, 753-757.

71. Turner, M.W. Mol. Immunol., **2003**, 40, 423-429.

72. Proença-Modena, J.L.; Acrani, G.O.; Brocchi, M. Future Microbiol. **2009**, 4, 223-240.

73. Snaith, A.; El-Omar, E.M. Expert. Rev. Gastroenterol. Hepatol. **2008**, 2, 577-585

74. Tahara T; Shibata, T.; Wang, F.Y.; Nakamura, M.; Yamashita, H.; Yoshioka, D.; Okubo, M., Maruyama, N.; Kamiya, Y.; Nakamura, M.; Fujita, H; Nagasaka, M.; Iwata, M.; Takahama, K.; Watanabe, M.; Nakano, H., Hirata, I.; Arisawa, T. Eur. J. Gastroenterol. Hepatol. **2009**, 21, 781-786.

75. Worthley, D.L.; Bardy, P.G.;Gordon, D.L.; Mullighan, C.G. Int. J. Cancer. **2007**, 120, 2751-2752.

76. Wang, F.Y.; Tahara, T.; Arisawa, T.; Shibata, T.; Yamashita, H.; Nakamura, M.; Yoshioka, D.; Okubo, M.; Maruyama, N.; Kamano, T.; Kamiya, Y.; Nakamura, M.; Fujita, H.; Nagasaka, M.; Iwata, M.; Takahama, K.; Watanabe, M.; Nakano, H.; Hirata, I. Dig. Dis. Sci. **2008**, 53, 2904-2908.

77. Larsen, F.; Madsen, H.O.; Sim, R.B.; Koch, C.; P. Garred. J. Biol. Chem. **2004**, 279, 21302-21311.

78. Ahmad, T.; Tamboli, C.P.; Jewell, D.; Colombel, J.F. Gastroenterology **2004**, 126, 1533-1549.

CHAPTER VI

HELICOBACTER PYLORI VIRULENT STRAIN EXPRESSING CELL-SURFACE LIPOPOLYSACCHARIDES LACKING FUCOSYLATED LEWIS *O*-CHAINS. OBSERVATION OF α-GLUCANS AND GLUCURONIC ACID-CONTAINING SERINE *O*-GLYCOPROTEINS

Helicobacter pylori virulent strain expressing cell-surface lipopolysaccharides lacking fucosylated Lewis *O*-chains. Observation of α-glucans and glucuronic acid-containing serine *O*-glycoproteins

José A. Ferreira[1], Rui Vitorino[1], Ana Reis[1], M. Rosário M. Domingues[1], Ceu Figueiredo[2,3], Mário A. Monteiro [4], Manuel A. Coimbra[1]

[1]Departamento de Química da Universidade de Aveiro, Campus de Santiago, 3810-193 Aveiro, Portugal, [2]IPATIMUP – Institute of Molecular Pathology and Immunology of the University of Porto, Porto, Portugal, [3]Medical Faculty of Porto, Porto, Portugal, [4]Department of Chemistry, University of Guelph, Guelph, ON N1G 2W1, Canada

Abstract

The present work concerns *Helicobacter pylori* virulent strain PTAV79 isolated from a gastric biopsy specimen of a patient with gastroesophageal reflux disease. This strain was recognized to yield virulence markers cytotoxin-associated gene (*cagA*) and vacuolating cytotoxin (*vacA*) and was found to express semi-rough cell-surface lipopolysaccharides (LPS; oligomeric *O*-chain-core-Lipid A~cell) with *O*-chains composed of LacNAc (i-antigen) units. The absence of fucosylated Lewis blood groups has been reported to negatively influence the bacteria's capability of colonizing the human stomach and promoting gastric malignancies. However, the results from *H. pylori* PTAV79 suggest that i-antigen phenotype did not compromise gastric colonization. This strain also found expressed high amounts of stearic acid and amylose-like glycans that were observed linked to glycerol (Gro) residues. Furthermore, Gro was detected carrying phosphodiester moieties suggesting the existence of glycerophospholipids. These structures are thought to act as anchoring points of amylose-like glycans to the outer cell-surface lipidic bilayer. Fine analytical and spectroscopic techniques, namely GC-EI-MS, FTIR, ESI-MS, MALDI-TOF-MS and NMR further permitted the identification of an unusual polysaccharide composed of [→3)-α-D-GlcA(1→4)-α-D-Glc(1→] repeating units generally known as aldobiouronic acid. In addition, a proteomic approach allowed the first report of a non-flagelar *H. pylori* glycoprotein exhibiting *O*-glucuronosyl serine residues.

Keywords: *Helicobacter pylori*, bacterial antigens, lipopolysaccharides, Lewis blood groups, amylose.

Introduction

Helicobacter pylori is a microaerophilic, spiral-shaped, flagellated Gram-negative bacterium that colonizes the human gastric mucosa. This microorganism is considered one of the most widespread bacterial pathogens with a prevalence of up to 90% in developing countries and a worldwide infection rate of around 50% (Farinha and Gascoyne 2005, Kusters *et al.* 2006).

Infection generally occurs during childhood and induces a strong local immune response in the gastric mucosa (Ferrero 2005). This response is not only ineffective in eliminating the bacterium from its preferred niche, but may actually contribute to the development of gastric lesions (Moran 2008). *H. pylori* infection leads to chronic gastritis in all individuals, a condition that will persist for the host lifetime if infection is not treated. An estimated 15% to 20% of infected individuals will develop more severe disease such as peptic ulcer disease, gastric carcinoma, and mucosa-associated lymphoid tissue (MALT) lymphoma (Montecucco and Rappuoli 2001, Sugiyama 2004, Ferreira et al. 2008). Furthermore, the close relationship between infection and gastric carcinoma (Graham 2000, Santacroce et al. 2008, Mbulaiteye et al. 2009) has granted *H. pylori* the recognition as a class 1 (definitive) human carcinogen (IARC Working Group 1994) by the World Health Organization.

Glycans on bacterial cell envelope have been long recognized as key mediators in the definition of host-microbial interactions and as main legislators in the establishment of symbiotic or pathogenic behaviours (Hooper and Gordon 2001). Like other Gram-negative bacteria, *H. pylori* expresses cell-surface lipopolysaccharides (LPS) that comprise, when biosynthetically complete, three structural domains: a polysaccharide (PS) known as *O*-chain, an oligosaccharide termed core, and a fatty-acid rich endotoxin moiety named lipid A (LPS: *O*-chain→Core→Lipid A~cell). Monteiro (2001) demonstrated that *H. pylori* expresses elongated *O*-chains exhibiting fucosylated glycosides analogous to some mammalian Lewis histo-blood-groups, namely internal Le^x units, with terminal Le^x or Le^y and, in some strains, with additional Le^a, Le^b, H-1, tumor associated sialyl Le^x antigens as well as blood groups A and B.

Bacterial camouflage based host's molecular mimicry has been pointed out as responsible for immune evasion, gastric adaptation and colonization thus contributing to the persistence of infection (Appelmelk *et al.* 2000, Moran 2008, Kobayashi 2009). In

addition, Le antigens also play a role in bacterial adhesion to gastric cells through galectin-3, a gastric receptor for polymeric Le^x (Fowler *et al.* 2006, Moran 2008). On the other hand the expression of fucosylated Le antigens has a strong influence in innate immune recognition of *H. pylori* by surfactant protein D (Moran *et al.* 2006). Also Le antigen expression affects both the inflammatory response and T-cell polarization that develops after infection (Moran 2008). In agreement with these considerations are the reports of clinical isolates from asymptomatic hosts lacking Lewis *O*-chains and expressing either elongated DD-heptoglycans (Monteiro *et al.* 2001) or α-(1→6) glucans (Altman 2003). These findings suggest that the presence of Lewis *O*-chain, even though not absolutely required for colonization, might result in the incapability of cells to induce significant pathology (Moran 2008). Here we report for the first time an *H. pylori* wild-type strain isolated from a symptomatic patient that expresses non-fucosylated *O*-chains.

On the other hand, the continuous increase in antibiotic-resistant *H. pylori* strains is becoming a serious worldwide threat (Vakil 2008) urging the development of alternative therapeutic and prophylactic strategies. Considering the proven success of carbohydrate-based vaccines in dealing with bacterial infections (Vliegenthart 2006) we further engaged in the identification and structural characterization of glycan antigen candidates to include in a future multivalent vaccine against *H. pylori*.

Material and methods

Bacterial cultures

Helicobacter pylori clinical isolate PTAV79 was obtained from a gastric biopsy specimen of a male patient with gastroesophageal reflux disease.

Definition of virulence profile

H. pylori virulence determinants cytotoxin-associated protein (*cagA*) and vacuolating cytotoxin (*vacA*) encoded by the *cagA* and *vacA* genes were accessed by polymerase chain reaction (PCR). Primers VA1F and VA1xR were used to amplify *vacA* s region, resulting in a fragment of 176 bp for type s1 variants and a fragment of 203 bp for type s2 variants (van Doorn et al. 1998a). To amplify the *vacA* m region, a mixture of forward primers MF1.1, MF1.2, MF1.3, and MF1.4 and reverse primer MR1 was used,

resulting in the amplification of fragments of 107 and 182 bp for m1 and m2 strains, respectively (van Doorn et al. 1998b). The presence of *cagA* was detected with primers *CagA*F and *CagA*R, yielding a product of 183 bp (van Doorn et al. 1998a). PCR primers and conditions were as previously described (van Doorn et al. 1998a, van Doorn et al. 1998b). PCR products were visualized by electrophoresis on 2% agarose gels as described by Sambrook et al. (1989).

Bacterial growth in Columbia blood agar

H. pylori cells isolated from gastric biopsies were recovered to pre-warmed Gelose Columbia solid media supplemented with 5% horse blood (bioMérieux, France) and incubated at 37ºC for 72 h, on a microaerophilic atmosphere generated by a CampyGen gas pack (Oxoid, United Kingdom). Cells were subcultivated after 48 h incubation periods in the conditions described above.

Bacterial growth in F12 liquid media

Cells were grown on Ham's F12 defined liquid media without the addition of enhancing growth factors. The medium was inoculated with cellular extracts obtained from CBA growth media. Cells were allowed to grow for 24 h in a glass flask under microaerophilic atmosphere under gentile stirring at 37ºC, as described by Testerman et al. (2001).

Purity assessment of bacterial growth

Purity assessment was assured by using a highly specific peptide nucleic acid probe in a fluorescence *in situ* hybridization procedure, according to the protocol described by Guimaraes et al. (2007). For every experiment a negative control was performed simultaneously where all the steps described above were carried out but where no probe was added during the hybridization procedure. Microscopy visualization was performed using an Olympus BX51 (OLYMPUS Portugal SA, Porto, Portugal) epifluorescence microscope equipped with one filter sensitive to the Alexa fluor 594 signalling molecule attached to the PNA probe (Excitation 530 to 550 nm; Barrier 570 nm; Emission LP 591 nm).

Extraction and purification of cell-surface glycans

Cell-surface glycans were isolated from cells using the hot phenol:water extraction according to Westphal and Jann (1965). The aqueous layer was dialyzed against distilled water using a 1,000 Da cut-off membrane and lyophilized. The resulting material was fractioned by Gel Permeation/Adsorption Chromatography (GPC) on a polyacrilamide Bio-Gel P-6 (fractionation range: 6,000-1,000 Da) (1 m length and 1.0 cm diameter) column using distilled water as the eluting solvent at constant flow rate of 0.33 mL/min. A portion of the initial material (approximately 7.5 mg) was suspended in degassed distilled water and introduced in the column. Fractions of 2.8 mL were collected. The mass content in the fractions was estimated on evaporative light scattering detector SEDEX55 (SEDERE France) and further assayed for total sugars with the phenol-H_2SO_4 method (Dubois et al. 1956). Exclusion and total volume were calibrated with blue dextran of 2,000 kDa and glucose, respectively.

Sugars composition and linkage analysis

Sugars composition analysis was performed by the alditol acetate method as described by Harris et al. (1988). The hydrolysis was done in 4 M trifluoroacetic acid (TFA) at 100ºC for 3 h, followed by reduction with $NaBH_4$ and subsequent acetylation with acetic anhydride in the presence of 1-methylimidazole. Alditol acetates derivatives were analyzed by gas chromatography-mass spectrometry (GC-MS), performed in an Agilent Technologies 6890N Network Gas Chromatograph connected to an Agilent 5973 Selective Mass Detector. The GC was equipped with a DB-1 capillary column (30 m length, 0.32 mm internal diameter, and 0.25 μm film thicknesses). The samples were injected in splitless mode (time of splitless 1.00 min), with the injector and detector operating at 220 and 230ºC, respectively, using the following temperature program: 100ºC (1 min) → 150ºC at 5ºC min^{-1} (8 min) → 159ºC at 0.5ºC min^{-1} (5 min) → 250ºC at 5ºC min^{-1} (2 min) → 320ºC at 2ºC min^{-1} (2 min). The carrier gas (He) had a flow of 1.7 mL min^{-1}, with an average linear velocity of 47 cm s^{-1} and a solvent delay of 9 min. The column head pressure was 5.34 psi. The mass spectrometer was operated in the electron impact mode at 70 eV, scanning the mass range *m*/*z* 40–500 and performing 3.18 scans s^{-1}. Linkage analysis was carried out by methylation with $NaOH/Me_2SO/CH_3I$, as described by Ciucanu and Kerek (1984). The methylated polysaccharides were hydrolysed with TFA

2M at 121ºC for 1 h, reduced by $NaBD_4$, and acetylated with acetic anhydride in the presence of 1-methylimidazole. The partially methylated alditol acetates were analyzed by GC-MS using the chromatographic conditions described previously, using the following temperature program: 45ºC (5 min) → 140ºC at 10ºC min^{-1} (5 min) → 170ºC at 0.5 ºC min^{-1} (1 min) → 280ºC at 15ºC min^{-1} (5 min)

Glucuronic acid was determined by reduction of carboxylic groups performed on partially methylated samples by an adaptation of the method described by Lindberg and Lönngren (1978) and Redgwell and Selvendran (1986). Samples were dissolved in 1 mL tetrahydrofuran and reduced with 20 mg of $LiAlD_4$ for 4 h at 65º C. The excess of LiAlD4 was destroyed by addition of 20 µL of ethanol and 20 µL of water followed by neutralization with a 2 M H_3PO_3 solution. Partially methylated reduced glycosides were then extracted with $CHCl_3/CH_3OH$ (2:1 *v/v*), evaporated to dryness and hydrolysed with 2 M TFA at 2M at 121ºC for 1h, reduced with $NaBD_4$, acetylated and analysed as described above for linkage analysis.

Partial acid hydrolysis and isolation of oligomeric units

A portion of fraction A (2.0 mg) and of fraction B (1.5 mg), both resulting from the Bio-Gel P6 column, were treated with 100 mM TFA for 30 min at 100º C. After hydrolysis, the TFA was evaporated under a steam of N_2 at room temperature and the resulting material was re-suspended in 200 µL of water and fractionated by Gel Permeation/Adsorption Chromatography on a polyacrilamide Bio-Gel P2 (fractionation range: 100-1,800 Da) (0.5 m length and 1.0 cm diameter) using degassed distilled water as eluent. Fractions of 1.0 mL were collected. The mass content in the fractions was estimated by evaporative light scattering detector SEDEX55 (SEDERE France) and the presence of sugars was confirmed by the use of phenol-H_2SO_4 (Dubois et al. 1956). In the case of fraction A, some of the non-hydrolyzed material, and corresponding to the void volume, was combined, concentrated and re-hydrolyzed with 500 mM TFA for 1 h at 100º C. The material resulting from the second hydrolysis was further fractionated in the above described conditions. The carbohydrate content of the fractions resulting from acid hydrolysis was determined by phenol-H_2SO_4 method (Dubois et al. 1956) and the protein content evaluated by the bicinchoninic acid (BCA) method according to Stoscheck (1990).

Gel electrophoresis and tryptic digestion

Fraction A was separated using the tricine system according to Schagger (2006). Following protein separation, gel was stained using colloidal coomassie and periodic acid schiff (PAS) to detect the presence of glycoproteins (Doerner and White 1990). The protein bands were excised with a pipette tip from the gel and transferred into an eppendorf. The gel pieces were washed three times with 25 mM NH_4HCO_3 /50 % ACN, one time with ACN and dried in a SpeedVac (Thermo Savant). Twenty five µL of 10 µg/mL sequence grade modified porcine trypsin (Promega) in 25 mM NH_4HCO_3 was added to the dried gel pieces and the samples were incubated overnight at 37ºC. Extraction of tryptic peptides was performed by addition of 10% formic acid /50% ACN three times being lyophilized in a SpeedVac (Thermo Savant).

Nano-HPLC

HPLC analyses were performed using an Ultimate 3000 ‘‘Dionex”. Twenty µL of each sample (2 µg of peptide extract) were injected onto a C18 trapping column (Zorbax 300SB-C18, 5 µm particle size, 5 x 0.3 mm, Agilent Technologies) using an auto sampler. The sample was washed over the trapping column for 3 min with 95% buffer A (water, 0.1% TFA), 5% Buffer B (ACN, 0.1% TFA) at a flow rate of 30 µL/min. Flow was then reversed over the trapping column, and sample was eluted onto a 150 mm × 75 µm Zorbax 300SB capillary analytical C18 column with 3.5 µm particle size (Agilent Technologies) at a flow rate of 0.3 µL/min. A linear gradient of 5% Buffer B to 55% Buffer B is run over a period of 35 min. The column was then washed with a 3 min gradient from 55% to 90% Buffer B, followed by a 5 min hold at 90% Buffer B. The column was then re-equilibrated in 5% Buffer B prior to future analyses. The peptides eluting off the monolithic capillary column were directly deposited onto 384-well MALDI plates at 20 s intervals for each spot using Probot (LcPackings) adding 170 nL of alpha-cyano-hydroxycinnamic acid (α-CHCA, Sigma) (20mg/ml in 70% acetonitrile/0.1% TFA with the addition of 10 fmol of Glu-fibrinopeptide as internal standard).

ESI-MS

Partially hydrolyzed fractions resulting from treatment of fraction A and fraction B with TFA were studied by ESI-MS in a Q-TOF (Micromass) instrument. Prior to ESI-MS analysis fraction B acid released oligosaccharides were exposed to a Dowex cation-

exchange resin to remove the excess of cations. Samples were introduced into the electrospray source at a flow rate of 10 μL min^{-1}. The cone voltage was set at 35 V and capillary voltage at 3 kV. Source temperature was at 80°C and desolvation temperature at 150°C. Tandem mass spectra (MS/MS) were obtained by collision-induced decomposition (CID), using argon as the collision gas (measured pressure in the Penning gauge ~6 x 10^{-5} mbar). In MS and MS/MS experiments, TOF resolution was set to ~9,000 (FWHM). The collision energies used for sodium adducts were 30 eV for all studied compounds. Data acquisition was carried out with a MassLynx 4 data system.

MALDI-TOF-MS

Material resulting from acid hydrolysis of fraction A with 500 mM TFA for 1 h at 100º C was analyzed by MALDI-TOF MS on 4800 MALDI-TOF/TOF analyser (Applied Biosystems, Fostercity, CA). The sample was mixed with α-CHCA in a proportion 1:1 and 0.5 µL of analyte:matrix mixture was placed on to the MALDI plate and left to dry at room temperature. The MS spectra were acquired on a MALDI-TOF/TOF mass spectrometer (4800 Proteomics Analyzer, Applied Biosystems, Europe) in the positive ion reflector mode. Spectra were obtained in the mass range between 800 and 4500 Da with ca. 1500 laser shots. MS/MS analysis of selected precursor ion was performed at collision energy of 2 kV with air as a collision gas at a pressure of $2x10^{-7}$ Torr.

Peptide mass spectra resulting from trypsin digestion and nano-HPLC separations were performed in the above described conditions. For each sample spot, a data dependent acquisition method was created to select the 10 most intense peaks, excluding those from the matrix or trypsin autolysis for subsequent MS/MS data acquisition.

Database search

Spectra were processed and analyzed by the Global Protein Server Workstation (Applied Biosystems, Foster City, CA, USA), which uses internal Mascot (Matrix Science Ltd, U.K.) software for searching the MS/MS data. Searches were performed against an internal database created based on all *Helicobacter pylori* available on Uniprot (2009-07-30) using the following criteria: 40ppm MS precursor tolerance, 2 missed cleavages, variable modifications for Asn, Ser and Thr residues (HexNac, Glucuronosyl, Hex). Positive identifications were accepted when confidence level was up to 95%.

Nuclear Magnetic Resonance spectroscopy

^{1}H, ^{13}C and ^{31}P NMR spectra were recorded on a Bruker AMX 600 spectrometer equipped with a TXI probe at 310 K. Two-dimensional (2D) NMR correlation spectroscopy (COSY), total correlation spectroscopy (TOCSY), heteronuclear spin quantum correlation (HSQC) spectroscopy and heteronuclear multiple bond correlation (HMBC) spectroscopy experiments were performed using the instrument's Bruker software. Prior to performing the NMR experiments, the samples were lyophilized three times with D_2O (99.9%). The HOD peak was used as the internal reference at δ_H 4.721 for ^{1}H NMR spectroscopy, and orthophosphoric acid (δ_P 0.0) as the external reference for ^{31}P NMR experiments. Just before the NMR experiments were carried out, a D_2O sample containing TMS (δ_H 0.00) was run to aid in the reference the HOD signal.

FTIR spectroscopy

FTIR spectra were collected on a Perkin Elmer BX Spectrometer with a single reflectance horizontal ATR cell (Golden Gate, equipped with a diamond crystal). The data was recorded in a spectral range of 4000 – 600 cm^{-1} with a resolution of 1 cm^{-1} and 256 scans were acquired and co-added before Fourier transformation.

Results

Clinicopathological and virulence characterization

H. pylori strain PTAV79 was recovered from a gastric biopsy specimen of a patient with gastroesophageal reflux disease. Polymerase chain reaction (PCR) characterization of this strain virulence profile highlighted the presence of *cagA*, the terminal gene of the *cag* pathogenicity island (PAI). The *cag* PAI encodes a type IV secretion system through which the CagA protein is injected into host epithelial cells (Backert and Selbach 2008). *H. pylori* strains containing *cagA* are associated with increased risk of peptic ulcer disease and gastric carcinoma (Figueiredo et al. 2002, Kusters et al. 2006). In addition, *H. pylori* PTAV79 was also found to carry the s1/m1 type *vacA* gene. *vacA* encodes the VacA cytotoxin, a protein that induces vacuolization in cultured epithelial cells (Kusters et al. 2006). *H. pylori* strains containing the s1/m1 genotype, meaning that the signal-region comprises allelic variant s1 and the middle-region comprises allelic variant m1, are

frequently associated with peptic ulceration and gastric carcinoma (Atherton et al. 1995, Figueiredo et al. 2002).

Isolation and pre-characterization of cell-surface glycans

H. pylori PTAV79 was characterized in relation to its glycan cell-surface phenotype. Glycosides-rich material was primarily isolated in the aqueous phase resulting from hot phenol:water extraction performed on intact bacterial cells. Approximately 8.5 mg of a heterogeneous sugars-rich material was obtained from 4 g of biomass. Sugars analysis of the non-purified extract presented on Table I confirmed heterogeneity by revealing a material mainly composed of Glc (57%) but also exhibiting considerable amounts of Gal (10%) and GlcNAc (13%) in proportions of approximately 1:1 as well as low percentages (<10%) of Gro (4%), Rib (6%), Man (3%), DD-Hep (3%) and LD-Hep (4%). Glc, Gal, GlcNAc, DD- and LD-Hep are common sugars in *H. pylori* LPSs (Monteiro 2001) thus suggesting the presence of this class of biomolecules. Gro residues have been found in *H. pylori* cell-surface as part of glycerophospholipids (Hirai et al. 1995) while Rib residues result from residual oligonucleotides coming from bacterial RNA. Man has been recurrently observed, even though always in residual amounts (<5% of total sugars), in *H. pylori* glycan-rich water extracts (Monteiro 2001). However, its origin and structural assignment is, at the moment, still unclear (Ferreira et al. 2009). On the other hand, the high amounts of Glc observed in *H. pylori* PTAV79 seems to be common among *H. pylori* strains (Monteiro 2001, Britton et al. 2005, Ferreira et al. 2009).

Table I. Sugars analysis of non-purified glycan-rich water extracts and fractions A and B resulting from elution in a Bio-Gel P6 column.

Fractions	Molar Ratio (%)							
	Gro	**Rib**	**Man**	**Glc**	**Gal**	**GlcNAc**	**DD-Hep**	**LD-Hep**
Non-purified	4	6	3	57	10	13	3	4
A	8	-	1	84	3	4	v	v
B	-	6	3	13	32	35	6	5

v – Vestigial amounts; > 0.5% total sugars

Fractionation of cell-surface glycans

With the objective of decreasing the molecular heterogeneity of glycan-rich water extracts and unveil more information about its composition, the isolated glycans were further fractionated in a polyacrylamide Bio-Gel P6 column (6 000 - 800 Da). Fractionation resulted on the elution profile shown in Figure 1, exhibiting two main fractions, A and B. Fraction A, corresponding to the void volume (>6,000 Da), comprised approximately 65% of the initial material, while fraction B corresponding to the inclusion volume (<6,000–1,000 Da), corresponded to the remaining 35%. Fraction A, corresponding to the void volume (>6,000 Da), comprised approximately 65% of the initial material, while fraction B corresponding to the inclusion volume (<6,000–1,000 Da), corresponded to the remaining 35%. Fraction A (Table I) was found to be most exclusively composed of Glc (84%), having low amounts of Gro (8%), Man (1%), Gal (3% total sugars) and GlcNAc (5%). Vestigial DD-Hep and LD-Hep residues were also observed. Conversely the oligomeric material (fraction B, Table I), yielded mainly Gal (32%) and GlcNAc (35%) in proportions of approximately 1:1. As a result, the percentage of Glc in this fraction was found to be significantly lower than what was observed for the non-purified material and fraction A (around 13%). Fraction B was also found enriched in both DD- (7%) and LD- (6%) Hep residues when compared to the non-purified material and fraction A. Furthermore, no Gro residues were found in fraction B. Thereby results suggest that high-molecular weight Glc-rich glycans were mainly isolated in fraction A while lower molecular weight material corresponding to LPS can be found in fraction B.

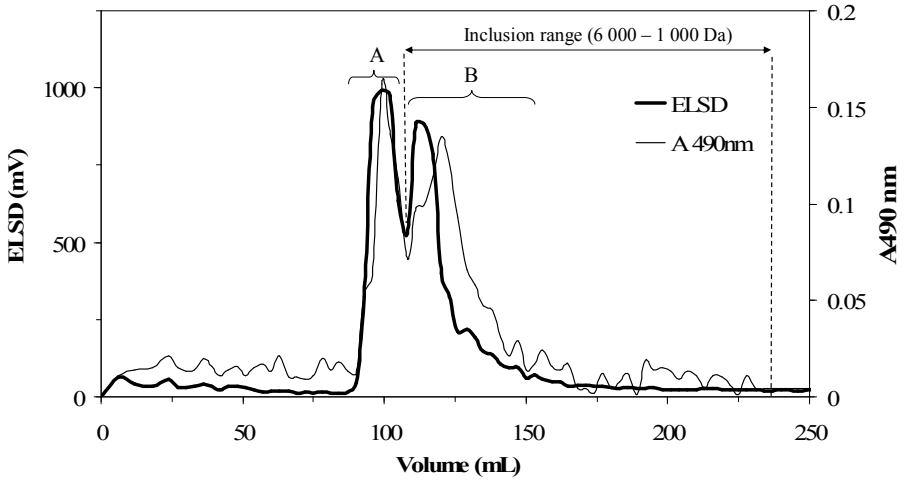

Fig. 1. *H. pylori* PTAV79 glycan-rich extract elution profile on a Bio-Gel P6 column. Letters A and B correspond to isolated fractions.

Structural studies on partially purified material

The linkage profile held by the identified sugars was evaluated by GC-EI-MS of the permethylated alditol acetate (pmaa) derivatives released after acid hydrolysis of the original glycans. Non-purified material (Table II) has shown to be mainly composed of *O*-4 linked Glc residues (around 56%) vowing for the presence of amylose-like polymers as described by Ferreira et al. (2009).

Table II. Sugar linkage profile and fatty acid composition of non-purified glycan-rich water extracts and fractions A and B resulting from elution in a Bio-Gel P6 column.

Linkage Type	Relative Molar Ratio (%)		
	Non-purified	Fraction A	Fraction B
LPS			
***O*–Chain**			
T-Gal	1.7	-	8.3
→3)Gal	7.1	v	25.2
T-GlcNAc	1.8	-	7.0
→4) GlcNAc	7.9	v	22.4
Core			
T-Glc[1]	2.8	-	5.5
→3)Glc	4.1	-	5.4
→4)Gal	2.7	-	4.2
→2)DD-*manno*-Hep	0.5	-	1.2
→2)LD-*manno*-Hep	0.9	-	2.5
→3)LD-*manno*-Hep	0.6	-	
→7)DD-*manno*-Hep	1.0	-	1.8
→7)LD-*manno*-Hep	0.5	-	0.9
→2,7)DD-*manno*-Hep	0.8	-	0.7
→3,7)LD-*manno*-Hep	1.4	-	1.2
Lipid A			
→6) GlcNAc	0.7	-	2.4
Glucan-rich glycans			
T-Glc		3.1	-
→3)Glc	-	5.7[2]	-
→4)Glc	55.8	65.2	9.3
→4,6)Glc	0.6	0.8	0.5
Fatty Acids			
C18:0 (stearic acid)	9.1	25.2	1.5

[1]Terminal Glc residues can either be addressed to amylose-like polymers or to non-reducing ends of the LPS core. [2]In the absence of LPS O-3 linked Glc residues were assigned to the Glucan-rich moiety.

v – Vestigial amounts; > 0.5% total sugars

However of considerable amounts of terminal *O*-3 linked Gal (7.1 %) and *O*-4 linked GlcNAc (9.7 %) recognized as LPS *O*-chain sugars were also detected. In addition, terminal and *O*-3 linked Glc, *O*-4 linked Gal, *O*-7 DD-Hep and *O*-2, *O*-2,7 and *O*-3,7 linked LD Hep core-belonging residues as well as *O*-6 linked GlcNAc commonly found in Lipid A (Monteiro 2001) confirmed the existence of LPS suggested by sugars analysis (Table I). Furthermore, the non-purified material revealed the presence of a C-18:0 fatty acid methyl ester (9.1 %, Table II). This reveals the existence of stearic acid, a common fatty acid of *H. pylori* Lipid A moiety (Monteiro et al. 2000, Moran et al. 1997).

After fractionation through the Bio-Gel P6 column the majority of the *O*-4 linked Glc and stearic acid residues were isolated in fraction A (Table II). In addition this fraction also showed low amounts of terminal (3.1% of total sugars) and *O*-3 linked Glc (5.7%).

Conversely, linkage analysis confirmed that fraction B was essentially composed of LPS (Table II), revealed by the existence of *O*-chain sugars, namely terminal (8.3% of total sugars) and *O*-3 linked Gal (25.2%) and terminal (7.0%) and *O*-4 linked GlcNAc (22.4%) residues. Lower amounts (<6%) of terminal and *O*-3 linked Glc, *O*-4 linked Gal, *O*-7 DD-Hep and *O*-2, *O*-2,7 and *O*-3,7 linked LD Hep units (Table II) that make up the core oligosaccharide region of the LPS (Monteiro 2001) were also observed. In addition ^{1}H 1D nuclear magnetic resonance (NMR) studies in fraction B (data not showed) revealed weak unresolved resonances at δ_{H1} 5.0-5.45 ppm. This signals showed that the Hep residues observed in sugars (Table I) and linkage (Table II) analysis were in α-*manno* configuration (Aspinall 1999, Aspinall and Monteiro 1996, Monteiro 2001).

ESI-MS spectra of the oligosaccharides released after partially acid hydrolysis with TFA revealed several ions originated from the LPS, resumed in Table III. The ions were found dehydrated as a result of strong acid treatment and protonated. Due to their high affinity for alkali metals, oligosaccharides normally ionize as sodium adducts (Ferreira et al., 2010, Zaia 2004). However, in this case, exposure to a Dowex cation-exchange resin prior to analysis to remove the excess of sodium ions resulted in the observation of only protonated species. Several core building blocks were identified (Table III), namely the ions at *m/z* 508 assigned to $[Hep_2\text{-}Kdo\text{-}H_2O+H]^+$, at *m/z* 536 to $[Hep(AEP)\text{-}Kdo\text{-}H_2O+H]^+$, *m/z* 700 to $[Hep_2\text{-}Hep(AEP)\text{-}H_2O+H]^+$, *m/z* 728 to $[Hep\text{-}Hep(AEP)\text{-}Kdo)\text{-}H_2O+H]^+$, *m/z* 860 to $[Hep_2\text{-}Hep(AEP)\text{-}Kdo)\text{-}H_2O+H]^+$, *m/z* 1082 to $[Hex\text{-}Hep_2\text{-}Hep(AEP)\text{-}Kdo)\text{-}H_2O+H]^+$, *m/z* 1244 to $[Hex_2\text{-}Hep_2\text{-}Hep(AEP)\text{-}Kdo\text{-}H_2O+H]^+$ and at *m/z* 1406 to $[Hex_3\text{-}$

Hep_2-Hep(AEP)-Kdo)-H_2O+H]$^+$. Assignments of Hex residues to either Glc or Gal as presented in Table III were made according to Monteiro (2001). The ions at *m/z* 508, *m/z* 536, *m/z* 700, *m/z* 860, *m/z* 1082, *m/z* 1244 and *m/z* 1406 were also found to carry Kdo residues (Table III) recognized as the anchoring point of the glycosidic region of the LPS to the Lipid A moiety (Monteiro 2001).

Table III. ESI-MS of the oligosaccharides obtained from the hydrolysis of fraction B. The presented assignments were confirmed by ESI-MS/MS and made according to previously published structures (Monteiro 2001).

m/z	assignment
Core Ions	
508	[Hep-Hep(AEP)-H_2O+H]$^+$
536	[Hep(AEP)-Kdo-H_2O+H]+
700	[Hep-Hep-Hep(AEP)-H_2O+H]$^+$
728	[Hep-Hep(AEP)-Kdo-H_2O+H]$^+$
860	[Hep-Hep-Hep(AEP)-Kdo-H_2O+H]$^+$
1082	[Gal-Hep-Hep-Hep(AEP)-Kdo-H_2O+H]$^+$
1244	[Glc-Gal-Hep-Hep-Hep(AEP)-Kdo-H_2O+H]$^+$
1406	[Glc-Glc-Gal-Hep-Hep-Hep(AEP)-Kdo-H_2O+H]$^+$
***O*-chain-Core Ions**	
396	[GlcNAc-Hep-H_2O+H]$^+$
711	[GlcNAc-Hep-Hep(AEP)-H_2O+H]$^+$
903	[GlcNAc-Hep-Hep-Hep(AEP)-H_2O+H]$^+$
942	[LacNAc-Hep-Hep-Hep-H_2O+H]$^+$
953	[GlcNAc-LacNAc-Hep-Hep-H_2O+H]$^+$
1123	[GlcNAc-Hep-Hep-Hep(AEP)-Kdo-H_2O+H]$^+$
1315	[GlcNAc-Hep-Hep-Hep-Hep(AEP)-Kdo-H_2O+H]$^+$
1430	[$LacNAc_2$-Hep-Hep-Hep-H_2O+H]$^+$
***O*-chain Ions**	
366	[LacNAc-H_2O+H]$^+$
528	[LacNAc-Hex+H]$^+$
569	[GlcNAc-LacNAc-H_2O+H]$^+$
731	[$LacNAc_2$-H_2O+H]$^+$
893	[$LacNAc_2$-Hex+H]$^+$
1096	[$LacNAc_3$-H_2O+H]$^+$

Furthermore, ESI experiments highlighted the existence of 2-aminoethylphosphate groups (AEP) linked to inner core Hep residues as it can be seen in the MS/MS spectrum of the ion at *m/z* 728 assigned to [Hep-Hep(AEP)-Kdo-H_2O] (Figure 2a). When induced to fragmentation by collision with a gas, the ion at *m/z* 728 originated three major ions at *m/z* 536 assigned to [Hep(AEP)Kdo-H_2O+H]$^+$ by loss of an Hep residue (Hep_{res}, 192 Da), the ion at *m/z* 508 assigned to [Hep-Hep(AEP)-H_2O+H]$^+$ resulting from the loss of a Kdo_{res} (220 Da) and the ion at *m/z* 316 assigned to [Hep(AEP)-H_2O+H]$^+$ by the combined loss of an Hep_{res} and a Kdo_{res} (412 Da) demonstrating the Hep-AEP linkage. These results together with previous reports (Monteiro 2001), suggest that the AEP moiety is *O*-7 linked to the innermost LD-Hep of the core region, linkage analysis (Table II) revealed vestigial amounts of *O*-3,7 linked LD-Hep.

The observation by ESI-MS of an AEP moiety was reinforced in a ^{31}P NMR experiment carried out at pD 6.0 (data not shown). The ^{31}P spectrum of intact fraction B exhibited a single resonance at δ 0.05 ppm that, according to Aspinall and Monteiro (1996), Aspinall et al. (1999), and Monteiro (2001) is characteristic of a phosphodiester group. In addition a 2D ^1H-^{31}P HMBC experiment (data not shown) highlighted connectivity between the phosphorus nucleus and a proton resonance at $\delta_{H\text{-}7}$ 3.72 ppm in a region of the spectrum that, according to Müller-Loennies et al. (1994), is occupied by H-7 protons of Hep residues. The information given by this 2D NMR experiment confirmed the *O*-7 linkage of the AEP motif to the inner core *O*-3 linked Hep residue that was suggested by linkage analysis.

The prevalence of *O*-3 linked Gal and *O*-4 linked GlcNAc residues in proportions of approximately 1:1 in fraction B suggests the expression of *O*-chains composed of LacNAc moieties [→3)Gal(1→4)GlcNAc(1→]. In accordance with this observation, the ^1H NMR spectrum of fraction B (data not shown) exhibited two dominant anomeric resonances at $\delta_{H\text{-}1}$ 4.69 ppm ($J_{1,2}$ 6.9 Hz), and at $\delta_{H\text{-}1}$ 4.47 ppm ($J_{1,2}$ 7.0 Hz) that, based on previous reports (Aspinall et al. 1999, Monteiro 2001, Monteiro et al. 2000), are attributed to β-Gal and β-GlcNAc respectively. The presence of amido-methyl protons (-$COCH_3$) in the GlcNAc units was responsible for the observation of a singlet at δ 2.05 ppm in the ^1H NMR spectrum (data not shown). The expression of LacNAc repeating units, suggested by NMR and linkage analysis (Table II), was confirmed by ESI-MS and MS/MS (Table III).

The ESI-MS spectra of the oligosaccharides released from partial acid hydrolysis exhibit the ions at *m/z* 366 assigned to [Hex-HexNAc-H_2O+H]$^+$, at *m/z* 528 assigned to [Hex_2-HexNAc-H_2O+H]$^+$, at *m/z* 569 assigned to [Hex-$HexNAc_2$-H_2O+H]$^+$, at *m/z* 731 assigned to [Hex_2-$HexNAc_2$-H_2O+H]$^+$, at *m/z* 893 assigned to [Hex_3-$HexNAc_2$-H_2O+H]$^+$ and *m/z* 1096 assigned to [Hex_3-$HexNAc_3$-H_2O+H]$^+$. MS/MS experiments further demonstrated the occurrence of Hex-HexNAc repeating units as it can be seen when inducing to fragmentation the ion at *m/z* 731 assigned to [Hex-HexNAc-Hex-HexNAc-H_2O+H]$^+$ (Figure 2b).

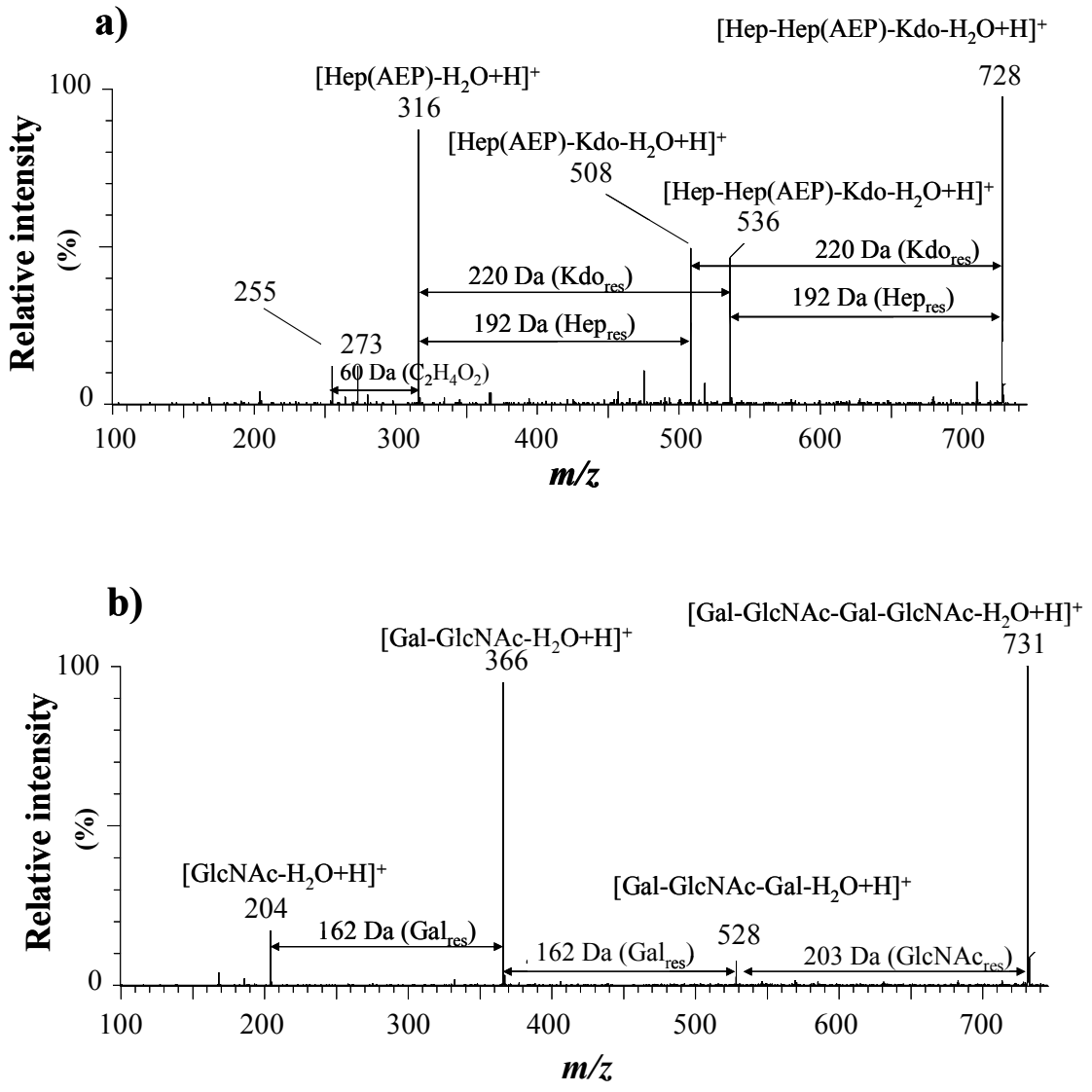

Fig. 2. ESI-MS/MS spectrum of a) the ion at *m/z* 728 assigned to the inner core structure [Hep-Hep(AEP)-Kdo-H_2O+H]$^+$ and b) the ion at *m/z* 731 assigned to the *O*-chain structure [Gal-GlcNAc-Gal-GlcNAc-H_2O+H]$^+$ resulting from acid hydrolysis.

The resulting MS/MS spectrum showed a dominant fragment ion at *m/z* 366 corresponding to $[Hex\text{-}HexNAc\text{-}H_2O+H]^+$ originated by the loss of a Hex-HexNAc motif (365 Da) and two low abundant fragments at *m/z* 528 corresponding to $[Hex\text{-}HexNAc\text{-}Hex\text{-}H_2O+H]^+$ by loss of a HexNAc residue (203 Da) and the ion at *m/z* 204 $[HexNAc\text{-}H_2O+H]^+$ by combined loss of two Hex residues and one HexNAc residue. In addition, the ions at *m/z* 903, assigned to $[HexNAc\text{-}Hep\text{-}Hep\text{-}Hep\text{-}Hep(AEP)+Na]^+$, at *m/z* 942, assigned to $[Hex\text{-}HexNAc\text{-}Hep\text{-}Hep\text{-}Hep\text{-}H_2O+H]^+$, at *m/z* 953, assigned to $[HexNAc\text{-}Hex\text{-}HexNAc\text{-}Hep\text{-}Hep\text{-}H_2O+H]^+$, at *m/z* 1123, assigned to $[HexNAc\text{-}Hep\text{-}Hep\text{-}Hep(AEP)\text{-}H_2O+H]^+$, at *m/z* 1315 $[HexNAc\text{-}Hep\text{-}Hep\text{-}Hep\text{-}Hep(AEP)\text{-}H_2O+H]^+$ and at *m/z*, assigned 1430 to $[Hex\text{-}HexNAc\text{-}Hex\text{-}HexNAc\text{-}Hep\text{-}Hep\text{-}Hep)\text{-}H_2O+H]^+$, show the linkage between the *O*-chain's most intern GlcNAc and inner core through an Hep residues.

Gathered structural information strongly suggests that *H. pylori* PTAV79 LPS exhibit a structural organization presented in Fig. 3 similar to what has been found among other *H. pylori* strains (Monteiro 2001).

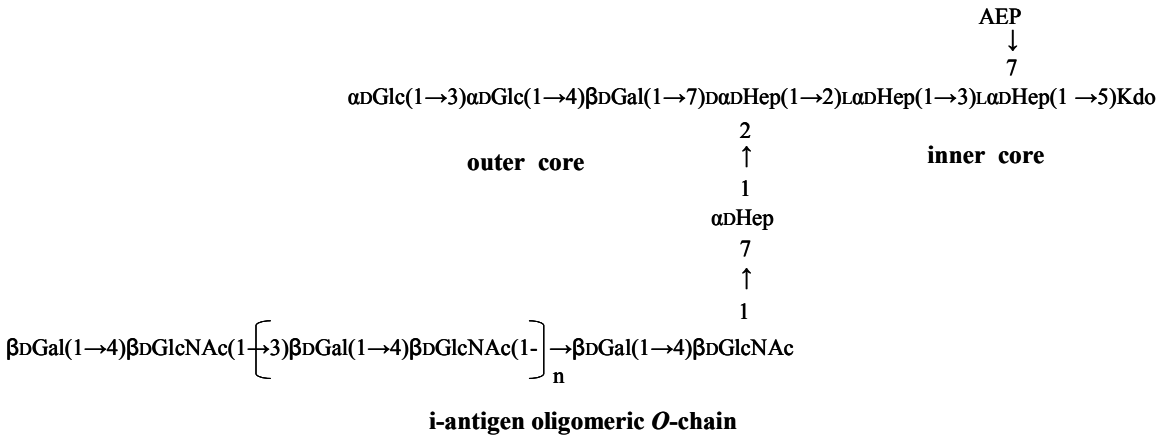

Fig. 3. Structural organization of *H. pylori* PTAV79 semi-rough LPSs showing an *O*-chain formed by i-antigens.

Detailed structural studies on H. pylori amylose-rich fraction A

Both sugars and linkage analysis show that fraction A is depleted of LPS (Table I and II) and is composed of amylose-like glycans. This fraction was also found to be enriched in Gro and stearic acid chains (Table I and II).

Figure 4 shows the FTIR spectrum of fraction B, highlighting the presence of CH, CH_2, and CH_3 asymmetric and symmetric stretching modes of fatty acids at 2959-2852 cm^{-1} (Adt et al. 2006). Furthermore, the polysaccharides fingerprint region at 1200–800 cm^{-1}

(Coimbra et al. 1998) yields characteristic absorbances at 1090 cm^{-1} and at 1015 cm^{-1}, suggesting the presence of hexuronic acids (Coimbra et al. 1998, Ferreira et al. 2001).

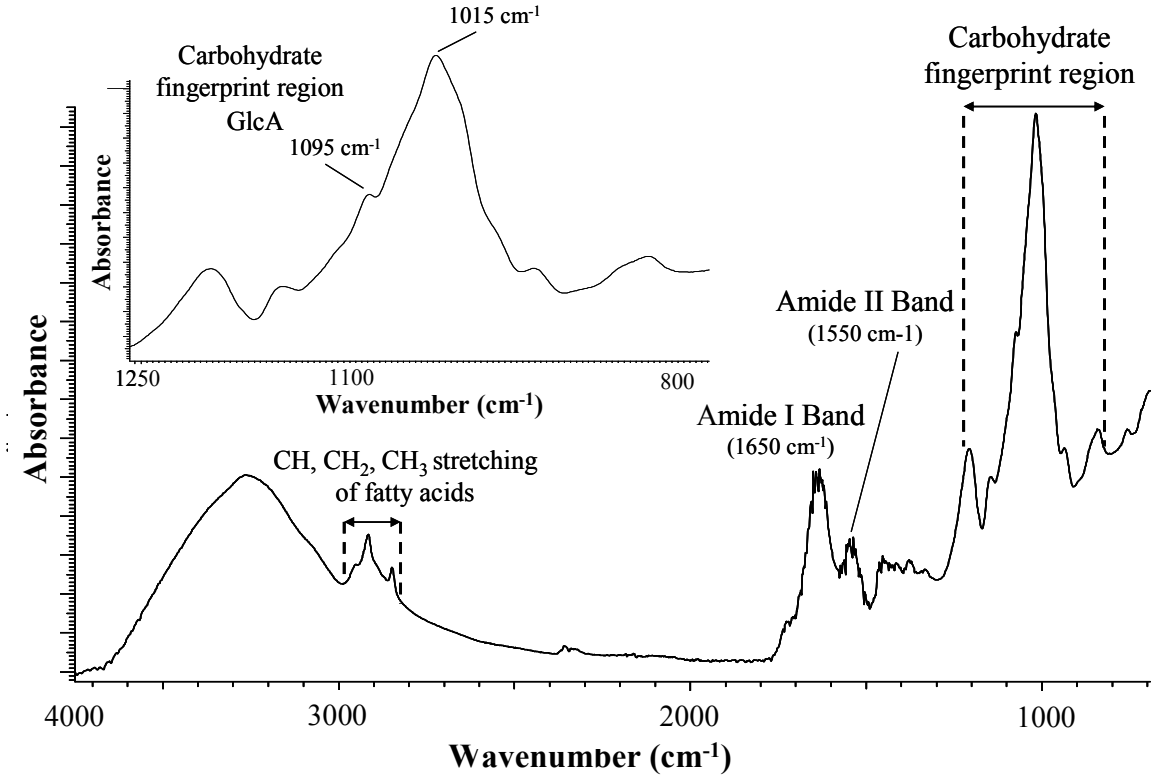

Fig. 4. FT-IR spectrum of fraction B highlighting the Amide bands derived from proteins and carbohydrate fingerprint region from 1200-800 cm^{-1} showing GlcA characteristic signals.

The presence of hexuronic acids was accessed by linkage analysis comprising the reduction of the carboxylic group with $LiAlD_4$ after methylation and prior to hydrolysis, reduction with $NaBD_4$ and acetylation. The GC-MS chromatogram resulting from this procedure exhibited two additional peak at $rrt^{1,4Glc}$ = 0.8 and $rrt^{1,4Glc}$ = 1.29 assigned to terminal GlcA and *O*-3 linked GlcA residues respectively.

The ^1H NMR spectra of fraction A (Figure 5 and Figure 6a) and HSQC showed three dominant α-anomeric resonances. Two major unresolved peaks were observed at $\delta_{H1/C1}$ 5.20/100.4 ppm (residue X) and assigned, according to linkage analysis, to *O*-4 substituted Glc residues. The two unresolved peaks are mostly likely to arise from two *O*-4 linked Glc residues exposed to two distinct chemical environments. A lower intensity doublet was found at $\delta_{H1/C1}$ 5.11/69.6 ppm ($J_{1,2}$ = 2.91 Hz) (Residue Y) and assigned, according to linkage analysis, to *O*-3 substituted GlcA. In addition, three vestigial

resonances were distinguishable at δ_{H1} 5.13, 5.07 and 4.92 ppm and were attributed to *O*-3 substituted Glc, terminal Glc, and terminal GlcA, respectively, based on theoretical values given by CASPER (Stenutz et al. 1998).

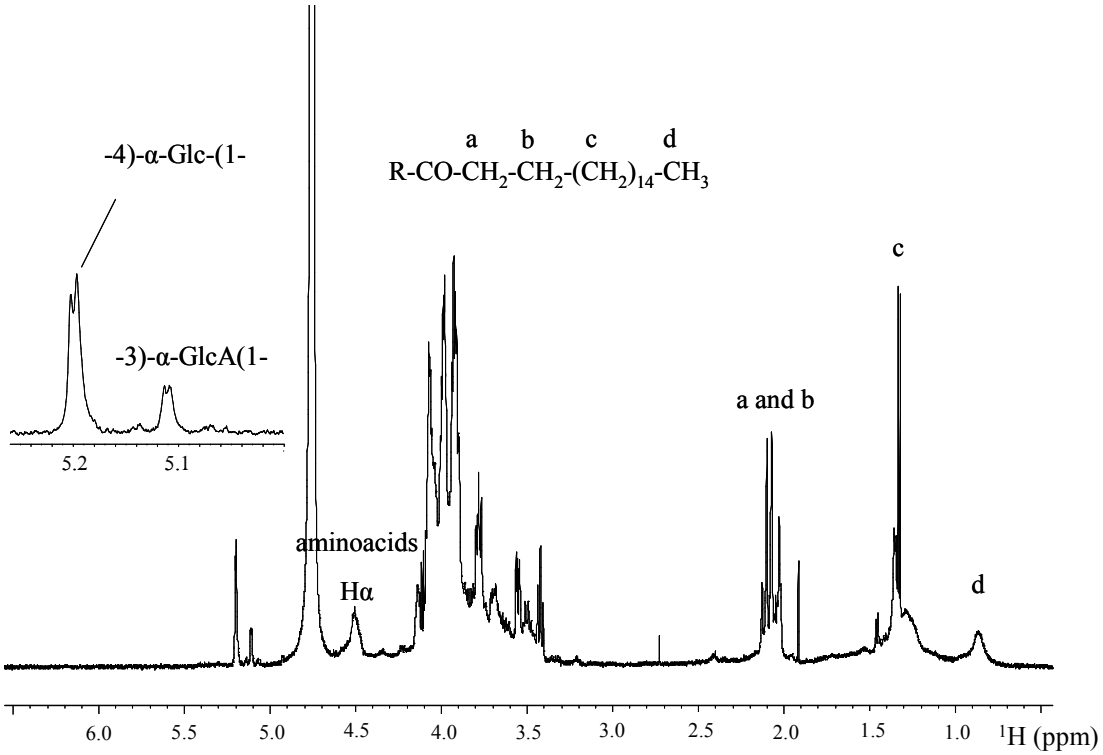

Fig. 5. 1H NMR spectrum of fraction A highlighting α anomeric resonances for *O*-4 linked Glc, *O*-3 linked GlcA residues and signals belonging to the C18 fatty acid chain.

2D ^{1}H–^{1}H COSY (Figure 6a), TOCSY, and ^{1}H–^{13}C HSQC (Figure 6b) experiments allowed to assign some of the ring protons and carbons of the major carbohydrate residues present in fraction A (Table IV).

Table IV. ^{1}H NMR and ^{13}C NMR chemical shifts of monosaccharide units present in *H. pylori* PTAV79 fraction A glycosides (δ, ppm; pD 6.0; 310 K).

Residue	H_1/C_1	H2/C2	H3/C3	H4/C4	H5/C5	H6/C6	H6/C6
X →4)-α-D-Glc-(1→	5.21 100.5	3.55 74.5	3.43 75.4	3.78 78.1	-	3.79/ 63.4	3.88/ 63.4
Y →3)-α-D-GlcA-(1→	5.11/ 99.6	3.96 74.6	3.84 -	--	-	-	-

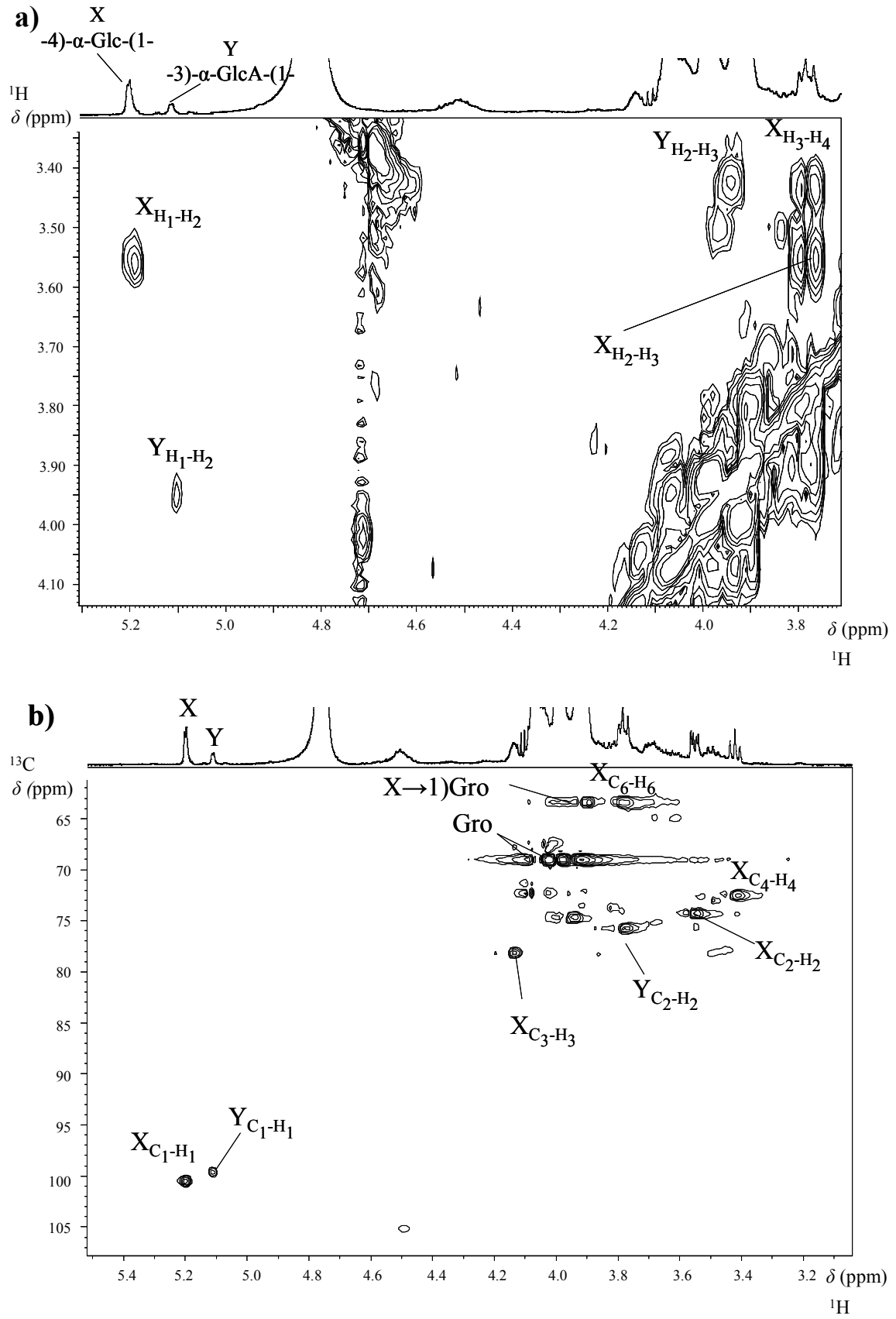

Fig. 6. a) ^{1}H-^{1}H COSY and b) ^{1}H-^{13}C HSQC NMR spectra of fraction A.

In addition the HMBC spectrum (Figure 7) presented in the α-anomeric region three cross-peaks, two corresponding to inner-residue connectivities between the C_1 and H_2 and H_3 of *O*-4 linked residues and an inter-residue connectivity between the C_1 and the H_4 of contiguous *O*-4 linked residue. The latter confirmed the existence of a [→1)-α-D-Glc-(1→4)-α-D-Glc-(1→] moiety characteristic of amylose-like glycans.

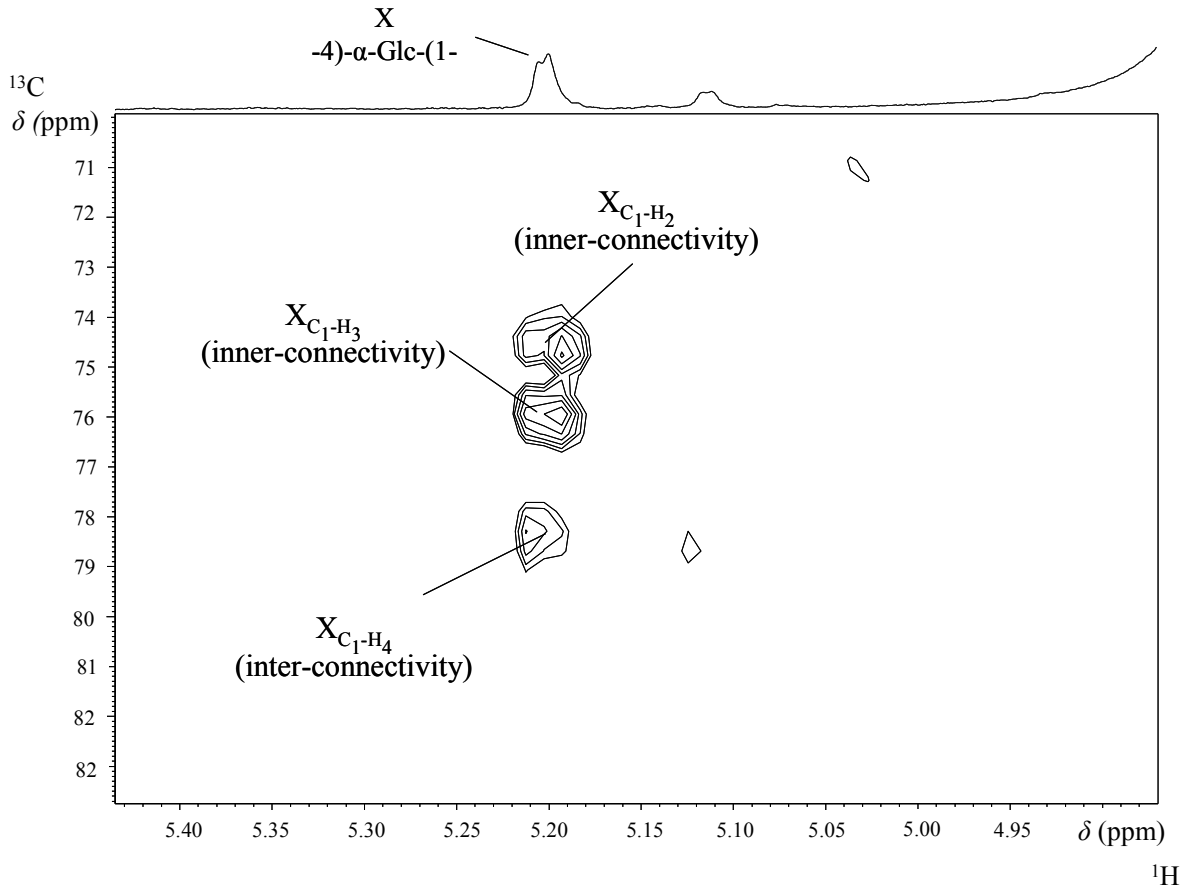

Fig. 7. ^{1}H-^{13}C HMBC NMR spectrum α-anomeric region exhibiting inner and inter-ring connectivities between *O*-4 linked Glc residues.

The ^{1}H NMR spectra in Figure 5 further highlighted signals identifiable, according to Gunstone et al. (1995) and Jie et al. (1995), with the C-18:0 fatty acid moiety, namely an unresolved multiplet at 0.86 ppm belonging to terminal methyl groups, a group of multiplets between 1.2 and 1.4 corresponding to methylene signals of $[(CH_2)_n]$ aliphatic chains, and multiplets at 2.26 and 2.06 and assigned to α and β methylene protons linked the ester carbonyl group.

In addition, the ^{1}H NMR spectrum of fraction A (Figure 5) also presented a broad band from $\delta_{H\alpha}$ 4.4 to 4.5 ppm originated by aminoacids H_α protons (Chary and Govil, 2008), suggesting the presence of proteins. It should be pointed out that aminoacids carrying either methyl or methylene groups can further contribute to the signals observed between 0.8 and 2.8 ppm. Further reinforcing the hypothesis of the existence of proteins in this extract, the FTIR spectrum (Figure 4) exhibited characteristic signals at 1650 cm^{-1} resulting from C=O group (amide I band) and at 1550 cm^{-1} from N-H group (amide II band) (Chapman et al. 1989).

Gathered information resulting from chemical, chromatographic, and spectroscopic analysis performed so far on fraction A has confirmed the presence of the amylose-like glycans suggested by linkage analysis (Table II). However, these studies have also revealed the presence of several unsigned structural motifs, namely terminal *O*-3 linked α-GlcA residues, Gro, fatty acids, and proteic material.

Partial acid hydrolysis of fraction A glycosides

In order to get more insights on fraction A molecular and structural organization, a strategy based on acid hydrolysis was adopted. Primarily, fraction A was submitted to acid hydrolysis with 100 mM TFA in order to obtain oligosaccharides that could be analysed by ESI-MS. The acid treated material originated the Bio-Gel P2 elution profiles presented in Figure 8 which show that a portion of the initial material remained unchanged upon acid treatment (Figure 8a), eluted in the void volume of the column. This material was found to be essentially sugar-rich (Figure 8b) as the proteic material was almost totally degraded (Figure 8c) upon exposure to acid.

Low molecular weight fragments isolated on the inclusion volume of the column were observed in the ESI-MS spectra (Figure 9a), revealing a dominant ion at *m/z* 439. Based on the MS/MS spectrum (Figure 9b), it was assigned to $[Glc\text{-}Glc\text{-}Gro+Na]^+$. Vestigial peaks at *m/z* 365, *m/z* 527, *m/z* 689 and *m/z* 851, assigned to $[Glc_2+Na]^+$, $[Glc_3+Na]^+$, $[Glc_4+Na]^+$ and $[Glc_5+Na]^+$, respectively, were also detected.

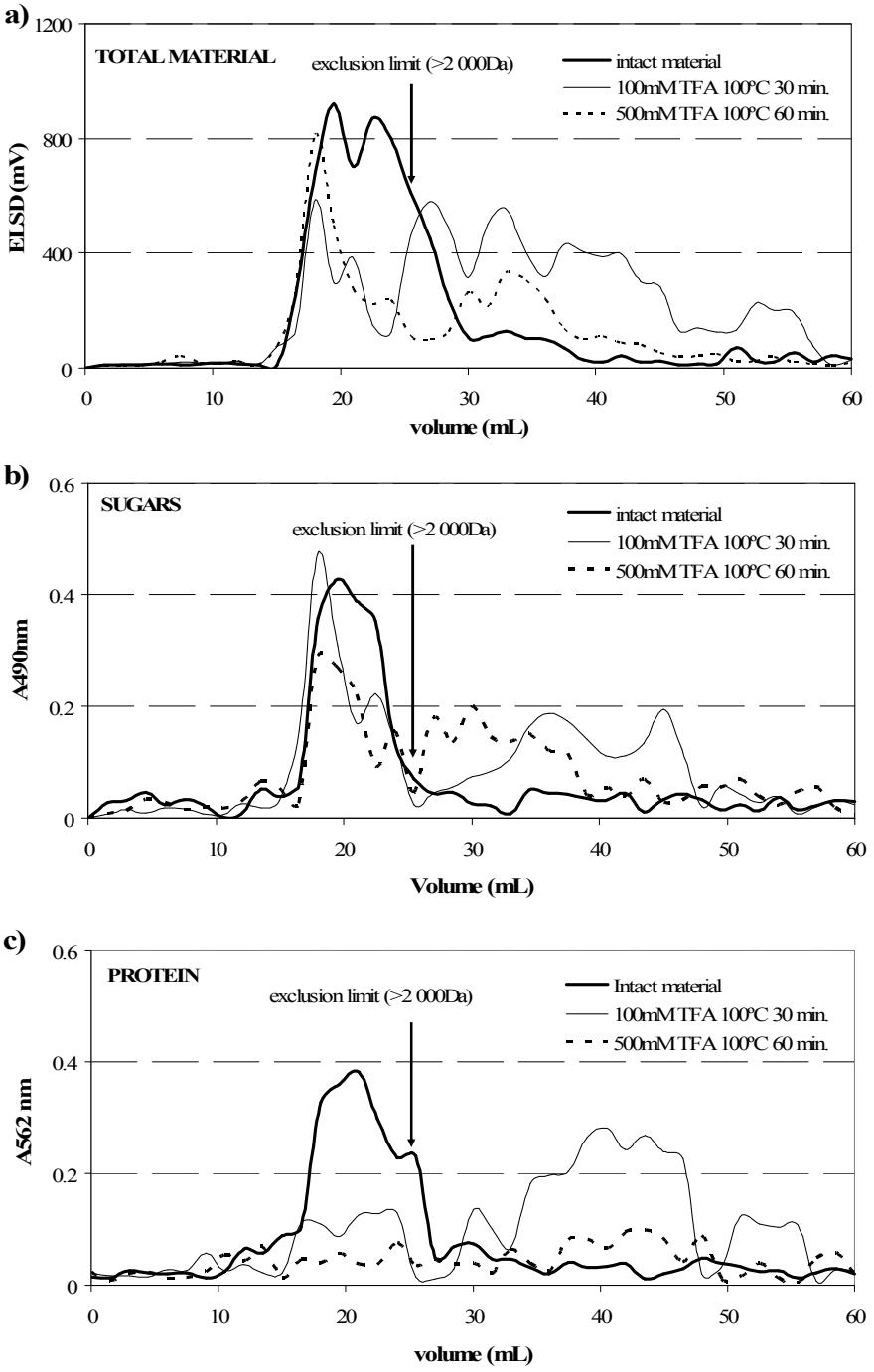

Fig. 8. Elution profiles determined by a) Lights cattering (total mass), b) A_{490} (total sugars, phenol-H_2SO_4 method) and c) A_{562} (total protein, BCA method) for intact fraction A, fraction A after hydrolysis with 100mM TFA for 30 min. and hydrolysis of acid-resistant material with 500 mM TFA for 60 min.

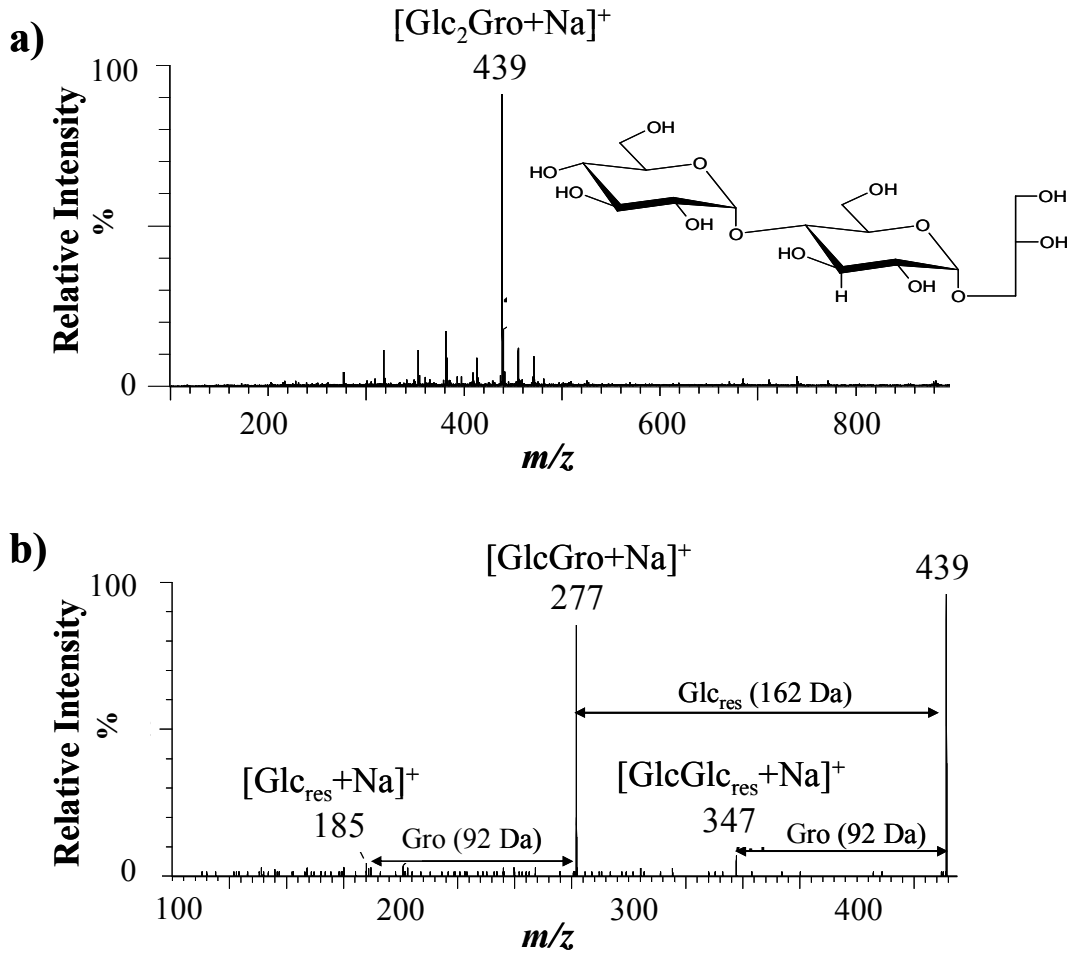

Fig. 9. a) ESI-MS spectrum of oligomeric material resulting from acid treatment of fraction A with 100 mM TFA at 100ºC for 30 min exhibiting a major ion at *m/z* 439 assigned to [Glc-Glc-Gro+Na]$^+$ and b) MS/MS spectrum of the ion at *m/z* 439.

The presence of the glycerol moiety was also evident in the NMR experiments. The HSQC of intact fraction A (Figure 6b) showed a cross peak at δ_{C1} 69.9 ppm with several resonances equivalent protons δ_H 3.98 and 3.91 ppm and at 4.07 ppm characteristic of *O*-substituted glycerol groups (Gunstone et al. 1995). Furthermore, the ^{31}P NMR experiments carried out at pD 6.5 (data not shown) revealed a single resonance at δ 0.01 ppm that, according to Aspinall and Monteiro (1996), Aspinall et al. (1999) and Monteiro (2001), is characteristic of a phosphodiester. This signal was found correlated through a 2D ^{1}H-^{31}P HMBC experiment with the above Gro-related resonances at δ_H 3.98 and 3.91 ppm, in accordance with the expect chemical shifts for proton belonging to CH_2-O-PO-R moieties (Gunstone et al. 1995). The HSQC spectrum also shows a broad low intensity peak around $\delta_{C/H}$ 3.98/63.9 which is thought to be correlated with Gro residues substituted with α-Glc

responsible for shifting the carbon resonances to upper fields (Gunstone et al. 1995). Even though ^{1}H-^{1}H COSY (Fig. 6a) and TOCSY (data not shown) spectra revealed to be fairly resolved in the region from 4.1 and 3.9, the observed signals suggest the expected connectivity between these resonances.

The ESI-MS data, highlighting a linkage between the α-(1→4)-Glc moiety and Gro, the observation of phosphorylation in the Gro by NMR, and the detection of considerable amounts of stearic acid in this fraction, suggests the presence o glycerophospholipids. These results further imply that glycerol could act as anchorage points of amylose-like glycans to *H. pylori* cellular-envelope. However, the extremely low abundance of material available associated to its high heterogeneity resulted in a major drawback in providing unambiguous data linking the fatty acid chain to glycerol residues. Still it should be pointed out that the prevalence of fatty acids in a polymeric fraction (Mw >6,000 Da) very soluble in water might only be explained by a strong association with polymeric hydrophilic molecules such as α-glucans.

Structural study of a polysaccharide containing aldobiouronic acid repeating units

The 100 mM TFA resistant material recovered on the Bio-Gel P2 void volume (Figure 8) was submitted to a new treatment using harsher hydrolytic conditions comprising 500 mM TFA at 100ºC for 1 h. The resulting Bio-Gel P2 elution profile highlighted that the bulk of the material, composed almost exclusively by sugars, remained unchanged (Figure 8b and 8c), thus on the void volume, further demonstrating its high resistance to the acid.

The oligomers originated from this hydrolysis were analyzed by MALDI-TOF-MS which resulted in spectra like the one presented in Figure 10. Major ions differing from each other in 388 Da ($GlcA_{res}Glc$) at *m/z* 699 were assigned to $[Glc_2\text{-}GlcA_2\text{-}H_2O+Na]^+$, at *m/z* 1037 assigned to $[Glc_3\text{-}GlcA_3\text{-}H_2O+Na]^+$, at *m/z* 1375 assigned to $[Glc_4\text{-}GlcA_4\text{-}H_2O+Na]^+$, at *m/z* 1713 assigned to $[Glc_5\text{-}GlcA5\text{-}H_2O+Na]^+$, at *m/z* 2051 $[\text{-}Glc_6\text{-}GlcA_6\text{-}H_2O+Na]^+$. Other ions at *m/z* 861 assigned to $[Glc_2\text{-}GlcA_3\text{-}H_2O+Na]^+$, at *m/z* 875 assigned to $[Glc_3\text{-}GlcA_2\text{-}H_2O+Na]^+$, at *m/z* 1199 assigned to $[Glc_3\text{-}GlcA_4\text{-}H_2O+Na]^+$, at *m/z* 1213 assigned to $[Glc_4\text{-}GlcA_3\text{-}H_2O+Na]^+$, at *m/z* 1537 assigned to $[Glc_4\text{-}GlcA_5\text{-}H_2O+Na]^+$, at *m/z* 1561 assigned to $[Glc_5\text{-}GlcA_4\text{-}H_2O+Na]^+$, at *m/z* 1875 assigned to $[Glc_5\text{-}GlcA_6\text{-}H_2O+Na]^+$ were also identified further suggesting a polysaccharide composed of a

aldobiouronic disaccharide GlcA-Glc repeating unit (Gloaguen et al. 1997, Govorchenko et al. 1971). Linkage analysis performed on the acid-resistant material collected on the void volume of the P2 column (data not shown) confirmed the presence of *O*-4 linked Glc and *O*-3 linked GlcA residues. This data suggests a polysaccharide composed of [→3)-α-D-GlcA(1→4)-α-D-Glc(1→] repeating motif. Even though the carboxylic acid group of the GlcA residue was found free, the HSQC spectrum of the intact material highlighted connectivity between a carbon resonance at δ_C 177.0 ppm thought to belong to C6 GlcA residues and multiplet at δ_H 2.09 ppm characteristic of a $-CH_2-CH_n$ group (data not shown). This suggests that some of the carboxylic groups in the GlcA moiety are esterified.

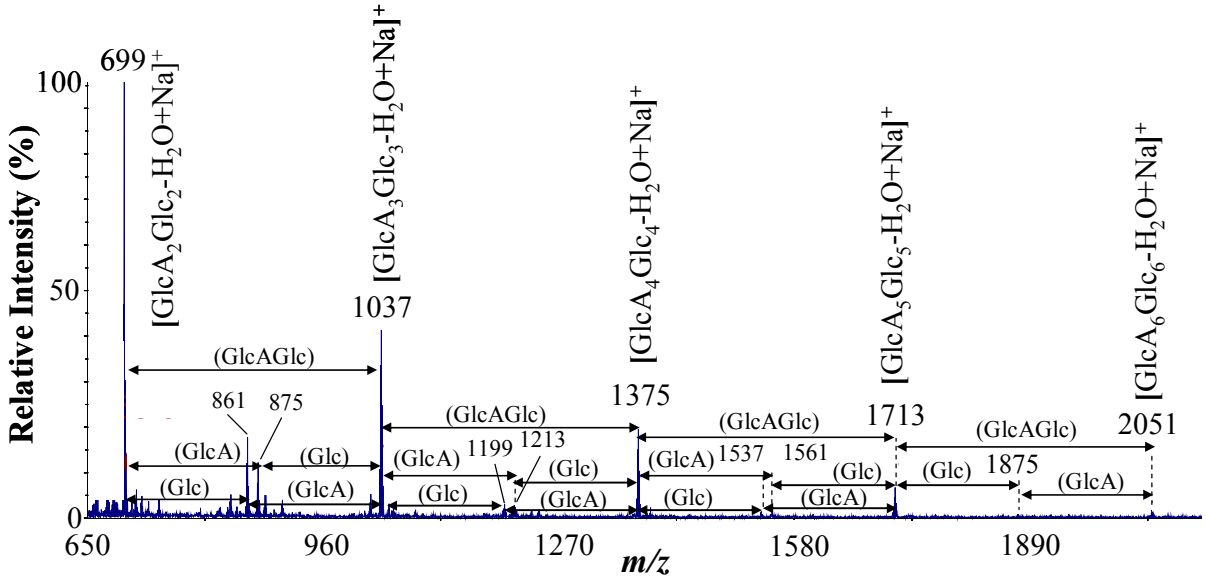

Fig. 10. MALDI-TOF-MS spectrum of a oligomeric fraction resulting from acid digestion of acid-resistant fraction A material with 500 mM TFA at 100ºC during 60 min.

Identification of a glycopeptide containing Ser O- *glucuronosyl moieties*

In order to separate the proteic from glycan-rich material, as well as to identify possible glycosylated proteins, fraction A was fractionated by SDS-PAGE. Under SDS-PAGE conditions (Figure 11) it exhibited four distinguishable bands when stained with coomassie blue. This observation confirmed the presence of proteins previously suggested by the FTIR (Figure 4) and NMR (Figure 5) spectra. The first and second bands were observed approximately at 45 kDa, the third band had an *M*w estimated around 28 kDa and the forth band, showing a large dispersion, corresponded to peptides with *M*w inferior to

11 kDa. However, when stained with PAS to reveal sugar-containing material only three bands were observed. The first and second bands appeared strongly stained with PAS and corresponded to non-migrated macromolecular glycosides with *M*w > 100 kDa and glycans with *M*w between 100 kDa and 38 kDa respectively. Conversely, the third band corresponding to an *M*w of around 28 kDa was found only slightly stained with PAS. Furthermore this material was also observable using coomassie blue, confirming the presence of a glycoprotein. The 28 kDa band then was then recovered from the gel, digested with tripsin and the resulting fragments were separated by nano-HPLC and analysed by MALDI-TOF-MS. MS/MS experiments (Figure 11b) allowed the identification of an ion at *m/z* 2308 corresponding to a modified peptide with the aminoacid sequence PSAVGYQPTLAGEMGKLQER exhibiting an additional 176 Da attributed to a GlcA residue. This post-translational modification was found to occur in the serine residue at the S2 position as shown by the identification of a_2 and b_2 fragmentations (nomenclature by Roepstorff and Fohlman 1984) resulting in the ions at *m/z* 333 and 361 corresponding to the P1-S2 sequence with an additional 176 Da (Figure 11 and Table V). Subsequent a- and b-type fragmentations confirmed the mentioned observation by yielding ions showing this modification (Table V). In addition, the y_{18} fragmentation corresponded to the sequence AVGYQPTLAGEMGKLQER (*m/z* 1948) while the y_{19} fragment showed an additional serine residue plus 176 Da (S(GalA)AVGYQPTLAGEMGKLQER, *m/z* 2211) (Figure 11 and Table V).

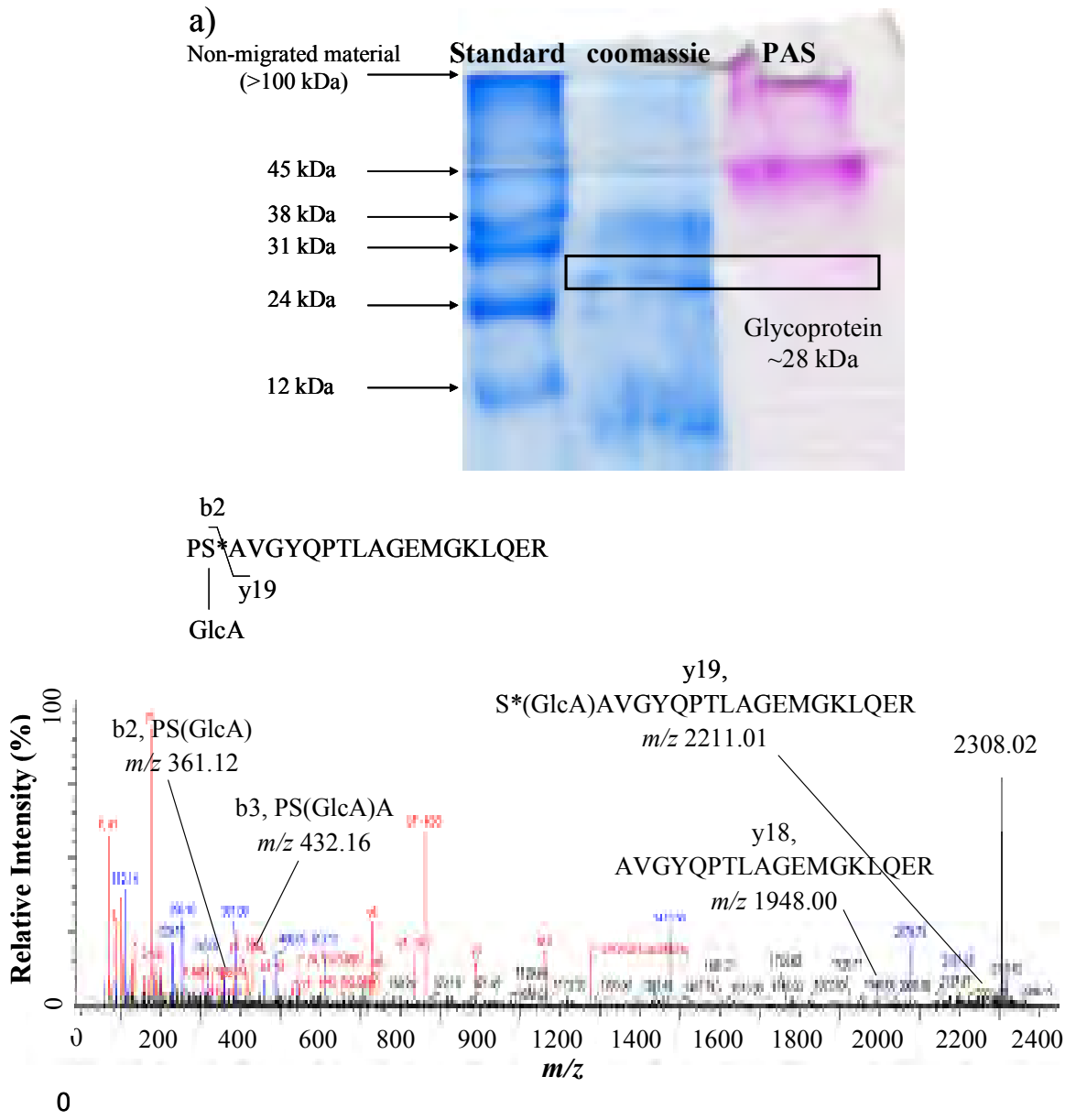

Fig. 11.a) Fraction A profile under SDS-PAGE conditions revealed with comassie blue (for proteins) and PAS (for glycans). The highlighted band stained both with comassie blue and PAS and corresponds to a glycoprotein of approximately 28 kDa. b) MALDI-TOF-MS/MS of the modified peptide resulting at *m/z* 2308.02 corresponding to the sequence PSAVGYQPTLAGEMGKLQER containing a GlcA in the in S2 aminoacid obtained from tryptic digestion of the 28 kDa band the. Specific *b* and *y* fragmentations confirming this posttranslational modification are highlighted.

Table V. MALDI-TOF-MS/MS a-, b- and y- type fragmentations for the 28 kDa tryptic digest PS(GlcA)AVGYQPTLAGEMGKLQER.

	Aminoacid	Characteristic Fragmentation (Da)			Theoretical Mass (Da)	Observed Mass (Da)	Match Error (Da)	Modification
		a	b	y				
1	P	70.70	98.06					
2	**S***	**333.13**	**361.12**	**2211.01**				
3	A	404.17	432.16	1948.00				
4	V	503.23	531.23	1876.96				
5	G	560.26	588.25	1777.89				
6	Y	723.32	751.31	1720.87				
7	Q	851.38	879.37	1557.81				
8	P	948.43	976.43	1429.75				
9	T	1049.48	1077.47	1332.69				
10	L	1162.56	1190.56	1231.65	2308.11	2308.02	-0.09	Glucuronosyl(S)[2]
11	A	1233.60	1261.59	1118.56				
12	G	1290.62	1318.62	1047.53				
13	E	1419.66	1447.66	990.50				
14	M	1550.70	1578.70	861.46				
15	G	1607.73	1635.72	730.42				
16	K	1735.82	1763.82	673.40				
17	L	1848.9	1876.9	545.30				
18	Q	1976.96	2004.96	432.22				
19	E	2106.01	2134.00	304.16				
20	R							

* Modified residue.

Discussion

H. pylori wild type strain PTAV79 was isolated from a symptomatic host with gastroesophageal reflux disease. Even though *H. pylori* is recognized as a highly fastidious microorganism (Stevenson et. al. 2000, Testerman et al. 2001), i.e. difficult to culture outside their normal environment, this strain showed abnormally low growth rates when sub-cultivated *in vitro* denoting its high adaptation to the gastric niche. Such behaviour resulted in a major drawback in obtaining enough biomass for a full structural characterization of its cell-surface glycans. So, from more than 4 g of cells, only approximately 8.5 mg of a highly heterogeneous material composed of LPS, proteic material and polysaccharides could be obtained. This resulted in a major challenge when addressing the structural organization of its components and a drawback as far as fully accessing certain specific molecular motifs.

H. pylori PTAV79 expresses LPS carrying i-antigens

LPS is a main component of *H. pylori* outer membrane and has strong implications on pathogenesis and virulence of the bacterium. The present study has demonstrated that *H. pylori* PTAV79 expresses semi-rough LPS formed by a conserved core region similar to what has been observed among other *H. pylori* (Monteiro 2001) and oligomeric *O*-chains composed of LacNAc (i-antigen) repeating units. Although clinical isolates normally express smooth phenotypes characterized by a polysaccharide moiety showing a core oligosaccharide and extended polymeric *O*-chains, in some cases semi-rough forms can also be observed (Monteiro et al. 2001). According to the LPS classification into glycotype families proposed by Monteiro et al. (2001), strains expressing semi-rough LPS are placed either in group G or H depending on their *O*-chains antigenic profile. Group G includes strains with *O*-chains having both Type 1 (Le^a, Le^b) and Type 2 (Le^x, Le^y) Le epitopes while group H concerns solely those expressing Type 1 structures. In addition to the above mentioned phenotypes, some strains often co-express other fucosylated epitopes such as Le^d [α-L-Fuc-(1-2)-β-D-Gal-(1-3)-β-D-GlcNAc], α-L-Fuc-(1-3)-α-L-Fuc-(1-4)-β-D-GlcNAc, β-D-GlcNAc-(1-3)-α-L-Fuc, α-L-Fuc-(1-3)-Fuc-(1-4)-β-D-GlcNAc as well as linear B blood-group [α-D-Gal-(1-3)-β-D-Gal-(1-4)-GlcNAc). However, as far as we know, *H. pylori* PTAV79 is the first strain reported to solely express semi-rough phenotypes composed of i-antigen *O*-chains. Also, none of the above described structural motifs were identified.

H. pylori strain PTAV79 was found to be devoid of fucosylated Le antigens. According to previously published works, the expression of Le and related blood groups by *H. pylori* has severe implications in several biological events directly correlated with pathogenesis such as modulation of immune response, influencing bacterial colonization and adhesion to gastric cells (Broutet et al. 2002, Heneghan 2001, Hynes et al. 2005, Moran 2008). It has also been described that strains with high expression of Le^x cause higher colonization density in patients than those with weaker expression (Heneghan et al. 2000) therefore enhancing the probability of developing gastric malignancies (Moran 1996, Rieder et al. 1997). Consequently, it is reasonable to think that the capability of strains like PTAV79 to evade immune response as well as successfully colonize the gastric mucosa and/or induce a pathological outcome might be seriously compromised. In agreement with these considerations is a report concerning a genetic engineered strain

having a knock out of the *rfb* gene (HP00437JHP0037), encoding a GDP-D-mannose pyrophosphorylase required for GDP-Fuc synthesis (Moran et al. 2000). This genetic modification resulted in LPS phenotypes composed of Fuc-lacking *O*-chains, thus i-antigens, like the ones encountered in strain PTAV79. Cells showing the described phenotype presented reduced capability of colonizing mouse stomachs (Moran et al. 2000) and ablated interaction with the human gastric mucosa of biopsy specimens *in situ* (Edwards et al. 2000). Also, a mutated *H. pylori* Sydney strain carrying a rough-form LPS devoid of Le *O*-chains, created by insertional mutagenesis of HP0826 (β4-*galT* gene), has been shown to still be capable of colonizing the murine model, although with less efficiency (Logan et al. 2000). Despite the lack of fucosylated Le antigens, *H. pylori* PTAV79 was isolated from a gastric biopsy specimen, vowing for its capability to induce successful colonization of the human gastric mucosa. It also suggests that the expression of i-antigen phenotypes does not compromise colonization. In addition other strains lacking Le epitopes and expressing LPS with either an elongated α-1,6-Glc side branch (Altman et al. 2003) and/or 2- and 3-linked D-*glycero*-α-D-*manno*-heptopyranose units (Monteiro et al. 2001) were also found capable of colonizing murine stomach models (Altman et al. 2003, Monteiro et al. 2001). Backed by the presented information and new insights brought by *H. pylori* PTAV79, we further reinforce the observation that the expression of fucosylated Le epitopes, in particular Le^x, even though recognized to render a positive contribute, are not a pre-requisite for a successful colonization.

When discussing the possible impacts of fucosylated Le epitopes upon pathology, it should be pointed out that a significant proportion of Le-negative strains have been identified among *H. pylori* from asymptomatic subjects (Monteiro et al. 2001, Rasko et al. 2000a). Le epitopes are known to be able to act as inflammatory agents responsible for immune activation upon *H. pylori* infection, frequently directing pro-inflammatory responses against the host (O'Keeffe and Moran 2008). A decreased or absent presentation of these antigens may lead to decreased immune-related symptoms and, consequently, an asymptomatic colonization. Despite these observations, available information suggests a correlation between infection with strain PTAV79 devoid of Le antigens and the development of gastric disorders. The identification of recognized pathogenicity markers *cagA* and type s1/m1 *vacA* (Kusters et al. 2006) further reinforces this strain's virulence potential (Wen 2009). Also, a significant proportion of gastroesophageal reflux disease

patients have shown *H. pylori* colonization (O´Connor 1999). Although the association between infection and development of reflux esophagitis remains highly controversial (Grande et al. 2008, Yagi et al. 2009), a recent review points out that *H. pylori* infection might induce an increase in acid secretion which can lead to gastroesophageal reflux disease (Souza and Lima 2009). The *H. pylori*-driven decrease of the stomach's pH may even have a direct impact in the modulation and establishment of the *O*-chains phenotype (Moran 2008). It has been demonstrated that upon decrease in pH there is a phase variable decrease in Le^x expression (Moran et al. 2002). On/off switching of fucosyltransferases expression due to a decrease in pH might be responsible for the observation of i-antigens in strain PTAV79.

Production of amylose-like glycans

Noteworthy is also the high amounts of amylose-like glycans expressed by *H. pylor*i strain PTAV79. According to Ferreira et al. (2009), *H. pylori* is known to bioaccumulate those polymers under specific environmental pressures. The mentioned report extensively discusses the biological importance of this class of glycosides and its implications in pathogenesis. It has been stated that its production can be regarded as part of a long time survival strategy under nutrient depletion (Bourassa and Camilli 2009). Also, they were implicated in the modulation/evasion of the host's immune response (Bittencourt et al. 2006, Gagliardi et al. 2007) and thought to contribute to the formation of strong and sticky framework responsible for promoting life on community and protecting the cell from external aggressions (Sutherland 2001).

Even though the exact environmental pressures triggering the expression of amylose-like glycans remains mostly unclear, it has been shown that its production is accompanied by a decrease in the overall expression of LPS (Ferreira et al. 2009). Such decrease was mostly attributed to a reduction in *O*-chain expression responsible for a shift from smooth LPS to semi-rough phenotypes. This was recognized as a typical behaviour among laboratory adapted strains upon sub-cultivation in solid medium (Ferreira et al. 2009). Interestingly, the same phenotype is now being described for *H. pylori* PTAV79 which is a freshly recovered clinical isolate further grown in F12 liquid medium. Moreover, growth in F12 was recognized to potentiate the expression of smooth LPS (Nilsson et al 2008, Ferreira et al. 2009) and decrease the amount of expressed amylose-

like glycans (Ferreira et al. 2009). However, upon growth in F12, *H. pylori* PTAV79 expressed mainly semi-rough phenotypes and high amounts of amylose-like glycans but not smooth type LPSs. Thus, the atypically high expression of polymeric amylose-glycans observed for this stain can be an environmental related response of a well adapted microorganism to the gastric niche when facing cultivation outside the human reservoir. On the other hand, it can in fact correspond to an *in vivo* phenotype. Nevertheless, F12 liquid media was found ideal for the rapid isolation, cultivation and identification of *H. pylori* from biopsy specimens overcoming fastidiousness (Sainsus et al. 2008) thus showing its potential of mimicking *in vivo* growth conditions. Reinforcing this last observation, cell-surface glycosides isolated from *H. pylori* strains from *in vivo* mouse models and fresh gastric biopsies have shown similar phenotypes to liquid media grown strains (Nilsson et al. 2008). Based on these considerations we are led to think that the observed cell-surface glycan pattern might indeed be fully representative of the *in vivo* phenotype. Surprisingly, evidences were found of amylose-like glycans linked to Gro residues. In the amylose-rich fraction it was also found a considerable amount of stearic acid which is known to be present at *H. pylori* cell surface (Hirai et al 1995, Inamoto et al. 1993, Moran et al. 1997). This fatty acid is generally regarded as belonging to Lipid A of the LPS moiety (Moran et al. 1997). This fraction was also found to contain phosphate groups in phosphodiester bonds. The expression of α-glucosylated glycolipids, namely cholesteryl-α-glucosides, cholesteryl-6'-*O*-acyl-α-glucosides, phospholipids like cholesteryl-6'-*O*-phosphatidyl-α-glucoside, and cholesteryl-6'-*O*-lysophosphatidyl-α-glucoside (Lebrun et al. 2006) are not unusual among *H. pylori* strains. Some of these structures were found to contain Gro residues with phosphate groups bridging the glycerolipidic moiety (Hirai et al. 1997). These results therefore suggest that amylose-like glycans might be linked to the bacteria's cell surface in the form of glyceroglycophospholipids with the α-*O*-4 linked Glc residues directly linked to Gro.

A polysaccharide composed of aldobiouronic acid repeating units

By submitting the cell-surface material extracted from *H. pylori* strain PTAV79 to an acid digestion with TFA 500 mM at 100ºC for 1h it was possible to unveil a highly acid resistant polysaccharide. The mentioned polysaccharide was found to be composed of [→3)-α-D-GlcA(1→4)-α-D-Glc(1→] repeating units. Such structural organization

comprising an uronic acid linked to neutral sugar is classified under the general name of aldobiouronic acid and has long been recognized as extremely resistant to acidic hydrolysis even at high temperatures and acid concentrations (Gloaguen et al. 1997, Govorchenko et al. 1971). Such property could be observed when submitting fraction A aldobiouronic acid containing material to strong acid hydrolysis at 100ºC for 1 hour.

Aldobiouronic acids are frequently found as part of bacterial capsular structures (Forsee 2009, Gloaguen et al. 1997, Yang et al. 1996). However, this is the first report for *H. pylori* of a polysaccharide recognizable by its unusual high acid resistance under harsh conditions. It is also worth mentioning that *H. pylori* cells face a pH gradient within the gastric mucosa, between the mucus layer and the gastric cell surface, from an expected pH 2 on the luminal side of the gastric mucus layer to almost pH 7 on the cell surface (Moran et al. 2002). Still, *H. pylori* is known to overcome this effect by producing and excreting an urease responsible for the metabolization of urea into CO_2 and ammonia thus buffering the cells surroundings (Kusters et al. 2006).

Structural resemblances between *H. pylori* PTAV79 extra-cellular aldobiouronic containing polysaccharide and hyaluronan, a linear polysaccharide formed by repeating units of D-GlcA and D-GlcNAc $[\rightarrow 4)$-β-D-GlcA$(1\rightarrow 3)$-β-D-Glc$(1\rightarrow]_n$ (Itano 2008), suggests similar functional properties. Hyaluronan is the major macromolecular polysaccharide component of the extra-cellular matrix and is distributed widely throughout human connective, epithelial, and neural tissues (Itano 2008). GlcA confers this polymer the capability of forming negatively-charged aggregates that imbibe water giving rise to hydrogels (Toole 2000) responsible for cellular hydration. The same structures can be thought to occur at the surface of *H. pylori* PTAV79 cells resulting in the formation of an additional protective layer against pH variations.

Also, it should be pointed out that the i-antigen phenotype expressed by *H. pylori* PTAV79 does not favour adhesion to the gastric epithelial cells (Moran 2008). Planktonic free swimming states along the mucus layer are thought to be promoted instead leading the bacteria to be exposed more frequently to pH gradients that might exert and trigger the expression of aldobiouronic acids.

H. pylori infection may further result in an increased gastric acid secretion that can contribute both to the observed gastroesophageal reflux (Souza and Lima 2009) and the expression of protective polysaccharides such as the one now described.

Identification of Ser O-glucuronidated protein

Glycan-rich water soluble material resulting from phenol:water extraction performed on intact bacteria are generally not completely devoid of proteic material. In particular, lower molecular weight peptides are expected since most of the macromolecular protein complexes are retained by the phenol phase (Shnyra et al. 2000). A proteomic approach permitted identifying in the aqueous fraction the existence of a 28 kDa glycoprotein containing Ser *O*-GlcA moieties. The presence of GlcA residues in the protein chain is responsible for an increase of the protein's hidrophilicity, thus explaining its presence in the aqueous fraction.

By matching the MALDI-TOF-MS/MS spectra resulting from this glycoprotein's tryptic digests against an internal database created based on all *Helicobacter pylori* available data on Uniprot (2009-07-30) revealed a putative protein. The failure in identifying a specific biologic role for the mentioned glycoprotein using this approach might result from the incapability of the database to fully represent the high genetic variability existing among strains.

Also, the occurrence of GlcA as a post-translational modification is quite uncommon and, as far as we know, has only been reported in human acidic proline-rich salivary protein PRP-1 (Jonsson et al. 2000). Most of all, reports directed towards a systematic evaluation of *H. pylori*'s proteomic profiles are up until now rather scarce. This is clearly illustrated when searching the PubMed database (*www.pubmed.gov*) using as keywords "proteomics and *Helicobacter pylori*". The mentioned insertion renders a mere total of 100 publications, 30% of which corresponding to studies published in the past two years. Among them, a proteomic study concerning reference strain NCTC 11637 points out that *H. pylori*'s proteins are subjected to a high degree of post-translational modification (Lock et al. 2001). Post-translational processing such as the insertion of GlcA now being described for strain PTAV79 may play an integral role in the pathogenicity and antigenic variability of this organism at the protein level.

Reports referring the exact post-translational events occurring in *H. pylori* proteins are scarcer. Moese et al. (2001) presented evidences of a tyrosine-phosphorylated *cagA* protein and descriptions for glycosylation were found to be limited to flagellar proteins (Schirm et al. 2003, Schirm et al. 2005, Schoenhofen et al. 2006). Such proteins have been shown to display up to 19 Ser/Thr *O*-linked sites modified with residues structurally

related to *N*-acetylpseudaminic acid (Schirm et al. 2003, Schirm et al. 2005). Interestingly, this presents similarities with what is now being described for *H. pylori* PTAV79, namely the insertion of acidic group containing sugars and the fact that Ser residues are recognized as ideal sites for *O*-glycosylation. This is, therefore, the first report of an *H. pylori* glycoprotein that does not concern events taking place in flagellar structures.

Concluding remarks

In resume, over the last twenty years the spotlight in the field of *H. pylori* cell-surface glycosides has been pointed out at the LPS, its structure, and its biological role. The present work suggests that *H. pylori*'s cell-surface is composed of a conundrum of glycosylated structures. In addition to LPS showing variable phenotypes, *H. pylori* strains have shown to express α-glucosylated biomolecules, namely amylose-like glycans (Ferreira et al. 2009) and glycolipids (Lebrun et al. 2006). Also, the identification for strain PTAV79 of structures composed of aldobiouronic acid building blocks and glycoproteins containing GlcA raises new questions. Among them, addressing how widespread is this kind of structures among *H. pylori* strains, unveiling their biosynthesis and the events triggering their expression is of primary concern. In addition, this newly revealed structures offer new potential targets when thinking about assembling a multivalent carbohydrate-based vaccine against *H. pylori*. Therefore, studies are being conducted in order to evaluate the immunogenic potential of these molecules against *H. pylori*.

Acknowledgments

This work was supported by Fundação para a Ciência e a Tecnologia (FCT) Project POCI/QUI/56393/2004, PhD grant SFRH/BD/19929/2004 and Natural Sciences and Engineering Research Council of Canada (NSERC).

Abbreviations

AA, Alditol Acetates; AEP, 2-aminoethylphosphate; BCA, Bicinchoninic acid; *cagA*, cytotoxin-associated protein; COSY, Correlated Spectroscopy; DD-Hep, D-glycero-D-manno-heptose; LD-Hep, L-glycero-D-manno-heptose; EI-MS, Electronic Impact-Mass Spectrometry; ELSD, Evaporative Light Scattering Detectors; ESI-MS, Electrospray Ionization-Mass Spectrometry; Fuc, Fucose; FTIR, Fourier Transform Infrared Spectroscopy; Gal, Galactose; GC-MS, Gas Chromatography-Mass Spectrometry; Glc, Glucose; GlcA, Glucuronic Acid; Gro, Glycerol; Hep, Heptose; Hex, Hexose; HMQC, Heteronuclear Multiple Quantum Correlated Spectroscopy; HPLC, High Performance Liquid Chromatography; Kdo, 3-deoxy-D-

manno-oct-2-ulosonic acid Le^a, Lewis a; Le^b, Lewis b; Le^x, Lewis x; Le^y, Lewis y; LacNAc, *N*-acetyl-β-lactosamine; LPS, Lipopolysaccharide; MALDI-TOF-MS, Matrix-assisted laser desorption ionization-Time of Flight-Mass Spectrometry; Man, Mannose; *M*r, molecular weight; NOESY, nuclear Overhauser Enhancement Spectroscopy; NMR, Nuclear Magnetic Resonance; OS, Oligosaccharide; PAS, Periodic Acid Schiff; PMAA, Partially Methylated Alditol Acetates; PCR, Polymerase Chain Reaction; PS, Polysaccharide; Rib, Ribose, SDS–PAGE, rrt, relative retention time; Sodium Dodecyl Sulfate–Polyacrylamide Gel Electrophoresis; Ser, serine, TFA, Trifluoroacetic acid; TOCSY, Total Correlated Spectroscopy, *vacA*, vacuolating cytotoxin.

References

Adt I, Toubas D, Pinon JM, Manfai M, Sockalingum GD. 2006. FTIR spectroscopy as a potential tool to analyse structural modifications during morphogenesis of *Candida albicans*. *Arch Microbiol.* 185: 277-285.

Altman E, Smirnova N, Li J, Aubry A, Logan SM. 2003. Occurrence of a nontypable *Helicobacter pylori* strain lacking Lewis blood group O antigens and DD-heptoglycan: evidence for the role of the core α1,6-glucan chain in colonization. *Glycobiology*. 13: 777-783.

Appelmelk BJ, Monteiro MA, Martin SL, Moran AP, Vandenbroucke-Grauls CM. 2000. Why *Helicobacter pylori* has Lewis antigens? *Trends Microbiol*. 8: 565-870.

Aspinall GO, Monteiro MA. 1996. Lipopolysaccharides of *Helicobacter pylori* Strains P466 and MO19: Structures of the O antigen and core oligosaccharide regions. *Biochemistry*. 35: 2498-2504

Aspinall1 GO, Mainkar AS, Moran A. 1999. A structural comparison of lipopolysaccharides from two strains of *Helicobacter pylori*, from which one strain (442) does and the other strain (471) does not stimulate pepsinogen secretion. *Glycobiology*. 9: 1235–1245.

Atherton JC, Cao P, Peek RM Jr, Tummuru MK, Blaser MJ, Cover TL. 1995. Mosaicism in vacuolating cytotoxin alleles of *Helicobacter pylori*. Association of specific vacA types with cytotoxin production and peptic ulceration. *J Biol Chem*. 270: 17771-17777.

Backert S, Selbach M. 2008. Role of type IV secretion in *Helicobacter pylori* pathogenesis. *Cell Microbiol*. 8:1573-1581.

Bittencourt VCB, Figueiredo RT, da Silva RB, Mourão-Sa DS, Fernandez PL, Sassaki GL. 2006. An α-glucan of *Pseudallesscheria boydii* is involved in fungal phagocytosis and Toll-like receptor activation. *J Biol Chem*. 281: 22614-22623.

Bourassa L, Camilli A. 2009. Glycogen contributes to the environmental persistence and transmission of *Vibrio cholerae*. *Mol Microbiol*. 72: 124-138.

Britton S, Papp-Szabo E, Simala-Grant J, Morrison L, Taylor DE, Monteiro MA. 2005. A novel *Helicobacter pylori* cell-surface polysaccharide. *Carbohydr Res.* 340: 1605-1611.

Broutet Nathalie; Moran Anthony; Hynes Sean; Sakarovitch Ch arlotte; Mégraud Francis. 2001. Lewis antigen expression and other pathogenic factors in the presence of atrophic chronic gastritis in a European population. *J Infect Dis*. 185: 503-512.

Chapman D, Jackson M, Haris PI. 1989. Investigation of Membrane Protein Structure using Fourier Transform Infrared Spectroscopy. *Biochem Soc Trans.* 17: 617-619.

Chary KVR, Govil G. 2008. Protein NMR: General Principles and Resonance Assignments. In Chary KVR, Govil G, editors. NMR in biological systems. From molecules to humans. Netherlands Springer. p. 163-210.

Ciucanu I, Kerek F. 1984. A simple and rapid method for the permethylation of carbohydrates. *Carbohydr Res*. 131: 209-217.

Coimbra MA, Barros A, Barrosa M, Rutledge DN, Delgadillo I. 1998. Multivariate analysis of uronic acid and neutral sugars in whole pectic samples by FT-IR spectroscopy. *Carbohydr Polym*. 37: 241-248.

Dubois M, Gilles DA, Hamilton JK, Rebers PA, Smith F. 1956. Colorimetric method for the determination of sugars and related substances. *Anal Chem*. 8: 350-356.

Edwards NJ, Monteiro MA, Faller G, Walsh EJ, Moran AP, Roberts IS, High NJ. 2000. Lewis X structures in the O antigen side-chain promote adhesion of *Helicobacter pylori* to the gastric epithelium. *Mol Microbiol*. 35: 1530-1539.

Farinha P, Gascoyne RD. 2005. *Helicobacter pylori* and MALT lymphoma. *Gastroenterology*. 128: 1579-1605.

Ferreira AC, Isomoto H, Moriyama M, Fujioka T, Machado JC, Yamaoka Y. 2008. Helicobacter and gastric malignancies. *Helicobacter*. 13: 28-34.

Ferreira D, Barros A, Coimbra MA, Delgadillo I. 2001 Use of FT-IR spectroscopy to follow the effect of processing in cell wall polysaccharide extracts of a sun-dried pear. *Carbohydr Polym.* 45: 175-182

Ferreira JA, Domingues, MRM, Reis A, Monteiro MA, Coimbra MA. 2010. Differentiation of isomeric Lewis blood groups by positive ion electrospray tandem mass spectrometry, *Anal Biochem.*. doi:10.1016/j.ab.2009.10.034.

Ferreira JA, Pires C, Paulo M, Azevedo NF, Domingues MR, Vieira MJ, Monteiro MA, Coimbra MA. 2009. Bioaccumulation of amylose-like glycans by *Helicobacter pylori*. *Helicobacter* 14:559-570.

Ferrero RL. 2005. Innate immune recognition of the extracellular mucosal pathogen *Helicobacter pylori*. *Mol Immunol.* 42: 879-885.

Figueiredo C, Machado JC, Pharoah P, Seruca R, Sousa S, Carvalho R, Capelinha AF, Quint W, Caldas C, van Doorn LJ, Carneiro F, Sobrinho-Simoes M. 2002. *Helicobacter pylori* and interleukin 1 genotyping: an opportunity to identify high-risk individuals for gastric carcinoma. *J Natl Cancer Inst.* 94:1680-1687.

Forman D, Graham DY. 2004. Impact of *Helicobacter pylori* on society-role for a strategy of "search and eradicate". *Aliment Pharmacol Ther*. 19: 17-21.

Forsee WT, Cartee RT, Yother J. 2009. Characterization of the lipid linkage region and chain length of the cellubiuronic acid capsule of *Streptococcus pneumoniae*. *J Biol Chem.* 84:11826-11835.

Fowler M, Thomas RJ, Atherton J; Roberts IS, High NJ. 2006 Galectin-3 binds to *Helicobacter pylori O*-antigen: it is upregulated and rapidly secreted by gastric epithelial cells in response to *H. pylori* adhesion. *Cell Microbiol.* 8: 44-54.

Gagliardi MC, Lemassu A, Teloni R, Marriotti S, Sargentini V, Pardini M. 2007. Cell wall-associated alpha-glucan is instrumental for *Mycobacterium tuberculosis* to block CD1 molecule expression and disable the function of dentric cells from infected monocyte. *Cell Microbiol*. 9: 2081-2092.

Gloaguena V, Plancked Y, Streckerd G, Vebret L, Hoffmann L, Morvan H. 1997. Structural characterization of three aldobiouronic acids derived from the capsular polysaccharide produced by the thermophilic cyanobacterium *Mastigocladus laminosus*. *Int J Biol Macromol.* 21: 73-79.

Govorchenko VI, Gorbach VI, Ovodov YS. 1972. Acetolysis of aldobiouronic and pseudoaldobiouronic acids. *Chemistry of Natural Compounds.* 8: 257-258.

Graham DY. 2000. *Helicobacter pylori* infection is the primary cause of gastric cancer. *J Gastroenterol*. 35: 90–97.

Grande M, Cadeddu F, Villa M, Attinà GM, Muzi MG, Nigro C, Rulli F, Farinon AM. 2008. *Helicobacter pylori* and gastroesophageal reflux disease. *World J Surg Oncol.* 6: 74-81.

Guimarães N, Azevedo NF, Figueiredo C, Keevil CW, Vieira MJ. 2007. Development and application of a novel peptide nucleic acid probe for the specific detection of *Helicobacter pylori* in gastric biopsy specimens. *J Clin Microbiol*. 45: 3089-3094.

Gunstone FD, Harwood JL, Padley FB. 1995. The Lipid Handbook. 2nd edition. London (UK). Chapman&Hall.

Harris PJ, Blakeney AB, Henry RJ, Stone BA. 1988. Gas-chromatographic determination of the monosaccharide composition of plant cell wall preparations. *J AOAC Int*. 71: 272-275.

Heneghan MA, McCarthy CF, Janulaityte D, Moran AP. 2001. Relationship of anti-Lewis x and anti-Lewis y antibodies in serum samples from gastric cancer and chronic gastritis patients to *Helicobacter pylori*-mediated autoimmunity. *Infect Immun.* 69: 4774-4781.

Heneghan MA, McCarthy CF, Moran AP. 2000. Relationship of blood group determinants on Helicobacter pylori lipopolysaccharide with host Lewis phenotype and inflammatory response. *Infect Immun*. 68: 937-941.

Hirai Y, Haque M, Yoshida T, Yokota K, Yasuda T, Oguma K. 1995. Unique cholesteryl glucosides in *Helicobacter pylori*: composition and structural analysis. *J Bacteriol.* 177: 5327-5333.

Hooper LV, Gordon JI. 2001. Glycans as legislators of host-microbial interactions: spanning the spectrum from symbiosis to pathogenicity. *Glycobiology* 11: 1R-10R.

Hynes SO, Keenan JI, Ferris JA, Annuk H; Moran AP. 2005. Lewis epitopes on outer membrane vesicles of relevance to *Helicobacter pylori* pathogenesis. *Helicobacter* 10: 146-56.

IARC Working Group on the Evaluation of Carcinogenic Risks to Humans, 1994. Schistosomes, liver flukes and *Helicobacter pylori*. *IARC Monogr Eval Carcinog Risk Hum* 61: 1-214.

Inamoto Y, Ariyama S, Hamanaka Y, Okita K, Kaneta Y, Nagate T, Kondou I, Takemoto T. 1993. Lipid analysis of *Helicobacter pylori*. *J Clin Gastroenterol.* 1: S136-S139

Itano N. 2008. Simple primary structure, complex turnover regulation and multiple roles of hyaluronan. *J Biochem*. 144: 131-137.

Jie LK, F MS, Lam CC. 1995. ^{1}H-Nuclear magnetic resonance spectroscopic studies of saturated, acetylenic and ethylene triacylglycerols. *Chem Phys Lipids*. 77: 155-171.

Jonsson AP, Griffiths WJ, Bratt P, Johansson I, Strömberg N, Jörnvall H, Bergman T. 2000. A novel Ser *O*-glucuronidation in acidic proline-rich proteins identified by tandem mass spectrometry. *FEBS Lett.* 475: 131-134.

Kobayashi M, Lee H, Nakayama J, Fukuda M. 2009. Roles of gastric mucin-type *O*-glycans in the pathogenesis of *Helicobacter pylori* infection. *Glycobiology*. 19: 453-461.

Kobayashi M, Lee H, Nakayama J, Fukuda M. 2009a. Carbohydrate-dependent defense mechanisms against *Helicobacter pylori* infection. *Curr Drug Metab*. 10: 29-40.

Kusters JG, van Vliet AHM, Kuipers EJ. 2006. Pathogenesis of *Helicobacter pylori* infection. *Clin Microbiol Rev*. 19: 449-490.

Lebrun AH, Wunder C, Hildebrand J, Churin Y, Zähringer U, Lindner B, Meyer TF, Heinz E, Warnecke D. 2006. Cloning of a cholesterol-α-glucosyltransferase from *Helicobacter pylori. J Biol Chem* 281: 27765-27772.

Lindberg B, Lönngren J. 1978. Methylation analysis of complex carbohydrates: general procedure and application for sequence analysis. *Methods Enzymol*. 50: 3-33.

Lock RA, Cordwell SJ, Coombs GW, Walsh BJ, Forbes GM. 2001 Proteome analysis of *Helicobacter pylori*: Major proteins of type strains NCTC 11637. *Pathology*. 33: 365-374

Logan SM, Conlan JW, Monteiro MA, Wakarchuck WW, Altman E. 2000. Functional genomics of *Helicobacter pylori*: identification of a beta-1,4 galactosyltransferase and generation of mutants with altered lipopolysaccharide. *Mol Microbiol.* 35: 1156-1167.

Mbulaiteye SM, Hisada M, El-Omar EM. 2009 *Helicobacter pylori* associated global gastric cancer burden. *Front Biosci.* 14: 1490-504.

Moese S, Selbach M, Zimny-Arndt U, Jungblut PR, Meyer TF, Backert S. 2001. Identification of a tyrosine-phosphorylated 35 kDa carboxy-terminal fragment (p35CagA) of the *Helicobacter pylori cagA* protein in phagocytic cells: Processing or breakage? *Proteomics*. 1: 618-629

Montecucco C, Rappuoli R. 2001. Living dangerously: how *Helicobacter pylori* survives in the human stomach. *Nat Rev Mol Cell Biol*. 2: 457-466.

Monteiro MA. 2001 *Helicobacter pylori*: a wolf in sheep's clothing: the glycotype families of Helicobacter pylori lipopolysaccharides expressing histo-blood groups: structure, biosynthesis, and role in pathogenesis. *Adv Carbohydr Chem Biochem*. 57: 99-158.

Monteiro MA; St Michael F; Rasko DA; Taylor DE; Conlan JW; Chan KH; Logan SM; Appelmelk BJ; Perry MB. 2001 *Helicobacter pylori* from asymptomatic hosts expressing heptoglycan but lacking Lewis *O*-chains: Lewis blood-group *O*-chains may play a role in Helicobacter pylori induced pathology. *Biochem Cell Biol.* 79: 449-459.

Moran AP, Khamri W, Walker MM, Thursz MR. 2005. Role of surfactant protein D (SP-D) in innate immunity in the gastric mucosa: evidence of interaction with *Helicobacter pylori* lipopolysaccharide. *J Endotoxin Res.* 11: 357-362.

Moran AP, Knirel B, Senchenkova SN, Widmalm G, Hynes SO, Jansson PE, J. 2002. *Biol Chem.* 277: 5785-5795.

Moran AP, Lindner B, Walsh EJ. 1997, Structural characterization of the Lipid A component of *Helicobacter pylori* rough- and smooth-form Lipopolysaccharides. *J Bacteriol.* 179: 6453-6463.

Moran AP, Lindner B, Walsh EJ. 1997. Structural characterization of the Lipid A component of *Helicobacter pylori* rough- and smooth-form lipopolysaccharides. *J Bacteriol.* 179: 6453-6463

Moran AP, Prendergast MM. 2001. Molecular mimicry in *Campylobacter jejuni* and *Helicobacter pylori* lipopolysaccharides: contribution of gastrointestinal infections to autoimmunity. *J Autoimmun*. 16: 241-256.

Moran AP, Sturegard E, Sjunnesson H, Wadstrom T, Hynes SO. 2000. The relationship between *O*-chain expression and colonization ability of *Helicobacter pylori* in a mouse model. *FEMS Immunol Med Microbiol.* 29: 263-270.

Moran AP. 1999 *Helicobacter pylori* lipopolysaccharide-mediated gastric and extragastric pathology. *Physiol Pharmacol.* 50: 787-805.

Moran AP. 2008. Relevance of fucosylation and Lewis antigen expression in the bacterial gastroduodenal pathogen *Helicobacter pylori*. *Carbohydr Res*. 343: 1952-1965.

Müller-Loennies S, Holst O, Brade H. 1994. Chemical structure of the core region of *Escherichia coli* J-5 Lipopolysaccharide. *Eur J Biochem.* 224: 751-760.

Nilsson C, Skoglund A, Moran AP, Annuk H, Engstrand L, Normark S. 2008. Lipopolysaccharide diversity evolving in *Helicobacter pylori* communities through genetic modifications in fucosyltransferases. *PLoS ONE*. 3: 1-14.

O'Connor HJ. 1999. *Helicobacter pylori* and gastro-oesophageal reflux disease-clinical implications and management. *Aliment Pharmacol Ther.* 13: 117-127.

O'Keeffe J, Moran AP. 2008. Conventional, regulatory, and unconventional T cells in the immunologic response to Helicobacter pylori. *Helicobacter*. 13: 1-19.

Rasko DA, Wilson TJ, Zopf D, Taylor DE. 2000. Lewis antigen expression and stability in *Helicobacter pylori* isolated from serial gastric biopsies. *J Infect Dis.* 181: 1089-1095

Redgwell RJ, Selvendran RR. 1986. Structural features of cell-wall polysaccharides of onion *Allium cepa*. *Carbohydr Res*. 157: 183-199.

Rieder G, Hatz RA, Moran AP, Walz A, Stolte M, Enders G. 1997. Role of adherence in interleukin-8 induction in Helicobacter pylori-associated gastritis. *Infect Immun.* 65: 3622-3630.

Roepstorff P, Fohlman J. 1984. Proposal for a common nomenclature for sequence ions in mass spectra of peptides. *Biomed Mass Spectrom.* 1984 11:601.

Sainsus N, Cattori V, Lepadatu C, Hofmann-Lehmann R. 2008. Liquid culture medium for the rapid cultivation of *Helicobacter pylori* from biopsy specimens. *Eur. J. Clin. Microbiol Infect Dis.* 27: 1209-1217.

Sambrook J, Fritsch EF, Maniatis T. 1989. Molecular cloning, a laboratory manual, 2nd edition. New York (USA). Cold Spring Harbor Laboratory Press.

Santacroce L, Cagiano R, Del Prete R, Bottalico L, Sabatini R, Carlaio RG, Prejbeanu R, Vermesan H, Dragulescu SI, Vermesan D, Motoc A, Losacco T. 2008. *Helicobacter pylori* infection and gastric MALTomas: an up-to-date and therapy highlight. *Clin Ter*. 159: 457-462.

Schagger H. 2006. Tricine-SDS-PAGE. *Nat. Protoc.* 1: 16-22.

Schirm M, Schoenhofen IC, Logan SM, Waldron KC, Thibault P. 2005. Identification of unusual bacterial glycosylation by Tandem Mass Spectrometry analyses of intact proteins. *Anal Chem.* 77:7774-7782.

Schirm M, Soo EC, Aubry AJ, Austin J, Thibault P, Logan SM. 2003. Structural, genetic and functional characterization of the flagellin glycosylation process in *Helicobacter pylori*. *Mol Microbiol.* 48:1579-1592

Schoenhofen IC, McNally DJ, Brisson JR, Logan SM. 2006. Elucidation of the CMP-pseudaminic acid pathway in *Helicobacter pylori*: synthesis from UDP-N-acetylglucosamine by a single enzymatic reaction. *Glycobiology*. 16: 8C-14C.

Shnyra A, Luchi M, Morrison DC. 2000. Preparation of endotoxin from pathogenic Gram-Negative bacteria. In: Evans TJ, editors. Septic Shock Methods and Protocols. New Jersey (USA): Humana Press Inc. p. 13-25.

Souza RC, Lima JH. 2009. *Helicobacter pylori* and gastroesophageal reflux disease: a review of this intriguing relationship. *Dis Esophagus*. 22: 256-263.

Stenutz R, Jansson PE, Widmalm G. 1998. Computer-assisted structural analysis of oligo- and polysaccharides: An extension of CASPER to multibranched structures. *Carbohydr. Res.* 306: 11-17;

Stevenson TH, Castillo A, Lucia LM, Acuff GR. 2000. Growth of *Helicobacter pylori* in various liquid and plating media. *Lett Appl Microbiol.* 30: 192–196.

Stoscheck CM. 1990. Quantitation of Protein. *Methods Enzymol*. *182:* 50-69.

Sugiyama T. 2004. Development of gastric cancer associated with *Helicobacter pylori* infection. *Cancer Chemother Pharmacol*. 54: S12-S20.

Sutherland I. 2001. Biofilm exopolysaccharides: a strong and sticky framework. *Microbiology.* 147: 3-9.

Testerman TL, McGee DJ, Mobley HLT. 2001. *Helicobacter pylori* growth and urease detection in the chemical defined medium Ham's F-12 Nutrient mixture. *J Clin Microbiol*. 39: 3842-3850.

Toole, BP. 2000. Hyaluronan is not just a goo! *J Clin Invest.* 106: 335–336.

Vakil N. 2008. *Helicobacter pylori* treatment: is sequential or quadruple therapy the answer? *Rev Gastroenterol Disord*. 8: 77-82.

van Doorn LJ, Figueiredo C, Rossau R, Jannes G, van Asbroek M, Sousa JC, Carneiro F, Quint WG. 1998a. Typing of *Helicobacter pylori* vacA gene and detection of *cagA* gene by PCR and reverse hybridization. *J Clin Microbiol.* 36: 1271-1276.

van Doorn LJ, Figueiredo C, Sanna R, Pena S, Midolo P, Ng EK, Atherton JC, Blaser MJ, Quint WG. 1998b. Expanding allelic diversity of *Helicobacter pylori vacA*. *J Clin Microbiol.* 36: 2597-2603.

Vliegenthart JFG. 2006. Carbohydrate based vaccines. *FEBS Lett.* 580: 2945–2950.

Wen S, Moss SF. 2009. *Helicobacter pylori* virulence factors in gastric carcinogenesis. *Cancer Lett.* 282: 1-8.

Westphal O, Jann K. 1965. Bacterial lipopolysaccharides: extraction with phenol-water and further applications of the procedure. *Methods Carbohydr Chem.* 5: 83-91.

Yagi S, Okada H, Takenaka R, Miyoshi M, Suzuki S, Toyokawa T, Kawahara Y, Yamamoto K. 2009. Influence of *Helicobacter pylori* eradication on reflux esophagitis in Japanese patients. *Dis Esophagus.* 22: 361-367.

Yang BY, Gray JSS, Montgomery R. 1996. The structure of stewartan, a capsular polysaccharide produced by *Erwinia stewartii* strain DC283. *Carbohydr Res.* 296: 183-201.

Zaia J. 2004. Mass spectrometry of oligosaccharides. *Mass Spectrom. Rev*. 23: 161-277.

CHAPTER VII

CONCLUDING REMARKS

7. Concluding remarks

Over the last ten years most attention has been devoted to the structural characterization of cell-surface LPS from several *H. pylori* strains. Of particular interest was the implication of *O*-chains bearing Le blood group determinants in adhesion to gastric cells, colonization of the gastric niche, and modulation/evasion of the host's immune system. Therefore, the detection of trace amounts of Le epitopes and the distinction between isomers Le^a/Le^x and Le^b/Le^y has been of primarily concern and a challenging analytical topic.

This thesis has demonstrated that the mentioned Le isomers can be detected in a nano-fentomole range by ESI-MS and distinguished based on their characteristic MS/MS spectra. Type 1 Lewis antigens (Le^a and Le^b) could be distinguished from Type 2 (Le^x and Le^y) on the basis of specific fragmentations of the GlcNAc unit. It was concluded that *O*-4 linked GlcNAc sugars are lost as residues, whereas *O*-3 linked sugars undergo fragmentation both as sugar units as well as sugar residues (unit -18 Da). Additionally, Type 2 Le antigens also showed a characteristic cross-ring cleavage $^{0,2}A_2$ of the GlcNAc. As a result, the product ions at *m/z* 388 and 305 were proposed as diagnostic for the presence of Le^x and at *m/z* 372 as diagnostic of Le^a. Also, the product ions at *m/z* 534 and 305, characteristic of Le^y, and at *m/z* 372, characteristic of Le^b, are proposed to distinguish the tetrasaccharide isomers Le^b/Le^y. These purposed ions can also be useful in the distinction of Le determinants within a mixture of both isomers. Despite the strong influence exerted by the type of analysers on MS/MS spectra, it was also concluded that LIT, Q-TOF and QqQ analyzers are capable of generating the ions purposed to distinguish the studied Le determinants.

Several studies have been pointing out that, in addition to the LPS, *H. pylori* expresses other cell-surface glycans, however their structures have remained until now mostly unaddressed. This thesis proved insights on some of these structural motifs by demonstrating *H. pylori* is capability to bioaccumulate amylose-like glycans (α-(1→4)-D-Glc polysaccharide) and to express mannose-rich glycans.

Bioaccumulation of amylose-like glycans was found enhanced with the subcultivation of the bacterium on agar medium, while LPS *O*-chains expression decreased. On the other hand, during exponential growth of the bacterium in F12 liquid medium, an opposite behaviour is observed, *i.e.* there is an increase in the overall amount

of LPS and decrease in amylose content. As such, it has been demonstrated that, under certain selective pressures induced by specific environmental conditions, *H. pylori* might be led to express a phase-variable cell-surface α-(1→4) Glc polysaccharide as part of a long-term survival strategy. Additionally, studies carried out in virulent clinical isolate *H. pylori* PTAV79 revealed that amylose-like glycans are linked to glycerol residues. The observation of high amounts of stearic acid, and glycerylphophodiester moieties in amylose-like rich fractions suggested the expression of glycoglycerophospholipids. These findings strongly suggest that amylose is anchored to the outer cell-surface lipidic layer.
Even though it is common to observe vestigial amounts of Man in *H. pylori* cell-surface glycan-rich extracts, its assignment has remained until now overlooked, most likely due to its low biological abundance. Taking advantage of the high amounts of Man expressed by clinical isolate *H. pylori* 968, it was possible to identify a highly branched mannan formed by a backbone of α-(1→6)-linked mannopyranosyl units showing up to 80% substitution in the *O*-2 position. Interestingly, it was concluded that the side chains contain *O*-2 linked Man residues both in α- and β-configurations. The described mannan is a part of a heteropolymeric structure containing Glc, Gal, and Glc, having a protein domain.

Structural studies conducted in *H. pylori* PTAV79 LPS allowed the identification of *O*-chains composed of LacNAc (i-antigen) units. The absence of fucosylated Lewis blood groups has been reported to negatively influence the bacteria's capability of colonizing the human stomach and promoting gastric malignancies. Results arising from this strain, however, showed that the expression of i-antigens does not compromise gastric colonization. *H. pylori* PTAV79 also expressed a polysaccharide composed by an aldobiouronic acid repeating unit of [→3)-α-D-GlcA(1→4)-α-D-Glc(1→]. This structure is though to play a role in cellular protection against acid environments by allowing the formation of hydrogels that aid buffering the surrounding media. In addition, a proteomic approach led to the first report of a non-flagelar *H. pylori* glycoprotein exhibiting *O*-glucuronosyl serine residues. Moreover, the expression of glucuronic acid by *H. pylori* is also being described for the first time.

In resume, the present thesis revealed the expression of several cell-surface structural motifs until now unknown in *H. pylori*, namely like the expression of heteropolymeric protein containing mannans, amylose-glycans, polysaccharides composed of albobiuronic acid repeating units, and glycoproteins containing *O*-glucuronosyl

residues. In addition, the newly described amylose and mannan glycans were found in association with fatty acids and proteins, respectively. The coexistence of these structures with the LPS in *H. pylori* cell-surface was further demonstrated.

This thesis has exposed new *H. pylori* cell-surface glycans that can act as players in host-microbial interactions and contribute to bacterial adhesion, resistance to external aggressions and modulation of immune responses. These structures offer new potential targets to include when considering the development of carbohydrate-based vaccines against *H. pylori*.

Future directions should comprise a comprehensive understanding of the events triggering the expression of the observed glycans, their biosynthesis, and biological role. Also, an evaluation of their capability to induce immune responses against *H. pylori* ought evaluation in order to determine their potential as carbohydrate-based vaccines.